FINAL PROJECT REPORT

THE SNAKE RIVER GEOTHERMAL DRILLING PROJECT: INNOVATIVE APPROACHES TO GEOTHERMAL EXPLORATION

DE-EE 0002848

John W. Shervais, Principal Investigator

UTAH STATE UNIVERSITY, LOGAN, UT 84322

EXECUTIVE SUMMARY

The Snake River Geothermal Drilling Project: Innovative Approaches to Geothermal Exploration (DE-EE-0002848) received its conditional award on March 5, 2010 with a start date of January 29, 2010. The award was finalized on July 9, 2010. The Lead PI is John Shervais at Utah State University, with co-investigators James Evans (Utah State University), Lee Liberty (Boise State University), Doug Schmitt (University of Alberta), and David Blackwell (Southern Methodist University). Our partner for the drilling activities was Drilling, Observation, and Sampling of the Earth's Continental Crust, Inc, a not-for-profit consortium of universities which coordinates continental scientific drilling in the United States. Cost share was provided by the International Continental Drilling Program (ICDP) and by two of the collaborating universities (Utah State University, University of Alberta).

The goal of our project was to test innovative exploration technologies using existing and new data, and to ground-truth these technologies using slim-hole core technology. The slim-hole core allowed us to understand subsurface stratigraphy and alteration in detail, and to correlate lithologies observed in core with surface based geophysical studies. Compiled data included geologic maps, volcanic vent distribution, structural maps, existing well logs and temperature gradient logs, groundwater temperatures, and geophysical surveys (resistivity, magnetics, gravity). New data included high-resolution gravity and magnetic surveys, high-resolution seismic surveys, three slimhole test wells, borehole wireline logs, lithology logs, water chemistry, alteration mineralogy, fracture distribution, and new thermal gradient measurements.

Phase 1 activities focused on data compilation and additional field studies, as well as on permitting and environmental review. Phase 2 drilling of the slim-hole wells began in September 2010 and continued with minor breaks until January 2012. Geophysical studies and well logging were carried out concurrently with drilling. The three drill holes were located to represent three distinct settings within the Snake River volcanic province: (1) the axial volcanic high, which contains the thickest accumulation of basaltic lava and the highest projected subaquifer heat flow, (2) the margin of the central plain, which is characterized by a large number of hot springs and comprises an official "warm water" thermal district that is not affected by the Snake River regional aquifer, and (3) the western plain, which is characterized by Basin-and-Range like faulting along the range fronts, young volcanism, and by high thermal gradients in deep wildcat petroleum wells.

The three locations studied were found to have distinctly different settings, stratigraphy, and geothermal potential, and together provided a robust test of the techniques studied here. The first site, Kimama, sits on the axial volcanic zone and is characterized by >2 km of basalt flows with minor intercalated sediment. The Snake River Regional Aquifer (SRRA) is exceptionally thick here (~980 m), almost twice as thick as found in deep wells to the NE. The aquifer has an isothermal temperature gradient (~3ºC/km), but below the SRRA thermal gradients are conductive at ~75ºC/Km. The base of the aquifer is controlled by the onset of groundmass smectite alteration. The second site, Kimberly, is dominantly underlain by rhyolite welded ash flow tuffs, with intercalated basalt and sediment near the top. This site lies south of the Snake River and is not affected by the SRRA. Thermal gradients in this well show cool water in the upper 300 m, with a rapid rise in temperature to 800 m depth; from 800 m to total depth (1958 m) temperatures are essentially isothermal at 50-58ºC. This represents an enormous warm water resource and documents the advective flow of warm water from the south (Cassia Mountains) or from below. However, these temperatures are too low for power generation.

The third site, Mountain Home, is unique in that it intersected a free-flowing artesian geothermal aquifer at depth. The Mountain Home site is characterized lacustrine sediments with interbedded basalt in the upper 1000 m, with basalt, basalt hyaloclastite, and basaltic sandstone in the lower 800 m. It is also characterized by steep geothermal gradient of ~75ºC/ Km from the surface to total depth at 1828 m, with a spike in temperature to ~149ºC adjacent to the geothermal fluid influx zone at 1745 m depth. This is supported by phyllosilicate studies which show a transition from smectite (clay) to corrensite (chlorite) around the influx zone, and then back to smectite deeper in the well. This indicates that hotter fluids from depth are being transported along the fracture zone intersected by the well at 1745 m. Chemical analysis of the artesian geothermal water shows that is low in total dissolved solids, and relatively sulfate-rich, plotting in the "volcanic waters" corner of a Giggenbach plot. Isotopically, is plots on a mixing line between meteoric water and equilibrated volcanic waters (unlike all other thermal waters in southern Idaho, which are essentially meteoric).

New high-resolution downhole and surface seismic data provide insights into stratigraphy and test the capabilities of seismic imaging in volcanic terranes. Downhole Vertical Seismic Profiles (VSP) data show low seismic attenuation, large seismic velocity contrasts at volcanic flow boundaries, and large near-surface static effects. Sedimentary interbeds correspond with slow velocity zones that relate to reflections on surface seismic profiles. Reflections observed on seismic profiles tie to flow boundaries in the upper 500 m depth. This reflection pattern suggests flow volumes from the latest eruption can be estimated with surface seismic methods. Downhole VSP and surface seismic results suggest seismic reflection methods are useful to image shallow flow boundaries.

Potential field studies (gravity, magnetics) were carried out in the Snake River Plain to provide regional geophysical mapping, and to characterize mid- to shallow-crustal features. This involved compiling and reprocessing existing gravity and aeromagnetic data, and collecting new gravity data to provide an unprecedented high-resolution potential field dataset for assessing subsurface structure. Gravity data were collected along several detailed transects (300-1200 m stations spacing) and provide the basis for new gravity anomaly maps of unprecedented detail. Representative rock samples were collected and their physical properties were determined in the laboratory to aid in quantitative modeling of measured geophysical anomalies. In addition to our potential field mapping efforts, we undertook two innovative applications for geothermal exploration. The first involved a technique to estimate depths to the bottom of magnetic sources that can be used to map the Curie temperature isotherm or estimate the thickness of basaltic fill within the Snake River Plain. The second involved novel methods to estimate the 3D geometry of subsurface alteration.

An extensive series of borehole geophysical logs were obtained at each site. Hydrogen-index neutron and γ-γ-density logs were deployed through the drill string to provide information on stratigraphy and alteration minerals. Electrical resistivity logs highlight the existence of some fracture and mineralized zones. Magnetic susceptibility together with the vector magnetic field measurements may provide a tool for tracking magnetic field reversals along the borehole. Sonic logs highlight the variations in compressional and shear velocity along the bore hole. Bore hole seismic measurements indicate that strong seismic reflections are produced at lithological contacts seen in core. Oriented ultrasonic borehole televiewer images were obtained over most of the wells; these allow for confident estimates of stress directions and/or placing constraints on stress magnitudes.

The data produced by this project have allowed us to produce a new conceptual model for the occurrence of geothermal resources in southern Idaho that may be used for more systematic exploration. In particular, this model will form the basis for a play fairway analysis of the region that will allow us to identify potential plays, and to assess these plays to develop a detailed list of prospects with a high probability of success. Our innovative approach, using seismic, gravity and magnetic, slim hole exploratory core holes, extensive core retrieval, and geochemical studies of both core and water samples, underscores the need for systematic and broad scale data collection (geologic and geophysical) as a prerequisite for fairway analysis.

Finally, our project exceeded its goals by discovering a new blind geothermal resource at Mountain Home AFB that has the potential to produce 10 MW of electricity for the U.S. Air Force. This will help them achieve their goal of energy independence, as mandated by the Department of Defence.

Table of Contents

Acknowledgements: *This work was performed under U.S. Department of Energy contract EE0002848 with Utah State University, and subawards issued under that contract to Boise State University, the University of Alberta, the U.S. Geological Survey (Menlo Park, CA), and DOSECC (Drilling, Observation, and Sampling of Earth's Continental Crust), a non-profit consortium dedicated to continental scientific drilling. Additional support was provided by the International Continental Drilling Program (ICDP, part of the German Research Centre for Geosciences, Potsdam, Germany), Utah State University (Logan, Utah, 84322), and the Institute for Geophysical Research, University of Alberta, Canada (Edmonton, AB T6G 2E1). The Operational Support Group of ICDP provided borehole wireline logging services. Cooperative work with personnel from the U.S. Geological Survey (Denver, CO), Brigham Young University, Southern Methodist University, the University of South Carolina, and the LacCore Lake Core Repository (University of Minnesota), is gratefully acknowledged and appreciated.*

CHAPTER 1:

OVERVIEW OF THE SNAKE RIVER GEOTHERMAL DRILLING PROJECT: INNOVATIVE APPROACHES TO GEOTHERMAL EXPLORATION

John W. Shervais and James P. Evans
Utah State University, Logan, UT 84322-4505

Eric H. Christiansen
Brigham Young University, Provo, UT 84602

Douglas R. Schmitt
University of Alberta, Edmonton, Alberta, T6G 2E1, Canada

Dennis Nielson, DOSECC, Inc.,
2075 Pioneer Road, SuiteB, Salt Lake City, UT 84104-4231

Lee M. Liberty,
Boise State University, Boise, ID 83725-1536

David D. Blackwell
Southern Methodist University, Dallas, TX 75275-0395

Jonathan M. Glen, and Duane Champion, U.S. Geological Survey, Menlo Park, CA 94025-3591

Alexander A. Prokopenko
University of South Carolina, Columbia, South Carolina, 29208

ABSTRACT

The Snake River volcanic province overlies a thermal anomaly that extends deep into the mantle and represents one of the highest heat flow provinces in North America, and an area with the highest calculated geothermal gradients. This makes the SRP one of the most under-developed and potentially highest producing geothermal districts in the United States. Elevated heat flow is typically highest along the margins of the topographic Snake River Plain and lowest along the axis of the plain, where thermal gradients are suppressed by the Snake River aquifer. Beneath this aquifer, however, thermal gradients rise again and may tap even higher heat flows associated with the intrusion of mafic magmas into the mid-crustal sill complex.

This project tested a series of innovative geothermal exploration strategies in three phases, at locations in southern Idaho. Phase 1 studies (January-August 2010) comprised compilation of existing data (geologic maps, well logs, heat flow measurements, and geophysical data), surface mapping, shallow seismic surveys, and potential field surveys (gravity and magnetics). Phase 2 (August 2010-January 2012) focused on the drilling of three intermediate depth (1.8-1.9 km) slim-hole exploration wells with a full suite of geophysical borehole logs and a vertical seismic profiles. Each of the exploration wells was cored to preserve a complete record of the stratigraphy and to assess hydrothermal alteration and its physical properties. Phase 3 (June 2011-June 2013) comprised data analysis and evaluation. Cost share was provided by a consortium of universities and by the International Continental Drilling Program (ICDP).

Our objectives were to implement and test a range of geophysical and geologic approaches to geothermal exploration. The slim-hole exploration wells were used to document thermal resources and to provide a lithologic and stratigraphic context for interpretation of the data obtained in Phase 1. A further objective was to establish the Snake River Plain as a viable target for the production of geothermal energy that is close to fast growing urban centers in southern Idaho and northern Utah. Idaho has been ranked 3rd among western states for geothermal power production by the Geothermal Task Force of Western Governor's Association (WGA), with an estimated 855 MW of near-term economic potential resources. As shown later in this report, we succeeded in finding a new medium temperature resource on Mountain Home AFB that is potentially capable of 10-20 MW of power production.

Major participants in this project included – in addition to Utah State University (Shervais, Evans) – the Shallow Geophysics group at Boise State University (Liberty), the Geothermal Laboratory at Southern Methodist University (Blackwell), the Institute for Geophysical Research at the University of Alberta (Schmitt), the US Geological Survey (Glen, Champion, Morgan), the US Continental Drilling Consortium (DOSECC), and the International Continental Drilling Program (ICDP-Potsdam).

INTRODUCTION

The Snake River volcanic province overlies a thermal anomaly that extends deep into the mantle and represents one of the highest heat flow provinces in North America, and an area with the highest calculated geothermal gradients (Figure 1-1; *Blackwell 1980; Blackwell et al 1989, 1991, 1992; Blackwell and Richards 2004*). This makes the SRP one of the most under-developed and potentially highest producing geothermal districts in the United States. Elevated heat flow is typically highest along the margins of the topographic Snake River Plain and lowest along the axis of the plain, where thermal gradients are suppressed by the Snake River aquifer. Beneath this aquifer, however, thermal gradients rise again and may tap even higher heat flows associated with the intrusion of mafic magmas into a geophysically imaged mid-crustal sill complex (*e.g., Blackwell 1989; Peng and Humphreys 1998*).

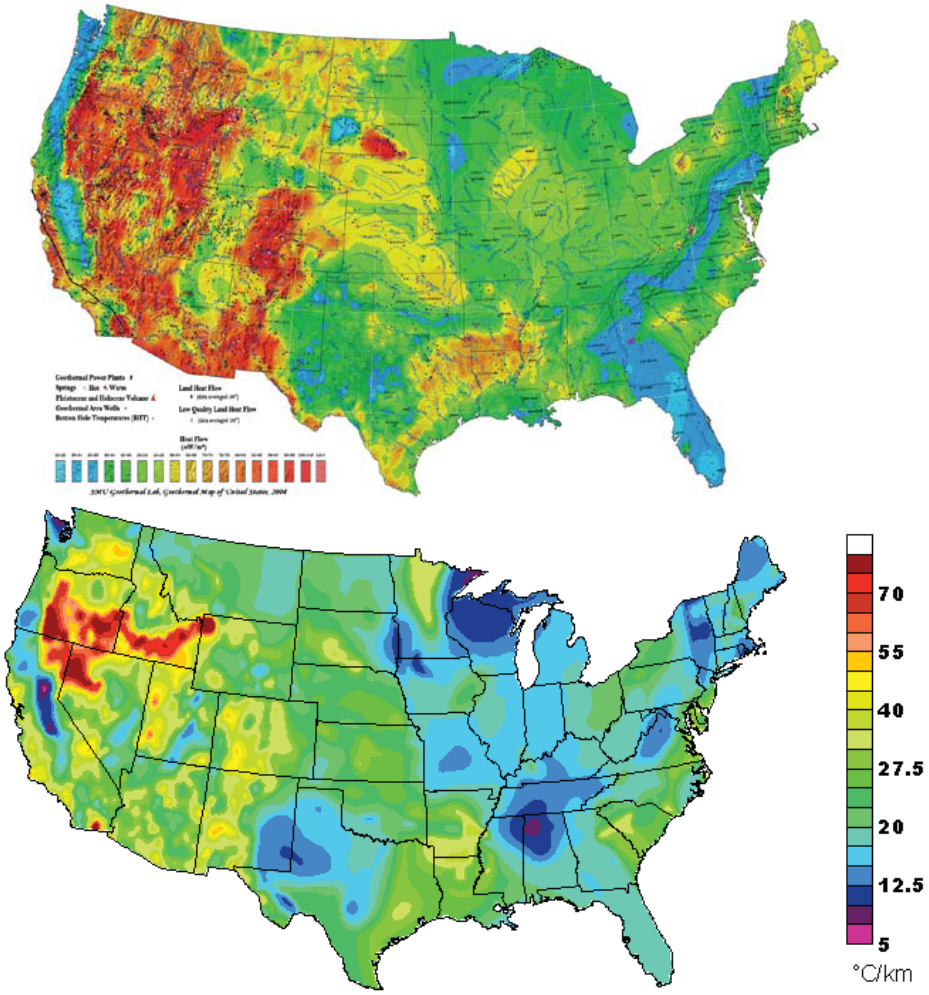

Figure 1-1. (A) Top. Heat flow map of United States showing generally elevated heat flow across much of western US, primarily in the Great Basin and southern Idaho. (B) Heat flow gradient map of United States, showing extremely high surface gradients concentrated in northern Great Basin and along Snake River Plain-Yellowstone trend. Both maps from Southern Methodist University Geothermal Laboratory and Professor David Blackwell.

The Snake River Geothermal Drilling Project (DE-EE-0002848) received its conditional award on March 5, 2010; the award was finalized on July 9, 2010, with a Kick-off Conference Call on July 12, 2010. The Lead PI is John Shervais at Utah State University with co-PI James Evans at *Utah State University*, and funded co-investigators Lee Liberty (*Boise State University*), Doug Schmitt (*University of Alberta*), and David Blackwell (*Southern Methodist University*). Our partner on the drilling activities was Drilling, Observation, and Sampling of the Earth's Continental Crust, Inc. (*DOSECC*), a nonprofit consortium of universities which administers the US Continental Scientific Drilling program. Cost share was provided by Utah State University, the University of Alberta, and the International Continental Drilling Program (*ICDP*), located at the GeoForschungsZentrum *(GFZ),* Potsdam, Germany.

REGIONAL SETTING: THE SNAKE RIVER VOLCANIC PROVINCE

The volcanism of the SRP is typically related to the passage of the North American plate over the Yellowstone mantle plume (Morgan, 1972). The arrival of the plume head is correlated with the eruption of the Columbia River and Steens flood basalts about 17 Ma (Figure 1-2); subsequent volcanism along the SRP may be associated with the plume tail (Pierce et al., 1992). The Yellowstone-Snake River Plain province is markedly bimodal, with basalt and rhyolite the most common volcanic rocks. Basalt erupted mainly from small shield volcanoes (Greeley, 1982). The central and eastern SRP comprises large collapse calderas with surrounding ignimbrite fields, overlain by a thin veneer of basalt. Well-studied individual ignimbrite sheets are as much as 100 m thick and have volumes of more than 1000 km^3 qualifying them as super-eruptions (e.g., Morgan and McIntosh, 2005; Christiansen, 2001; Ellis et al., 2012).

The eastern SRP is a topographic depression that cuts across Basin and Range structures, and is characterized by a thin carapace of basalt (100m-1500m) that overlies rhyolite volcanics and tuffaceous sediments (Champion et al 2002; Geist et al 2002a,b; Hughes et al 2002). The eastern SRP is underlain by a 10 km thick mid-crustal sill complex that has been imaged seismically that represents layered magma chambers where the basalts fractionate (Peng & Humphries, 1998; Shervais et al 2006).

The central SRP represents a critical transition from the broad western province to the well-defined eastern province, but it has received comparatively little study compared to the eastern SRP. It contains basalt, rhyolite, and lacustrine sediments that vary greatly in proportion from place to place, and it lacks the well-defined rhyolite eruptive centers that underlie the eastern SRP. It is the only part of the plain that has not been penetrated by a deep drill hole that samples a large section of basalt and that has not been extensively explored for geothermal resources. Recent mapping projects provide a new framework for understanding the central plain, and for site selection (Kauffman et al, 2005).

The western SRP is a NW-trending graben bounded by en-echelon normal faults exposing rhyolite, and filled with up to 4 km of basalt and sediment (*Wood & Clemens 2002; Shervais et al 2002; White et al 2002; Shervais and Vetter 2009*). Large epicontinental lakes deposited several km of Miocene-Pleistocene sediments, which are both overlain and underlain by basalt (Shervais et al 2002). These sediments are relatively impermeable and form an insulating blanket that traps heat flux from below. The western province is also underlain by a mid-crustal mafic sill similar to that imaged under the eastern plain (*Hill and Pakiser 1967*), but it lies north of the projected hotspot track based on reconstructions of North American plate motion (*Gripp and Gordon, 1990, 2002*).

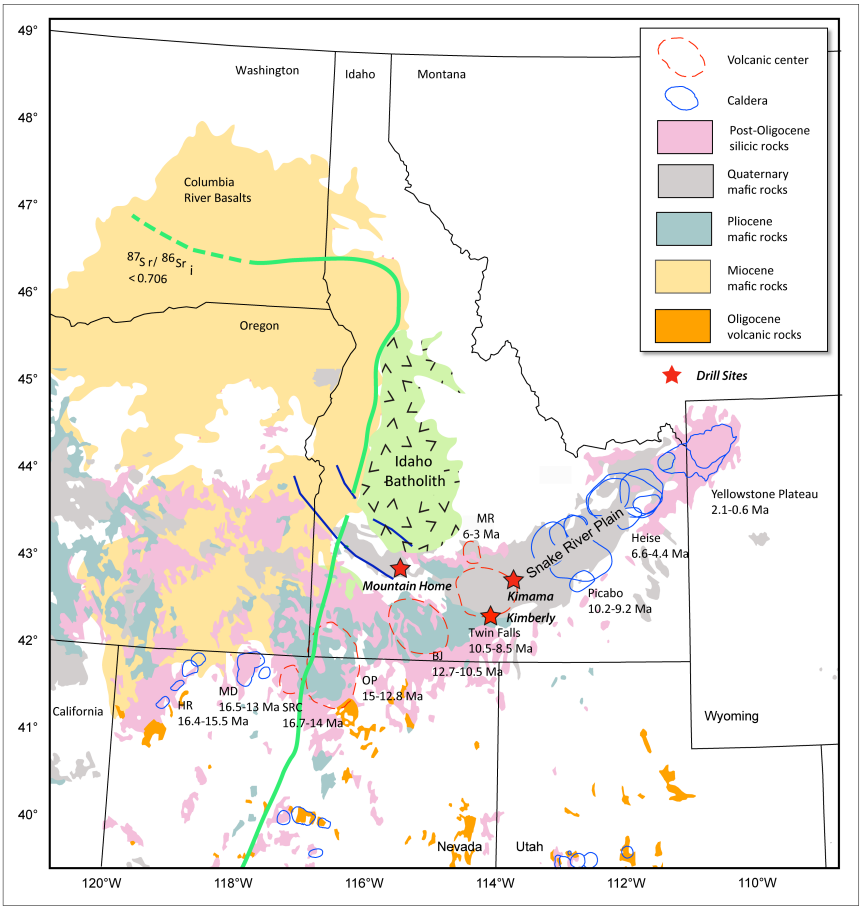

Figure 1-2. Simplified geologic map of the northwestern United States. Rhyolitic volcanic centers and calderas related to the Yellowstone hotspot are younger to the northeast. Basalts overlie older rhyolites. Stars show the location of the Project Hotspot drilling sites; the Kimberly well is in red. Names of volcanic elds and caldera complexes as follows: HR-High Rock, MD-McDermitt, SRC-Santa Rosa-Calico; OP-Owyhee Plateau; BJ-Bruneau-Jarbidge, MR-Magic Reservoir Boundaries are dashed where less certain or buried.

GEOTHERMAL POTENTIAL OF SNAKE RIVER VOLCANIC PROVINCE

Geothermal power has long been used in southern Idaho, but it has been confined almost exclusively to direct use applications such as space heating and aquaculture *(e.g., Sherman 1982; Mitchell et al 2003; Neely 1996; Fleischmann, 2006).* There is only one site where geothermal resources are used for power generation – the Raft River Valley site *(Nathenson et al 1980; Peterson et al 2004; Neely and Galinato 2007).* Nonetheless, the potential for power generation is significant, especially using binary generation systems that can exploit lower temperature resources (*Sanyal and Butler 2005; Neely and Galinato 2007*).

The deep-seated mantle hotspot that undlies the Snake River volcanic province has thinned the lithosphere and fueled the intrusion of up to 10 km of hot basaltic magma into the lower and middle crust. The heat from these intrusions, and from rhyolites formed by the basalt, drives the high heatflow and geothermal gradients observed in deep drill holes from throughout the Snake River Plain (*Blackwell 1978, 1980, 1989; Brott et al 1976, 1978, 1981; Lewis and Young 1989*). Heat flow in the SRP tends to be high along the margins of the plain (80-100 mW/m^2-s) and low when measured in shallow drill holes along the axis of the plain (20-30 mW/m^2-s). However, deep drill holes (>1 km) in the axial portion of the plain are characterized by high heat flows and high geothermal gradients below about 500 m depth (*Blackwell 1989*). This discrepancy is caused by the Snake River aquifer – a massive aquifer system fed by the Lost River system north of Idaho Falls that extends under the plain and emerges at Thousand Springs, Idaho. This aquifer varies in thickness from <100 m to >450 m in the eastern-most SRP. Thermal gradients through the aquifer are static until the base of the aquifer is reached, then rise quickly at deeper levels in the crust (*e.g., Blackwell 1989; Blackwell et al 1992; Smith 2004*). Below the aquifer along the axis of the plain, heat flow values are comparable to heat flow values along the margins of the plain or higher (75-110 mW/m^2-s; Blackwell 1989). Bottom hole temperatures for wells along the margins of the plain near Twin Falls are typically around 30-60ºC at 400-600 m depth (*Baker and Castelin 1990*) and as high as 120ºC at 2800 m depth in the axial region of the plain (*Blackwell 1989)*.

There is a direct link between the volume of magma added to the crust and crustal heat flow, such that estimates of magmatic flux based on geochemical constraints can be used to calculate expected heat flux, and measured heat flux can be used to estimate the magmatic flux. Since most SRP rhyolites are thought to represent crustal melts formed in response to intrusion of mafic magma into the lower and middle crust, the volume of rhyolite and basalt allows us to infer the volume of mafic magma trapped in the crust.

PROJECT OBJECTIVES

Our goals were to [1] identify new geothermal resources in the undeveloped Snake River Plain region, or failing that, to [2] characterize the thermal regime at depth in such a way as to further exploration goals in more focussed efforts, and [3] to document specific exploration methods and protocols that can be used effectively in these terranes. In this report, we summarize our results and present our recommendations for future work. One of our primary accomplishments was the discovery of a moderately high-temperature resource (~140-150ºC) under Mountain Home Air Force Base, which has the potential to be developed as an electric resource that will contribute to Defense Department goals for energy independence on U.S. military installations. Our successful partnership with the USAF on this project presents a model for future cooperative efforts.

Our project used a combination of traditional geologic tools (geologic mapping, petrologic studies, and geochemical investigations of rocks and water samples) and geophysical techniques (high-resolution active source seismic reflection-refraction surveys, detailed ground-based gravity and magnetic surveys), along with relatively deep slim hole test wells that allowed us to document the underlying stratigraphy (ground truth), geothermal gradients below the surface aquifers, fracture densities, and hydraulic conductivities.

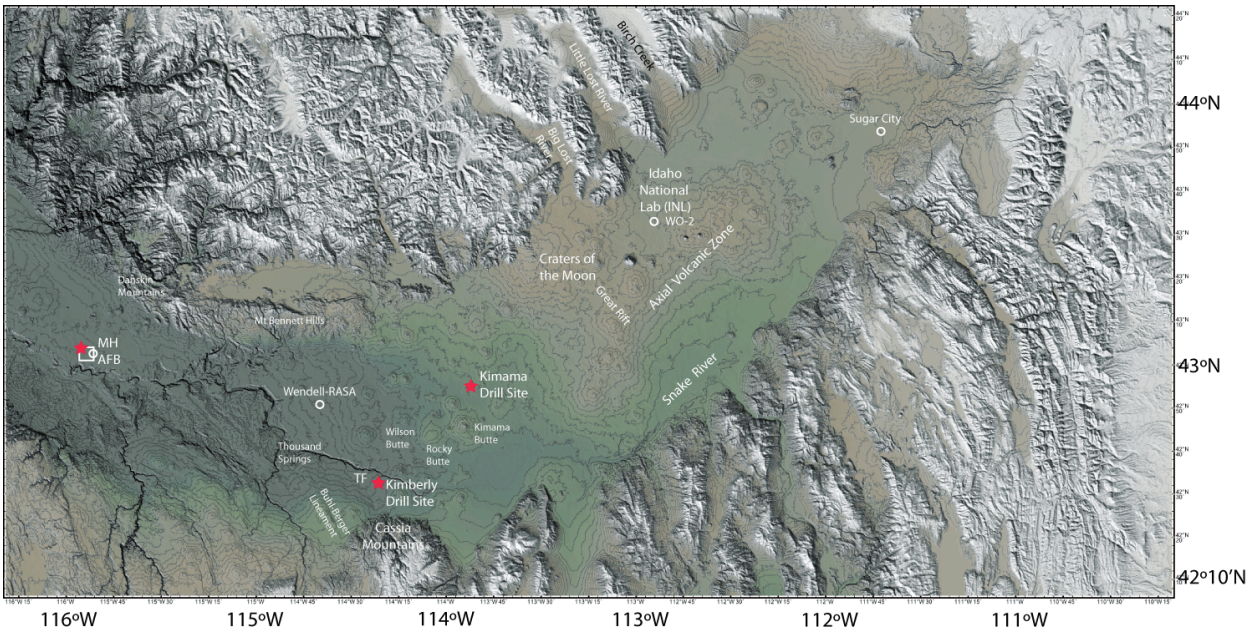

Figure 1-3. Shaded relief-topographic map of Snake River Plain, derived from NASA 10 m DEM data and contoured at 30 m intervals in GeoMap App. Lowest elevations are green, highest are white. DOE-funded drill sites shown as red stars; older drill sites noted as white circles. MH = Mountain Home, TF = Twin Falls. Features discussed in text labelled in white text.

Our objectives were to implement and test a range of geophysical and geologic approaches to geothermal exploration. The slim-hole exploration wells will be used to document thermal resources and to provide a lithologic and stratigraphic context for interpretation of the data obtained in Phase 1. A further objective was to establish the Snake River Plain as a viable target for the production of geothermal energy that is close to fast growing urban centers in southern Idaho and northern Utah. Because State, Federal, and private lands are available in close proximity within our study areas, commercial geothermal development will have a range of options for obtaining access to land and permits. Idaho has been ranked 3rd among western states for geothermal power production by the Geothermal Task Force of Western Governor's Association (WGA), who estimated that Idaho has 855 MW of near-term economic potential resources (Peterson et al 2004; Fleishmaann 2006; Neely and Galinato 2007).

Our project proceeded in three phases designed to explore innovative new exploration techniques in this greenfield setting. Phase 1 studies comprised map and data compilation, shallow seismic surveys, potential field surveys (gravity and magnetics), compilation of existing well data, and the construction of three dimension structure sections. Phase 2 comprised three deep (1.8-1.9 km) slim-hole exploration wells with a full suite of geophysical borehole logs and a vertical seismic profile to extrapolate stratigraphy encountered in the well into the surrounding terrain. Phase 3 focused on post-drilling science and data integration (Figure 1-3).

This project had as its focus an undeveloped "greenfield" region noted for its high heat flow and the common development of low-temperature passive geothermal, but which has not been developed for electrical generation. Impediments to geothermal exploration in this region have largely centered around the difficulty in imaging through the overlying cover of seismically opaque basalts that overlie much of the plain, the effects of the Snake River Aquifer on thermal gradients, and – despite the long-standing use of low temperature geothermal for passive space heating in two important districts (Boise and Twin Falls) – a fundamental lack of data on the depth and distribution of heat sources, up-flow zones, and basement structure.

Young volcanic active regions with high heat flow offer significant geothermal energy potential, and many of these areas have not been explored for economic resources. However, the application of traditional geophysical methods can be problematic -- especially in bi-modal volcanic terranes where young basalts impede seismic wave transmission and present challenges to detailed interpretations. These regions may also be poorly characterized structurally, since young volcanic rocks tend to blanket the underlying basement and mask structural trends and elements that are more easily observed in other areas.

CHAPTER 2:

PERMITTING AND ENVIRONMENTAL REVIEW

John W. Shervais
Utah State University, Logan, Utah

Lee Liberty
Boise State University, Boise, Idaho

ABSTRACT

Permitting and environmental review of the drill sites and adjacent areas was required by the National Environmental Protection Act. One of the drill sites was located on a Department of Defense facility (Mountain Home AFB) and was permitted under a Categorical Exclusions by the USAF. The other two sites (Kimama and Kimberly) were surveyed for cultural and biological assessment by USU Archeological Services, Incorporated. Their survey found no endangered species at either site, and no significant cultural artifacts. The Mountain Home AFB site was permitted under a categorical exclusion by the USAF, so we did not have to carry out NEPA studies at this site. Permitting for the seismic surveys was minimal, as they were conducted along county roads or privately-owned farm roads.

Permitting of geothermal test wells is done by the Idaho Department of Water Resources (IDWR). These regulations require that casing (¼" thick steel) be set to 10% of total depth, with 1" annulus, cemented and pressure tested. Wells must also be bonded and installation of a blow-out preventer is required when bottom hole temperatures exceed 100ºC.

The ease of permitting and environmental review were largely due to three factors: (1) the use of private land minimized NEPA requirements relative to what would be required on BLM or other Federal land; this holds also for university-owned state lands (Kimberly); (2) within the areas of interest, specific sites were selected based in part on prior disturbance, such that the impact of drilling operations was minimal; and (3) permits for the Mountain Home AFB site were handled by the USAF, which allowed us to focus our efforts on the KImama and Kimberly sites.

INTRODUCTION

A cultural and biological assessment of the Kimama and Kimberly drill sites was carried out by USU Archeological Services, Inc., in July 2010; their report is included as an Appendix to this report. The survey found no endangered species at either site, and no significant cultural artifacts. Both sites have been disturbed by previous activities and it was concluded that drilling operations would have no significant impact on the either location. The USAF provided DOE with a Categorical Exclusion (CX) for the site on Mountain Home AFB. All required NEPA permits for Mountain Home AFB were handled by the USAF and their environmental personnel.

Permitting for surface seismic investigations was obtained by Professor Lee Liberty of Boise State University. Seismic surveys were conducted along either county roads, or on privately owned farm roads. The following descriptions of the Kimama and Kimberly drill sites are taken from the USU Archeological Services report by Dr. Kenneth P. Cannon.

KIMAMA

The Kimama Drill Site is located in Lincoln County in the SW ¼ of Section 5, T7S, R23E and is on private property which is owned by the Robert and Arlene Jones Living Trust. The drill site at the intersection of the county road and a farm two-track. The drill site is on a slightly rolling upland at an elevation of approximately 4200 feet AMSL. The sandy loam soils have basalt cobbles on the surface. The site is surrounded by degraded sagebrush shrub lands. There are several sagebrush and rabbitbrush plants growing on the site, but a majority of the vegetation consists of weedy species.

The Kimama Townsite is the remains of a small railroad and agricultural town that was initially inhabited in the 1880s, with expansion in the 1910s and 1930s. The archaeological remains consist of five historic period features, as well as surface and subsurface deposits of historic debris. Remnants of the Kimama Townsite are present east of the county road, however, the drill site lies west of the County Road and will not impact any remnants of the townsite.

The Kimama Drill Site area was surveyed using an intensive pedestrian survey (15-m transects) that consisted of 1.14 acres. The survey included the drill site proper, plus the staging area. Scattered around the site were various modern materials associated with the farm operation. These included broken glass, blue tarps, rusted metal, pieces of various discarded farm equipment, concrete, plastic, and shotgun shells. None of this material is of historic age and consequentially not significant. There are several sagebrush and rabbitbrush plants growing on the site, but a majority of the vegetation consists of weedy species. There were no threatened or endangered species identified on the site or the areas in the immediate vicinity.

KIMBERLY

The Kimberly Drill site is located in Twin Falls County in the SW ¼ of Section 15, T10S, R23E and is on the property of the University of Idaho Research Center in a disturbed area that is used to park and store tractors. The area surrounding the drill site is currently planted in crops. The drill site is on an relatively flat upland terrace above an unnamed intermittent stream at an elevation of approximately 3900 feet AMSL. The sediments are sandy loams. The site is surrounded by agricultural fields. Alfalfa grows on the northern edge, corn to the east, and grass to the west. A paved road and sheds sit to the south. A majority of the site is bare soil. The few plants growing consist of weedy species and introduced crops.

The Kimberly Drill Site intensive pedestrian survey (15-m transects) consisted of 1.13 acres and included the drill site proper which is located in the area currently used for parking farm equipment surrounded by fields of corn and alfalfa. No cultural resources were found during this intensive pedestrian survey.

The Kimberly Drill Site is surrounded by agricultural fields with alfalfa on the northern edge, corn to the east, and grass to the west. A paved road and sheds sit to the south. A majority of the site is bare soil. The few plants growing consist of weedy species and introduced crops. Table 2 lists the species found on the Kimberly Drill Site. Plant names are those given by the USDA PLANTS database. There were no threatened or endangered species identified on the site or the areas in the immediate vicinity.

MOUNTAIN HOME

The Mountain Home Drill site is located in Elmore County on Mountain Home Air Force Base (AFB). The drill site (and the AFB) is on a rolling upland terrace above the Snake River, which lies 6 miles to the south. The drill site was covered with cheat grass, and lay just west of an area used to dump construction waste. The drill site was permitted under a categorical exclusion by the USAF, so we did not have to carry out NEPA studies at this site. In addition, the USAF obtained the drilling permit for this site.

SEISMIC SURVEY PERMITTING

Seismic surveys were carried out at all three drill sites. Seismic lines were laid out along existing county roads or along privately-owned farm roads. Permits were obtained from Lincoln and Elmore Counties for the Kimama and Mountain Home sites, respectively. A traffic control plan was not required for either county permit due to the non-stationarity of our seismic survey and the limited traffic and lane restriction along these rural roads. The Kimberly site did not require a county permit because seismic surveys were conducted along farm roads between agricultural fields. All of the roads accessed for the seismic surveys were either dirt or gravel and no damage occurred during the survey.

DRILLING PERMITS

Permitting of geothermal test wells is done by the Idaho Department of Water Resources (IDWR). The Idaho Department of Water Resources regulations require that geothermal test wells be cased to 10% of total depth with ¼" steel casing and a 1" cemented annulus. In order to drill below this casing with HQ-size rod, we needed to install 4½" diameter casing in a 6½" diameter hole. IDWR does not require a pressure test for a low-temperature well. However, once bottom hole temperatures reach 100^{o}C, the well is considered high-temperature by IDWR. At this point, the well must have a pressure test (IDWR requires 1000 psi) and an annular BOP must be installed. Should the well fail the pressure test, the well will be terminated since there is little opportunity to re-cement without considerable cost.

CHAPTER 3:

FIELD STUDIES AND DATA COMPILATIONS

John W. Shervais
Utah State University, Logan, Utah

ABSTRACT

Prior to the initiation of drilling, existing data were compiled to document the surface and subsurface geology of the study area, and to guide site selection, supplemented by field studies where appropriate. Geologic maps of the central and western Snake River Plain were compiled to document the distribution of volcanic vents and their eruptive products, and to evaluate the distribution and nature of mapped faults. Additional mapping of faults and lineaments was carried out in the Twin Falls area using NASA 10m DEM data and the program GeoMapApp. Geophysical data includes new gravity and magnetic maps produced from the most recent database, and published resistivity maps, which indicate basalt thickness. Subsurface data compiled includes ground water temperature maps, and lithologic logs of deep water wells throughout the region, along with water temperature data where available.

These data compilations were used to review and modify final site selections, to characterize the sites selected, and document the selection process. Detailed evaluations of these data are presented in the following chapter.

INTRODUCTION

The Snake River Plain has been studied in varying detail for decades, producing a vast store of information on its geology, hydrology, and volcanic features. These data form the basis for any new study of the SRP and can be used to guide further investigations. However, much of this data exists in the form of open file reports, state bulletins, and other 'grey' literature, or in databases that contain scans of paper records rather than digital data, making it more of a challenge to access and compile effectively. We compiled data from a wide range of sources, some of the more important being U.S. Geological Survey open file reports, USGS Water Resources Bulletins, maps published by the USGS and by the Idaho Geological Survey, USGS geophysical data bases for gravity and magnetic data, the Idaho Department of Water Resources (Water Resources Bulletins and water well logs), the Idaho State Department of Lands (oil and gas well logs), and unpublished mapping by the PI and his colleagues. Heat flow data were taken largely from the SMU database which reports heat flow for large numbers of wells in this area.

We also accessed data from published reports in scientific journals, which often present results in the form of figures and maps but not the primary data used to compile them. In these cases, we used these figures as representative of the primary data. In this chapter we discuss the data compiled and present summaries where appropriate. Detailed information on each site is presented in the following chapter.

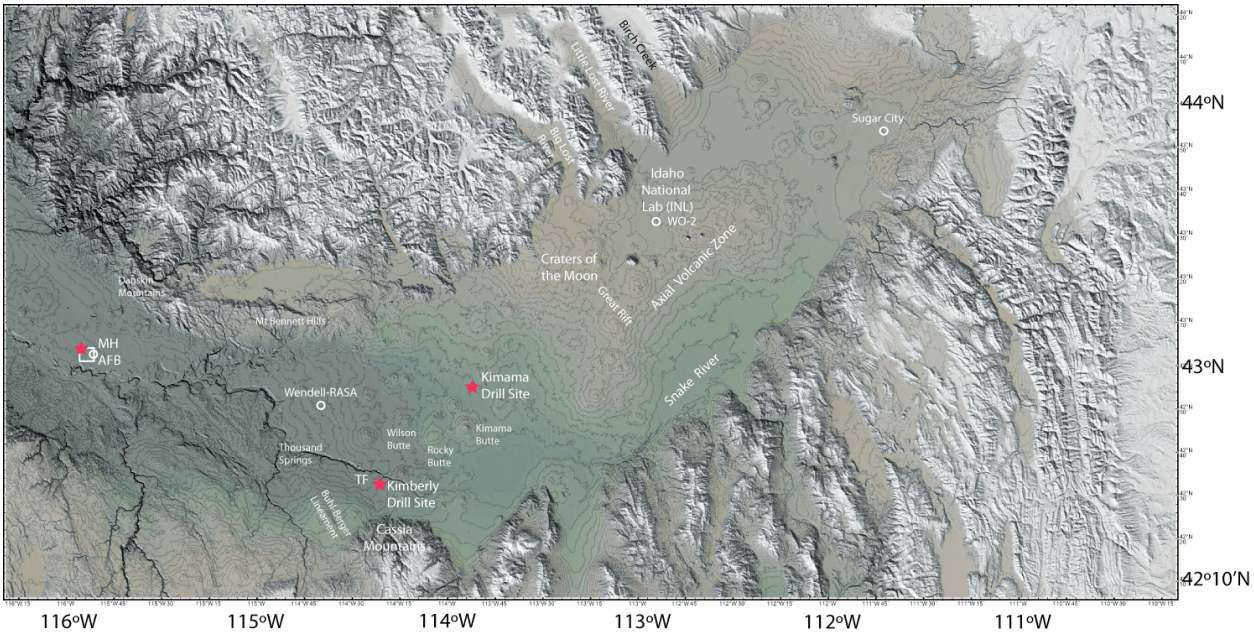

Figure 3-1. Topographic-relief map of southern Idaho showing location of the three drill sites (red stars), previous drill sites (white circles) and some of the features referred to in the text.

GEOLOGIC MAP AND DATA COMPILATION

Geologic Mapping

Geologic maps represent a first-order tool for evaluating the geologic history of an area and for understanding its structure and origin. In recent years, traditional geologic maps have been supplemented by high resolution digital topography that allows the surface manifestations of subsurface features (particularly faults) to resolved in detail. In addition, in volcanic terranes like the Snake River Plain, volcanic vents form conspicuous features that may be mapped remotely and then field checked.

Geologic mapping in the central SRP northeast of Twin Falls has been carried out over the last decade by the PI and his students, and by personnel of the Idaho Geological Survey, resulting in the publication of several geologic maps at 1/24000 or 1/100,000 scales *(Kauffman et al, 2005a, 2005b; Shervais et al, 2006c, 2006d; Cooke et al, 2006a, 2006b; Matthews et al., 2006a, 2006b)* and unpublished thesis maps *(Cooke, 1999; Matthews, 2000; Hobson, 2009; DeRaps, 2009).* This mapping ties into published mapping by the US Geological Survey in the Craters of the Moon 1/100,000 sheet *(Kuntz et al 2007)* and into unpublished mapping by the PI and his graduate students east of longitude 114ºW in the Sid Butte, Senter Butte, Kimama Butte, and Black Ridge Crater 1/24000 quadrangles. The PI prepared a field guide to this area for the 2005 national meeting of the Geological Society of America and led a field trip based on this guide (*Shervais et al., 2005*). Extension of this mapping into the Lake Walcott 1/100,000 sheet was carried out on a reconnaissance basis, using existing geologic maps and new mapping by the PI and his students. Finally, this mapping was compiled into a single map sheet that covers the entire central SRP (Figure 3-2).

The principal result from the geologic mapping is to show that Quaternary volcanism is widespread throughout the central SRP, with young vents occurring both along the margins of the plain and near its center. Nonetheless, young volcanic vents are dominant within the axial volcanic zone. While some vents with similar ages may align parallel to the NS-trending volcanic rift zones defined by *Kuntz (1992; Kuntz et al 2002),* other young vents are as likely to define other alignments, e.g., Wilson Butte and Rocky Butte, which are aligned ~WNW and have nearly identical ages and compositions (Figure 3-2). These trends are often highlighted on regional magnetic maps, since basalts with similar ages will commonly have the same magnetic polarity, resulting in striped magnetic alignments.

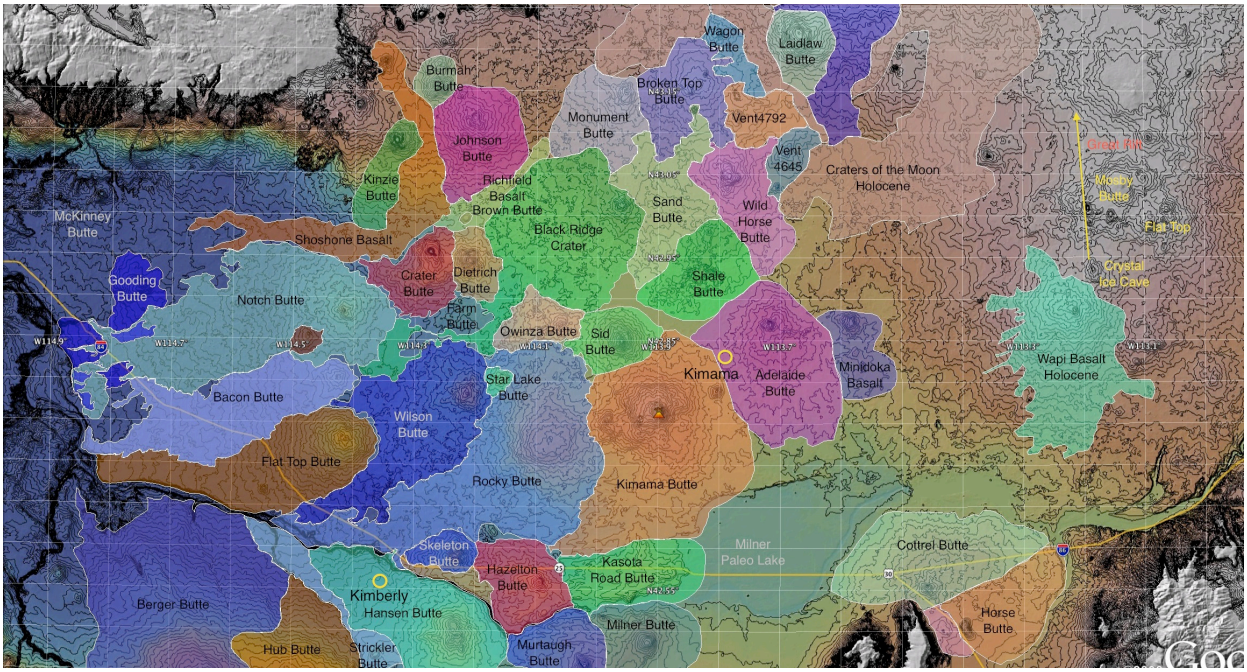

Figure 3-2. Geologic map compilation for the central Snake River plain. The youngest volcanoes are associated with Craters of the Moon and the Great Rift (eastern quarter of map). Pleistocene volcanism dominates along the central volcanic axis of the plain, while older, largely Pliocene volcanoes are exposed along the margins. Source vents are typically small shield volcanoes and are commonly characterized by summit craters; cinder cones are relatively minor and small. Sources listed in text.

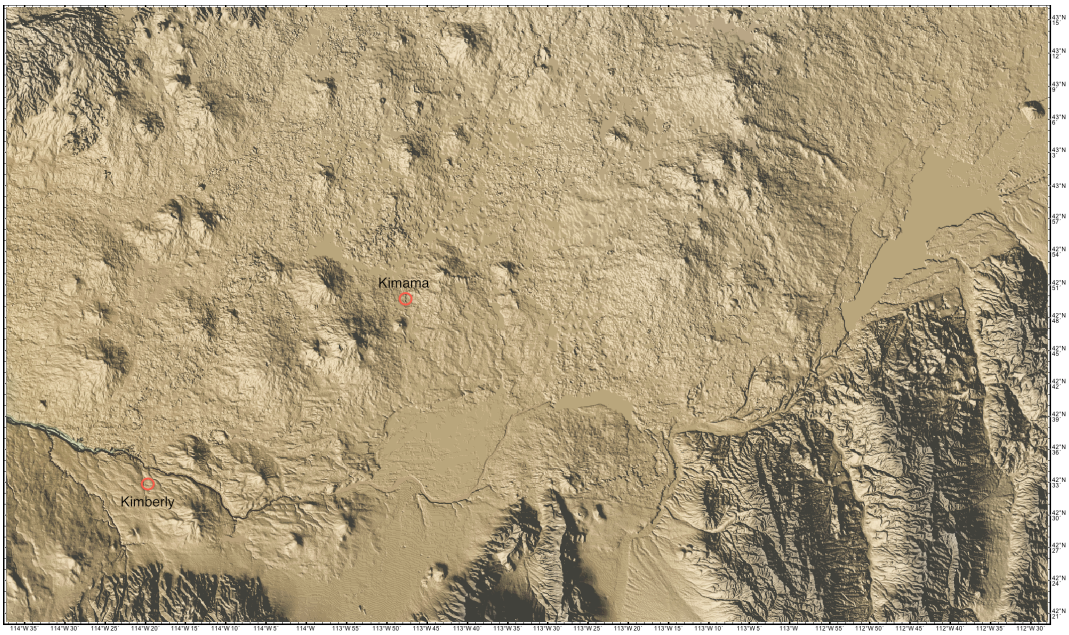

Figure 3-3. High-resolution (10 m) digital topography of central Snake River Plain, showing concentration of volcanic vents along the central axis of the plain. The Snake River is confined to a shallow moat along the southern margin of the plain, where it has been periodically ponded by lava dams to form lake deposits (smooth, flat topography). Kimberly and Kimama drill sites shown as small red circles.

Basaltic Vent Distribution

Young basaltic volcanism tends be concentrated along the axial volcanic high, with older vents dominantly exposed along the margins of the plain (Figures 3-2, 3-3). Unlike the eastern plain, however, this trend does not continue to the SW. Northwest of Twin Falls, vents become less common and the basalt flows thin out and become intercalated with fluvial and lacustrine sediments. This is well-documented in the Wendell-RASA well (342 m), which has 122 m of young Quaternary basalt (<400 ka) separated from older basalts deeper in the well by 60 m of sediment *(Whitehead and Lindholm, 1985).* The older basalts (1.0-4.5 Ma) are themselves underlain by more sediment. Basalt flows also thin towards the margins of the plain, where they may sit directly on rhyolite or on sediment horizons that rest on rhyolite. This is in contrast to the 1500 m deep WO-2 well at the INL site, which contains ~1200 m of basalt with minor intercalated sediments on top of 300 m of rhyolite, with no intervening sediments and no major sediment horizons within the basalt *(Morgan, 1990; Hackett et al 2002; William Hackett, unpublished well log).* The concentration of young Quaternary volcanism near the Axial Volcanic Zone, and the nexus of volcanic rift zones, which trend NNW and EW makes this region a high priority for geothermal exploration (Shervais et al 2005, 2006a, 2006b).

Vent concentrations are highest between the Great Rift and the Twin Falls-Shoshone area (Figures 3-1, 3-3), so our model suggests that this region, centered around our Kimama drill site, is more likely to encounter high temperature resources at depth than areas lying farther west; the Great Rift itself lies within Craters of the Moon National Monument, and is off-limits to exploration.

Structural Mapping

Regional reconnaissance mapping of structural trends in the Twin Falls-Kimberly area has been carried out by the PI using NASA 10 m DEM data in the software GeoMapApp (*Goodwillie and Ryan, 2009*). These data are used to produce shaded relief maps and topographic maps with 10 m contour intervals that are more detailed than published 1/24,000 topographic maps, and which reveal structural lineaments more clearly than topographic maps or air photographs (Figure 3-4). Mapping was done in GeoMapApp so that sun position and sun angle could be varied to highlight structures in different orientations, and then compiled onto a fixed base map. These lineaments reflect in part western SRP fault trends (WNW) and in part more northerly trends that may represent a transition between the western SRP trends and the NS-oriented Basin and Range trends. This mapping will be discussed in more detail under the Site Selection discussion for Kimberly.

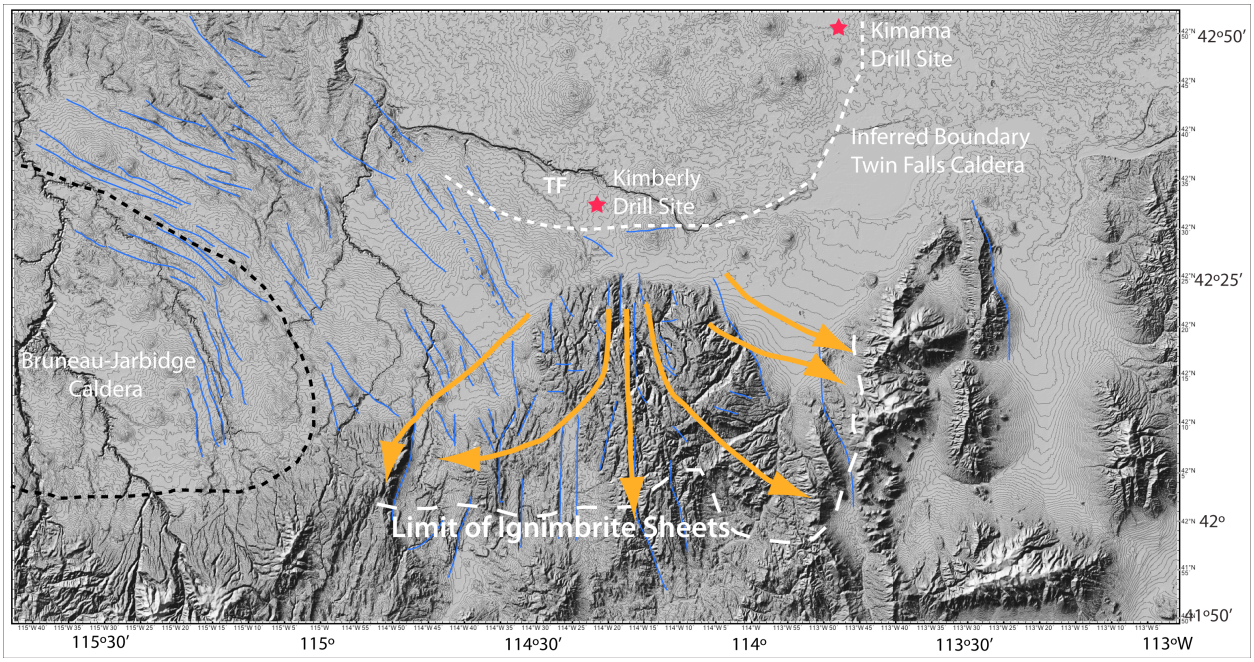

Figure 3-4. Shaded relief map of Twin Falls area, with 10m contours calculated from NASA 10 m DEM data using GeoMapApp. Blue lines show faults mapped from lineaments in 10 m data. Yellow arrows show directions of ashflow sheets in Cassia Mountains, mapped by McCurry et al 1996, with southern extent of ash sheets marked by long-dash white line. Southern margin of the Twin Falls caldera complex, inferred from regional Bouger gravity anomaly, shown with dashed white line. Drill sites marked with red stars; TF = City of Twin Falls.

Geologic Mapping Western Snake River Plain

We have also prepared geologic maps of eight 1/24,000 quadrangles in the Mountain Home area for publication by the Idaho Geological Survey (Figure 3-5). These quadrangles, which were mapped prior to this project, have been combined into a single map sheet in Arc GIS for publication. This map covers Mountain Home AFB and a large part of the surrounding region.

In the western SRP around Mountain Home, digital topography derived from NASA 10m DEMs and unpublished mapping by Shervais document the concentration of volcanic vents (Figure 3-5). All of the volcanoes are younger than about 1.8 Ma (Pliocene-Pleistocene), with the youngest vents (<750 ka) characterized by high K_2O and MgO (Shervais and Vetter, 2009). Mapping by Shervais (Shervais et al 2002) documents two groups of faults, many of which can be readily seen on the digital topography as steep fault scarps (Figure 3-6). The dominant fault system trends ~N50W, essentially parallel to the range front fault system, and likely related to the same stress fields that produced the range front faults and the overall structure of the western SRP graben. The secondary fault system trends ~N80W, oblique to the the trend of the graben and to the range front fault system. However, these faults are roughly parallel to the trend of gravity anomalies discussed in the next section, and may represent a surface expression of the fault system that borders these buried structures.

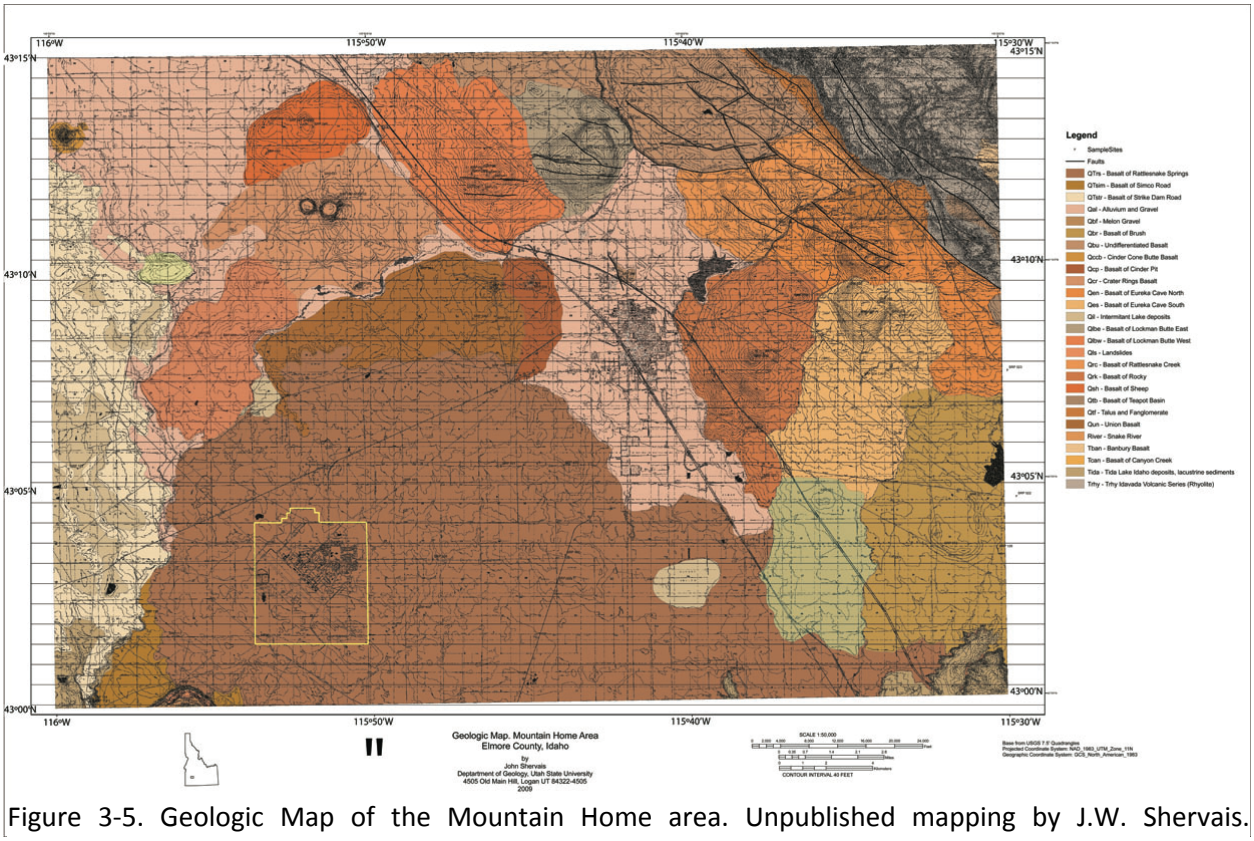

Figure 3-5. Geologic Map of the Mountain Home area. Unpublished mapping by J.W. Shervais. Mountain Home AFB outlined in yellow. Diagonal lines thru central area are the railroad and instate highway. Primary maps at 1/24,000 scale.

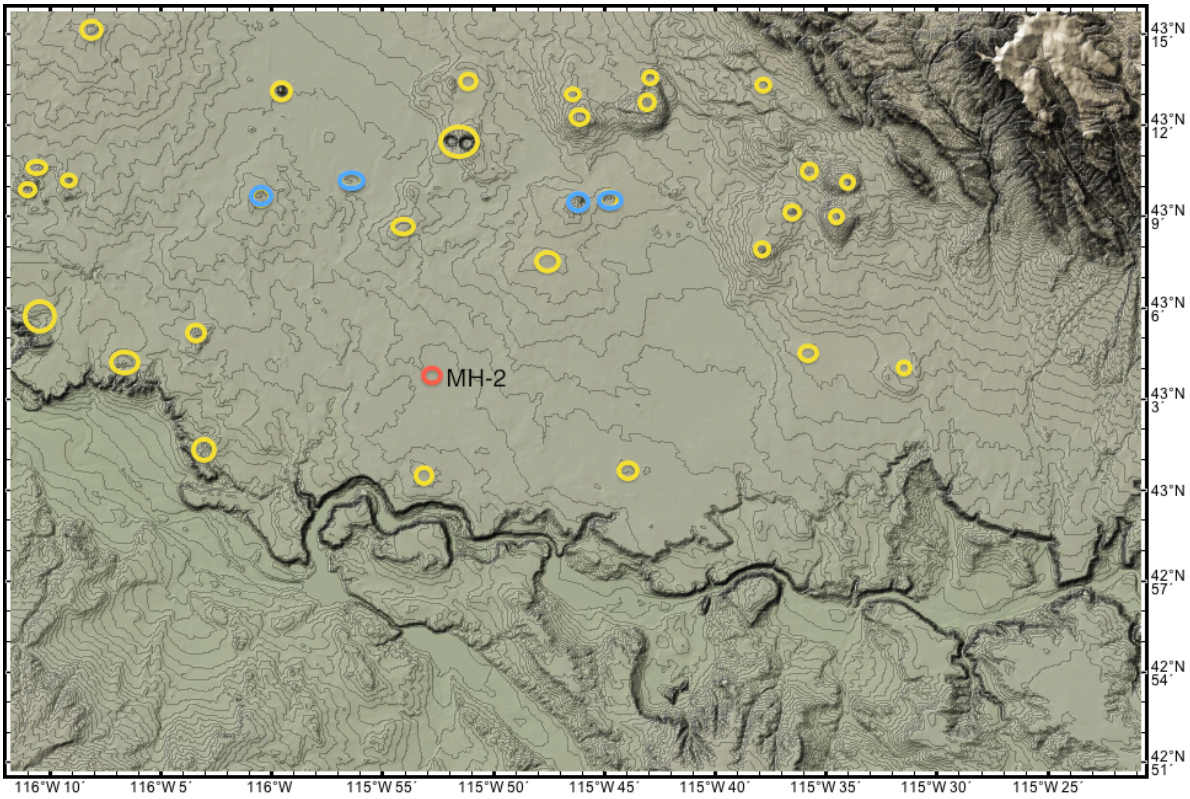

Figure 3-6. Digital topographic map of area around Mountain Home AFB, showing location of drill hole MH-2. Also shown are locations of Pliocene-Pleistocene tholeiitic basalt vents (yellow circles), and Pleistocene high-K basalt vents (blue circles).

Groundwater Temperatures

Water well and shallow geothermal well data were compiled from drillers logs (off of the State of Idaho Department of Water Resources website) and from previous compilations published by the Idaho Department of Water Resources and US Geological Survey (*Street and deTar, 1987; Lewis and Young, 1989; Baker and Castelin, 1990*). Well logs are especially useful in the Twin Falls region because of the large number of shallow geothermal wells, which are generally deeper than water wells and are more likely to have temperature data. These data are discussed later in this chapter. In the area around Kimama, groundwater data were compiled and analyzed by *Smith (2004), McLing et al (2002), Johnson et al (2000),* and *Rohe et al (2002).* Though we do not have access to the database that supports these publications, the figures in *Smith (2004)* are sufficiently detailed to allow us to use their results here.

The Idaho National Laboratory site is thoroughly documented by numerous deep drill holes that penetrate the Snake River Aquifer. Figure 3-7 show temperature profiles for several deep wells that intersect both the upper and lower boundaries of the aquifer, as indicated by inflections in the temperature gradients. Gradients within the aquifer are nearly isothermal,

indicating advective heat transfer, while gradients above and below the aquifer are steep, indicating conductive heat transfer.

These inflections bracket the aquifer thickness, which in map view defines a deep channel of cold water that transects the INL site from northeast to south (Figure 3-7b), fed by influx from the Big Lost, Little Lost, and Birch Creek rivers. The deepest lower boundary of the aquifer in this channel is 500-550 m, but most wells show a lower contact at 250-350 m depth.

Smith (2004) published a compilation of groundwater temperatures for the eastern and central SRP that documents both the flow of water through the system, and its change in temperature as it flows (Figure 3-8). Groundwater temperatures are low at the eastern margin of the SRP, and are low along the margins where major river systems (Snake and Wood Rivers) dominate the groundwater system. Temperatures are high along the central axis of the plain, coincident with the axial volcanic high (Figure 3-8a). Temperatures increase progressively from east to west along the axis, consistent with heating from below by a significant thermal anomaly. Inferred flow patterns for subsurface water suggest that flow is greatest along the margins (corresponding to the primary river drainages), and relatively low along the central axis, allowing the water heat as it flows west (Figure 3-8b).

The change in groundwater temperatures, from about 8.5ºC at its entry into the aquifer to 17ºC at the western end of the axial flow zone, requires significant heat flux from below. A model for this was presented in Smith (2004). This model postulates an influx of cold water at the NE end of the SPR that becomes progressively heated as it flows to the SW (Figure 3-9). A heat flux of ~110 mW/m2 is postulated to provide the heat needed to elevate groundwater temperatures, based on observed sub-aquifer heat flow. Blackwell et al (1992) calculate that a heat flux of 190 mW/m2 is required by thermal mass balance calculations.

Thermal gradients and heat flux are discussed in more detail later in this chapter.

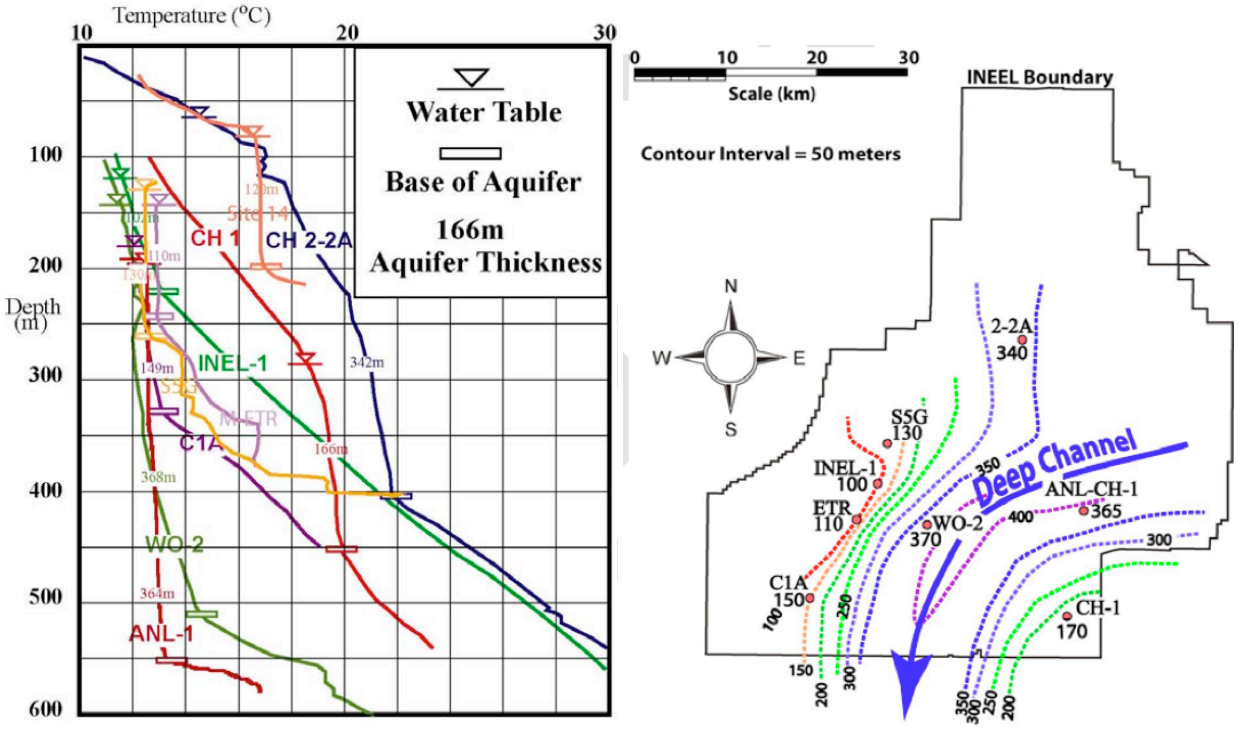

Figure 3-7. (a) Left: Thermal profiles in deep wells at the INL site. Upper inflection from conductive to isothermal represents top of the Snake River aquifer; lower inflection from isothermal to conductive represents the base of the aquifer. (b) Right: Aquifer thickness and the lower inflections define a deep channel that underlies the INL, caused by the influx of cold groundwater from the Centennial Mountains to the north. This cold water plume flows SW along the northern margin of the SRP. From Smith 2004.

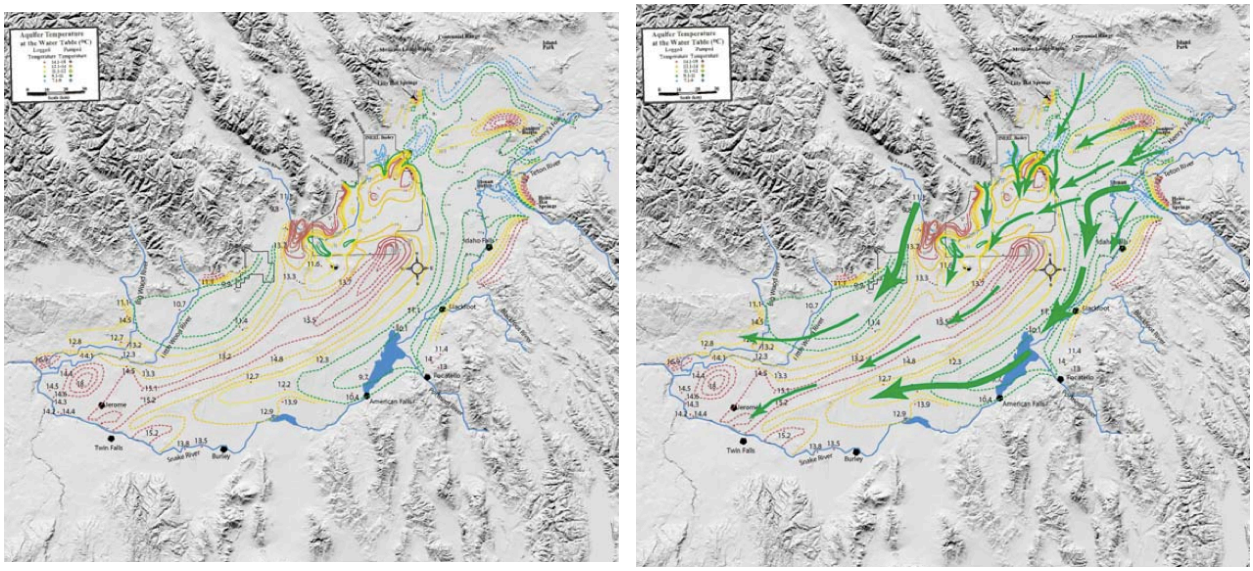

Figure 3-8. Groundwater temperatures and inferred flow paths, from Smith 2004. (a) groundwater temperatures contoured from cold (blue, green) to warm (yellow, red). Note axial zone of high groundwater temperatures that correspond to the central volcanic axis of the SRP; (b) Inferred flow paths for cold water in subsurface.

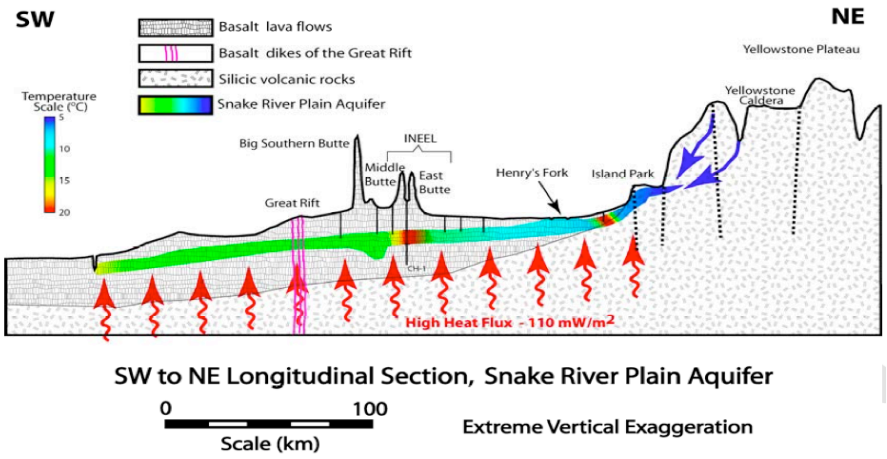

Figure 3-9. Model of groundwater flow under central axis of Snake River Plain, from Smith 2004. Cold water influx from mountains is warmed from below by conduction of high geothermal gradient, and by advection of heat in thermal fluids. Water becomes progressively warmer as it moves westward long the volcanic axis.

GEOPHYSICAL DATA COMPILATION

Gravity data for the State of Idaho *(Kucks 1999)* were used by Liberty to produce regional Bouguer anomaly maps for both the central SRP north of Twin Falls and for the western SRP near Mountain Home. The gravity database was compiled within Arc GIS and maps were produced using a gradational color scale to indicate relative anomalies. The maps were plotted with the station locations indicated so that the density of data stations relative to the anomalies could be assessed. In addition to the Bouguer anomaly maps, Liberty produced "upward continued" gravity models for the western SRP that emphasized mid- to lower crustal structures and minimized the affects of density variations in the shallow crust (e.g. the presence and thickness of basalt flows).

Gravity maps for the central and eastern SRP are dominated by a pronounced linear gravity high off to the west which represents the eastern continuation of the western SRP gravity high (see below). Low gravity along the margins represents sediment filled basins, rhyolite ash flows, or Paleozoic carbonates (Figure 3-10). The roughly circular to ovoid gravity modest high north of Twin Falls (red circle in Figure 3-10) is interpreted to represent a buried rhyolite eruptive complex, with an outer "moat" that has been filled by higher density basalt flows, and a lower density central peak that likely represents resurgent rhyolite domes or flows. As shown in Figure 3-10, both the Kimama and the Kimberly sites lie on the rim of this circular feature.

Magnetic maps of the central and eastern SRP are characterized by a striped magnetic texture that is oriented approximately East-West north of Twin Falls (in the central SRP) and ~N50-55E farther to the east (Figure 3-8). This texture is interpreted to represent bands of different age basalt, where relatively young flows (<780 Ka) have positive magnetic anomalies (red stripes) while the older Pleistocene and Pliocene basalts have negative magnetic anomalies (blue stripes). Young basalts are dominant along the axial volcanic zone, positive (red) anomalies rarely extending outside the plain (Figure 3-11).

Bouguer gravity maps of the entire western SRP produced by Lee Liberty (Boise State University) document a pronounced gravity high which trends obliquely across the trend of the SRP graben (Figure 3-12). This is most evident in Figure 3-9a, which is a simple Bouguer gravity map. This image is refined using an upward continuation of the gravity from 5 km depth, removing surface effects and high-lighting the deep seated anomalies (Figure 3-12b). This map further delineates the oblique gravity high, which we interpret as a faulted horst block within the overall WSRP graben. The city of Mountain Home lies on the northern margin of this anomaly, while Mountain Home AFB lies along its southern margin. This is shown clearly in Figure 3-13, which shows a close-up of the Bouguer anomaly map for this area.

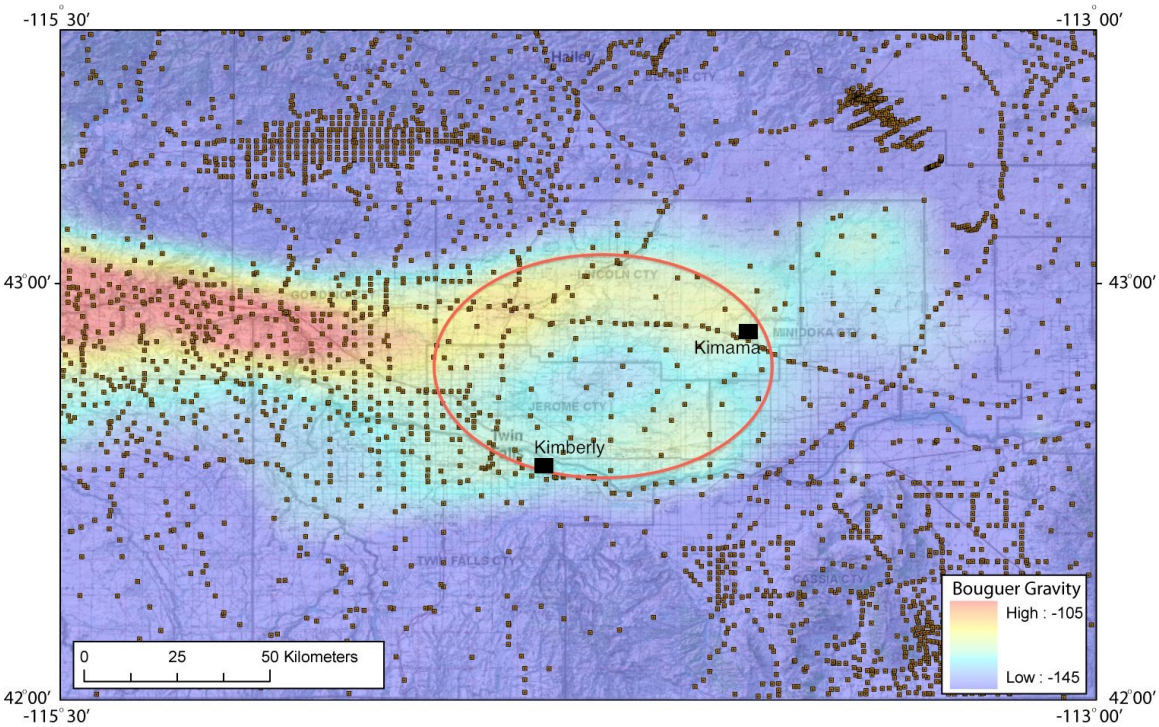

Figure 3-10. Bouger gravity map of central SRP showing ovoid anomaly of high gravity thought to represent the Twin Falls eruptive complex, now buried beneath 2+ km of basalt. Location of Kimama and Kimberly drill sites shown as black boxes. The circular structure of high gravity may represent infilling of a caldera moat by more dense basalt; resurgent rhyolite domes with lower density in the center of the structure may prevent this infilling and result in the central peak of lower gravity.

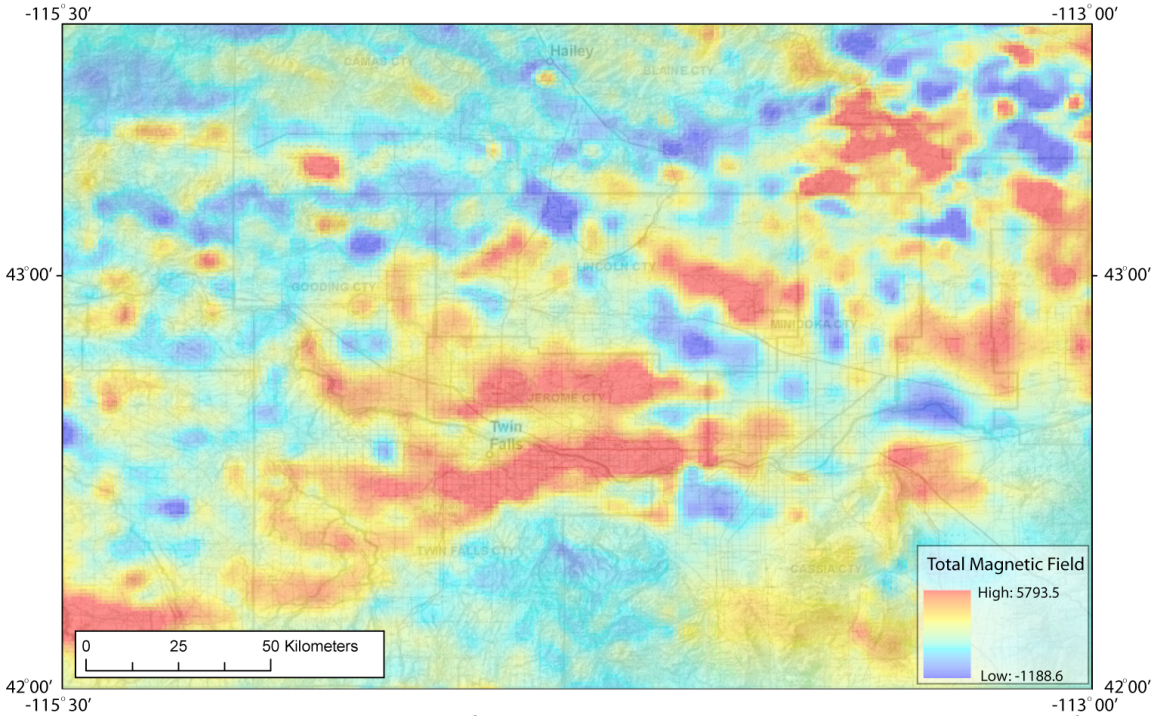

Figure 3-11. Magnetic anomaly map of central SRP near Twin Falls. Linear anomaly belts reflect ages of surface volcanics, with young (normal polarity) vents dominant along central axis. Note the ~EW trends near Twin Falls, similar to fault trends in western SRP.

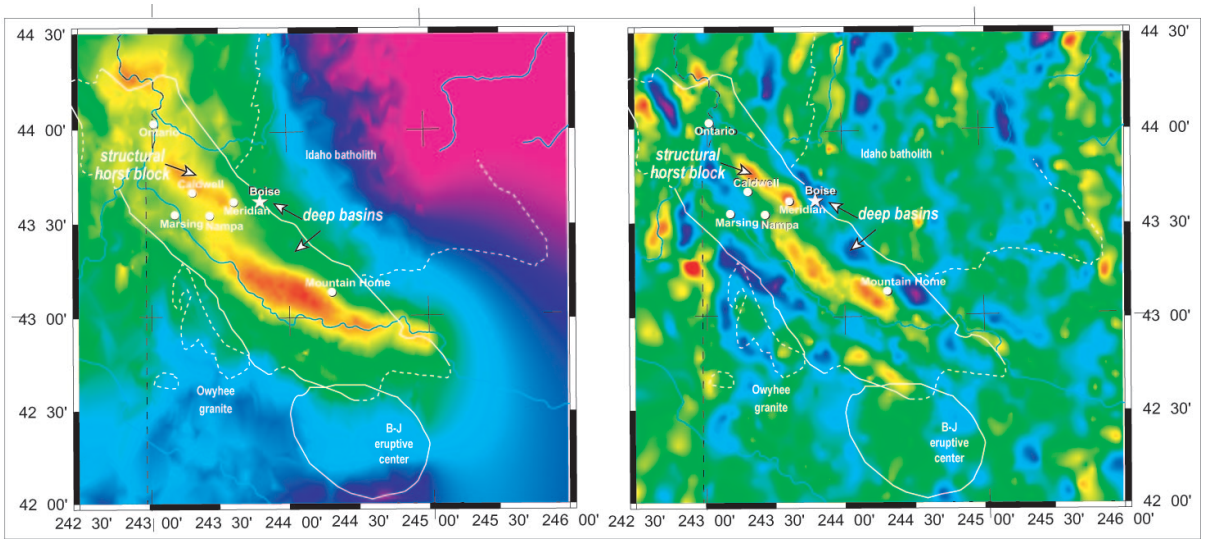

Figure 3-12. (a) Bouguer gravity anomaly map and (b) upward continued Bouguer gravity map, of the western Snake River Plain. The upward continued map emphasizes deeper crustal features, including deep basins along the margins of the WSRP and a prominent gravity high trending obliquely to its axis; we interpret this positive anomaly as a buried horst block.

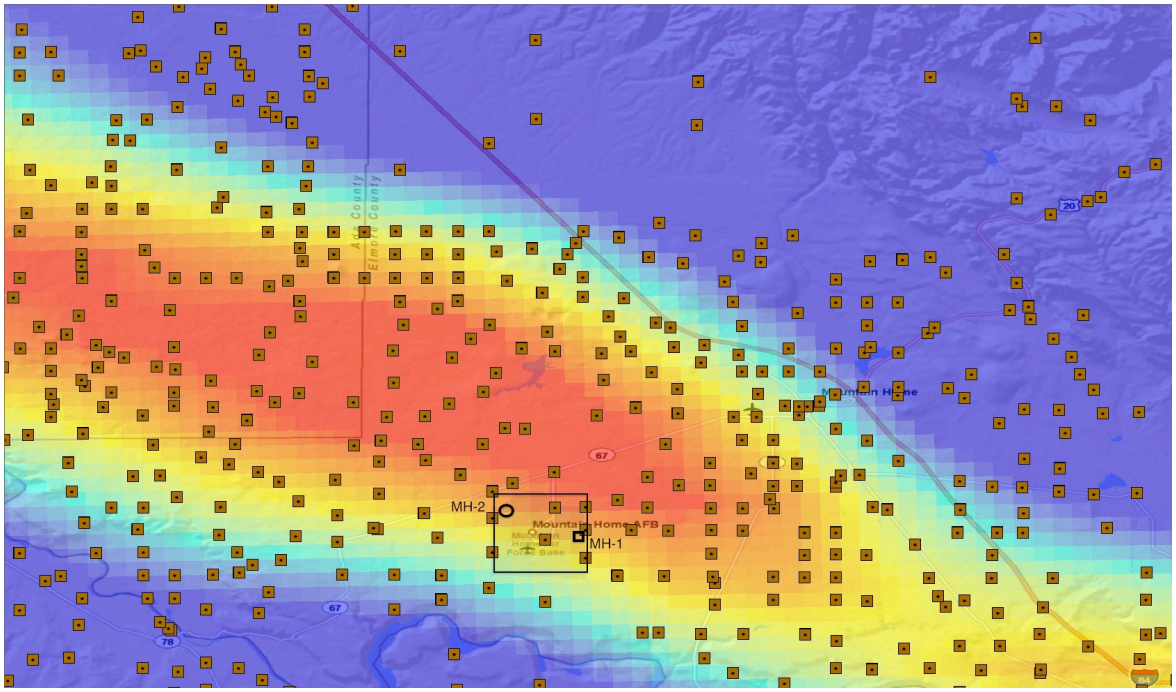

Figure 3-13. Bouger gravity map of the western SRP around Mountain Home AFB. Mountain Home AFB is located on the southern margin of a pronounced gravity high that trends across the SRP graben at an oblique angle; this trend is similar to that observed in the N80W fault system on the surface. Black box outlines approximate location of Mountain Home AFB; black circle and square represent locations of drill holes MH-2 (this project) and MH-1, respectively.

Lindholm (1996), in a major study of the Snake River Aquifer, estimated the thickness of Quaternary basalts in the Snake River Plain using well logs and resistivity surveys (Figure 3-14). Resistivity is low in water saturated rocks, and high in older rocks with little pore space or permeability. The Kimama drill site sits on the axial volcanic high, in an area with a projected Quaternary basalt thickness of 3000-4000 feet (~1.0 to 1.2 km). Kimberly is known to sit on a thin basalt cover over rhyolite, based on exposures in the Snake River Canyon, and Mountain Home is known to sit on thin basalt cover (<200 m) over lake sediments, based on well logs from MH-1 test well and on exposures south of the drill site.

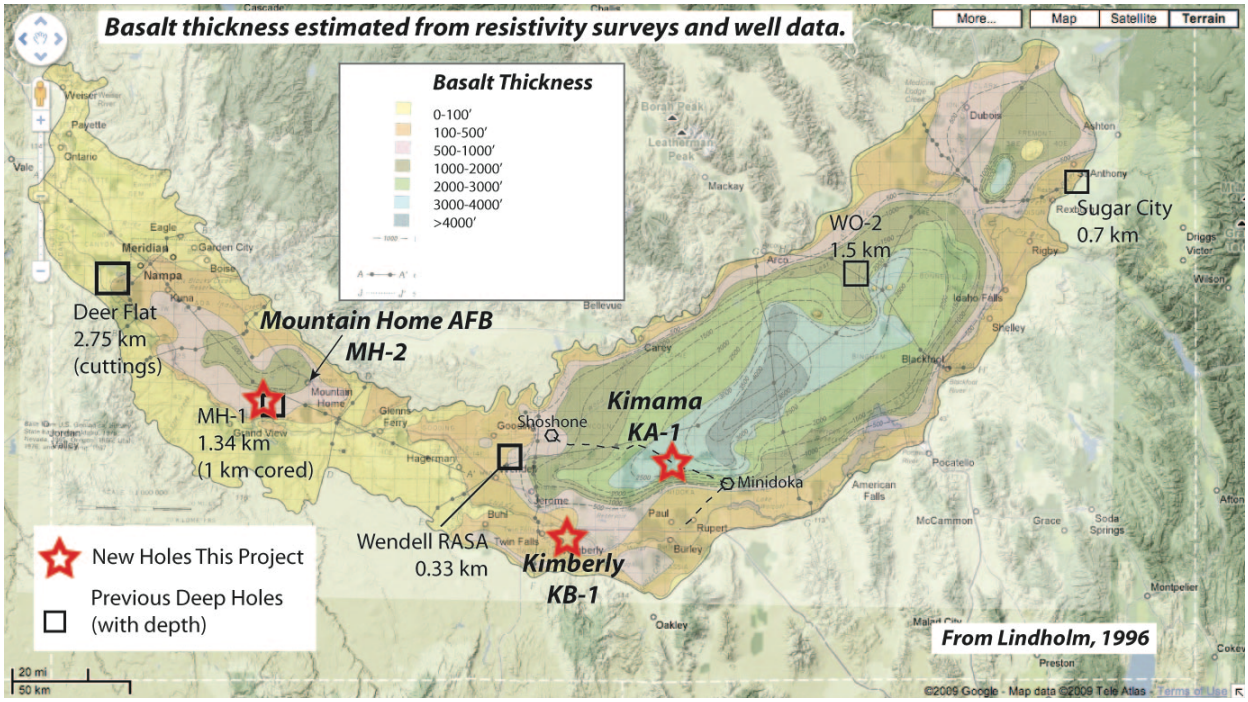

Figure 3-14. Estimated thickness of Quaternary basalt in the Snake River Plain, based on well logs and resistivity surveys, from Lindholm, 1996, superimposed on a base map of terrane from Google Maps. Also shown are locations of holes drilled for this project, and select deep holes drilled in the past.

HEAT FLOW AND GEOTHERMAL GRADIENT STUDIES

The Snake River Plain in southern Idaho represents the track of deep-seated mantle hotspot that has thinned the lithosphere and fueled the intrusion of up to 10 km of basalt into the lower and middle crust. The heat from these intrusions, and from rhyolites formed by the basalt, drives the geothermal gradients and high heat flow observed in deep drill holes from throughout the Snake River Plain (Blackwell 1978, 1980, 1989; Brott et al 1976, 1978, 1981; Lewis and Young 1989). Blackwell and the SMU Geothermal Laboratory (Blackwell, 1989; Blackwell et al 1992) have carried out geothermal gradient measurements and heat flow calculations in the Snake River Plain for decades, and their database is the most complete available.

Heat flow in the SRP tends to be high along the margins of the plain (80-100 mW/m^2-s) and low when measured in shallow drill holes along the axis of the plain (20-30 mW/m^2-s). However, deep drill holes (> 1 km) in the axial portion of the plain are characterized by high heat flows and high geothermal gradients below about 500 m depth (Blackwell 1989). This discrepancy is caused by the Snake River aquifer – a massive aquifer system fed by the Lost River system north of Idaho Falls that extends under the plain and emerges at Thousand Springs, Idaho. Thermal gradients through the aquifer are static until the base of the aquifer is reached, then rise quickly at deeper levels in the crust (e.g., Blackwell 1989; Smith 2004). Below the aquifer along the axis of the plain, heat flow values are comparable to heat flow values along the margins of the plain or higher (75-110 mW/m^2-s; Blackwell 1989). Bottom hole temperatures for wells along the margins of the plain near Twin Falls are typically around 30-60ºC at 400-600 m depth (Baker and Castelin 1990) and as high as 120ºC at 2800 m depth in the axial region of the plain (Blackwell 1989). This data are discussed on more detail below.

Average surface heat flow along the margins of the eastern SRP is approximately 100 ±15 mWm^{-2} for all groupings. Sub-aquifer heat flow measured in the deep wells USGS G2A and INEL-1 is ~107-110 mWm^{-2} -- roughly equivalent to that found on the margins, where the aquifer has little or no influence (Blackwell et al 1992, pages 40, 49). Further, groundwater temperatures along the central volcanic axis become progressively elevated from ~8ºC along the margins at the eastern end of the SRP, to temperatures >15ºC west of the Great Rift. The heat required to change groundwater temperatures in aquifer from 8ºC to 14.5ºC = 287.3 MW. In contrast, surface heat loss above the aquifer is only ~42.3 MW. Thus the total heat flux from below the aquifer is 329.6 MW. The heat flow required a to achieve this flux = 190 mWm^{-2} (Blackwell et al 1992, page 51).

The western SRP is also characterized by high geothermal gradients. This is illustrated best by two deep wildcat oil wells drilled along the margins of the western plain. The Bostic 1A well was drilled on the north side of the western plain, east of Mountain Home. It produced a bottom hole temperature of 195ºC at 2900 meters. It is characterized by high heat flow, and a positive geothermal gradient to TD. This well was later studied by a group from Los Alamos National Lab as part of the Hot Dry Rock Project (Arney 1982; Arney et al 1982, 1984). The 2900 meter deep Anschutz Federal well was drilled on the south side of the graben. This well achieved a high temperature of 125ºC, with the high temperatures at shallow depths but not at deeper levels, giving it a negative gradient at depth.

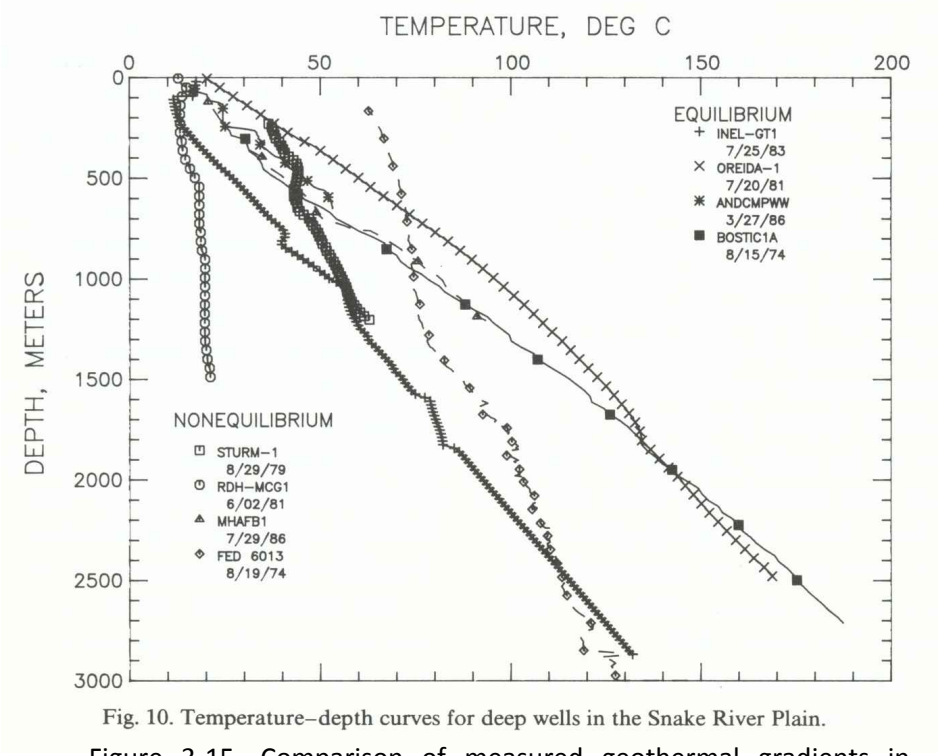

Figure 3-15. Comparison of measured geothermal gradients in selected deep wells from the Snake River Plain, including both equilibrated and unequilibrated wells. From Blackwell et al 1992.

Geothermal gradients for a selection of deep wells in the SRP are shown in Figure 3-15. The highest thermal gradients are observed in two western SRP wells: Bostic 1A and Oreida-1; these steep continuous gradients are essentially conductive and show no sign of convective cooling. The 1986 geothermal test well on Mountain Home AFB (MH-1) follows a similar steep gradient but terminates at 1300 m depth (4404 feet). The MH-1 gradient is non-equilibrium and thus can be expected to increase in temperature over time at depth.

Anderson Camp (ANDCMPWW) is the closest well to Kimberly; it follows a high temperature gradient similar to Bostic 1A and MH-1, though it is much shallower. This led us to expect that Kimberly to have a higher gradient and higher bottom hole temperatures because it lies south of the river and outside the influence of the Snake River aquifer.

WELL LOGS

All water wells drilled in the State of Idaho are required to submit drilling and cutting logs to the Idaho Department of Water Resources, which maintains a website for accessing this data. The data are simply scans of paper logs filled in by hand, which must be transferred manually to LogPlot® in order to evaluate the collated data. Data quality is variable, from actual identification of rock types to "hard red rock" and "soft brown rock," with all gradations in between. Nonetheless, most logs distinguish basalt, rhyolite, and sediment of various kinds (sand, mud), so it is possible to get a general sense of local stratigraphy from these logs. In addition, many of the logs contain information on water temperature, especially for wells drilled in the Twin Falls Geothermal District -- many of which are drilled for passive space heating.

Well log data for oil and gas wells are maintained by the Idaho State Department of Lands. These data are more complete and of higher quality, but none of the wells were close enough to our target areas to provide useful guidance.

We focused our efforts on water wells around the axial volcanic zone (near Kimama) and those in the Twin Falls Geothermal District (near Kimberly). Data searches were conducted section by section, as larger searches (e.g., by county) returned too much data, or truncated data records. Data searches in the Kimama area proved to be unhelpful, because there are few water wells in this area (much of it unfarmable), and because few wells exceed 300-400 feet in depth. The deepest wells near Kimama for which records are available are ~700 feet deep, and almost entirely in basalt (as expected). Data searches in the Twin Falls area were more fruitful, as there a many passive geothermal wells that range in depth from ~1400 to 2200 feet (Figure 3-16). These well logs establish depth to the basalt-rhyolite contact, and show that significant sedimentary interbeds are present within the rhyolite section. They also establish a water temperature of ~37-42ºC these wells, at depths up to 2200 feet (Figure 3-16), suggesting that significantly higher temperatures might be encountered at depth (though they were not!).

In the end we had only two wells that provided deep records along the axial volcanic zone: the 5000 foot (1500 m) WO-2 well at the Idaho National Laboratory, and the 1125 foot (343 m) Wendell RASA (Regional Aquifer Study Area) well near Wendell, Idaho (Figure 3-1). Neither well is particularly close to the Kimama drill site. The 1500 m WO-2 well is most similar what we expected to encounter: about 1200 m of basalt with minor sediment intercalations, bottoming

into 300 m of rhyolite. The Wendell RASA well section consists of two basalt sections separated by a fluvial sediment layer, all sitting on older sediments (Figure 3-17). The estimated age of the lower basalts is circa 4.5 Ma, based on paleomagnetic reversals, comparable to some of the oldest basalts exposed on the surface in this area.

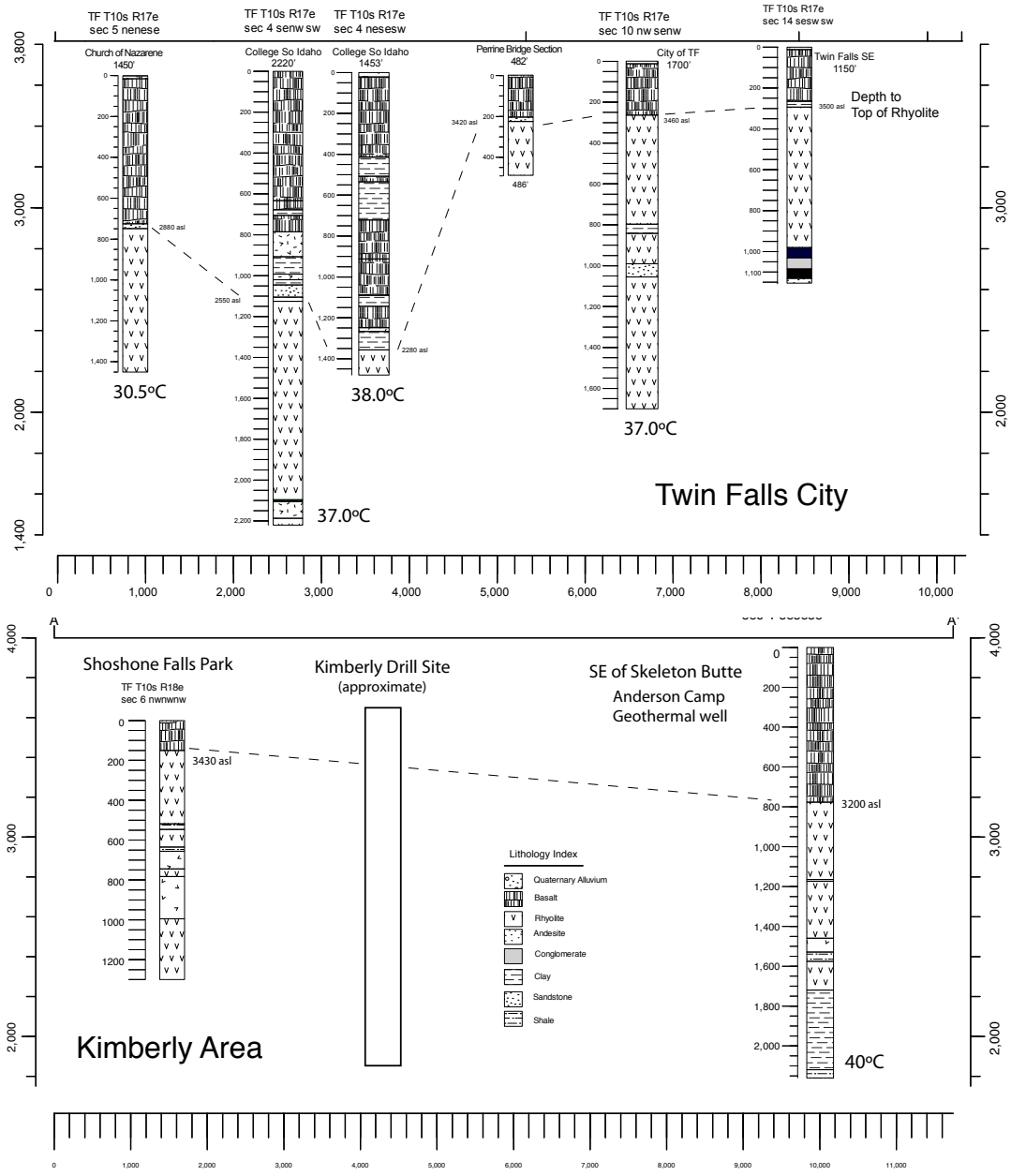

Figure 3-16. Wells logs and temperatures for passive geothermal wells in Twin Falls city (top) and Kimberly area (bottom).

Based on the depth of the basalt-rhyolite contact in WO-2, and the age of the deepest basalts in Wendell RASA, we estimated that we would encounter the basalt-rhyolite contact in the Kimama well between 3300 to 4000 feet (1000-1200 m) depth. To provide a margin of uncertainty, we budgeted the Kimama hole based on an inferred stratigraphy with 4000 feet of basalt (1200 m), penetrating 1000 feet (300 m) into basement, for a total budgeted depth of 5000 feet (1500 m).

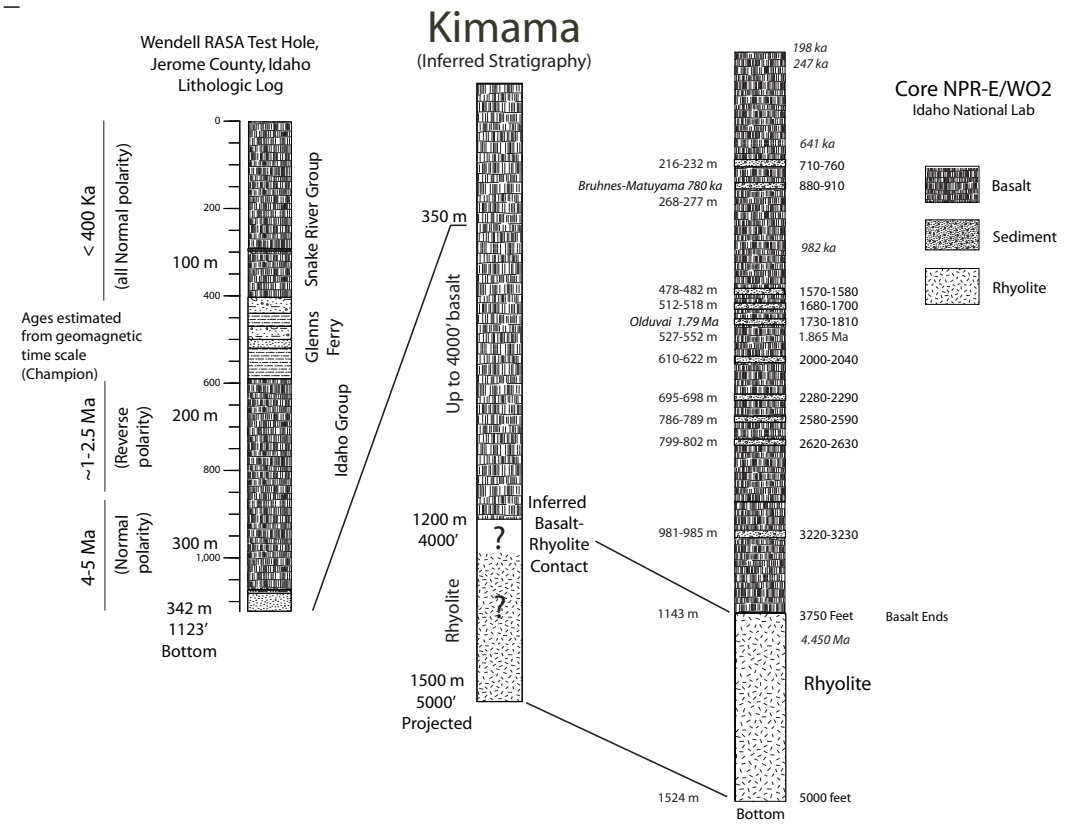

Figure 3-17. Comparison of inferred Kimama stratigraphy with that observed at WO-2 (Idaho National Lab) and Wendell RASA (USGS, near Wendell, Idaho). See Figure 3-1 for locations. Note that our actual section at Kimama differed significantly from this model. Not to scale.

At Mountain Home, we had the advantage to of having the 1988 MH-1 well, drilled ~5 km east of our proposed site, plus the 2900 m Bostic 1A well, located much farther east but sampling a significantly thicker section, and bottoming in rhyolite (Figure 3-18). Both logs are characterized by an upper most basalt section overlying a thick lacustrine sedimentary sequence, with episodic lava flows. Beneath the lacustrine sediments are more volcanics, dominantly basalt to about 2500 m, with rhyolite below that. In detail, however, there are some significant differences, such as how much basalt on top, and the overall thickness of the lake section. We used MH-1 as a general model to guide our drilling since it lies relatively close to MH-2, and sits in the same location relative to the gravity anomalies

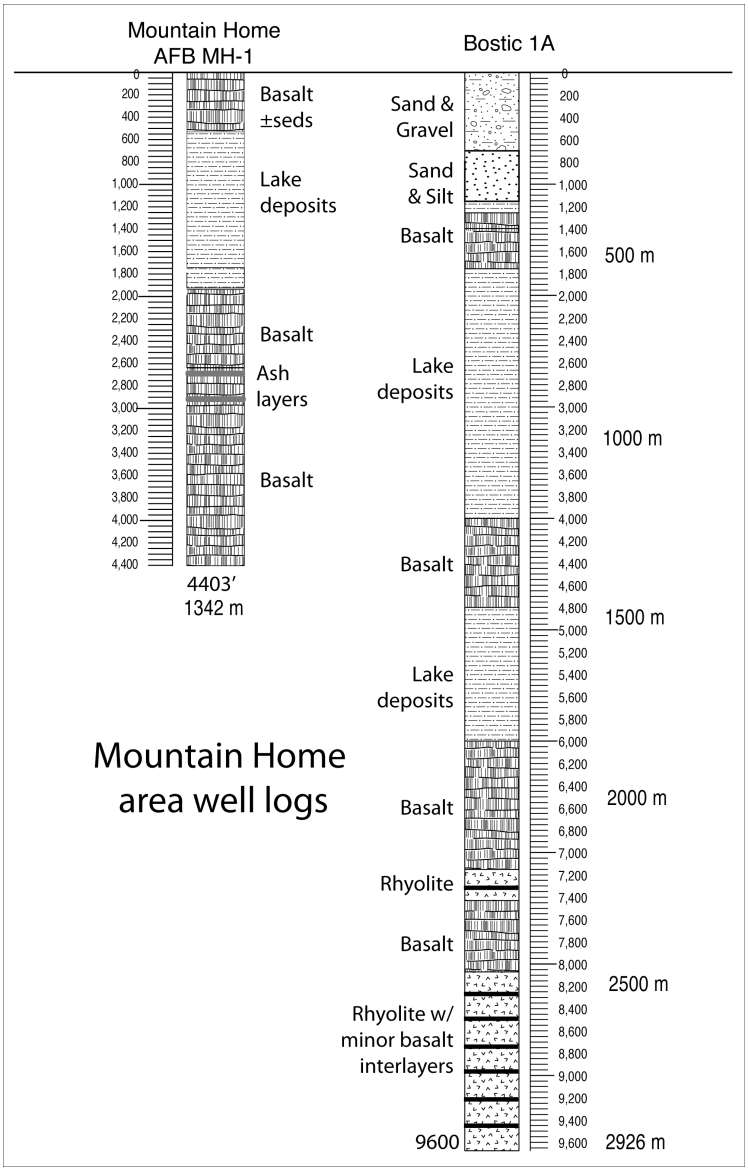

Figure 3-18. Comparison of well logs from two Mountain Home area wells: the 1988 MH-1 geothermal test well, and the 2900-meter deep Bostic 1A well (Lewis and Stone, 1988; Arney et al, 1982, 1984).

CHAPTER 4:

SITE CHARACTERIZATION AND SELECTION

John W. Shervais
Utah State University, Logan, Utah

ABSTRACT

Three locations were chosen for slim hole test wells as part of this project: Kimama 1500 m target depth, Kimberly 1800 m target depth, and Mountain Home 700 m target depth. Each site was selected with a specific objective in mind. The Kimama site targeted high sub-aquifer heat flow along the axial volcanic zone of the central SRP; the Kimberly site targeted the buried margin of the Twin Falls eruptive complex, located in an established passive geothermal district; and the Mountain Home site targeted high thermal gradients in the western SRP along a steep gravity gradient thought to represent the faulted margin of a buried hörst block. Sites were selected based on the Phase 1 field studies and data compilation. This chapter presents the rationale for selecting each site, and characterizes their setting.

INTRODUCTION

Two new intermediate depth (1.9 km) slim-hole exploration wells were drilled in the central Snake River Plain near Twin Falls, Idaho, during Phase 2 of this study, along with a third 1.8 km well on Mountain Home AFB in the western SRP graben. These wells were used to validate the surface and geophysical studies of Phase 1 in order to further constrain the extent and quality of the geothermal resources in this region. Locations for these wells were chosen using the field studies and data compilations discussed in Chapter 3 of this report. Each site was selected to represent a distinct setting within the Snake River volcanic province (axial volcanic zone, margin, and western SRP graven).

The new central SRP holes were located west of the Great Rift and NE of Twin Falls, Idaho, and close together longitudinally so that they overlie similar age and composition basement. The 1912 m deep Kimama well was sited to test the extent of geothermal resources along the axis of the plain, beneath the Snake River aquifer, in an area where the enhanced volcanism of the axial volcanic high and elevated groundwater temperatures imply a significant flux of conductive or advective heat flow from below (*e.g., Smith 2004; Smith et al, 2002).* Fracture systems here may be related to the volcanic rift zones or Basin and Range extension.

The 1958 m deep Kimberly well was sited to evaluate geothermal resources along the margins of the plain, focusing on a buried caldera complex and the ring-fractures that define its margins. High measured heat flow along the margins of the plain suggest that thermal resources are closer to the surface but the shallow resources may be more prone to disturbance by excessive pumping (*Brott et al 1981; Lewis and Young 1989*). The Kimberly site is located in an existing thermal water district characterized by numerous low temperature wells (~40ºC) that are used for passive space heating.

The 1812 m deep Mountain Home AFB test hole is sited on the margin of a buried horst block in the western SRP graben system (Shervais et al 2002; Wood and Clemens 2002), in a setting similar to the Basin-and-Range province. This site was also chosen because it may provide a geothermal energy resource to the US Air Force.

KIMAMA – ELEVATED HEAT FLUX UNDER THE VOLCANIC AXIS

The primary goal of the Kimama drill site was to test the extent of geothermal resources along the axis of the plain, beneath the Snake River aquifer, in an area where elevated groundwater temperatures imply a significant flux of conductive or advective heat flow from below (*e.g., Smith, 2004*). The use of shallow temperature gradient drill holes to define a thermal anomaly is not a meaningful test in this situation because of the refrigeration effect of the massive shallow groundwater flow.

This site was chosen because it sits on an axial volcanic zone that is defined by high topography to the east (Figure 3-1) and by electrical resistivity (ER) logs that define a buried keel of basalt underlying the topographic high (Figure 3-14). The ER logs define the depth to saturated basalt – generally interpreted to represent the base of the younger Quaternary basalts, and excluding older Pliocene basalts which have limited porosity (*e.g., Lindholm 1996*). Based on these ER logs and nearby wells, the depth to base of Pleistocene basalt at the Kimama site is about 850 m (2800 feet). For comparison, the WO-2 borehole on the Idaho National Laboratory (INL) site is located on the same ER depth contour, and sampled 1200 m (3900 feet) of basalt (Figure 3-14). The basalt thickness estimated from ER measurements most likely corresponds very approximately to the base of the Snake River aquifer, which is sealed by authigenic mineralization of the older basalts that seals off permeability (*e.g., Morse and McCurry 2002*). The Wendell-RASA borehole, situated near the 500 m ER depth contour, encountered 335 m (1100 feet) of basalt plus sediment, but did not encounter rhyolite basement (Figure 3-17).

Detailed assessments of groundwater temperatures and flow paths beneath the Idaho National Lab and adjacent areas have been made by *Smith (2004), Smith et al (2002),* and *McLing et al (2002).* They show that the base of the Snake River aquifer varies from 200 m to 500 m depth, based on the inflection depth of groundwater temperatures in deep wells, which change from isothermal within the aquifer to conductive below the aquifer (Figure 3-7). Thick portions of the aquifer correspond to massive inputs of cold water from (1) the combined Snake River-Henrys Fork River drainages and (2) the Centennial Mountains, including the Big Lost River, Little Lost River, and Birch Creek drainages (Figures 3-1 and 3-8).

This flux of cold water is concentrated in groundwater plumes that follow the southern and northern margins of the Snake River Plain, paralleling flow of the Snake River (in the south) and the Little Wood River (in the north), and skirting the thick axis of basalt volcanism that underlies the central volcanic axis of the plain (Figure 3-8). Groundwater temperatures form a linear high along the central axis of the Snake River Plain that corresponds with both the axial topographic high and the axial volcanic keel (*Smith 2004; McLing et al 2002*). The elevated groundwater temperatures are especially remarkable in light of the massive flow of cold water documented by deep wells and by cold springs that emerge from the aquifer west of Twin Falls. As discussed in Chapter 3, it requires over 287 MW of heat flux to raise the groundwater temperature from 8ºC to 14.5ºC (*Blackwell et al 1992*). Since over 42 MW are lost above the aquifer, a total flux of 329 MW is required; this translates to a heat flow of ~190 mW/m^2 (*Blackwell et al 1992*)!

The conceptual model for this process is shown in Figure 3-9, taken from *Smith (2004),* which depicts a longitudinal profile along the axis of the central and eastern SRP. Cold water enters the system from the surrounding mountains, fed by major river systems from the north,

east and southeast. This plume of cold water is gradually heated from below by the high plume-derived heat flux, which is focused under the axis of the plain (Figure 3-9). The axial heat flux is enhanced by the intrusion of the mid-crustal sill complex, which advects heat into the middle crust as magma, and continuously releases latent heat of fusion as the sills cool and crystallize (*Shervais et al 2006b*).

We selected the Kimama site for several reasons, based on the analysis above. First, it sits within the an area that has a high concentration of Quaternary volcanic vents. Second, it sits on the Axial Volcanic Zone where heat from the underlying mantle plume and sill complex should be highest. Third, it sits above the elongated plume of warm ground water defined by *Smith (2004),* which shows that this heat is being advected to the surface. Finally, as shown in the following section, it appears to sit above the eastern margin of a buried caldera complex, which may provide enhanced pathways for heat transport along its ring fracture system.

Our budgeted depth for the Kimama drill hole was 1500 m, in order to penetrate the Snake River Regional Aquifer and well into the underlying volcanic rocks. We estimated the basalt thickness at about 1200 m, similar to hole WO-2 at the Idaho National Laboratory site, or less (Figure 3-17). This proved to be incorrect; even after drilling to 1912 m depth, we had still not intercepted rhyolite basement. However, the abundance of fluvial and lacustrine sediments near the bottom of the hole suggest that we were relatively close to the basalt-rhyolite contact, based on results from the Kimberly hole.

Our selected location is on private land located just north of the former Kimama township site (Figure 4-1). This site was chosen because it sites squarely on the keel of the axial volcanic high; it is not too far east of the proposed rhyolite site at Kimberly, and it is about 40 km west of the Great Rift – a volcanically active rift zone with anomalous crust that has likely been affected by hydrothermal circulation *(Kuntz et al 1982).* Note that the Great Rift lies within Craters of the Moon National Monument, and is off-limits to development.

The Kimama site was also chosen for its logistical advantages: it is located off of a wide, well-graded gravel road less then half a mile from paved highways, about 25 miles north of a major town (Burley). This allows us to house the drillers and science crews in local motels, so we do not have to provide lodging and meals onsite. The site has an existing power line and the landowner has contracted to provide a power drop to our office and lab trailers, so that we did not need to use diesel generators for electric power. The owner has also contracted to drill a water well on the property so that we did not have to lease a water truck, purchase water in town, and truck it to the site. The site is favorably located for development of a geothermal resource.

The site has been disturbed by previous development, including the construction of two airstrips for crop dusters (one is currently active but the other has been abandoned), and several dirt or gravel roads that cross the property. No endangered species are present, and there are no culturally significant artifacts, as determined by consultants at USU Archeological Services, Inc., who conducted cultural and biological surveys in July 2010. A copy of their report was transmitted to DOE.

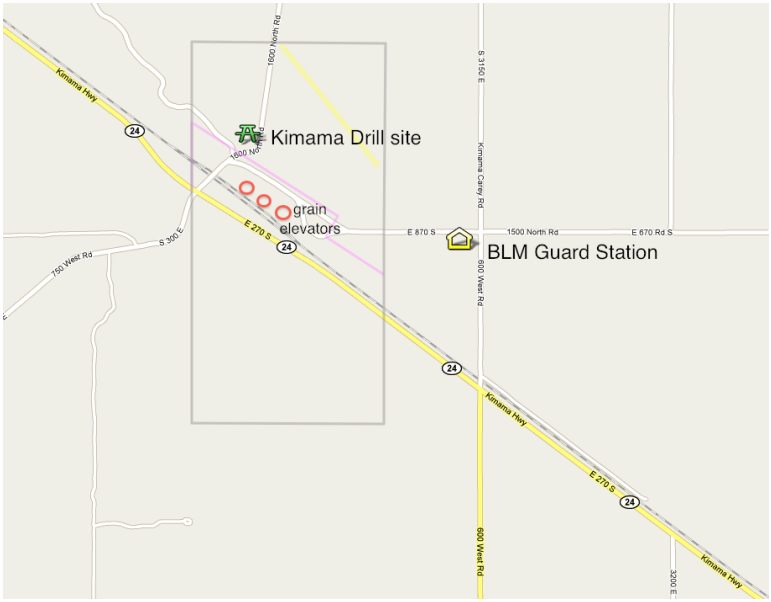

Figure 4-1. Detailed location map of the Kimama drill site, Lincoln County, Idaho. Drill site location shown by green derrick symbol. BLM guard station shown a yellow house.

KIMBERLY – UP-FLOW ALONG A BURIED CALDERA MARGIN

The primary goal of the Kimberly drill hole is to assess the geothermal potential of up-flow zones along a buried caldera margin. The large number of shallow geothermal wells in the Twin Falls area makes this area one of the best characterized stratigraphically, and a prime location to explore for higher temperature resources at depth (*Street and deTar, 1987; Lewis and Young, 1989; Baker and Castelin, 1990*). The proposed drill site lies south of the Snake River where groundwater flow is dominated by water that originates in the mountains to the south, and penetrates deeply into the crust where it is heated before upwelling in the Twin Falls low-temperature geothermal district (*Street and deTar, 1987; Baker and Castelin, 1990).* Geothermal wells in the Twin Falls Groundwater Management Area range in temperature from around 30ºC to 72ºC, with the highest temperature occurring along the Buhl-Berger lineament. High temperatures are also found in the Kimberly area (up to 55ºC) near the site of our proposed deep well (*Baker and Castelin, 1990).*

Stratigraphy in the Twin Falls area is well-defined by exposed sections and by well data that extend to depths of 700 m below surface (mbs). The oldest volcanic rocks in region are ash flow tuffs and pyroclastic deposits of the Idavada Group (*circa* 10-12 Ma); these have been subdivided into more detailed local units, but may be conveniently grouped together here for discussion *(e.g., Street and DeTar 1987; McCurry et al, 1996; Bonnichsen et al 2008).* These are commonly overlain by fine-grained lacustrine sediments (mudstone, shale, siltstone) that are generally correlated with the Glenns Ferry Formation (*Street and DeTar 1987)*.

Overlying this in places is the Twin Falls rhyolite, also known as the Shoshone Falls rhyolite, a circa 4.5 Ma lava flow that is exposed in the Snake River Canyon from Shoshone Falls in the east to west of the Perrine Bridge in Twin Falls (*Bonnichsen et al 2008)*. The Twin Falls rhyolite lava flow varies from zero to 150 m thick. Where it is exposed in the Snake River Canyon north of Twin Falls, the upper surface is an exhumed paleo-flow top marked by ogives and ramp structures. We interpret this unit to represent a post-caldera rhyolite flow erupted from ring fractures along a caldera margin that is now buried by younger basalt flows. Similar caldera-margin lavas are well-known in other eruptive centers, most notably the Yellowstone caldera *(e.g., Christiansen, 2001).* These ring fractures are our proposed target for fluid up-flow.

This sequence is overlain by 100-300 m of basalt, commonly with a thin horizon of fine- to medium grained fluvial sediments separating the rhyolite from the basalt. Where the Twin Falls rhyolite lava flow is not present, lake sediments continue upwards to the base of the basalt. This succession is well-documented in water wells and geothermal wells through the region, with the contact of “rhyolite” underlying sediment (all that can be discerned from most drillers records) varying in elevation from as low as 2300 feet above sea level (650 m asl) to a high of 3400 feet asl (1100 m asl) (Figure 3-16).

We have compiled and mapped surface structural elements in a region surrounding Twin Falls between about longitudes 114ºW and 115.6ºW and latitudes 42º-43ºN (Figure 3-4). Our base map, as described previously, is derived from a NASA 10 m resolution DEM for the United States (http://seamless.usgs.gov/index.php), contoured with 10 m contour intervals in GeoMapApp (Goodwillie and Ryan, 2009). The resulting contour map was combined with a greyscale shaded relief image from the same 10 m data, with the maps in separate layers to enable toggling between them. Lineaments were identified from existing geologic maps, from lineations in the shaded relief map, or from offsets in contours that define lineaments (Figure 3-4). Using the live GeoMapApp projection, sun illumination angles were altered to enhance the visibility of lineaments with different orientations.

The lineaments form three groups, based on orientation and location (Figure 3-4). West of Buhl and north of the Bruneau-Jarbidge eruptive center, the lineaments trend approximately 275º-285º, or roughly parallel to range front faults in the western SRP *(e.g., Shervais et al 2002; Wood and Clemens, 2002)*. Lineaments with these trends also form the northern border of the Bruneau-Jarbidge eruptive center *(Bonnichsen et al 2008).* South and west of this region, the lineaments trend more northerly (~325º), including those within the Bruneau-Jarbidge eruptive center (Figure 3-4). This includes the Buhl-Berger lineament identified by *Street and DeTar (1987),* which cuts Berger Butte and may control its elongate shape. Finally, lineaments in the Cassia Mountains and in the Rogerson graben trend ~NS to 005º, more or less parallel to regional basin and range trends. There are some exceptions to these groups: Hansen Butte near Kimberly appears to be cut by an EW-trending fault, and there are many small cross-faults within the Cassia Mountains.

Overall, the pattern suggests a transition from western SRP orientations in the NW to Basin-and-Range orientations in the south. For the most part these lineaments can be shown to represent normal faults that offset topography, and many form small grabens that can be in both the topographic map and in the shaded relief map. The lineaments are more common where the underlying basement rock is older (rhyolite, lake sediments, or Paleozoic sediments), less common where underlain by Tertiary basalt, and essentially absent in areas covered by Quaternary basalts. This relationship implies that the faulting itself is older than Quaternary, and most likely formed coevally with the western SRP graben and Basin-and-Range extension. We note, however, that the absence of surface manifestations of these faults in the Quaternary basalts does not mean that they are absent in the subsurface. Indeed, it seems likely that since some faults are present in the late Pliocene age basalts, faulting continued up to the Pliocene-Pleistocene boundary, and that faults with these same orientations are likely to underlie the younger Quaternary basalts. The orientation of Rock Creek Canyon south of Twin Falls is subparallel to the Berger Butte trend, suggesting that the course of this creek is itself control by pre-existing fractures.

Also shown on the 10 m DEM topographic map are measured flow directions for ash-flow tuffs in the Cassia Mountains, as mapped by *McCurry et al (1996),* along with the southern extent of these ash-flow sheets (Figure 3-4). These flow directions are based on hundreds of field measurements and document clearly a source vent located north of the central Cassia Mountains, in the vicinity of Kimberly, Idaho. As we noted earlier, post-caldera rhyolite flows are exposed in the Snake River Canyon NW of Kimberly, suggesting that the now buried southern margin of the caldera vent which erupted these ash flows is somewhere near Kimberly, and that the central vent lay somewhere north of Kimberly. The inferred boundary of the Twin Falls caldera complex is shown on Figure 3-4 as a dashed white line.

In order to clarify the possible location of the source vent for the Cassia Mountains ash-flow tuffs, we produced a Bouguer gravity map of the central SRP covering an area slightly larger than the 10 m DEM topographic map. The Bouguer gravity map is characterized by low gravity along the margins corresponding to sediment-filled basins, rhyolite ash flows, or Paleozoic carbonate basement (Figure 3-10). The pronounced gravity high to the west continues beneath the western SRP, and may represent a buried horst block within the WSRP graben (see section on Mountain Home drill site for detailed discussion of the western SRP gravity structure). North of Twin Falls is a prominent gravity low surrounded by a rim of slightly higher gravity material (dashed white line). We interpret this structure to represent a buried caldera complex associated with eruption of the rhyolite tuffs. The Kimberly drill site lies along the southern margin of this structure, which lies more-or-less where we predicted it based on geologic mapping. The Kimama drill site lies along the NE margin of this same structure (Figure 3-10).

The area underlain by the ring-like structure is covered with a more-or-less uniform carapace of Quaternary basalts, so it cannot be interpreted to result from the distribution of surface basalt flows. The relative density contrast, the shape, and the size of this structure are all consistent with its interpretation as a buried eruptive complex *(e.g. Morgan et al 1984).* It also lies in the appropriate location for the source vent of the Cassia Mountain ash-flows. Richard Smith of INL developed the concept of using gravity to locate buried caldera complexes in the mid-1990's, which he applied to the eastern SRP with some success *(Smith et al 1994).* We believe that his approach will also work in the central SRP and provides an innovative way to see below the thick carapace of basalt, and to test the geothermal potential of these ring fracture systems.

The proposed depth of the Kimberly drill hole was 1.8 km. This depth was chosen based on estimates of rhyolite thickness outside the plain. In the end we were able to drill to 1.96 km depth through cost savings in our drilling plan, as discussed in Chapter 7.

The Kimberly drill site is on the University of Idaho Extension Farm, located 3 km NE of Kimberly town and 10 km east of Twin Falls (Figure 4-2). This location was chosen because it lies on the southern margin of the topographic Snake River Plain, and on or near the margin of the Twin Falls caldera complex, as defined by outflow sheets in the nearby Cassia Mountains *(McCurry et al 1996)* and by the regional Bouguer gravity anomaly discussed above. This site offered the logistical advantage of being located just off a state highway, on property owned by the University of Idaho, which is a partner in the Project Hotspot initiative. The infrastructure present includes power, water, diesel fuel station, and a variety of buildings. Our well-head site was located in dirt parking lot north of the main office buildings and greenhouse that will absorb noise from the drill rig, and which has easy access from existing farm roads.

Figure 4-2. Detailed location maps for the Kimberly well site. (a) top: map view shows location of the University of Idaho Research facility 5 miles east of Twin Falls, Idaho. (b) satellite view of Kimberly site, showing rig location in former agricultural field and tractor park.

MOUNTAIN HOME – GEOTHERMAL POTENTIAL OF THE WESTERN SRP GRABEN

The primary science goal of the Mountain Home drill core was to assess the geothermal potential under the AFB, building on results from a geothermal test well drilled in 1985-86 *(Lewis and Stone, 1988).* The previous geothermal test well had a BHT of 93ºC, but it was not possible to perform a pump test due to the hole size. Our goals for this hole were to sample basalts and lacustrine sediments in the upper 300 m of the section, which were not sampled by the existing Mountain Home Air Force Base (MH-AFB) MH-1 test hole, and to drill deep enough to assess geothermal resource potential in this setting. A geologic map of this area is being prepared for publication (Figure 3-5).

The western SRP has a long history of passive geothermal space heating applications, especially within the city of Boise. Previous wells (MH-1, Bostic 1-A: Figure 3-18) have documented elevated temperatures at depth that are close to those needed to sustain geothermal development, and elevated groundwater temperatures are found in some areas *(Lewis and Stone 1988; Arney 1982; Arney et al 1982, 1984).* A prominent gravity anomaly in the regional Bouguer gravity map *(Liberty, personal communication, 2010)* has been shown near Boise to represent an uplifted horst block in the subsurface *(Wood, 1994).* This same gravity high extends to the east beneath Mountain Home, and can be seen in both the Bouguer gravity anomaly map (Figure 19a) and an upward continued gravity map that removes shallow density variations and emphasizes deep crustal structures (Figures 3-12 and 3-13).

Mountain Home AFB sits on the southern edge of this prominent gravity anomaly, as can be seen in the more detailed Bouguer gravity map in Figure 3-13, which shows the gravity contour map without and with the gravity stations used to produce it. This gravity high that has been interpreted by *Shervais et al (2002)* to represent a buried horst block with the larger western SRP graben. This interpretation is consistent with reflection seismic data from Boise-Caldwell area that documents a buried horst block below the Glenns Ferry formation *(Wood 1994)*.

The difference in stratigraphy between the MH-1 well *(Lewis and Stone 1988)* and Bostic 1A well *(Arney et al 1984)* is best explained by their positions relative to the inferred basement high, with MH-1 bottoming on top of the inferred horst block (but near its southern margin) and Bostic 1A traversing a thick section of sediments and volcanic flows filling the small graben that lies north of the horst block, and south of the Danskin Mountains (Figure 18). There may in fact be vertical upflow zones along both the northern and southern margins of this inferred horst block, explaining the elevated bottom hole temperatures found in both wells *(Lewis and Stone 1988; Arney et al 1982, 1984).*

Our drill site is located in the undeveloped NW corner of MHAFB (Figure 4-3). This site is less than 5 km from the original MH-1 (1342 m) geothermal exploration well, which was drilled along the eastern margin of the Base. The overall stratigraphy at this site was expected to be more or less identical to that found in the MH-1 well. This site is within a few hundred meters of an existing 150-meter deep monitoring well (MW-3-2), and near two other monitoring wells, so the upper stratigraphy is well-known. However, no core is available from the monitoring wells. Logistically, the site is located near the MH AFB contractors gate, easily accessible from the main paved road via a gravel road built by USAF engineers.

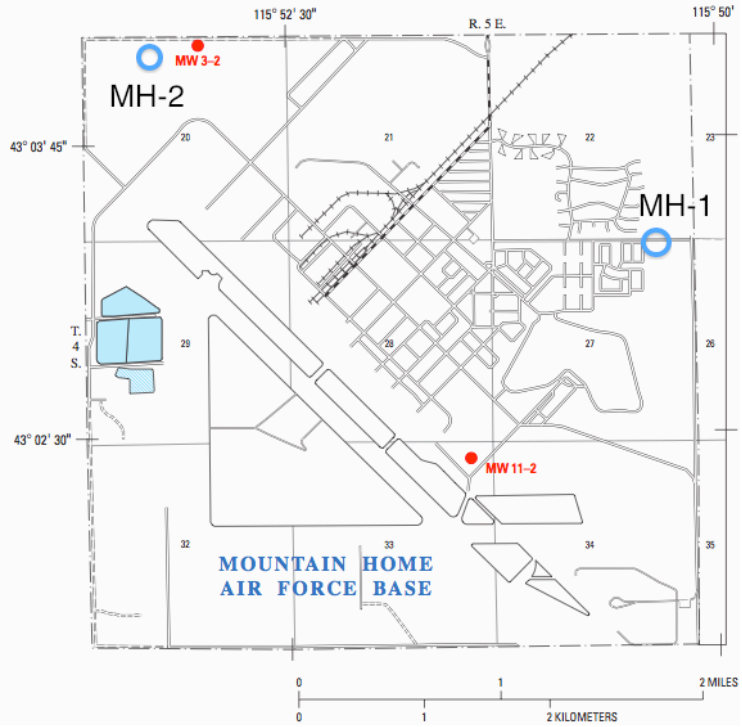

Figure 4-3. Detailed location map for the Mountain Home well site, MH-2. Also shown are location of 1988 test well MH-1 and monitoring wells MW-3-2 and MW-11-2.

CHAPTER 5:

POTENTIAL FIELD STUDIES

Jonathan M.G. Glen
U.S. Geological Survey, 345 Middlefield Road, MS 989 Menlo Park, CA 94025; jglen@usgs.gov

Claire Bouligand
Institut des Sciences de la Terre, Université Joseph Fourier, BP53 Cedex 9, 38041 Grenoble, FRANCE; Claire.Bouligand@ujf-grenoble.fr

ABSTRACT

Project Hotspot was undertaken to study the surface expression of the Yellowstone hotspot along the Snake River Plain volcanic province (SRP), which is thought to represent the magmatic track of a deep-seated mantle plume located under North America. The primary goal of this project was to document the volcanic, thermal, structural, and stratigraphic history of a continental hotspot, to understand how the hotspot has affected the evolution of continental crust and mantle, to evaluate the geothermal potential across the Plain, and to develop innovative techniques for geothermal exploration in volcanic settings.

We have performed potential field studies in the Snake River Plain to provide regional geophysical mapping to characterize mid- to shallow-crustal features. This involved compiling and reprocessing existing gravity and aeromagnetic data, and collecting new gravity data to provide an unprecedented high-resolution potential field dataset for assessing subsurface structure.

Gravity data were collected along several detailed transects (stations spaced about 1/4- to 1-mile apart along profiles). Because Project Hotspot largely involved the study of three deep drill holes along the central and western SRP (Kimama - located along the central volcanic axis of the SRP; Kimberly - located near the margin of the plain; and Mountain Home - located in the western plain), much of our data collection was focused in these areas.

Representative rock samples were also collected concurrently with the gravity data, and their physical properties (density and magnetic susceptibility, and magnetic remanence) were determined in the laboratory to aid in quantitative modeling of measured geophysical anomalies. Together, these data provide a region-wide geophysical framework for detailed mapping and modeling of subsurface structures.

In addition to our potential field mapping efforts, we undertook two innovative applications for geothermal exploration. The first involved a technique, introduced by Bouligand et al. (2009), to estimate depths to the bottom of magnetic sources that can be used to map the Curie temperature isotherm or estimate the thickness of basaltic fill within the Snake River Plain. The second involved novel methods, developed as part of this project, to estimate the 3D geometry of subsurface alteration. To test these methods we applied them to several well-developed hydrothermal areas in Yellowstone National Park, where surface alteration has been extensively mapped, that provide critical independent control to assess our results.

Introduction

Potential field geophysics (gravity and magnetics) is a valuable tool for regional characterization of subsurface geology and structures in the mid to upper crust. These methods work particularly well when there are strong contrasts in rock properties that result in prominent gravity and magnetic anomalies, like in the Snake River Plain (SRP) where relatively dense and magnetic volcanic units that contrast sharply with low density tuff and low density and weakly magnetic sediments.

The purpose of this work was to (1) perform potential field mapping of the Snake River Plain that could provide a regional characterization of subsurface structures, (2) to apply innovative methods for characterizing geothermal potential across the plain, (3) develop novel techniques for geothermal exploration in volcanic settings.

As part of our mapping effort, we processed existing aeromagnetic data available for the SRP and surrounding region, and collected detailed high-resolution gravity data along several profiles (Figure 5-1) spanning the western and central portions of the SRP. The focus of the gravity data collection included prominent geophysical anomalies that may represent buried lavas or sediments, feeders to early SRP volcanism (dikes, or volcanic vents), buried calderas, pre-Tertiary basement, or major intrusives. On a more local scale important for geothermal feasibility studies, the detailed profile data can aid identification of faults and fractures that can serve as conduits for hydrothermal fluid flow.

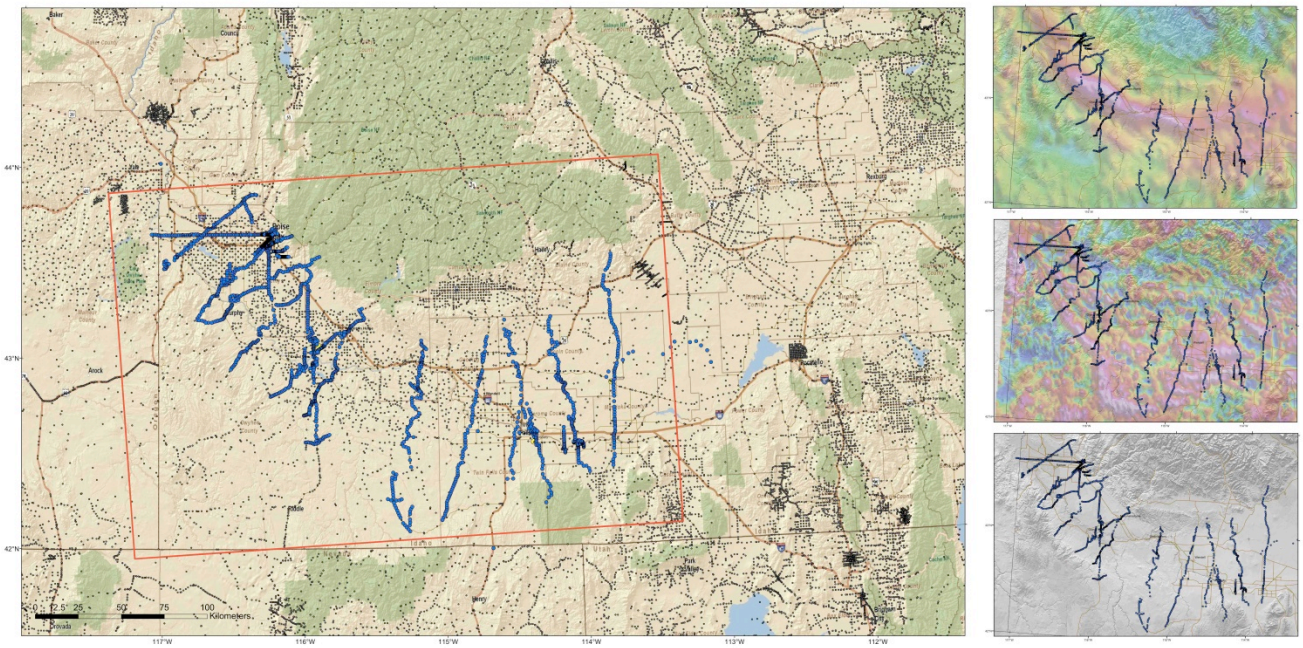

Figure 5-1a. Index map showing new (blue circles) and existing (small grey circles) gravity data collected in the Snake River Plain and surrounding areas. Large yellow circles show the locations of ICDP drill holes. The red box show the extent of maps portrayed on the right of the figure. The locations of new gravity data are plotted with the Isostatic gravity map (top right), magnetic residual map (middle right), and topography (lower right).

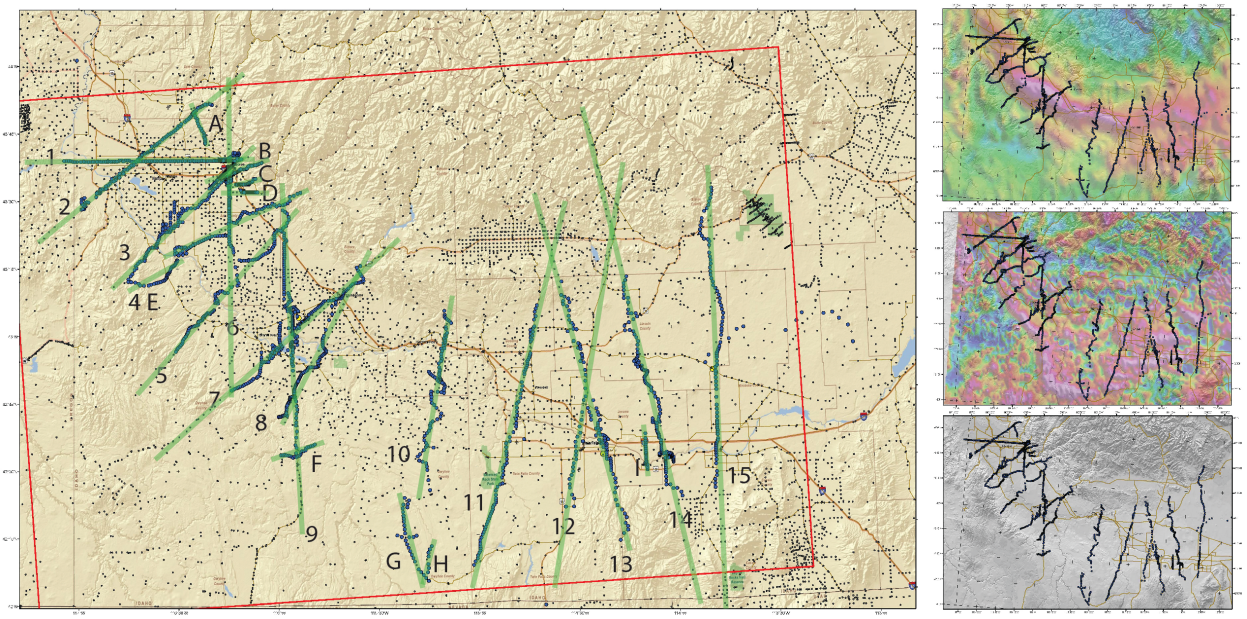

Figure 5-1b. Index map showing profiles referred to in this report. Symbols same as in figure 5-1a.

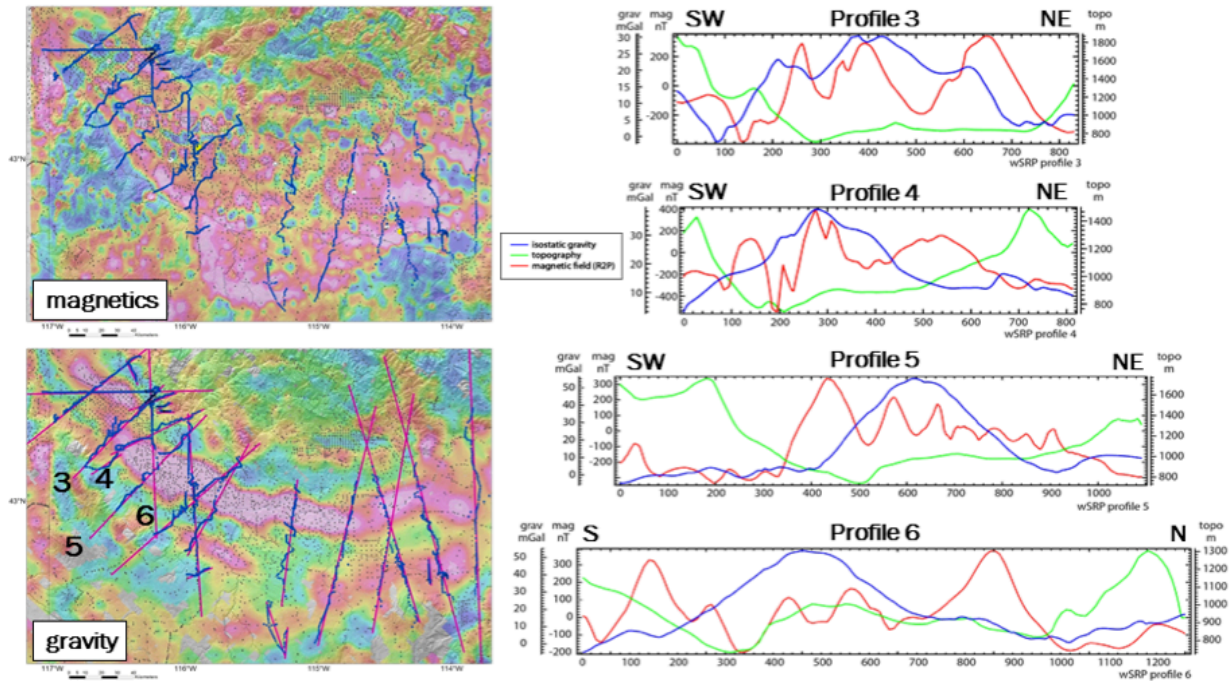

Figure 5-1c. Map of residual reduced to pole (top) and residual isostatic field (bottom) for the central and western SRP showing gravity data (black and blue symbols, and profile (pink lines). Also shown are profile data [topography (green), isostatic gravity (blue), and reduced to pole magnetic field (red) along profiles (3 through 6) across the western SRP.

Gravity data

The U.S.G.S. collected 1866 new gravity stations throughout the western and central Snake River Plain (Figure 5-1) during three field sessions between August 2010 and June 2011 using Lacoste Romberg and Scintrex CG-5 gravimeters. Stations were distributed largely along several long profiles, oriented perpendicular to the axis of the plain (Profiles 1-15, Figure 5-1b,c), spanning the western and central portions of the SRP. These profiles were designed to aid 2D modeling, which is possible because many of the regional intrabasin structures are aligned with the axis of the plain. Several of the profiles were selected to cross drill holes (at Kimama, Kimberly, and Mountain Home) to help constrain local geology around the holes and to make use of core and borehole data in potential field modeling. The distribution of profiles was also planned in order to map the transition from western to eastern SRP and to aid future 3D modeling. This proved difficult in places where access to private lands, lack of roads, or bridges prevented us from collecting continuous, densely-distributed data along long and relatively straight transects crossing the plain. Profiles were also selected to take advantage of existing regional data, and to target prominent magnetic and gravity anomalies of interest. Gravity stations were taken with nominally 0.5-1km spacing between stations in areas where gradients were large or more sparsely (1.5-2km) in low gradient areas, or where access or time were limited. Several short, detailed profiles (75-100m station spacing) were also taken in areas of specific interest (Profiles A-I, figure 5-1b). The gravity data were tied to several base stations, some of which were established for the purpose of this project.

Gravity data were tied to primary base stations located at Boise, ID (BOCY, U141), Mountain Home, ID (MTHB), Buhl, ID (BUHL), Jackpot, NV (JPOT), and Ontario, OR (ONTA) that were established by the U.S. Defense Mapping Agency and NOAA-National Geodetic Survey (Jablonski, 1974; D. Winester, pers. comm. 2010), as well as two additional secondary bases established for the purpose of this study. Gravity values at these secondary bases, located at Mountain Home (MTHC) and Twin Falls (TFPO), Idaho, were determined through multiple calibration loops tied to the primary base stations.

Gravity station locations and elevations were obtained using a Trimble® GeoXH differential Global Positioning System instrument. The GeoXH receiver uses the Wide Area Augmentation System (WAAS) which, combined with a base station and post-processing using Continually Operated Reference Station (CORS) satellites, results in sub-meter vertical accuracy.

Prior to data interpretation, gravity data need to be reduced in order to reflect anomalies arising from lateral changes in the density of subsurface materials. This required correcting for several other factors which affect observed gravity. These corrections follow standard gravity reduction procedures (Blakely, 1995) that include: (a) an instrument-drift correction which compensates for drift of the gravimeter spring with time. The drift value is calculated by

assuming a linear drift between the day's opening and closing measurements performed at the same base station; (b) a tidal correction which makes up for the gravity effects of the sun and moon; (c) a latitude correction, which accounts for the variation of the Earth's gravity with latitude; (d) a Free-air correction that accounts for the variation in elevation between a gravity station and sea level using a free air gravity gradient .3086 mgal/m; (e) the Bouguer correction, which compensates for the mass between the station and sea level, and utilizes the average density of continental crystalline crust , 2.67 g/cm^3; (f) the curvature correction, which corrects the Bouguer correction for the effect of the Earth's curvature; (g) Terrain corrections that account for the effects of surrounding topography (this includes a "field" correction that accounts for terrain to a radial distance of 53m from the station that is estimated in the field, and corrections extending to 166.7km that are computed using digital terrain models); and (h) an isostatic correction that removes a regional gravity field caused by isostatic compensation of topographic loads.

New gravity data were combined with pre-existing gravity data from the surrounding areas (including parts of ID, OR, NV, UT, WY and MT) downloaded from the PACES (Pan-American Center for Earth and Environmental Studies, 2009) data portal. Existing data coverage across much of the western and southern SRP was generally poor (3-6 mi spacing) for detailed profiling, but provided good regional coverage off-axis of profiles that help to fill in the regional map between profiles and to extend profiles beyond the plain. Prior to combining new and existing data, PACES data had to be edited and re-reduced.

The PACES database incorporates datasets from a large number of different sources of varying quality, and contains duplicate or erroneous data. Data had to be carefully edited for: 1) repeat stations that can be difficult to identify due to station locations or gravity values that differ because of truncated digits, errors in projection, or differences in data reduction; 2) stations that are bad, due to erroneous locations, readings, elevations,…etc. In some cases, these stations can be 'fixed' (e.g., by correcting elevations using digital terrain models), while in other cases the data may need to be omitted; 3) datum shifts between various datasets that comprise the study database. The final edited dataset was then reduced (terrain corrections and gravity anomalies were recomputed using standard programs, described above) to be merged with our new data. After editing, over 30,000 gravity data within the broader study area (Snake River Plain and surrounding area – covering ~3º x 6 º window centered on the SRP) were used from the PACES database. A comparison of profiles, showing data from the original PACES database with the final edited data set that includes new data, is shown in Figure 5-2.

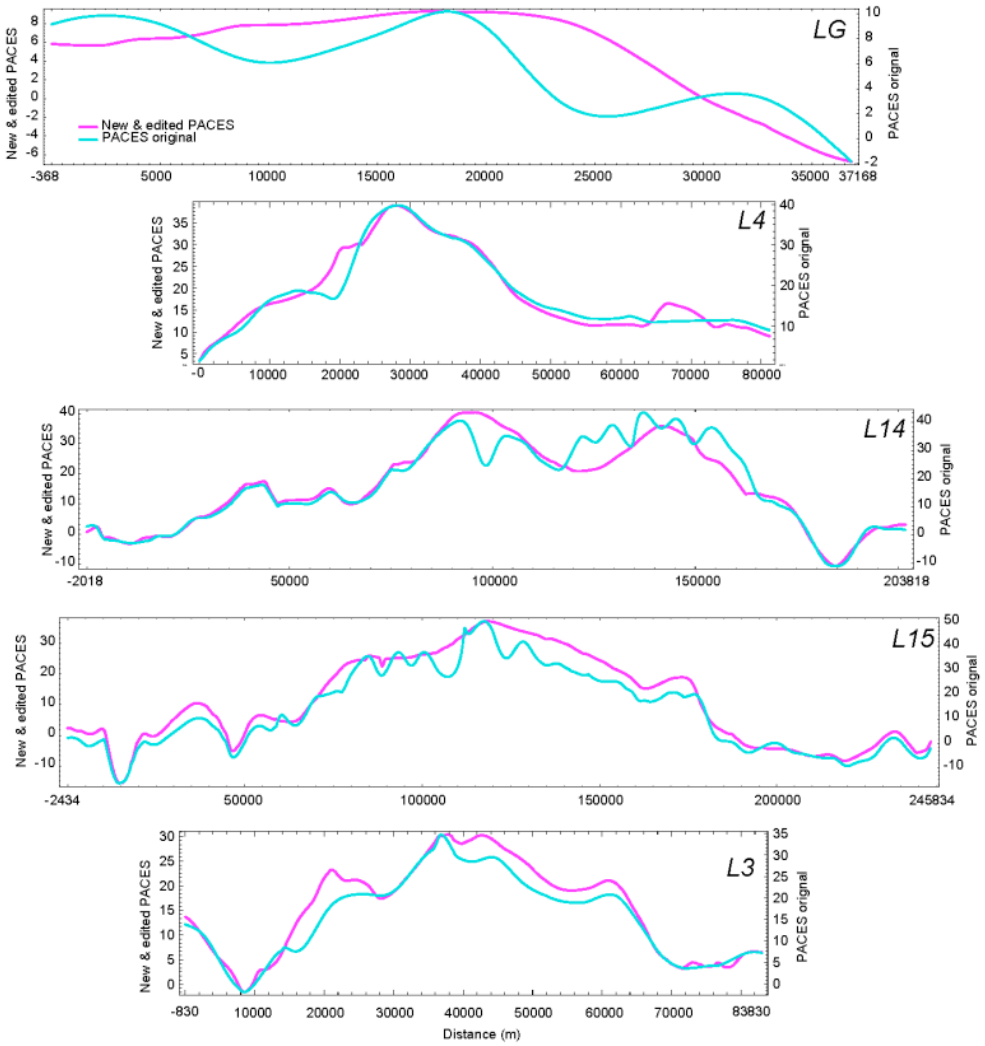

Figure 5-2. Examples of some profiles (see figure 5-1b for profile locations) showing original PACES data (light blue) versus the edited PACES data set combined with new data (pink) collected for this project.

Magnetic Data

Regional and State grids

The regional magnetic grid used in this report was derived from the Magnetic Anomaly Map of North America (Bankey et al., 2002; http://crustal.usgs.gov/projects/namad/). We have also used a higher resolution grid for the State of Idaho (McCafferty et al., 1999). For more detailed studies (e.g., looking at Curie Temperature depths) we regridded individual survey data used in the State compilation.

The southern part of the state compilation spanning the greater SRP area, consists of a patchwork of over 30 individual surveys of varying quality conducted over the past 40 years

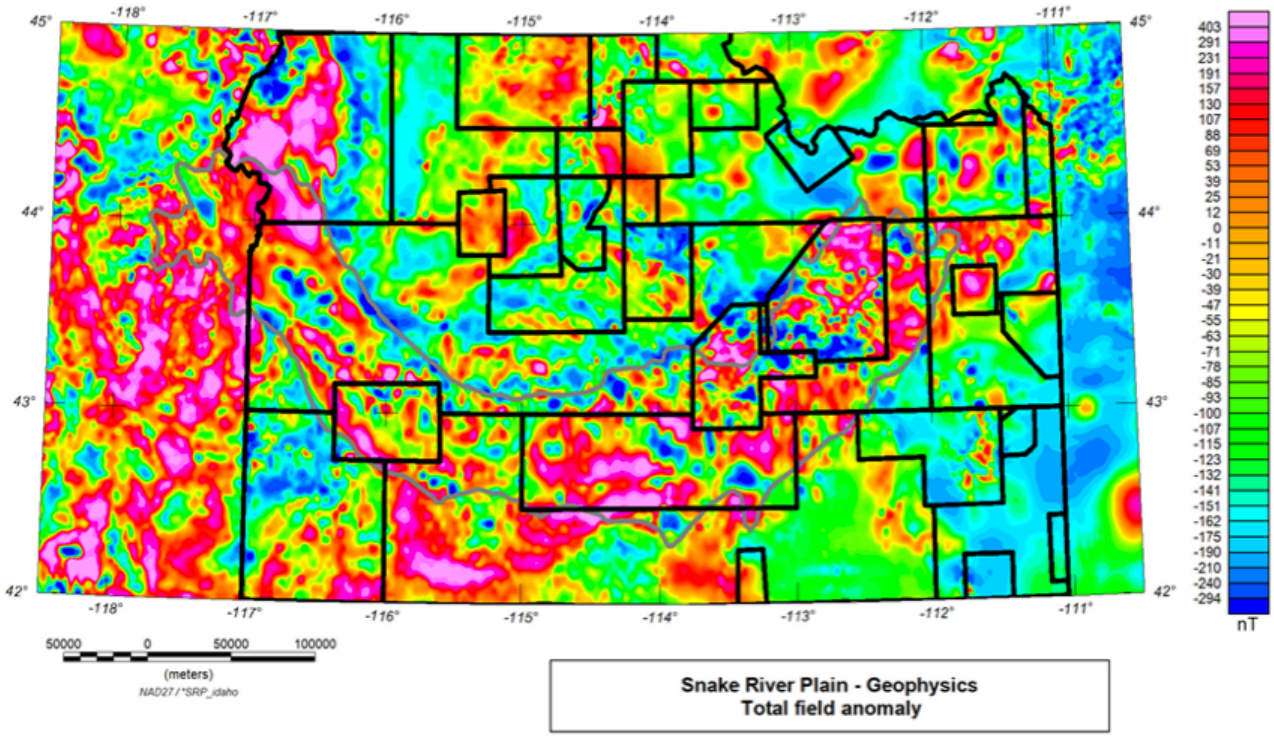

Figure 5-3. Index showing outlines of individual aeromagnetic surveys used in the Idaho State compilation, superimposed on the regional aeromagnetic compilation for North America.

(Figure 5-3). These surveys have been flown at different times with varied flight elevations, flight-line spacings, and subject to different data-reduction procedures. Aeromagnetic data coverage along the SRP (particularly in the southern and western segments) is generally poor with widely spaced (3-6mi spacing) flight lines.

Magnetic map compilations used here reflect the magnetic-anomaly field [total field intensity minus the Definitive International Geomagnetic Reference Field (DGRF)]. Individual surveys for the State compilation grid were reduced to a common elevation of 305 m (1,000 ft). Draped surveys flown at a constant elevation above or below this datum level were analytically continued upward or downward (Hildenbrand, 1983) so that the data would be consistent with adjacent surveys. Older surveys for which the original digital data were not available were digitized (from contoured maps) along flight-line/contour-line intersections, which is considered to be the most accurate method of recovering the original data.

Alteration surveys

For the alteration study, we used data from both a high-resolution aeromagnetic survey (flown at 250m height above terrain with 400 m flightline spacing) conducted over YNP in 1997 (Figure 5-4; USGS, 2000) and ground surveys we performed in the Fall of 2010 for this study. The aeromagnetic survey provides uniform data coverage over a large area that includes terrain difficult to access on the ground, while ground data provide detailed information on shallow sources. Ground-based magnetic surveys were made using a cesium-vapor magnetometer (Bouligand et al., in press). These surveys include several 4-5 km long transects that cross thermal features within three primary study areas (Firehole River, Smoke Jumper Hot Springs, and Norris Geyser Basin; Figure 5-4) and a detailed survey over an area around Lone Star Geyser. The detailed survey was conducted along approximately north-northwest oriented lines with a line spacing of about 10 m (near thermal features) to 50 m (far from thermal features) and with a few transverse tie lines. Diurnal magnetic field variations were recorded using a proton-precession base-station magnetometer which remained at a fixed location, and used to apply diurnal corrections to magnetic anomaly profile data.

Physical-Property Data

Nearly 1000 field susceptibility measurements were made on outcrop located typically at or near gravity stations. In addition, over 75 hand samples were collected for performing laboratory measurements of density and magnetic susceptibility. Densities (grain, saturated-bulk, and dry-bulk) were determined using the buoyancy method with an electronic balance, and magnetic susceptibility measurements were made using a Kappameter® KT-5.

Potential Field Methods

Spatial variations in gravity and magnetics (potential fields) result from lateral contrasts in rock-density, and rock-magnetic properties (induced and remanent magnetizations), respectively, and can be used to map and model subsurface features such as faults and fracture zones, geologic contacts, metamorphism, or alteration that juxtapose rocks with contrasting rock properties. As a result, potential field methods are useful for characterizing areas where much of the surface is covered by young deposits that conceal deeper units or structures. Furthermore, gravity and magnetic data can be obtained relatively quickly over large tracts of land making them particularly suitable for regional studies.

The size, geometry, and depth to a potential field source, the character of the geomagnetic field, and the rock properties of a source and its surroundings, all determine the character of a source's anomaly. Despite this complexity, and the inherent non-unique nature of potential field model solutions, potential field data can provide concrete constraints on the geometry and inferentially, the origin of anomaly sources, particularly when combined with other geologic

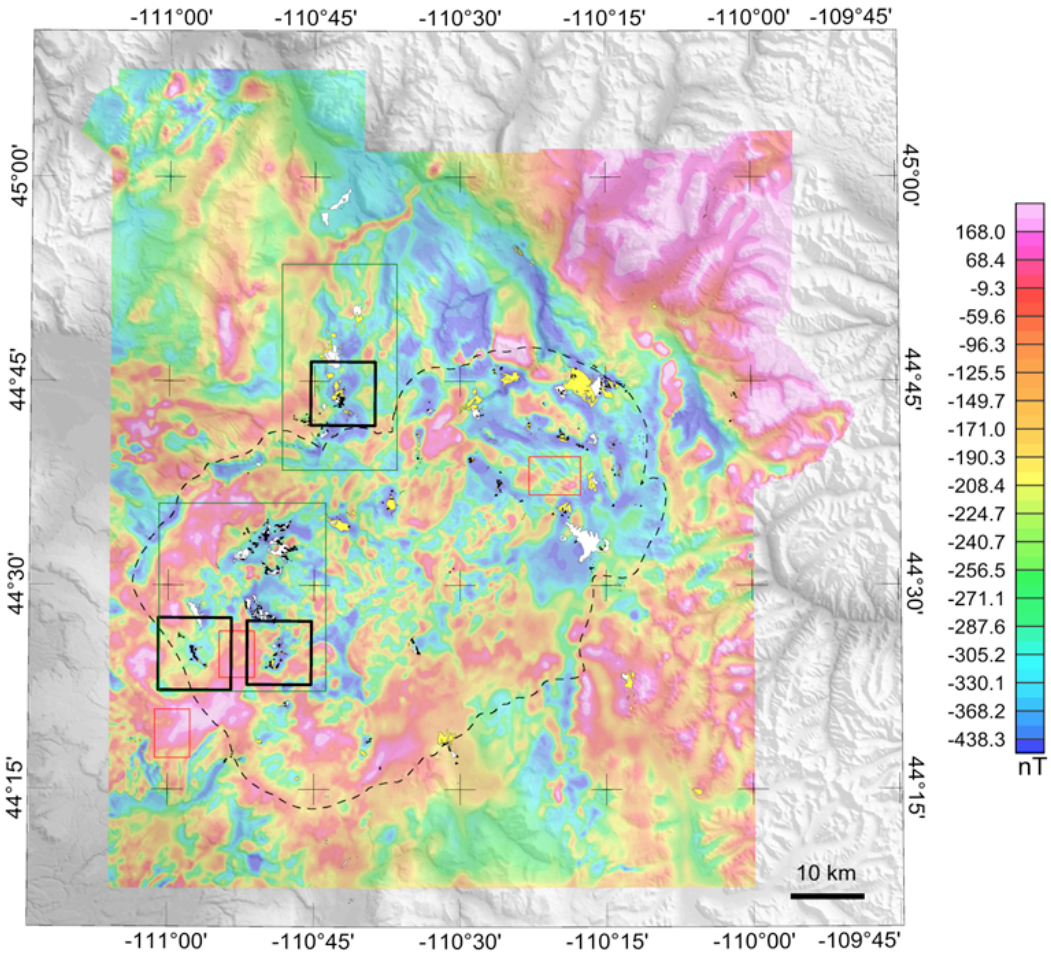

Figure 5-4. Map of the high-resolution aeromagnetic survey of Yellowstone National Park plotted over shaded topography. Aeromagnetic anomalies are reduced to the pole. Hydrothermal alteration and deposits are represented in yellow and white, respectively. Thermal features are located by black triangles. The dashed outline represents the 0.6 Ma Caldera rim (after Christiansen, 2001). Study areas are indicated by black squares. Note that magnetic lows are generally associated with thermal features, hydrothermal alteration or deposits. Black thick rectangles show the location of study areas.

constraints such as the regional tectonic framework, surface geology, and seismic or electrical data.

Some general conclusions can be drawn from the character of geophysical anomalies and their likely sources. The shallower the depth to a potential field source body, the higher the amplitude, the shorter the wavelength, and the steeper the gradients of its potential field anomaly. As a result, high-amplitude, short-wavelength anomalies, which often have steep gradients, are produced by sources at shallow depths in the crust. In contrast, long-wavelength anomalies having smooth gradients commonly reflect deep sources. Anomalies with wavelengths of hundreds of kilometers, for example, most likely arise from sources in the lower

crust. Although wide, shallow, thin sources with gently sloping sides, can produce similar anomalies, such cases can usually be recognized with regional geologic mapping.

Gravity maps indicate anomalies that arise from lateral density contrasts that may arise from deviations from isostatic equilibrium, density contrasts between rock bodies, or lateral variations in temperature within the crust. Contrasts in rock density may be due to lithologic or structural contacts between rock units, partial melting, or phase transitions. Magnetic anomalies, on the other hand, reflect variations in the magnetization of the crust (including induced and remanent magnetizations), which, to a large extent (i.e., in rocks with small remanent components) reflect variations in the magnetic susceptibility of rocks caused by changes in the concentration and mineralogy of magnetic minerals within the crust. It is often assumed that the induced component need only be considered because of present field remanent overprints that are parallel to the induced component, or low intensity remanence components. Remanence however, may have a significant effect, particularly in the case of strongly magnetic units such as mafic igneous rocks that occur throughout the SRP.

Generally, gravity and magnetic highs arise from mafic and ultramafic igneous and crystalline basement rocks, whereas lows arise from felsic igneous, sedimentary, or altered basement rocks. Metamorphism and alteration, can strongly affect the susceptibility of an originally homogeneous rock body by leading to the non-uniform production or destruction of magnetic minerals. Igneous outcrops not associated with magnetic anomalies might be thin or contain low concentrations of primary magnetic minerals, or have lost them due to alteration. In the SRP, many of the most prominent gravity and magnetic anomalies (Figures 5-5 and 5-6, respectively) arise from mafic volcanic or intrusive rocks.

In contrast to gravity data, magnetic data highlight shallow and mid-crustal features as opposed to deep sources. This is due, in part, to the more rapid attenuation of magnetic fields with distance to their source than gravity. The fact, too, that there are significantly fewer gravity data off-axis from the detailed profiles, limits the ability of gravity data to resolve small-scale features, rendering the gravity method most effective at resolving broad, deep crustal structures on a regional map scale.

To aid interpretation of gravity and magnetic data, we have applied several filtering and derivative methods that help to delineate structures and to constrain the depths and geometry of sources. Features of interest include: intrabasin and basin-bounding faults, pre-existing crustal structures that could have guided extension and magmatism associated with the hotspot, intrusive bodies that may have fed early SRP volcanism, or calderas emplaced during passage of the hotspot.

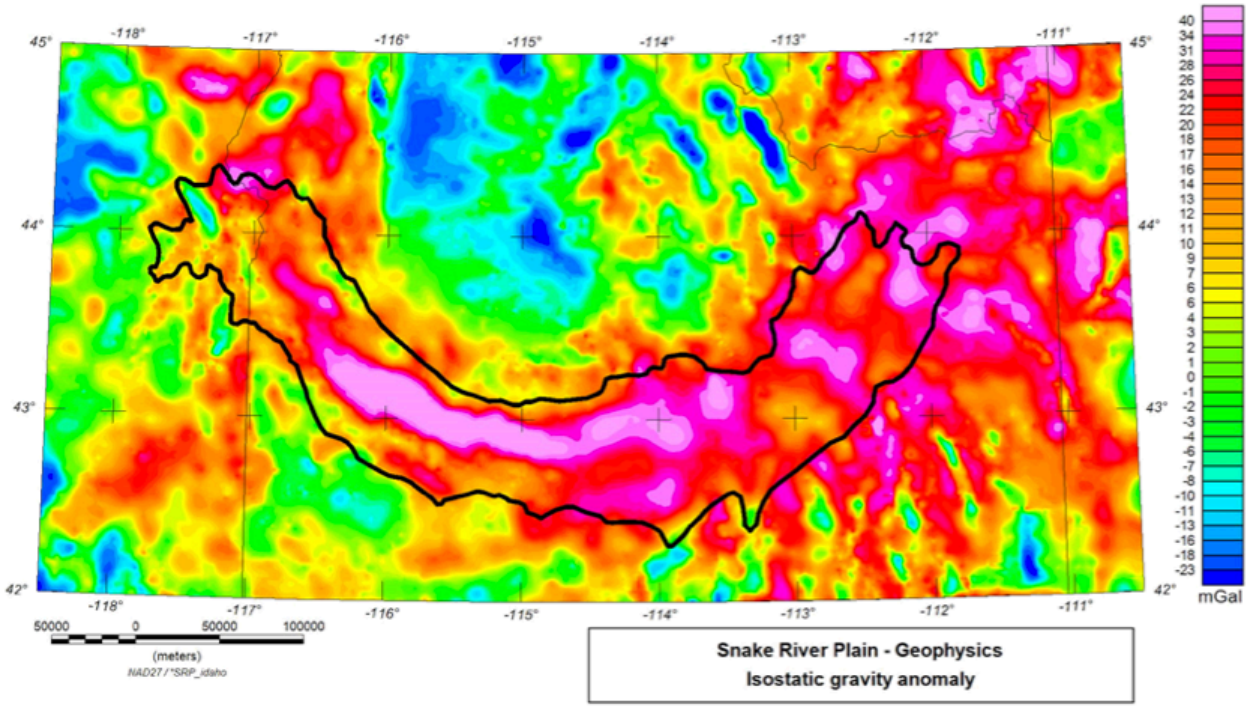

Figure 5-5. Map of isostatic gravity. Outline of SRP topographic depression is shown for reference.

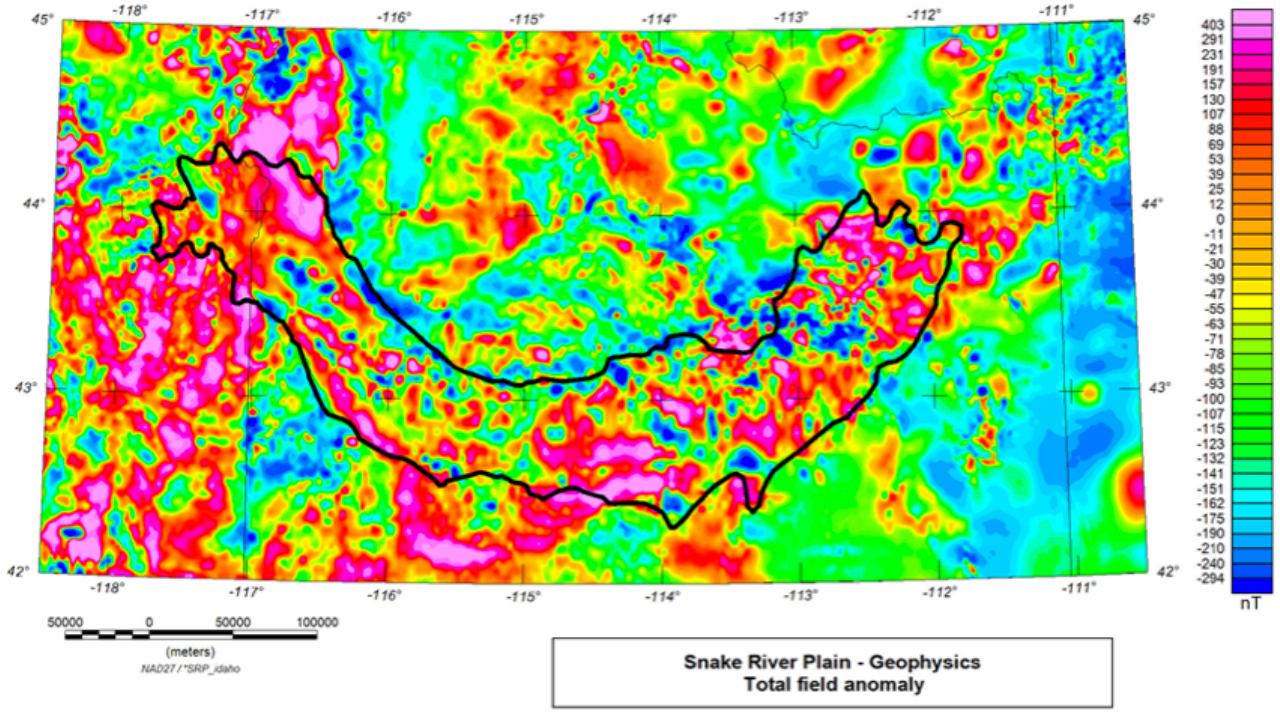

Figure 5-6. Map of Total magnetic field anomaly. Outline of SRP topographic depression is shown for reference.

Reduction-to-the-magnetic-pole

Because the regional magnetic field and the direction of magnetization are seldom vertical, magnetic anomalies are commonly laterally displaced from their sources and may have distorted, asymmetrical shapes. This effect often increases the complexity and difficulty of magnetic anomaly interpretation. A reduction-to-the-magnetic-pole (RTP) transformation and resulting map (Figure 5-7) removes the effect of the direction of the earth's magnetic field and the direction of magnetization by transforming the data to their expression at a vertical field and magnetization as if measured at the north magnetic pole. This can help interpretation of magnetic anomalies because it approximately centers magnetic anomalies over their causative sources and will produce a symmetrical anomaly over a symmetrical source. However, it assumes that remanent magnetization is either negligible or in the same direction as the Earth's magnetic field (valid for induced magnetization or, recent volcanic terrain, or rocks whose remanence is dominated by an expected normal overprint). A more detailed discussion of reduction to the pole can be found in Baranov and Naudy (1964) and Blakely (1995).

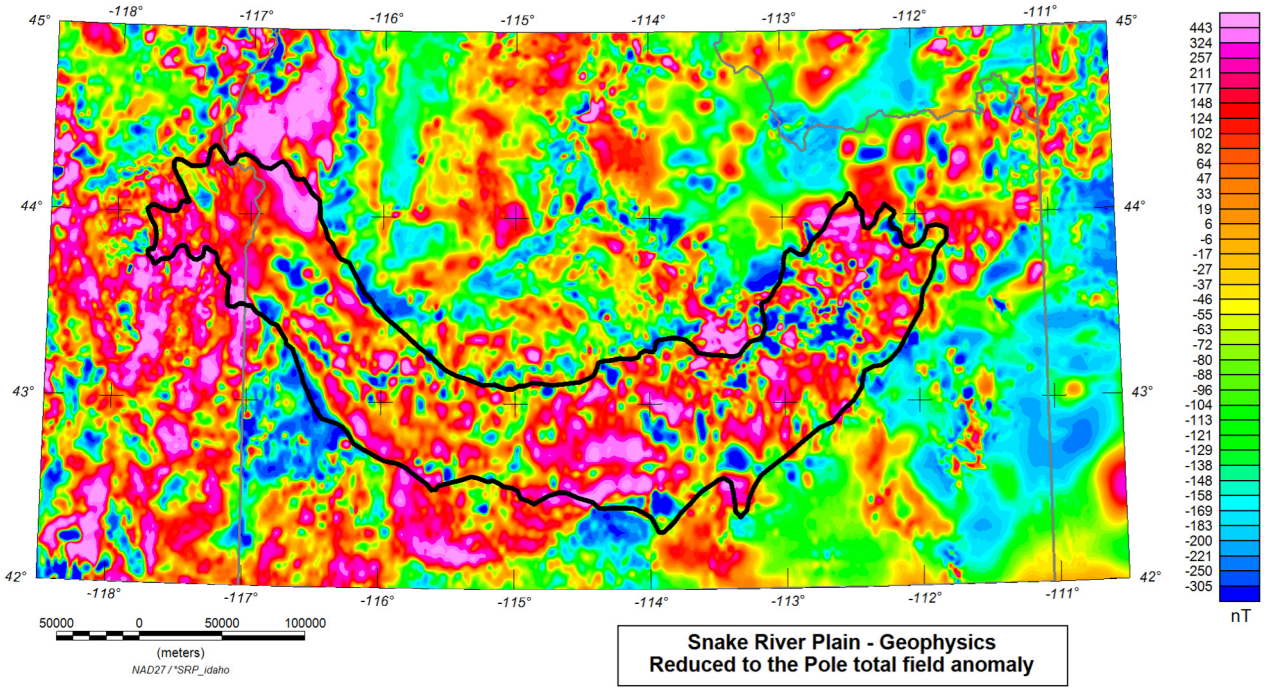

Figure 5-7. Map of Total magnetic field anomaly. Outline of SRP topographic depression is shown for reference.

Residual maps

A simple tool for emphasizing near-surface sourced anomalies is to upward continue a potential field grid, which retains information on the regional field, and subtract this from the original grid. In so doing, the long-wavelength anomaly field is removed, leaving the short-

wavelength field that originates in the shallow subsurface. It should be noted that this practice will result in removing any low-frequency content that may arise from shallow, but broadly-distributed features. In general, however, this can be taken into account since any widely-extensive but shallow units should be identified by mapping. Examples of residual magnetic and gravity maps for the central and western SRP are given in Figures 5-8 and 5-9, respectively.

Magnetic Potential (pseudogravity)

Crustal magnetism differs from, and is more complex than, gravity which varies due simply to the crustal density distribution. Magnetism varies because of differences in both the concentration and type of magnetic minerals within the crust (analogous to the relation between density and gravity), and crustal remanent magnetization. Furthermore, because crustal magnetization is seldom vertical, except at the magnetic poles, anomalies are asymmetric and not centered over their sources. Magnetic data also tend to highlight shallower features than gravity, because magnetic field strength attenuates more significantly with distance to the source than does gravity.

Because of this complexity, magnetic anomalies can be difficult to interpret and to compare with gravity. The pseudogravity (Figure 5-9) or magnetic potential transformation (Baranov, 1957; Blakely, 1995) removes asymmetry of anomalies (leading to anomalies that more effectively lie centered over their sources). In addition, it helps highlight regional magnetic features masked by high-frequency anomalies.

The magnetic and gravity potentials are related by a directional derivative, thus the total magnetic field can be transformed into an equivalent gravity field. Magnetic potential, or pseudogravity, maps are produced by the transformation of the magnetic field into the equivalent gravity field assuming a density distribution equal to the magnetization distribution (Baranov, 1957). The ratio between magnetization and density is held constant (in this application, the ratio is a magnetization contrast of 0.001 cgs-units to a density contrast of 0.10 g/cm^3), and, remanent magnetization is assumed to be either negligible or in the same direction as the Earth's magnetic field. This process amplifies long wavelengths (deeper sources) at the expense of short wavelengths (shallow sources). The pseudogravity transformation is a useful tool because it simplifies the interpretation of magnetic anomalies and allows for easier comparison of regional gravity and magnetic features. In addition, because gravity anomalies have their steepest gradients approximately over the edges of their causative sources, especially for shallow sources, the magnetic potential map can be used to approximate the edges of magnetic sources (Blakely, 1995). While this method significantly simplifies the interpretation of magnetic sources, its underlying assumptions (e.g., remanence is negligible) can limit its use. A map of the magnetic potential for the study area is shown in Figure 5-10.

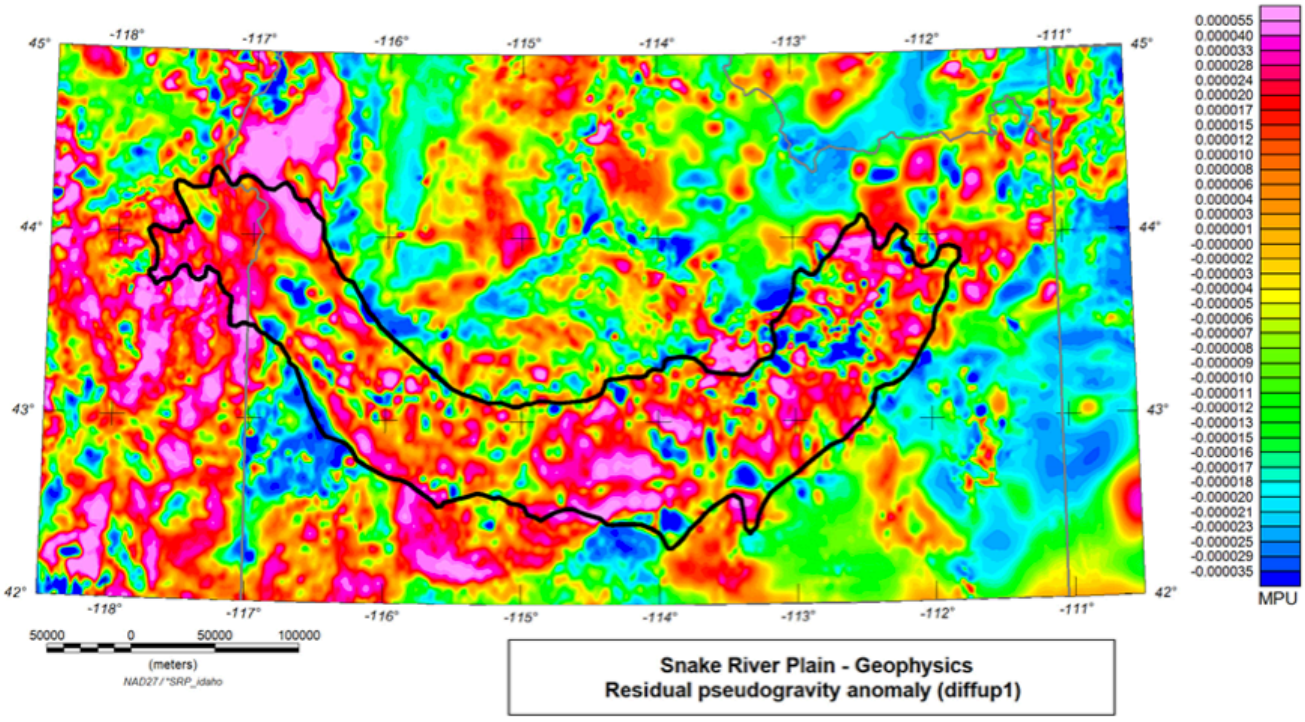

Figure 5-8a. Map of residual pseudogravity for the central and western SRP. Contours are shown to highlight anomalies.

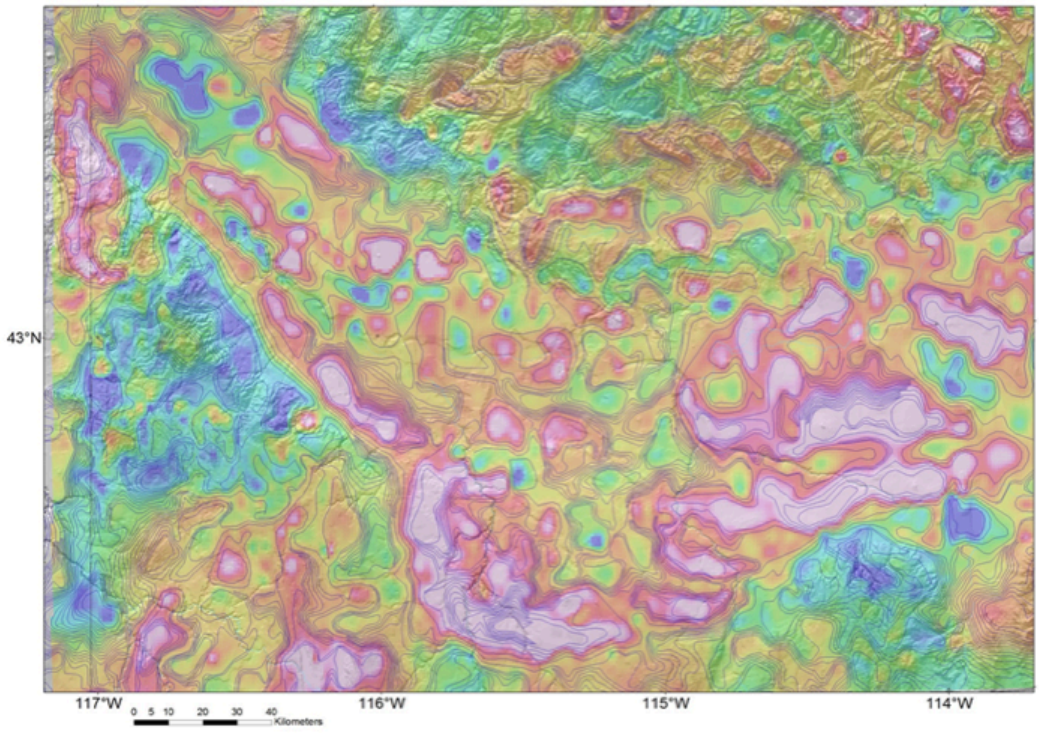

Figure 5-8b. Map of residual pseudogravity for the central and western SRP. Contours are shown to highlight anomalies.

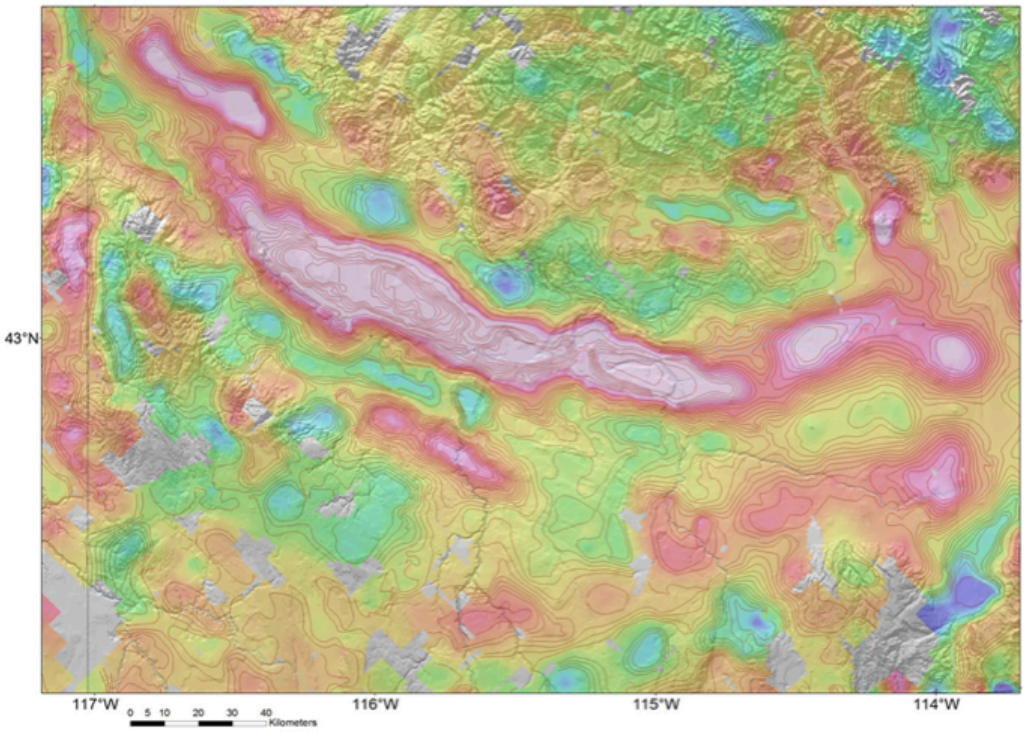

Figure 5-9a. Map of residual isostatic gravity for the central and western SRP. Contours are shown to highlight anomalies.

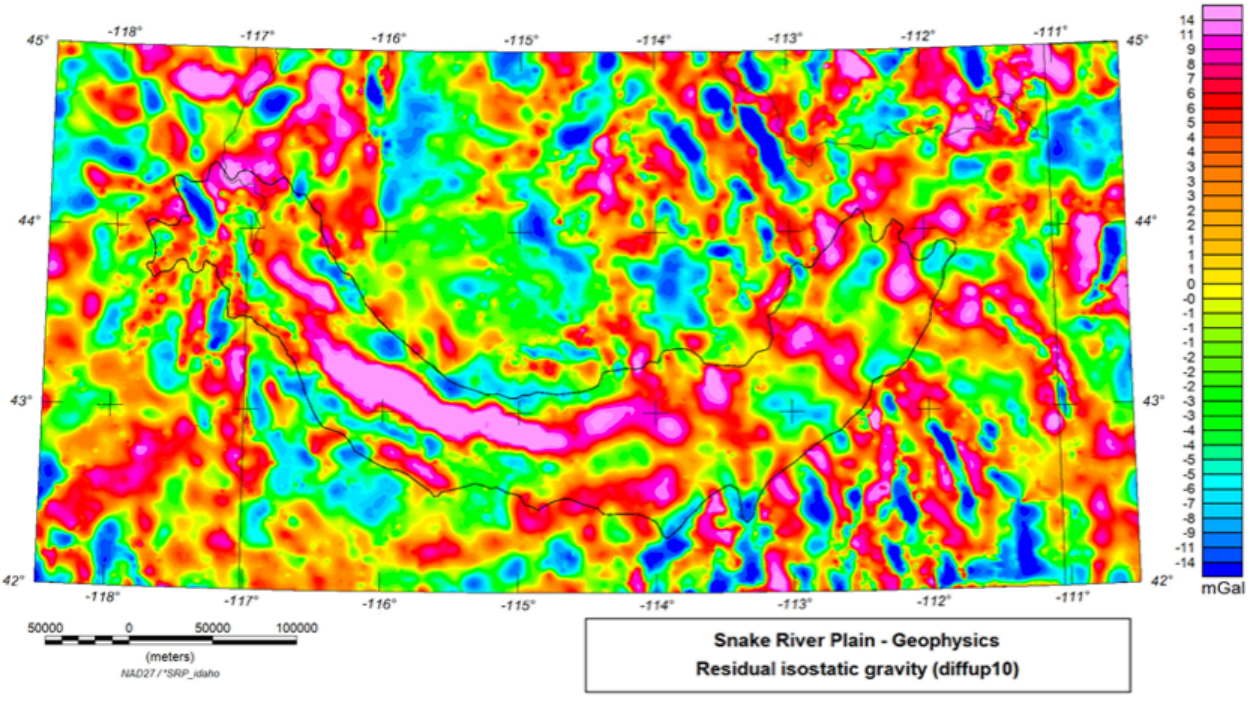

Figure 5-9b. Map of residual isostatic gravity. Outline of SRP topographic depression is shown for reference.

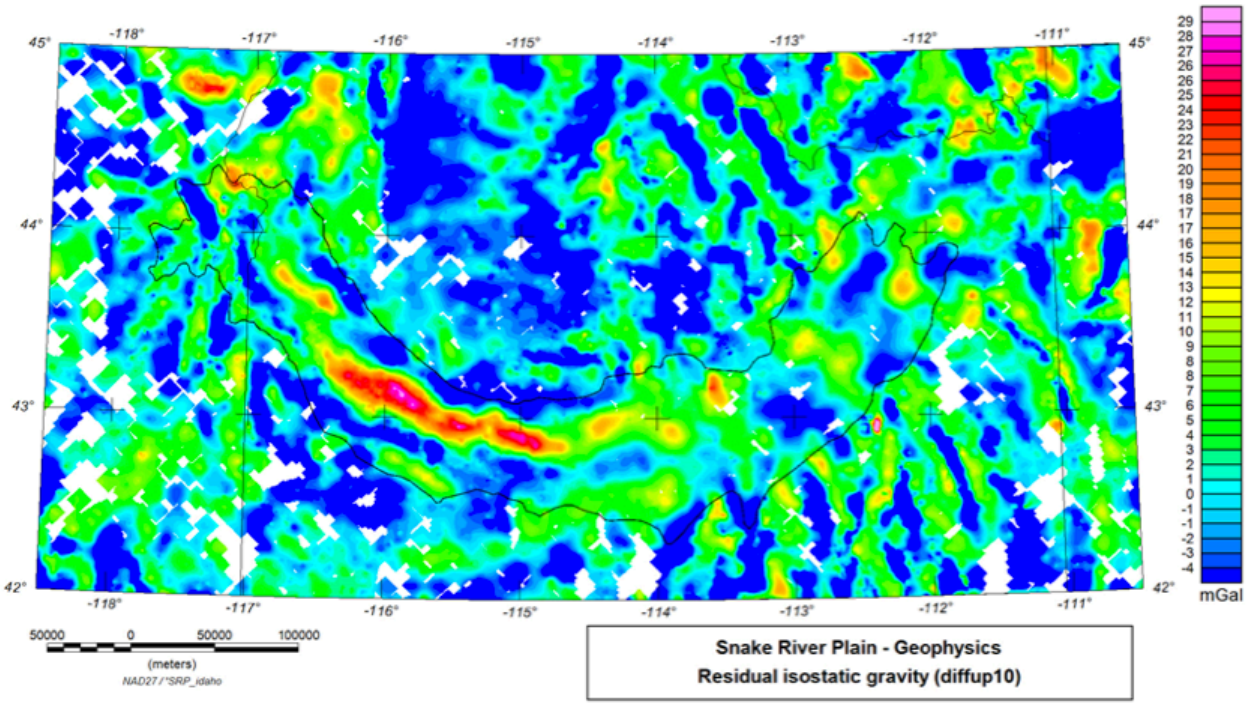

Figure 5-9c. Map of residual isostatic gravity. Outline of SRP topographic depression is shown for reference. This plot differs from 5-9b in the color range scale and gridding specifications to highlight the central gravity high in the western SRP.

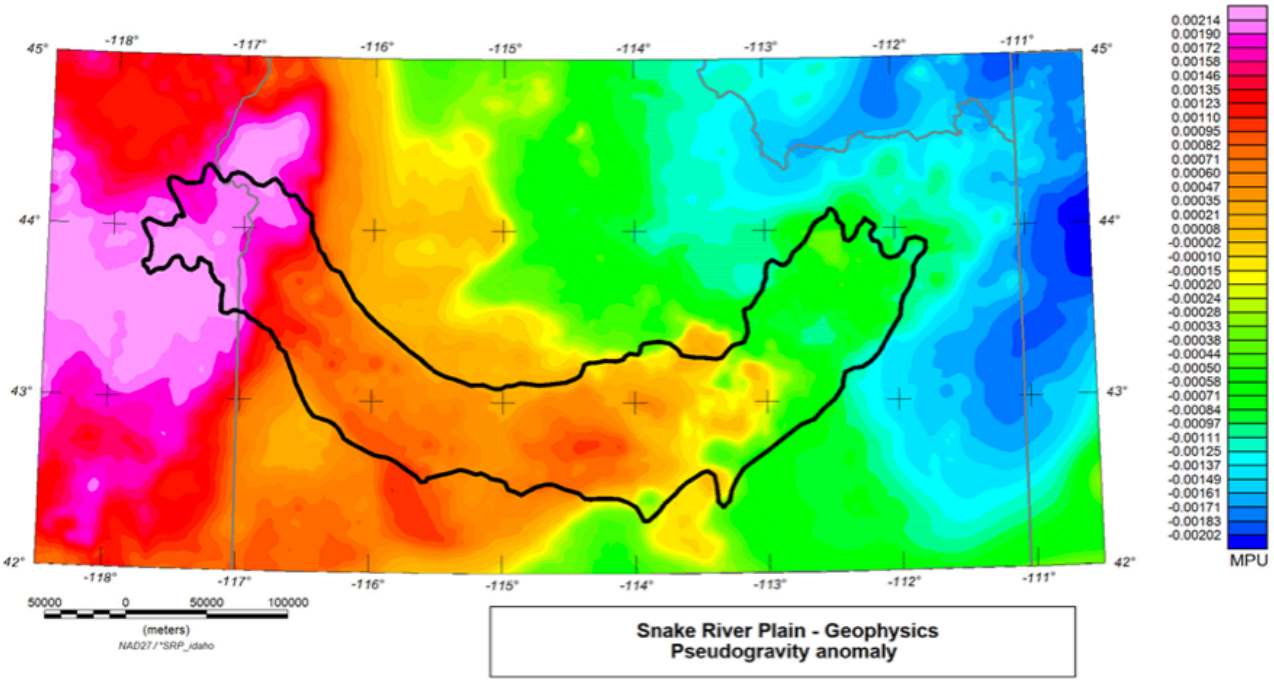

Figure 5-10. Map of pseudogravity. Outline of SRP topographic depression is shown for reference.

Maximum Horizontal Gradients

Maximum horizontal gradients (MHG; Blakely and Simpson, 1986) reflect abrupt lateral changes in the density or magnetization of the underlying rocks, and tend to lie over the edges of bodies with near vertical boundaries (Cordell and McCafferty, 1989; Grauch and Cordell, 1987). They are calculated for both gravity and magnetic data to estimate the extent of buried sources, and to define the boundaries of geophysical domains, and internal domain structures.

Match Filtering

Another method we have employed is a matched bandpass filtering technique (Syberg, 1972; Phillips, 2001) applied to the frequency spectrum of gravity and magnetic data (Figures 5-11 and 5-12, respectively), that allows anomalies arising from different crustal levels to be isolated, provided that the depths of anomaly sources are sufficiently distinct.

The longest wavelength band reflects variations in density and magnetization of the deepest sources. The intermediate bandpass layers represent sources from intermediate to shallow depths that may outcrop at the surface. The shallowest layer, resulting from the highpass filter and reflecting the shortest wavelength anomalies, is due to sources at the surface or in the shallow sub-surface. It is apparent that some anomalies in this layer also result from noise in the data (e.g. aeromagnetic survey boundaries). Despite this, even the shallowest layer appears to resolve coherent fabrics that may be used to distinguish regional domains and structures. As with residual maps, however, it is important to keep in mind that broad anomalies might arise from uniform, thin, extensive, but shallow rocks.

Curie temperature depth calculations

We have applied a recently-developed method for mapping depth to the Curie-temperature (Tc) isotherm from magnetic anomalies (Bouligand et al., 2009) in an attempt to provide a measure of heat flow in the Snake River Plain. Such methods are based on the estimation of the depth to the bottom of magnetic sources assumed to correspond to the temperature at which rocks lose their spontaneous magnetization. The method is based on the spectral analysis of magnetic anomalies that incorporates a representation where magnetization has a fractal distribution defined by three independent parameters, the depths to the top (zt) and bottom (zb) of magnetic sources and a fractal parameter (b) related to the geology. Depths (zt and zb) are obtained assuming a constant fractal parameter and applying a sliding window swept across the study area to compute the radial power spectrum. In order to obtain discrete values within the SRP that are not influenced by regions outside the plain, we applied a window size of 50 km (note that Bouligand et al., 2009 used window sizes of 100-200 km).

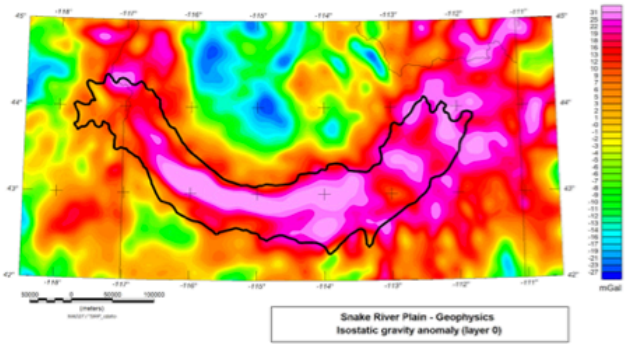

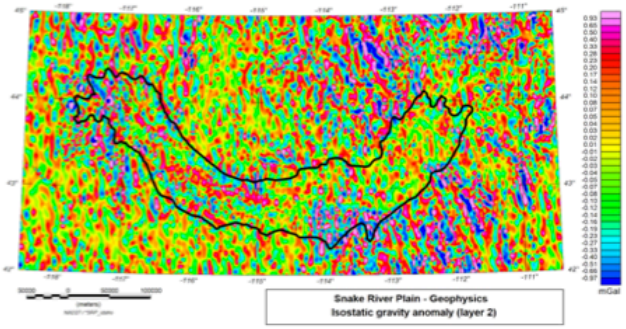

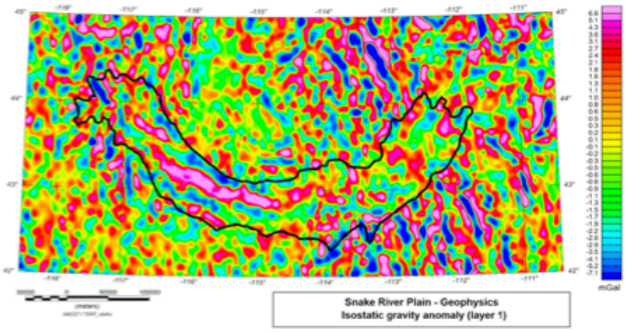

Figure 5-11. Match-filtered maps of isostatic gravity for the central and western SRP showing deep (lower left), intermediate (lower right) and shallow (upper right) depth layers. Depths correspond nominally to 14, 5, and 2.25km respectively.

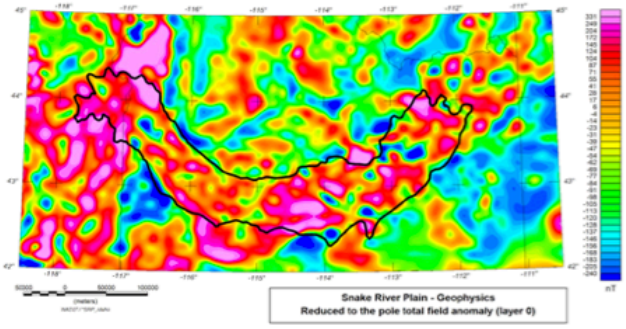

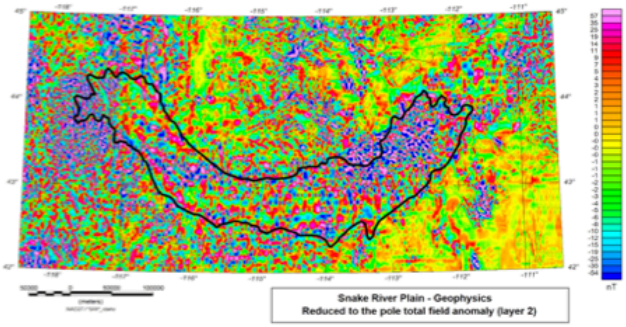

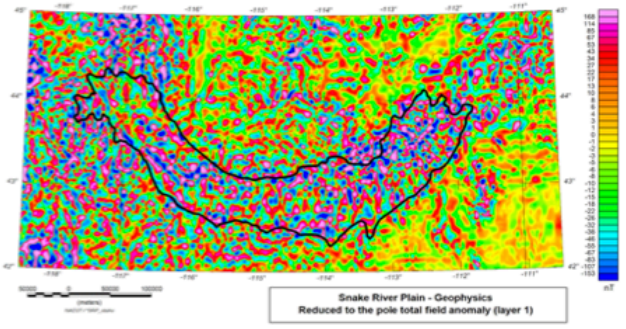

Figure 5-12. Match-filtered maps of the magnetic reduced to pole field for the central and western SRP showing deep (lower left), intermediate (lower right) and shallow (upper right) depth layers. Depths correspond nominally to 14.5, 4, and 1.5km respectively.

The resulting depth to the bottom of magnetic sources shows some features that broadly correlate with prominent heat-flow anomalies, such as the Battle Mountain High (BMH, Sass et al., 1971). The estimated values for the Tc depth, however, are unrealistically shallow (few km; Figure 5-13), possibly arising from our having used a window size that is too small to recover

low wavenumbers in the radial power spectrum [we note that Bouligand et al., 2009, reported Tc depths of 10-15 km for the BMH, and 15-23 km for the Eastern Snake River Plain using a window size of 100 km].

A more likely explanation for the shallow depths is that the bottom of magnetic sources reflect a lithologic contact as opposed to the depth to the Tc isotherm. The methodology assumes a model of crustal magnetization composed of a single layer of fractal random magnetization. If a layer of strongly magnetic volcanics such as basalt were to overly very weakly magnetic basin sediments or tuff, the magnetic signal due to the basalts may mask the magnetic signal due to weaker underlying units. If this is the case for the SRP, the method could provide an estimate of the thickness of superficial volcanic rocks. Further work incorporating independent geophysical and geologic datasets will be needed to assess whether the method can effectively be used to map basalt thicknesses.

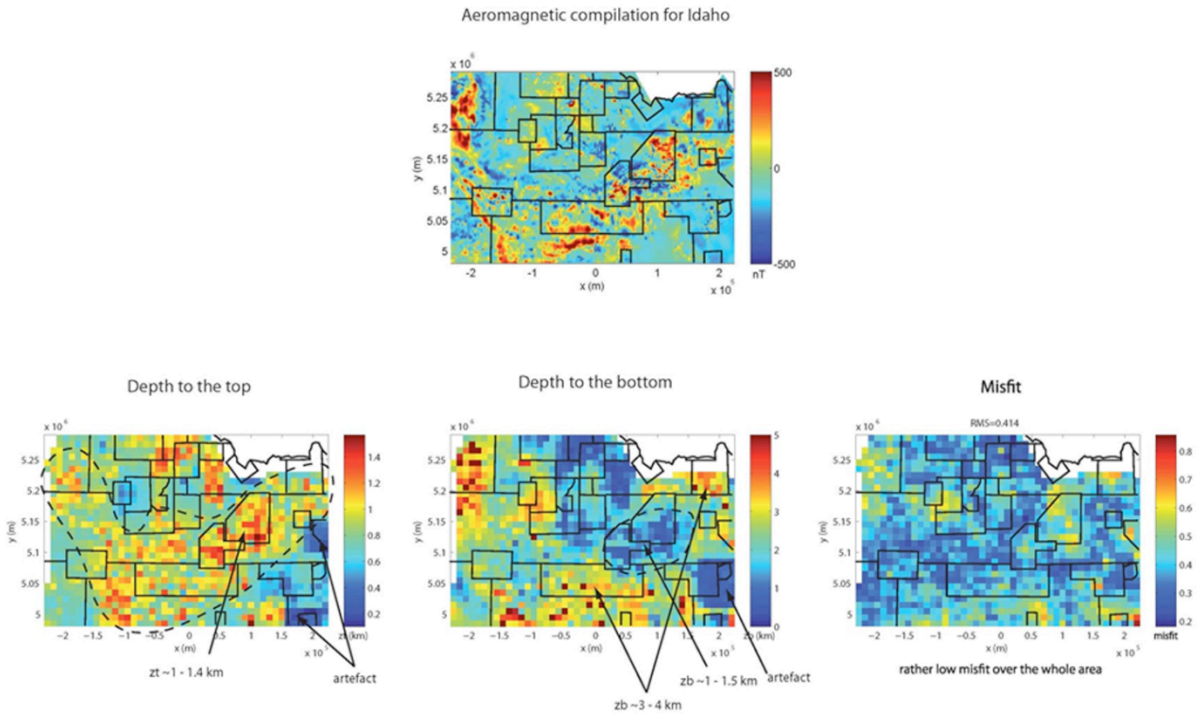

Figure 5-13. Results from depth-to-source calculations performed on the Idaho State aeromagnetic compilation grid showing: original aeromagnetic grid (top), depth to top (lower left), depth to bottom (lower center), and misfit (lower right). Superimposed on each map is an outline of the individual surveys used to construct the compilation. In some places (noted on figure) there appear to be artifacts resulting from the contrasting survey specifications.

Alteration Mapping

The distribution of hydrothermal alteration can be an important parameter for understanding the evolution of geothermal systems. Unfortunately, the extent of alteration in the subsurface can be grossly underestimated by geologic mapping or remote sensing methods that are restricted to surface exposures. As a result, extensive subsurface alteration often remains hidden, significantly limiting exploration efforts to characterize the potential of undiscovered geothermal resources.

As part of our research for this project, we developed geophysical methods for mapping alteration that do not rely on surface outcrops. Due to the fact that hydrothermal alteration modifies the magnetic properties of the volcanic substratum, magnetic methods can be used to constrain the 3-dimensional (3D) distribution of hydrothermal alteration at depth. To test these methods we applied them to areas in Yellowstone National Park where several well-developed hydrothermal systems occur, surface exposures of alteration have been extensively mapped, and a high-resolution aeromagnetic survey is available (U.S. Geological Survey, 2000). The aeromagnetic map of the park (Figure 5-4) reveals that areas of hydrothermal activity and surface alteration are commonly characterized by magnetic lows. This was noted by Finn and Morgan (2002) who suggested that the lows result from a significant decrease of the substratum magnetization associated to hydrothermal alteration.

We selected four thermal areas for study that display these magnetic lows associated with hydrothermal alteration (Figures 5-4, 5-14): area 1 along Firehole River, area 2 around Smoke Jumper Hot Springs, area 3 in Norris Geyser Basin, and area 4 (which is a subarea of area 1) around Lone Star Geyser. These hydrothermal areas have different characteristics in terms of topography, nature of surrounding rocks, hydrothermal water chemistry, occurrence and composition of hydrothermal deposits, and nature of hydrothermal alteration reactions.

In addition to applying our analyses to airborne data, we also collected ground-based magnetic surveys to provide more detailed mapping of magnetic anomalies, and to better understand the relationship between magnetic lows and hydrothermal alteration. Magnetic grids constructed from airborne and ground-based data were used to invert the distribution of magnetization, relying on various simplifying assumptions and taking the topography into account. These models were used to infer the distribution of hydrothermal alteration.

Ground magnetic data reveal that high-amplitude, short-wavelength anomalies, typical of unaltered volcanic terrain are significantly smoothed and subdued over volcanic substrata demagnetized by hydrothermal alteration (Figure 5-14). This is an important observation that provides a new tool for mapping areas of hydrothermal alteration by searching areas characterized by amplitudes lower than a regional threshold.

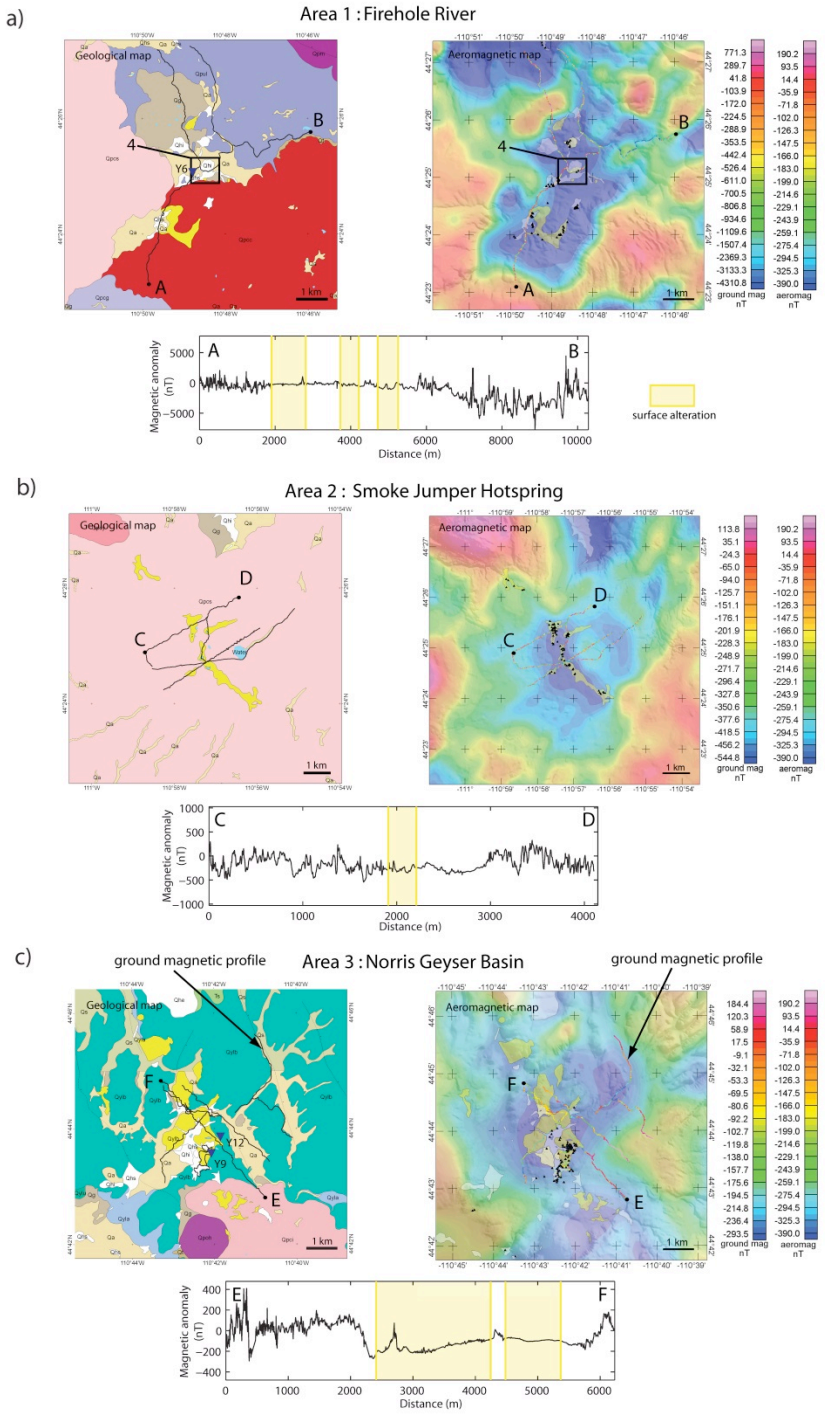

Figure 5-14. Geologic map (left), aeromagnetic map (right) and one ground magnetic profile (bottom) for study areas 1-3: Firehole river (a), Smoke Jumper Hot Springs (b), and Norris Geyser Basin (c). Areas of hydrothermal alteration and deposits are located by yellow and white polygons on both geological and aeromagnetic maps. Endpoints of displayed magnetic profiles are indicated by letters (AB, CD or EF). Extent of surface alteration (deduced from the geologic map) along these profiles is represented in yellow. Location of study area 4 (Lone Star Geyser) is indicated by a black square.

The application of inverse methods to high-resolution airborne and ground magnetic grids yielded three-dimensional models of the distribution of magnetization and geometry of hydrothermal alteration. This revealed that the largest degree of demagnetization (alteration) and maximum thicknesses of demagnetized (altered) substratum, reaching a few hundred meters, are associated with hydrothermal vents and with superficial hydrothermal alteration (Figure 5-15). Our three dimensional models of magnetization provide estimates of the volume of buried hydrothermal alteration ranging from 10 to 20 km^3 buried within each of our 10 x 10 km^2 study areas.

Within the three hydrothermal sites that we investigated in Yellowstone National Park, subdued short-wavelength signals indicate pervasive demagnetization (alteration) of the shallow substratum that extends over larger areas than initially mapped by geology. In addition, magnetic lows observed in the aeromagnetic survey and the damped short-wavelength signals observed in ground magnetic profiles over areas of hydrothermal activity and alteration indicate that demagnetization occurs in both the shallow and deep substratum within all the investigated areas including both liquid- and vapor-dominated systems.

This demonstrates a valuable tool for geothermal exploration and the study of active geothermal systems. It also suggests that these methods should be useful for characterizing the mineral potential of fossil hydrothermal systems that may host epithermal ore deposits.

Discussion

Gravity

In general, isostatic gravity anomalies reflect lateral density variations in the middle to upper crust and can be used to infer changes in lithology, or identify features, such as faults, calderas, granitic basement, mafic intrusives, or sedimentary basins. Regionally the SRP is characterized by elevated average gravity values relative to surrounding regions, reflecting infilling by dense mafic volcanic rocks and related intrusive rocks, and possibly significant amounts of mafic underplating related to SRP magmatism.

Superimposed on this regional high is a prominent central gravity high extending along the western and central SRP (features g3-g7, Figure 5-16). In the deep layer of the match-filtered gravity (Figure 5-11) this appears as an arcuate high that sweeps continuously from western through central SRP. Detailed profile data help to illuminate the finer details of this feature and reveal that it actually consists of several segmented anomalies (Figures 5-8b, 5-9c). Intermediate and shallow layers of the match filtered gravity suggest that western and southern SRP segments are not part of the same feature, since there is an abrupt break in the anomaly corresponding with a change in the trend of segments (from NW-trending in the

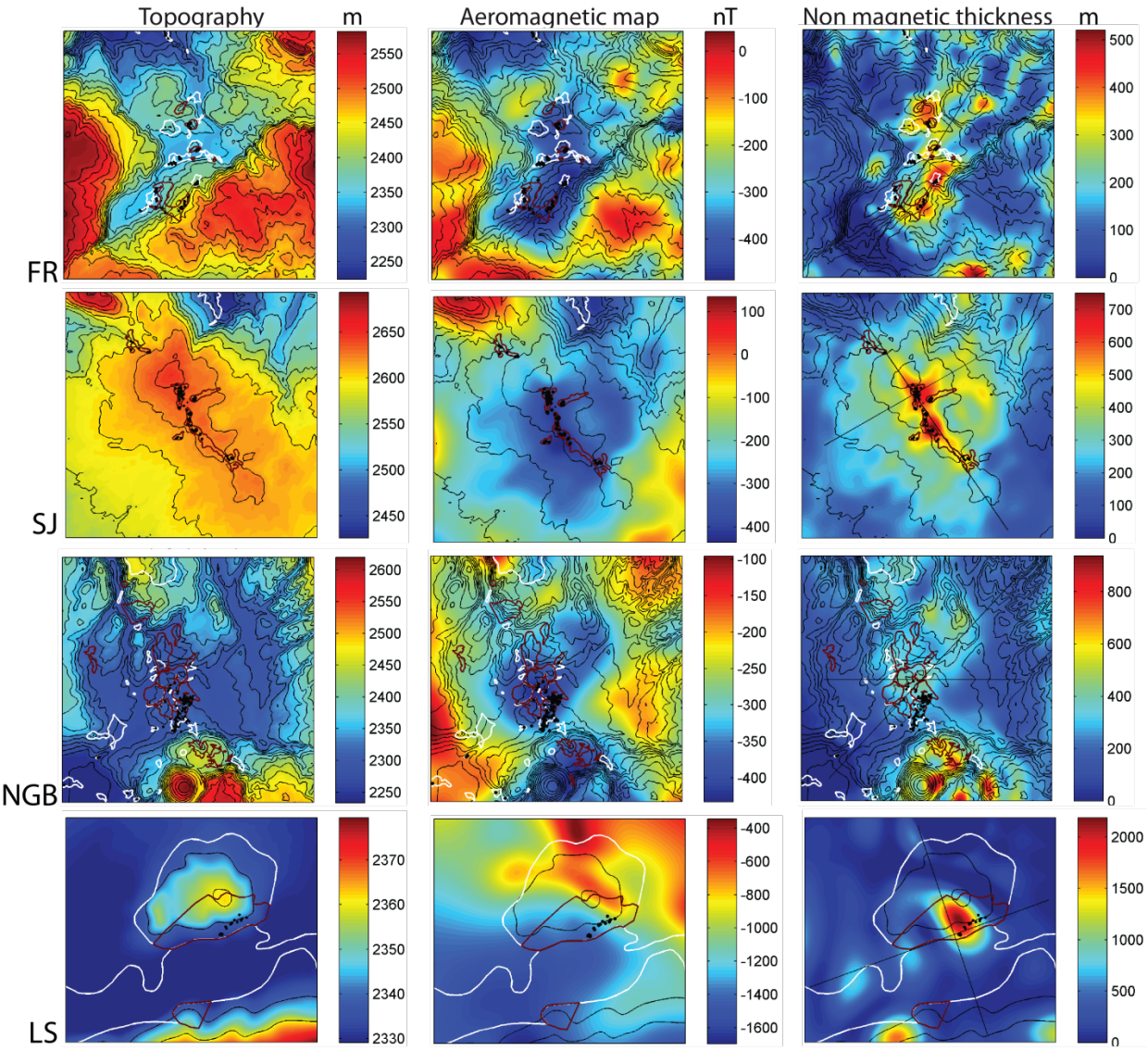

Figure 5-15. Alteration maps for (top to bottom): area 1 (Firehole River), area 2 (Smoke Jumper Hotsprings), area 3 (Norris Geyser Basin), and area 4 (Lone Star Geyser), presented at a constant elevation level (2855 m, 2940 m, 2885 m, 2402 m, respectively for the four areas). (from left to right): topography, observed aeromagnetic anomaly (not reduced to the pole), and non-magnetic thickness computed assuming a constant magnetization of 3 A/m. Magnetization direction is supposed to be those of a GAD field. Hydrothermal alteration and deposits are indicated by brown and white thick lines, respectively. Thermal springs are located by black dots. Black lines are topographic contours represented with a 20 m spacing.

western SRP, to NE-trending in the southern SRP). It is noteworthy that the segments of the high appear to be distributed in a left-stepping en echelon fashion that would suggest a possible oblique WNW shear. They also have a NW orientation that is significantly more northerly in orientation than the overall WNW trend of the regional gravity high defined by the string of highs g3-g5 (Figure 5-16). This NW orientation is much more closely aligned with the trend of magnetic anomalies in the western SRP (feature m2, m3, m4, m6, Figure 5-17) and

with several other smaller gravity anomalies (features g1, g9, Figure 5-16). In several places, these features closely coincide with Quaternary faults (Figure 5-18) suggesting the deep-seated sources may be influencing active faulting.

A small northwest-trending gravity high at the top of the western SRP (feature g1, Figure 5-16) has been interpreted as a horst block, based on seismic and deep drill hole data (Wood, 1994). This corresponds with a prominent magnetic low (feature m3, Figure 5-17) suggesting that it probably consists largely of reversely magnetized flows. Another NW-trending gravity high occurs along the western margin of the western SRP (feature g9, Figure 5-16) that may also represent a fault block with very similar size and orientation. In fact all three segments (g1-g3) have similar geometries and orientation suggesting they are structurally controlled. It may also indicate that they formed at the same time or under similar regional stress regimes, or were influenced by the same regional structural fabric.

Along the margins of the central gravity high are several gravity lows that likely arise from a range of different sources. A few examples include sedimentary basins containing low-density alluvial fill that occur along the northeastern margin of the western SRP (feature g2, Figure 5-16), caldera filled with low-density tuff (feature g10, Figure 5-16), and granitic basement outcropping southwest of the western SRP (feature g8, Figure 5-16).

The central SRP (and region immediately to the south) is dominated by three prominent WSW-trending gravity highs (features g6, g12, g13, Figure 5-16) and intervening low (feature g10, Figure 5-16) that closely resemble the trend of a sequence of magnetic highs (features m10, m11, m9, m7, Figure 5-17), suggesting a common regional significance that may relate them in age and origin, or link them through a common regional stress field or through influence by a pre-existing structural fabric.

Magnetics

In general, magnetic anomalies reflect lateral variations in magnetic sources in the middle to upper crust that can arise from changes in lithology, or structures such as faults or contacts that juxtapose units with contrasting rock properties. Short-wavelength and high-amplitude magnetic anomalies typically reflect shallow volcanic rocks that are moderately to strongly magnetic. Strongly magnetic volcanic and associated intrusive rocks filling the SRP produce a regional high that is punctuated by numerous large amplitude, short-wavelength anomalies. This contrasts sharply with the more subdued anomaly pattern north and south of the plain. Discrete anomalies (10's-100 km wide) may reflect buried structures or intrusive bodies (e.g., dike swarms, fault blocks, calderas, plutons). Magnetic lows may be associated with reversely magnetized units (feature m3, Figure 5-17), altered volcanic rocks, silicic intrusions or basement rock, weakly magnetic volcanic tuff, or sedimentary rocks.

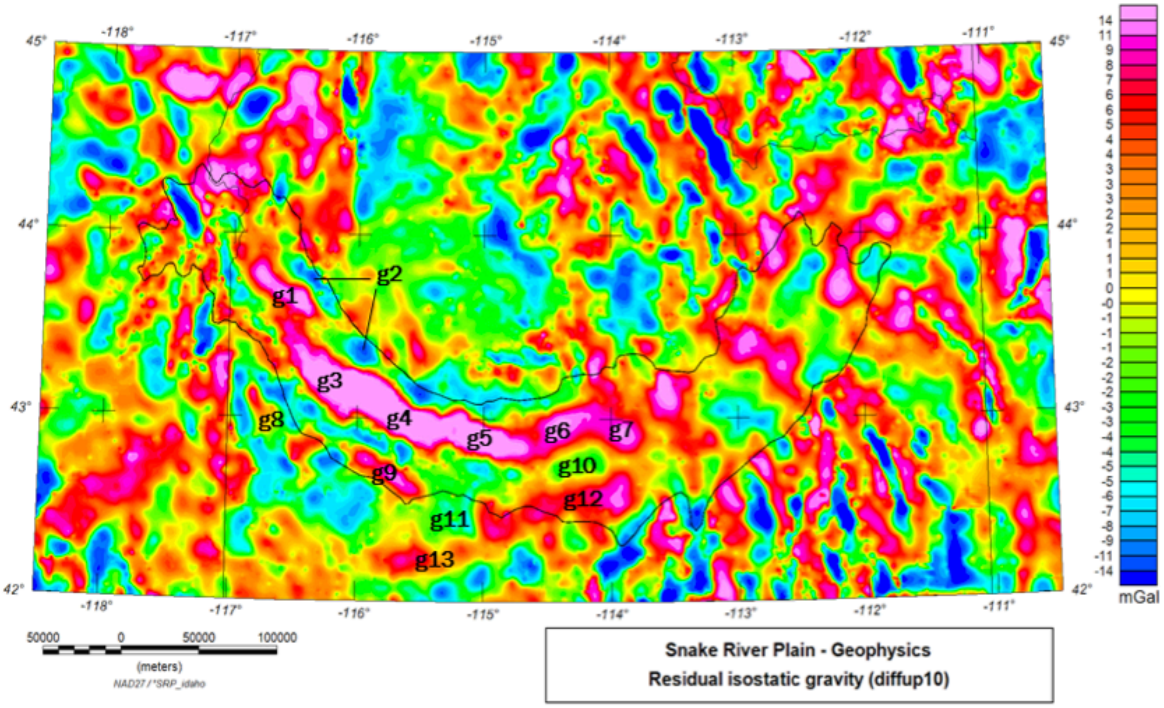

Figure 5-16. Map of isostatic gravity. Several features discussed in text are labeled. Outline of SRP topographic depression is shown for reference.

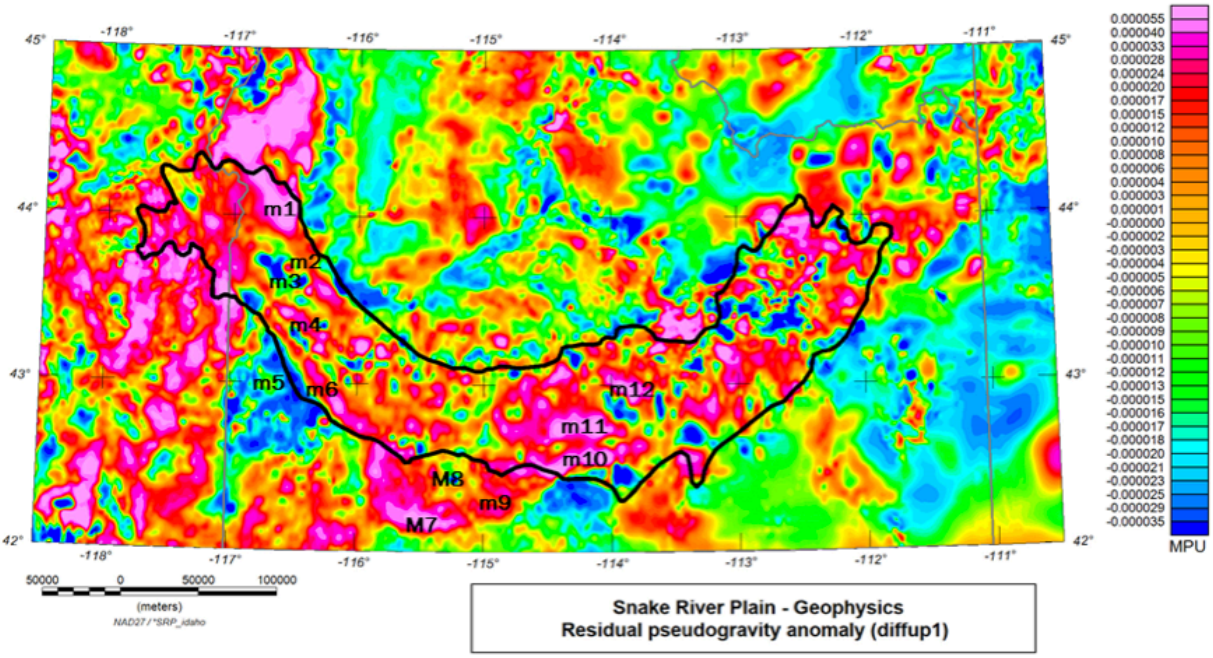

Figure 5-17. Map of residual pseudogravity. Several features discussed in text are labeled. Outline of SRP topographic depression is shown for reference.

Prominent long-wavelength magnetic highs extending north from the northern end of the western SRP occur over Tertiary volcanics related to the Columbia River Basalt Group. Likewise, prominent highs in eastern Oregon (southwest of the northern end of the SRP) are due to outcropping strongly magnetic Quaternary and Tertiary volcanics.

The western SRP is characterized by a dominant NW-trending fabric that includes several narrow linear magnetic highs (features m2 and m6, Figure 5-17) and lows (feature m4, Figure 5-17). Aside from these discrete linear highs, the western plain reflects a relatively lower magnetic relief than the eastern SRP, that is likely due in part to a thicker section overlying sediments. Prominent NW-trending highs along the margins of the western plain (features m2 and m6, Figure 5-17) resemble anomalies in northern Nevada that are due to mid-Miocene mafic dike swarms thought to be related to inception of the Yellowstone hotspot (Glen and Ponce, 2002) and have a common origin.

The central SRP (and region immediately to the south) is dominated by a sequence of relatively long-wavelength EW-trending elongate magnetic highs (features m10, m11, m9, m7, Figure 5-17). This broad regional similarity may indicate these features are similar in age and origin, or linked through a common regional stress field or through influence by a common pre-existing structural fabric.

A prominent triangular low southwest of the western SRP (feature m5, Figure 5-17) is coincident with a moderate gravity low (feature g8, Figure 5-16) of the same general size and is located over Mesozoic intrusive rocks possibly related to the Idaho Batholith. Another low (feature m8, Figure 5-17) and corresponding gravity low (feature g11, Figure 5-16) are situated over the inferred center of the Bruneau-Jarbidge caldera suggesting these anomalies may be due to infilling of low density, weakly magnetic volcanic tuff. Magnetic and gravity highs along the margin of this low (feature g13, m4, Figures 5-16 and 5-17) may reflect dense, magnetic intrusions related to emplacement of the caldera.

The regional field depicted by the deepest match filtered layer of pseudogravity reveals a string of anomaly highs extending across the eastern SRP (Figure 5-19). These highs are similar in size, and roughly correlate with, the inferred eastern SRP calderas including Bruneau-Jabridge, Twin Falls, Picabo, and Heise volcanic fields. It is noteworthy that this regional magnetic trend follows southwestward along the track of calderas and may also image the northeastern end of the Owyhee-Humbolt field at the edge of the state magnetic grid.

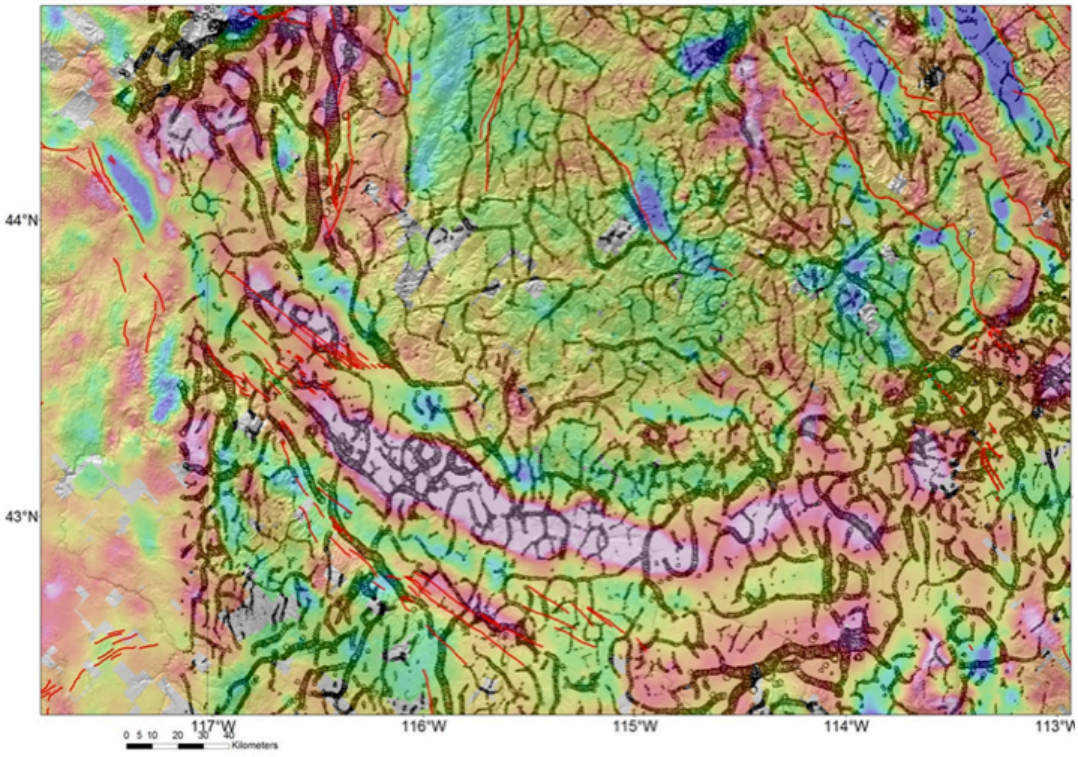

Figure 5-18. Map showing the residual isostatic field for the central and western SRP overlain with maximum horizontal gradients (circles sized to magnitude of MHG) that reflect the edges of gravity sources, and Quaternary faults (red lines).

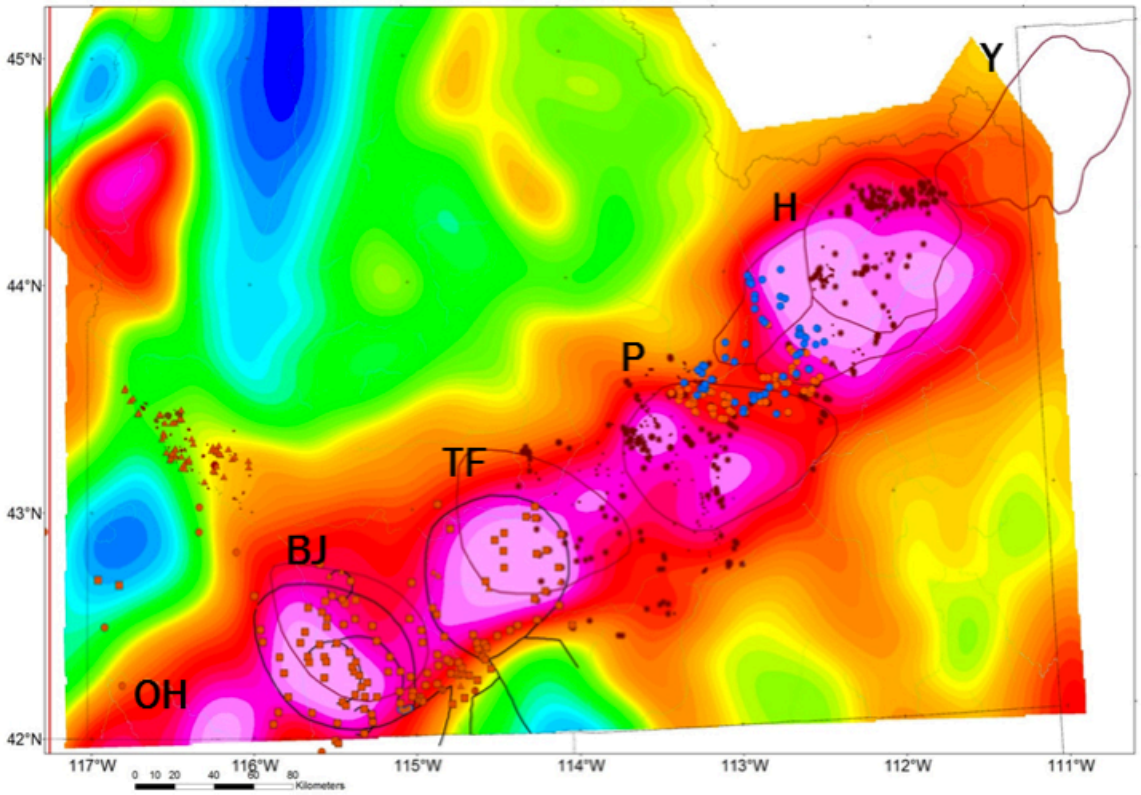

Figure 5-19. Map of the deepest match-filter layer of the pseudogravity of the Idaho state compilation (corresponding to ~15.5 km depth). Also shown are various mapped vents (symbols) and interpreted outlines of caldera boundaries (including OH – Owyhee-Humboldt, BJ – Bruneau-Jarbidge, TF – Twin Falls, P – Picabo, H – Heise, and Y – Yellowstone volcanic fields). Brown outlines are caldera boundaries from Pierce and Morgan (1992). Black outlines show caldera boundaries for BJ and TF calderas after Bonnichsen and Godchaux (2002).

Summary

We have performed potential field studies in the Snake River Plain to provide regional geophysical mapping to characterize mid- to shallow-crustal features. This involved compiling and reprocessing existing gravity and aeromagnetic data, and collecting new gravity and rock-property data throughout the western and central Snake River Plain to provide an unprecedented high-resolution potential field dataset for assessing subsurface structure. To aid interpretation of gravity and magnetic data, we have applied several filtering and derivative methods that help to delineate structures and to constrain the depths and geometry of sources. Features of interest include: intrabasin and basin-bounding faults, pre-existing crustal structures that could have guided extension and magmatism associated with the hotspot, intrusive bodies that may have fed early SRP volcanism, and calderas emplaced during passage of the hotspot.

The potential field maps suggest:

- The western and central branches of the SRP have distinct geophysical characteristics
- The long-wavelength character of the pseudogravity field may be used to map the regional crustal extents of calderas across the eastern SRP
- The central gravity high in the western SRP is segmented suggesting the mid-lower crust may be dissected into discrete structural blocks
- These segments have trends that parallel prominent linear magnetic anomalies suggesting that magnetic and gravity sources may be related (or influenced by a common structural fabric)
- NW-trending magnetic and gravity anomalies in the western SRP are aligned with Quaternary faults suggesting that deeper crustal structures imaged by the potential field data may be controlling active faulting

In addition to our potential field mapping efforts, we developed inversion methods, using magnetic data, to model the 3-dimmensional extent of subsurface hydrothermal alteration. We tested these methods in Yellowstone National Park where hydrothermal systems are well-studied and where surface alteration has been extensively mapped. These applications demonstrate the effectiveness of this technique to study subsurface alteration of active geothermal systems, and to identify major long-lived structures that conduct subsurface fluid flow. Beyond their obvious value for geothermal exploration, these methods can also be used to characterized the mineral potential of fossil hydrothermal systems that host epithermal ore deposits.

Future work will entail:

- Two-dimensional potential field modeling along gravity profiles
- Developing a fully-3D potential field model
- Further investigation into methods for estimating depth to base of magnetic sources in order to constrain the thickness of basin-filling basalts
- The application of alteration mapping methods, developed for this project, to study hydrothermal systems within the SRP
- Continued investigation of the use of long wavelength match-filtered pseudogravity to map the extent of calderas

CHAPTER 6:

SEISMIC IMAGING AND VERTICAL SEISMIC PROFILES

Lee M. Liberty[1], Douglas R. Schmitt[2], John W. Shervais[3]

[1]Center for Geophysical Investigation of the Shallow Subsurface, Boise State University, Boise, ID 83725-1536
2Institute for Geophysical Research, Dept. of Physics, University of Alberta, Edmonton, AB T6G 2E1
[3]Department of Geology, Utah State University, 4505 Old Main Hill, Logan, UT 84322-4905

ABSTRACT

Hotspot: The Snake River Geothermal Drilling Project was undertaken to better understand the geothermal systems in three locations across the Snake River Plain with varying geological and hydrological structure. A series of surface and borehole seismic profiles were obtained at each of three sites (Kimama, Kimberly, Mountain Home). New high-resolution downhole and surface seismic data tied to drill holes related to the Snake River Geothermal Drilling Project (ICDP Project Hotspot) provide insights into stratigraphy and test the capabilities of seismic imaging in volcanic terranes. The downhole data at the drill sites in southern Idaho show low seismic attenuation, large seismic velocity contrasts at volcanic flow boundaries, and large near-surface static effects. Lithologic and seismic boundaries observed in borehole data tie to reflections on surface and borehole seismic images. The Kimberly site drilled through 1,958 m of mostly rhyolite, with thin sedimentary interbeds throughout the section. Sedimentary interbeds at depth correspond with slow velocity zones that relate to reflections on surface seismic profiles. Reflections observed on seismic profiles tie to flow boundaries in the upper 500 m depth. This reflection pattern suggests flow volumes from the latest eruption can be estimated with surface seismic methods. The Kimama site drilled through 1,912 m of mostly basalt with sedimentary interbeds at depth. Mountain Home drilled through 1821 m of sediments with intercalated basalt. Downhole and surface vibroseis seismic results suggest seismic reflection methods are useful to image shallow flow boundaries. High fold to obtain wide angle coverage is necessary for data acquisition. High frequency attenuation is observed at all three sites and can be countered by geophone groups to match coherent noise patterns, and a focus on lower frequency acquisition. The potential for large static effects need to be addressed in processing and with an accurate velocity model tied to borehole information, improved seismic imaging may be achieved with prestack migration methods. We recommend high fold wide angle seismic imaging methods to optimize seismic results in these complex geologic environments.

INTRODUCTION

Seismic imaging in volcanic terranes is often difficult due to large seismic velocity contrasts between volcanic rocks and sediment interbeds, large lateral variations in stratigraphy, and the potential for mode converted (p-wave to s-wave) energy to partition the seismic signal and degrade the quality of the seismic stack (e.g., Pujol et al., 1989; Pujol and Smithson, 1992; Ziolkowski et al., 2003). The objective of our project was to assess seismic imaging capabilities at three sites to recognize geothermal potential in a variety of volcanic settings within the Snake River Plain, Idaho. Specifically, we examined up-flow zones along the southwest margin of a buried caldera margin (Kimberly), tested the extent of surface imaging capabilities along the axis of the Snake River Plain in an area where elevated groundwater temperatures imply heat flow from below (Kimama), and provided the geophysical framework to site a new geothermal well (Mountain Home). In addition to surface seismic data collection, a suite of downhole geophysical logs and geochemical measurements were used to calibrate and compare to our results. Here, we present seismic results from three field sites to conclude that high temperature zones in the subsurface correlate with seismic velocity contrasts and, within limits, surface seismic methods can be used to improve geothermal exploration.

At all sites, we acquired seismic data using a 12,000 lb IVI Minivib source and 240-360 vertical 10-14 Hz geophones spaced at 4 m. Downhole data were acquired using a Sercel 3-component borehole geophone at 2 m spacing at both Kimberly and Kimama sites, and a vertical component downhole geophone at the Mountain Home site at a spacing of 2 m. Data were acquired along dirt/gravel roads with geophones planted along the adjacent shoulder. Our results suggest that surface seismic methods can image major boundaries in volcanic terranes High fold to obtain wide angle coverage is necessary for data acquisition. High frequency attenuation is observed at all three sites and can be countered by geophone groups to match coherent noise patterns, and a focus on lower frequency acquisition. The potential for large static effects need to be addressed in processing. We recommend wide angle seismic imaging using multi-component acquisition capabilities to improve seismic imaging capabilities.

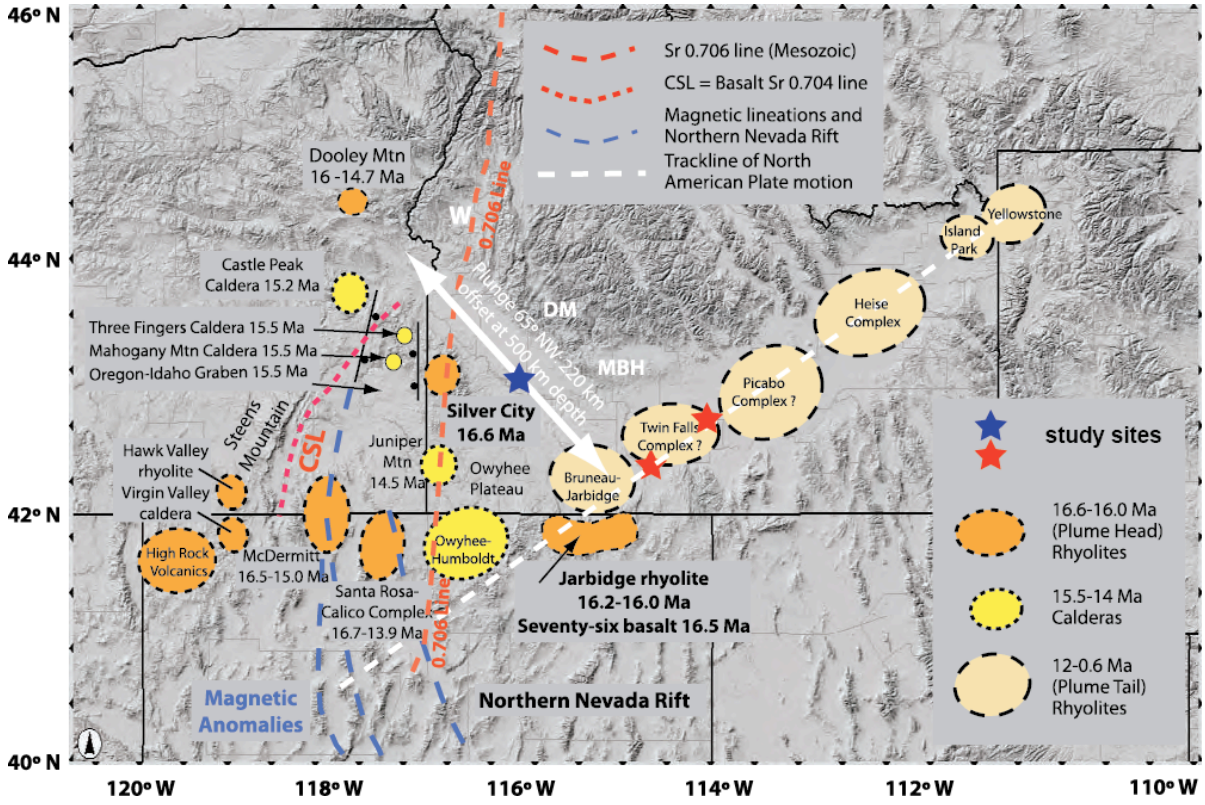

Figure 6-1. Digital topographic map of southern Idaho and surrounding area showing location of eruptive centers related to the track of the Yellowstone Hotspot (revised from Shervais and Hannan, 2008). The Kimberly and Kimama sites (red stars) are located on the perimeter of the Twin Falls eruptive complex. The Mountain Home site (blue star) is located on the eastern margin of the western Snake River Plain graben.

KIMBERLY SEISMIC RESULTS

The Kimberley site, located in the Twin Falls region and along the southwest margin of the Twin Falls volcanic complex (Figure 6-1), is well known for its low enthalpy geothermal resources. Here, the ground water is recharged in the mountains to the south, seeps deeper into the crust where it is heated, then upwells forming an artesian system [*Street and deTar*, 1987]. The borehole and surface seismic profiles are located along the west flank of Hansen Butte, immediately south of the Snake River (Figure 6-2) and the lithology consists of basalt, rhyolite, and sediment layers in the upper 430 m, which overlie a thick sequence of rhyolite with rare thin sediment interbeds to 1,958 m depth (Shervais et al., 2011).

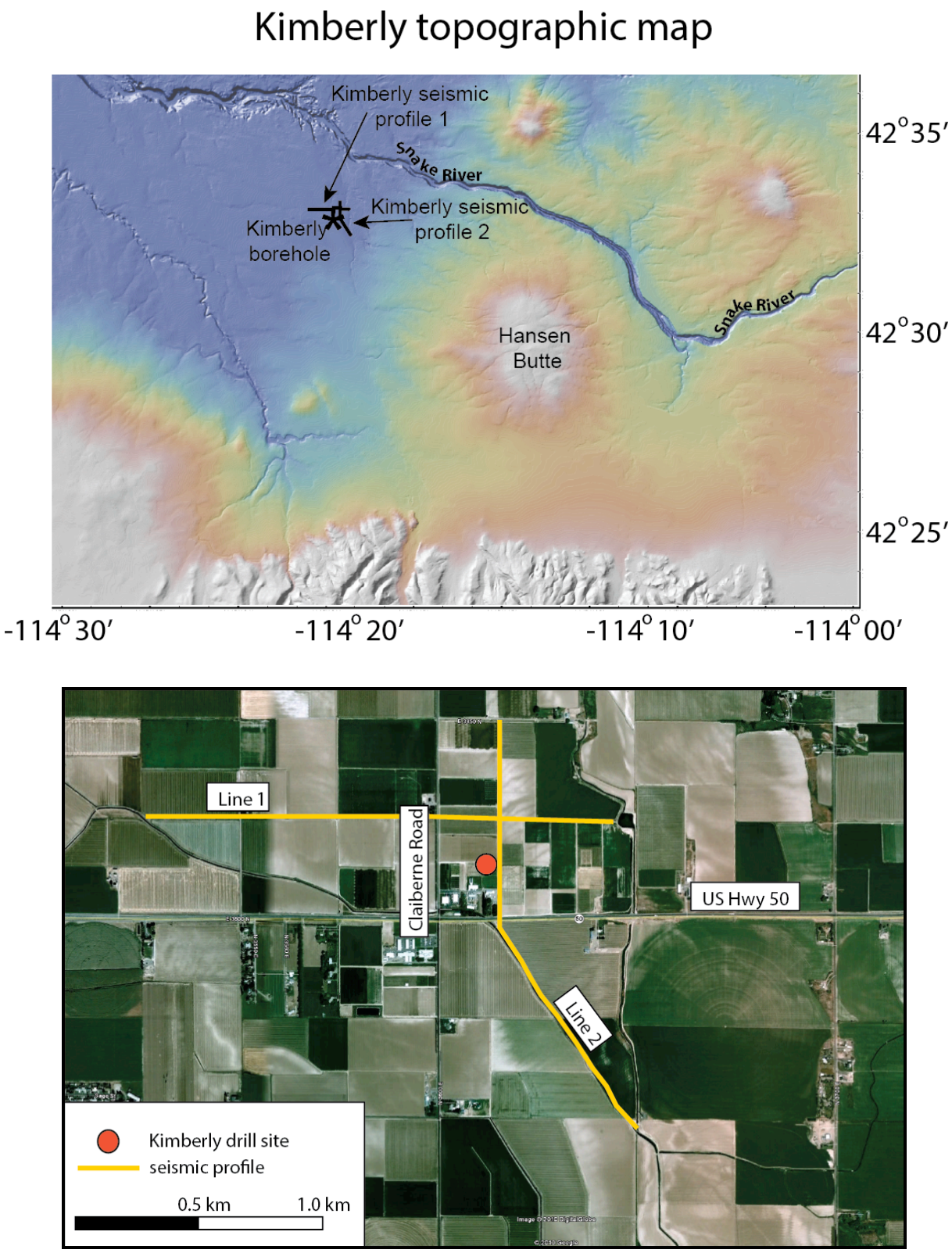

Figure 6-2. (top) Topographic map showing the Kimberly drill site and seismic profile locations on the northwest flank of Hansen Butte near Kimberly, Idaho. (bottom) Aerial photo of the Kimberly site.

Kimberly Vertical Seismic Profile (VSP)

A 1.9 km deep vertical seismic profile (VSP) at the Kimberly site shows clear first arrivals using the University of Alberta 12,000 lb IVI P-wave vibroseis source. The data were collected at 2 m depth intervals using four 3-component Sercel 10 Hz downhole geophones with a vibroseis sweep from 20-160 Hz. The source was stationed approximately 17 m from the Kimberly borehole. The first arrivals suggest relatively low attenuation of the p-wave seismic energy at the dominant frequency of 30-40 Hz, but at higher frequencies, we observe attenuation with increasing depth. Although we acquired data to above 100 Hz, direct arrival energy above this frequency was not recorded at depths greater than ~300m (Figure 6-3). At these higher frequencies, low velocity tube wave arrivals (at water velocity) and multiple downgoing arrivals that parallel the first break direct arrival dominate the VSP wave field. Although tube waves are not an issue for a surface seismic campaign, this observation suggests that little high frequency coherent seismic energy is returned below a few hundred meters at Kimberly. However, lower frequency (10's of Hz) imaging to geothermal target depths (upper 2 km) is feasible with this source. This conclusion is consistent with other seismic studies conducted in volcanic terranes (e.g., Pujol and Smithson, 1991; Ziolkowski et al., 2003) and suggests meter-scale flow boundaries may be difficult to resolve with seismic methods, but larger flow boundaries may still be imaged.

We picked first arrivals to estimate P-wave interval velocities (Figure 6-3b). A first order least squares fit to the calculated interval velocities suggests a general increase from 4,000 m/s near the surface to 6,000 m/s at 1.9 km depth. The increase in velocity with depth is typical of seismic velocity measurements with increasing confining pressure for similar igneous rocks (e.g., Christensen, 1984). Low velocity zones appear where sediment interbeds are identified in the Kimberly lithologic log (Shervais et al., 2011 and this report) and many of these zones correlate with fluctuations in downhole water temperature (Figure 6-3c). The calculated velocity values for the thin sedimentary interbeds are likely overestimated due to the influence of the adjacent high velocity rhyolite seismic velocities and a necessary smoothing filter used to calculate interval velocity values. However, thick sedimentary interbeds observed at 0.4 km and 0.6 km depth record interval velocities of 2,000-3,000 m/s and reflect fine-grained unconsolidated sediments that were logged within these zones (Shervais et al, 2011). In summary, seismic velocity variations correlate with changes in lithology at the Kimberly site. One exception to this observation is a velocity boundary at 1.65 km depth that does not correlate to any major lithologic boundary.

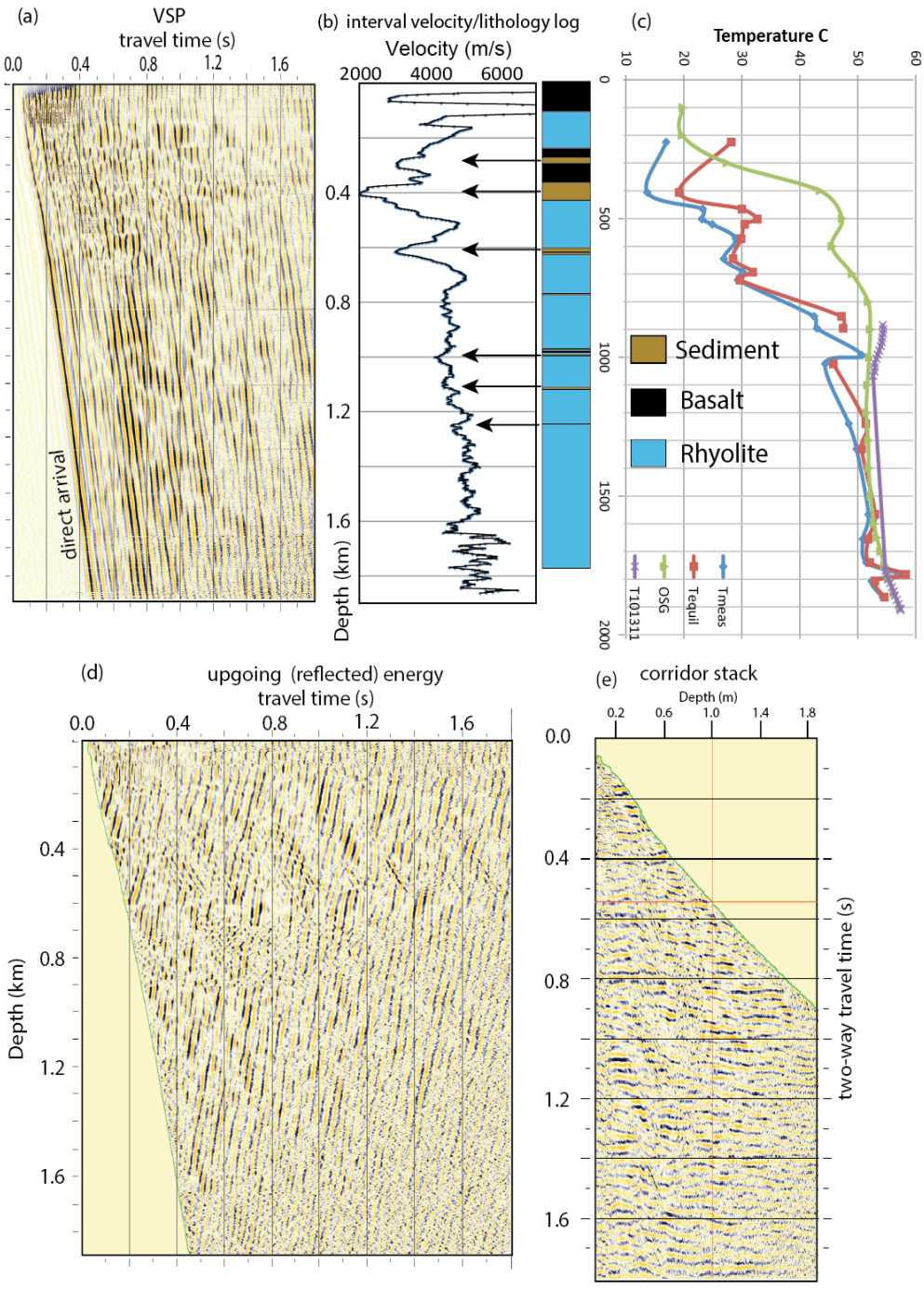

Figure 6-3. (a) Vertical component VSP from Kimberly with no processing to emphasize direct down going (direct) arrivals. (b) First arrivals were picked to calculate interval velocities to compare with lithologic and temperature logs (c). (d) Down going arrivals were removed through signal processing to emphasize reflected arrivals. Green line represents first arrival travel time. (e) Corridor stack in two-way travel time is used to tie VSP results to surface seismic results. Borehole location is shown in Figures 6-1 and 6-2.

Removal of the downgoing VSP seismic energy using a median subtraction filter highlights upgoing reflections from seismic boundaries at depth (Figure 6-3d). Reflections projected back to direct first arrival travel time indicate that many velocity (and reflecting) boundaries tie to sediment interbeds both at and below VSP depths. A corridor stack (Figure 6-3e), produced by doubling of the travel time of these filtered results, simulates a surface source and receiver to compare with surface seismic reflection profile. The amount of reflected energy observed on the corridor stack is very encouraging and suggests surface seismic methods using this vibrator source can provide adequate energy to image seismic boundaries at borehole depths.

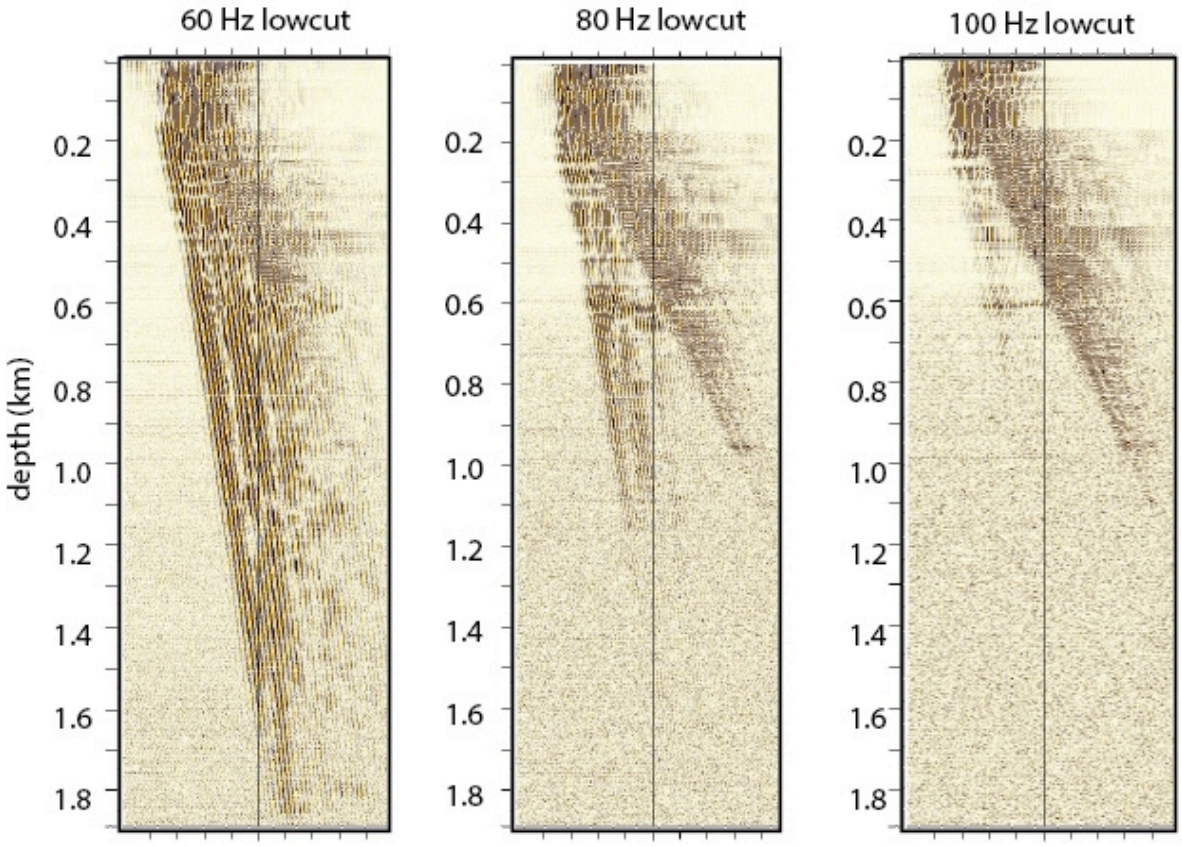

Figure 6-4. VSP filter panel results from Kimberly borehole showing attenuation of high frequency signals with depth. Note that little first arrival signal above 100 Hz appears below 300 m depth.

Kimberly - Static effects on imaging

One observation that the corridor stack analysis provides is that travel time delays for some reflections suggest static effects may present difficulties with surface seismic analyses (Figure 6-3e). Static time shifts occur when large lateral seismic velocities are encountered. To further examine static or small travel time effects with seismic imaging methods, we acquired a walkaway VSP at a range of receiver depths (Figure 6-4). These data were collected by moving the vibroseis truck at 4 m intervals along the road adjacent to the Kimberly borehole and recording downhole 3-component data. Our results show a large and repeatable pattern of travel time shifts at a range of receiver depths that is consistent with large velocity changes along this 200 m long seismic test. Static measurements of more than 60 ms (two-way travel time) appear within lateral distances of less than 50 m and these travel time variations are nearly identical for all depths below 500 m. This analysis suggests that the majority of problems related to static effects occurs at less than 500 m depth and is likely related to lateral changes in shallow flow boundaries. To succeed with surface seismic imaging techniques to image deeper stratigraphy, these static effects must be addressed with advanced seismic processing methods. Typically, these long-wavelength static effects can be addressed with a refraction static analysis via turning ray tomography methods (e.g., Cox, 1999). However, in a terrane where velocity inversions from shallow volcanic layers are common, the assumptions of first arrival tomography to extract a near-surface velocity distribution are violated. Under these conditions, borehole measurements with a layer stripping approach to reflection processing may provide the best imaging results. In addition to a reduced imaging capability that results from lateral near-surface contrasts, the large changes in seismic velocities with depth are responsible for much of the high frequency attenuation that was observed in Figure 6-4. Therefore, gaining a handle on the velocity field in volcanic terranes is essential to accurately image the subsurface with seismic methods. Borehole controls to obtain seismic velocity information is therefore a critical component to high quality surface seismic measurements.

We next examined the horizontal components from the downhole VSP data to determine the role of mode converted shear wave signals derived from the seismic source or converted from shallow layers. Although small amplitude shear wave arrivals are observed on the vertical offset VSP results, these signals are at very low amplitude and we conclude that converted waves do not play a significant role at near vertical incidence, as expected by Zoeppritz equation calculations (Aki and Richards, 1980). However, at wider angles, coherent shear wave arrivals suggest much of the p-wave energy has been partitioned and a multi-component approach to imaging in volcanic terranes for geothermal targets may be beneficial (e.g., Hannsen et al., 2003; Stewart et al., 2003; Behara, 2006). Figure 6-5 shows shot gathers for our wide angle 3-component VSP experiment. Our results show that at wide angles (shallow depths relative to the imaging angle), s-wave energy matches the amplitude of the vertical component

(p-wave energy). Although some horizontal energy is expected in a VSP experiment due to non-vertical raypaths, coherent signals along both the inline and crossline sensors support this observation of mode converted energy playing a large factor in signal attenuation and that these data may be beneficial in seismic imaging in these complex geologic environments.

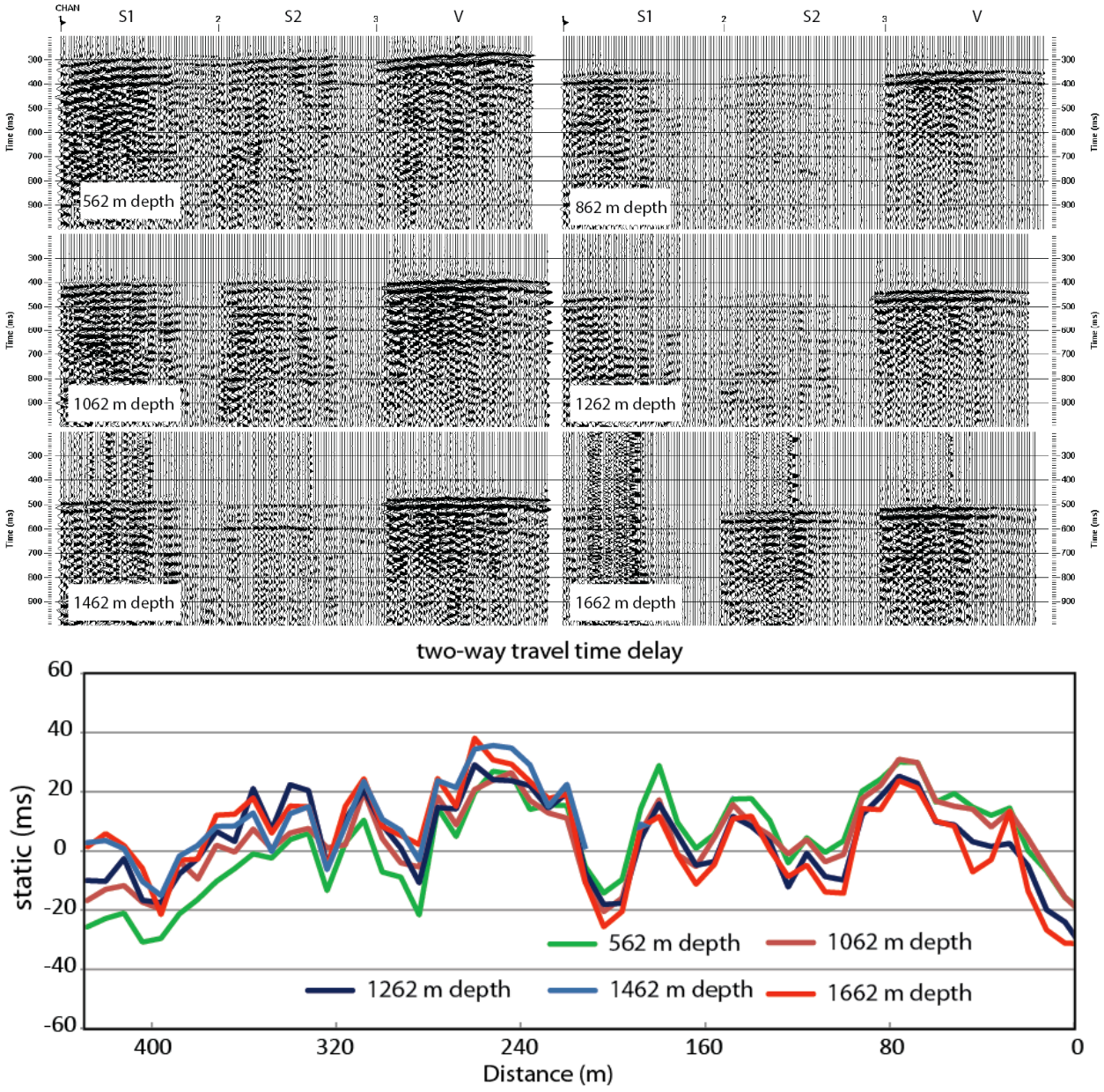

Figure 6-5. (top) Relative amplitude walkaway seismic profiles at a range of geophone depths for both horizontal (S1 and S2) and vertical (V) receivers. Note that the horizontal energy decreases in amplitude (relative to the vertical component) with depth, related to converted wave partitioning at greater raypath angles (bottom). Static effects from the walkaway survey showing two-way travel time delay times from a range of receiver depths. These data were calculated by subtracting the average direct wave velocity calculated at each receiver depth. Surface source locations were along seismic profile 2.

Kimberly Surface seismic results

Surface seismic profiles from Kimberly were acquired along dirt roads associated with the University of Idaho Kimberly agricultural research facility (Figure 6-2). We used an IVI minivib II seismic source and 360 channel 4-m spaced 10-14 Hz vertical geophones to acquire these data. The maximum source-receiver offset ranged from 720-1,440 m, providing relative wide angle coverage for the target depths upwards of 2.0 km. The 2.0 km west to east seismic profile 1 was acquired along a farm field access road, approximately 300 m north of the Kimberly borehole (Figure 6-2). This profile crosses seismic line 2 at position 1,150 and Claiberne Road at position 1,320. The 1.7 km long north to south seismic profile 2 was acquired along the Kimberly well access road. The profile crosses US Hwy 50 at position 2,200 and crosses the borehole location at position 2,150. We processed these data using a standard processing approach summarized by Yilmaz (2001). Processing steps included precorrelation gains to recover high frequency signals, deconvolution, detailed velocity analyses, a focus on residual and horizon statics, and post-stack Kirchoff migration. The data were depth converted using velocities derived from the VSP survey (Figure 6-3).

Interbedded basalt, rhyolite and sedimentary interbeds in the upper 0.5 km below land surface provide large seismic impedance contrasts to produce a highly reflective zone observed on both seismic profile 1 and 2 (Figure 6-6). Profile 1 shows a near continuous reflector that varies between 0.3-0.6 km depths and is likely associated with the sequence of interbedded basalt, rhyolite, and sediments (Figure 6-3). Deeper and more discontinuous reflectors are likely associated with sedimentary interbeds observed in the borehole cores (Figure 6-3). A more transparent zone of reflectivity below one km depth is consistent with few flow boundaries noted in the Kimberly borehole. Profile 2 shows a package of south-dipping reflectors associated with the top of volcanic rock/sediment flow boundaries. This reflector topography may suggest the last eruptive flow associated with Hansen Butte flowed on pre-existing topography that shallows to the north. Reflections below 0.5 km depth are more discontinuous and likely result from sedimentary interbeds that exceed a few meters thick, consistent with borehole logs. Large static shifts were accommodated with a residual statics approach and iterative velocity analyses. This approach did not optimally address the large static corrections (Figure 6-5) and resulted in an improper stacking velocity model, but significantly improved the stack.

At the location of the Kimberly borehole on profile 2 (Figure 6-6), we superimposed an acoustic synthetic seismogram derived from VSP first arrival picks. This synthetic seismogram was derived using a 30 Hz zero phase Ricker wavelet, similar to the source signature output from the minivib seismic source. We observe a strong correlation between reflections observed

on the surface profiles and borehole seismic measurements and suggests that surface seismic imaging techniques can be used to track flow boundaries and possibly geothermal target zones.

In summary, although significant energy loss is observed from frequency attenuation, scattering and mode conversions (e.g., p-wave to s-wave), we were able to image major flow boundaries related to volcanic processes at the Kimberly site. We believe seismic imaging methods in volcanic terranes can be used to accurately map flow boundaries related to past eruptions. If these flow boundaries are conduits to high temperature fluid flow, seismic methods can be used to image targets related to geothermal exploration. A tie between borehole seismic measurements and subsurface physical property measurements may provide the necessary link between reflectivity and key target zones for geothermal exploration. Additionally, a data acquisition strategy of large fold and possibly inline or 3-D receiver groups may help attenuate both coherent and random noise, and improve data quality (e.g. Regone, 1997). Processing steps that include a velocity model from borehole measurements, a layer stripping approach to build an accurate velocity model away from the borehole, and prestack migration methods may provide an improved seismic image in complex volcanic terranes.

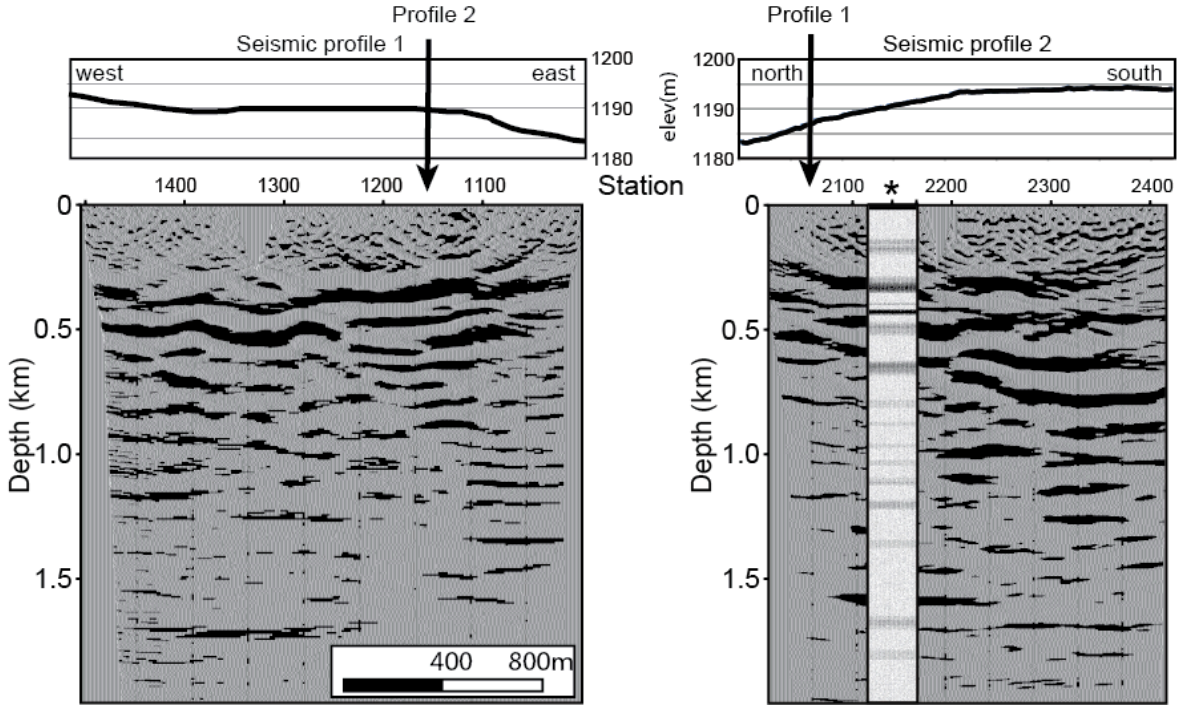

Figure 6-6. Migrated and depth converted surface seismic profiles from the Kimberly site with elevation profiles. (left) West-east profile 1 (right) North-south profile 2. Synthetic seismogram computed from VSP velocity profile is superimposed at the Kimberly well location. Note the volcanic and sedimentary rock interbeds between 300-600 m depth are imaged on both profiles.

KIMAMA SEISMIC RESULTS

The Kimama site is located on the axis of the Snake River Plain that blanketed with thick overlapping basalts originating from a series of vents along the eastern limits of the Twin Falls volcanic complex (Figures 6-1 and 6-7). The Kimama site was chosen because it sits on an axial volcanic zone that is defined by high topography to the east and by a buried basalt ridge underlying the topographic high (Lindholm, 1996). The Snake River Plain cold water aquifer [*Hubbell et al.*, 1997] underlies the site. The aquifer is in part recharged by flow of water from the mountains to the north and east, with the general underground flow to the west and southwest, and significant discharge into the Snake River in the Thousand Spring area, NW or Twin Falls. The flow of these fluids cools the aquifer zone resulting in a nearly isothermal (15-17ºC) convective geotherm ≥980 m depth, and a steep conductive gradient (75ºC/km) below that depth (Figure 6-8). The general lithology at Kimama consists of primarily of basalt flows interbedded with weak, wind-blown sediments deposited during volcanic hiatuses (Figure 6-8).

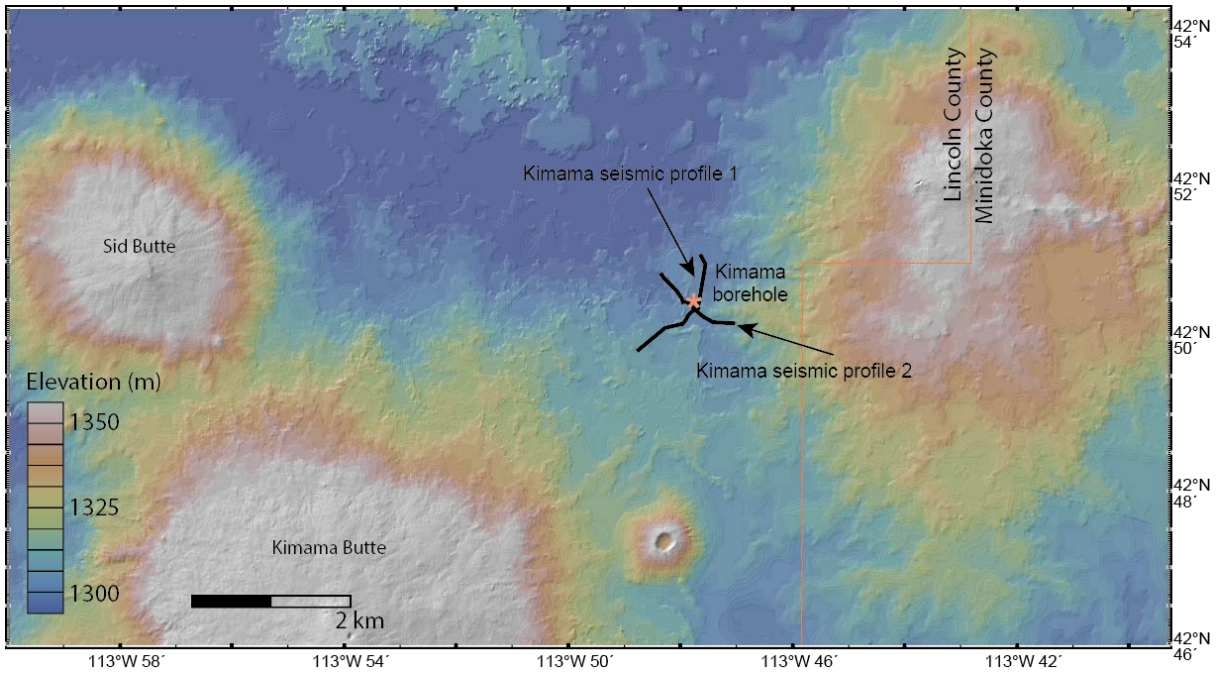

Figure 6-7. Topographic map from the Kimama field site showing borehole and surface seismic locations near multiple volcanic vents that flank the east side of the Twin Falls volcanic complex.

Kimama Vertical Seismic Profile (VSP)

A vertical seismic profile (VSP) at Kimama was acquired between 0.2 and 1.2 km depth using the University of Alberta 12,000 lb IVI P-wave vibroseis source. The data were collected at 2 m depth intervals using four 3-component Sercel 10 Hz downhole geophones. The data were collected with a vibroseis sweep from 20-160 Hz and the vibroseis truck stationed approximately 20 m from the Kimama borehole. Access with the VSP tool to depths greater than 1.2 km was not possible due to the borehole conditions at the time of our seismic survey. Our borehole seismic results show strong p-wave first arrivals and a series of downgoing arrivals that parallel the first arrival wave train (Figure 6-8). The clear first arrivals suggest relatively low attenuation of the p-wave seismic energy around the dominant seismic frequency of ~30 Hz and that the vibrator source was adequate to propagate energy (one way) to target depths that exceeded one km. A first motion arrival time of 0.37 s at 1,000 m depth suggests an average p-wave velocity of 2,700 m/s for the top km at the site. However, interval velocity measurements derived from first arrival picks between 200-1,000 m depth suggest seismic velocities increase from ~3,000 m/s to ~5,000 m/s with an average interval velocity in this depth range of 4,150 m/s. The increase in velocity with depth is typical of seismic velocity with increasing confining pressure for similar rocks (e.g., Christensen, 1984). The large disparity in seismic velocities between the upper 200 m depth and the depths measured with the VSP is consistent with unconsolidated, unsaturated sediments that were logged from the surface to approximately 15 m depth and alternating fractured and dense dry basalts logged to a water table depth of 80 m (Twining and Bartholomay, 2011). Dry unconsolidated sediments can have p-wave seismic velocities of less than 500 m/s while dry basalts and other igneous rocks have measured velocities of 10-50% below saturated rocks of the same composition (e.g., Christensen et al., 1973; Christensen, 1982). A direct measurement of these slow near surface seismic velocities was observed with surface seismic methods and is discussed below.

The coherent arrivals that immediately follow the first arrival on the VSP image are likely from seismic energy trapped between the surface and a large velocity contrast layer in the near surface (Figure 6-8a). This downgoing reverberatory signal likely results from the very large, near surface velocity contrast between unconsolidated, unsaturated sediments and the underlying volcanic rocks. A strong series of slower velocity “down going” arrivals matches water velocity speeds and is consistent with tube wave energy traveling at a water velocity.

Removal of the down going first arrival seismic energy using a median subtraction filter algorithm highlights reflections from seismic boundaries at depth (Figure 6-8b). These “up going” reflections intersect the first arrivals at the reflector depth and can be used to calibrate surface seismic results. We produced a corridor stack by doubling of the travel time of the filtered up going reflection image (Figure 6-8c). This corridor stack simulates a surface source

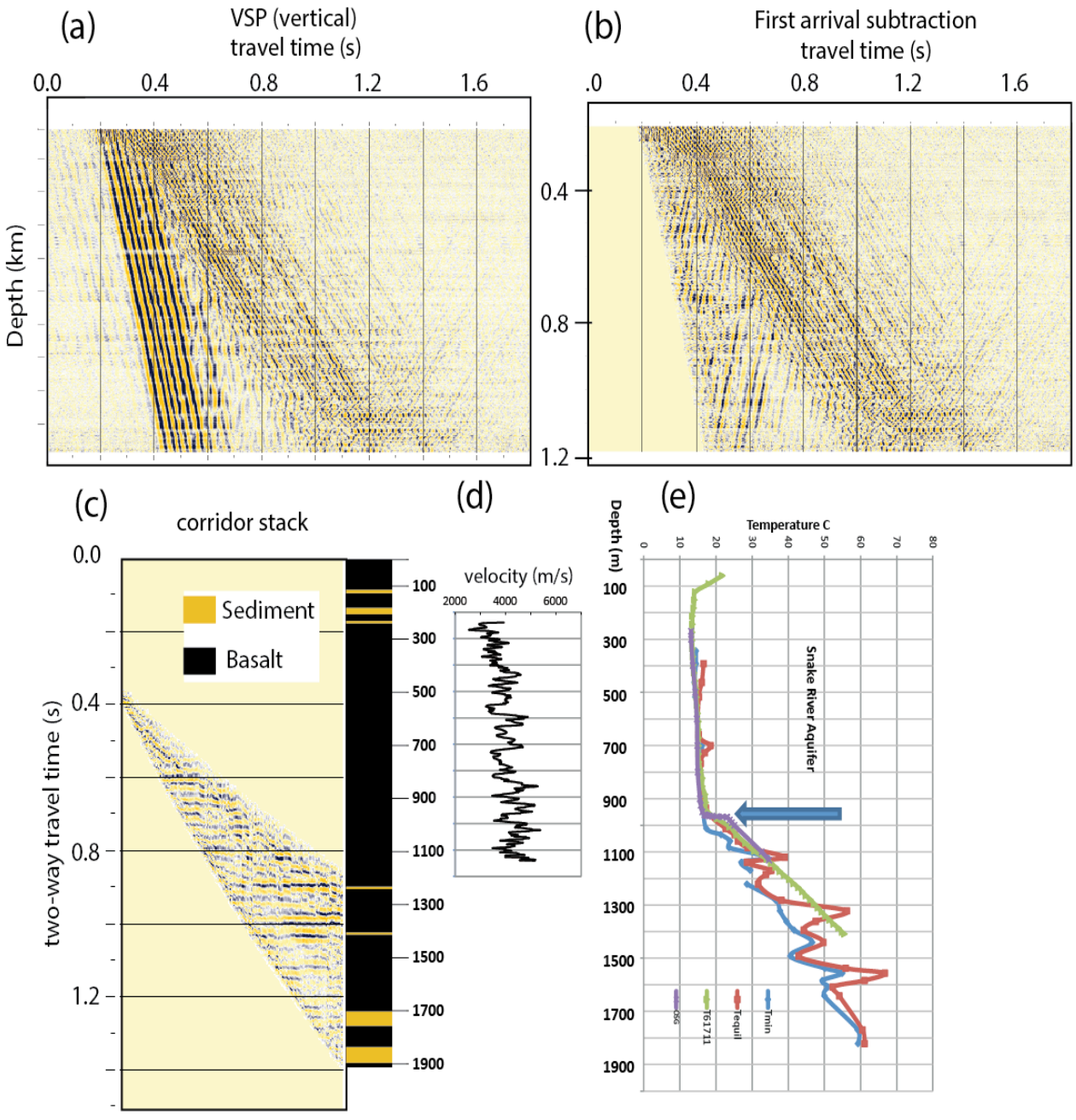

Figure 6-8 (a) Vertical component VSP from Kimama borehole to emphasize direct downgoing arrivals from surface to depth. (b) Downgoing arrivals were removed through signal processing to emphasize reflected (up going) arrivals. (c) Corridor stack in two-way travel time is used to tie VSP results to surface seismic results. (d) Interval velocity log derived from first arrival picks showing a steady increase in p-wave velocities with depth. (e) Downhole temperature log showing the correlation between reflections and temperature spikes. Location of the Kimama borehole is shown on Figures 6-1 and 6-7.

and receiver to compare reflection travel times with surface seismic reflection results. Reflections to depths that approach 2 km are consistent with sediment interbeds that are logged in the Kimama well (Shervais et al, 2013). A zone between 1,100-1,600 m depth contains numerous reflections and is consistent with the transition from relatively uniform Snake River Aquifer volcanic rocks to a zone containing numerous sedimentary interbeds that contain anomalously high water temperatures (Figure 6-8e). Our VSP results suggest that sedimentary interbeds at geothermal target depths can be mapped with seismic methods at Kimama and that the minivib seismic source provides adequate resolution and signal penetration to characterize the upper few km.

Kimama Surface seismic results

We acquired three 360-channel surface seismic profiles using an IVI minivib source and 10-14 Hz geophones. We acquired data at 4 m source and receiver spacing with a source sweep from 20-160 Hz along Lincoln County operated gravel roads (Figure 6-7). We acquired two 1.4 km long south to north profiles, separated by the Kimama Highway. The Kimama borehole was located immediately north of the Kimama Highway (Figures 6-7 and 6-9). The 2.0 km west-east profile crossed to within a few meters of the Kimama borehole. The western portion of this profile was acquired on an unimproved dirt road while the eastern portion of the profile was shot on the Lincoln County gravel road. We processed each profile by applying precorrelation gains to normalize sweep frequencies. After correlation, we performed a detailed velocity analysis for each common mid-point gather, applied deconvolution, statics, bandpass filters, and post stack Kirchoff migration. Travel time to depth conversions were based on VSP first arrival measurements.

Surface seismic results show reflections associated with shallow (<200 m) sedimentary/ basalt interbeds (Figure 6-9) that were logged in the Kimama borehole but were not imaged in the VSP due to our survey restrictions (Figure 6-8). These reflections show considerable topography away from the Kimama borehole and suggest variable thickness volcanic flows were derived from adjacent volcanic vents (Figure 6-7). These flow boundaries suggest that the younger (shallower) flows were deposited on pre-existing topography, which results here from the geometry of previous basalt flows. Improved reflections to the north of Kimama Highway when compared to the profile to the south likely reflect a more straight profile compared to the winding road to the south (Figure 6-7). The west-east profile (Figure 6-9) shows reflections that match shallow sedimentary interbeds, with increasing reflector topography towards the east. The far eastern portion of this profile suggests an additional flow may sit upon the flows logged in the Kimama borehole. Deeper reflections are best observed on the west-east profile where coherent reflections are observed between 1.1-1.5 km depths. These reflections in both the VSP results (Figure 6-8) and the surface seismic results (Figure 6-9) show a surprising coherency

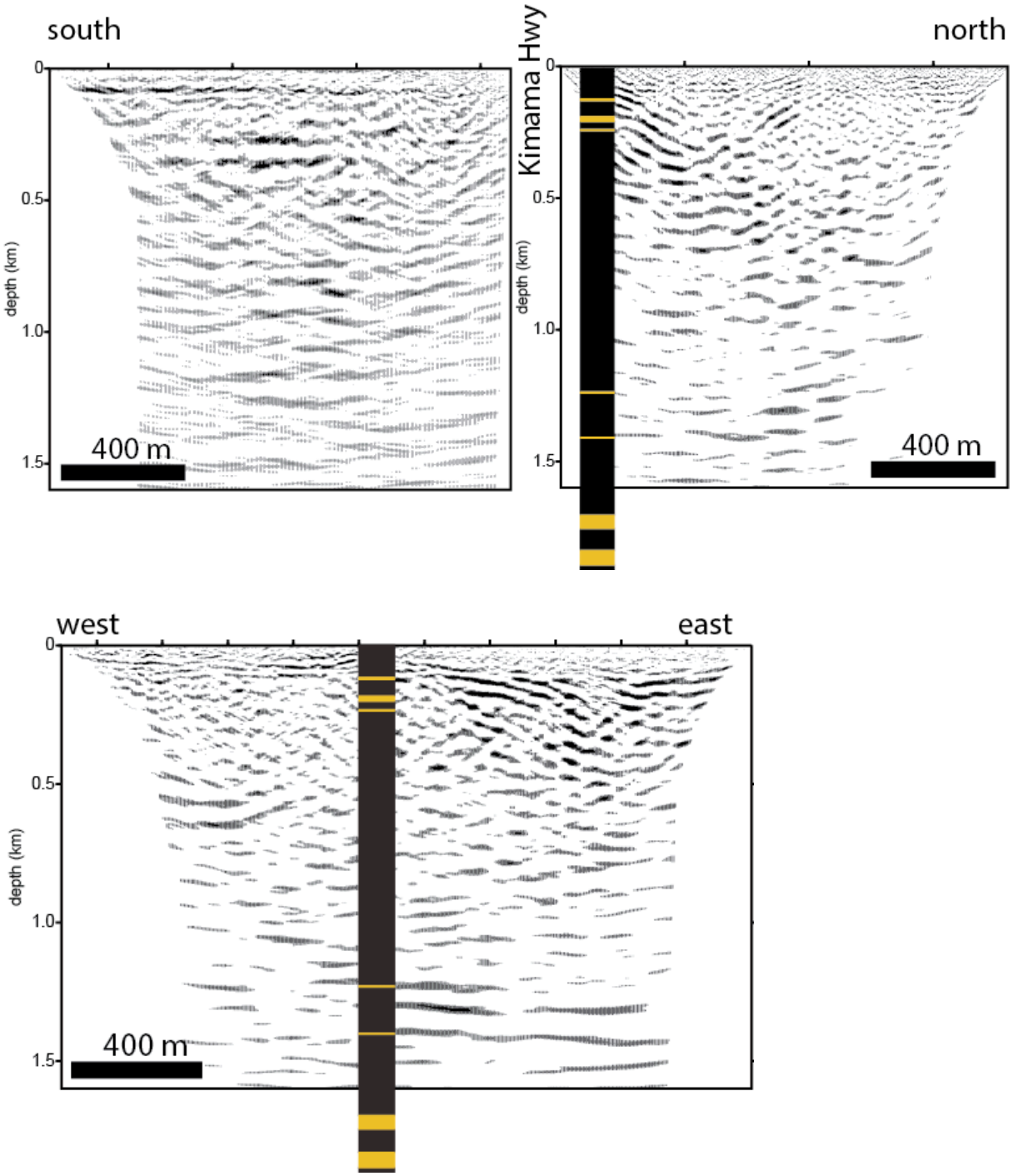

Figure 6-9. (top) Kimama south to north surface seismic profiles and (bottom) west to east profile. Simplified lithologic map for the Kimama borehole shows basalt (black) and sediment interbeds (yellow). Profile locations are shown on Figure 6-7.

that represent this sedimentary interbeds observed in the borehole logs. Poor data quality below 1.5 km depth likely represents a decrease in signal returns, increased static effects from flow boundaries, and a narrow aperture with respect to imaging depths. To provide an improved image of the deeper targets, longer profiles would provide this greater ray path aperture by recording longer source-receiver offsets. Profile orientation in this complex geologic environment may also be a factor (Figure 6-9). For example, acquiring a seismic profile along an orientation that minimizes flow boundary topography between may help reduce the effects of scattering.

MOUNTAIN HOME SEISMIC RESULTS

The Mountain Home site, located on and adjacent to the Mountain Home Air Force Base (AFB), is a site with the planned installation of a binary power system (Figure 6-10). The primary goal of the Mountain Home drill core was to assess the geothermal potential under Mountain Home AFB, building on results from earlier geothermal test wells (e.g., Arney et al., 1982). A bottom hole temperature of the 192 degrees C was encountered at the nearby Griffith-Bostic well at a depth of 2.9 km and similar temperatures were anticipated at the Mountain Home site.

Geologically, the Mountain Home borehole sits upon surface Quaternary basalt flows that range in thickness to more than 200 m. Below, near-shore lacustrine sediments of the Idaho Group, which occupy the Western Snake River Plain, are found to depths that exceed 600 m (e.g., Wood, 1994; Figure 6-1 and 6-10). Below, Tertiary basalts and sediment interbeds are encountered in the deepest boreholes.

Mountain Home Vertical Seismic Profile (VSP)

A 1.2 km deep vertical seismic profile (VSP) at the Mountain Home site shows clear first arrivals using the University of Alberta 12,000 lb IVI P-wave vibroseis source (Figure 6-11). The data were collected at 2 m depth intervals using a single vertical component geophone. A source sweep from 20-160 Hz was used with the vibroseis truck stationed approximately 15 m from the Mountain Home borehole. The first arrivals in the upper 300 m show a high velocity arrival related to the steel casing that masked the underlying (and slower) direct arrival through the formation. As with the Kimberly and Kimama wells, we observe relatively low attenuation of the p-wave seismic energy at the dominant frequency of 30-40 Hz, but at higher frequencies, similar attenuation effects are observed.

We picked first arrivals to estimate P-wave interval velocities (Figure 6-11f). A first order least squares fit to the calculated interval velocities suggests a general increase from 3,000 m/s near the bottom of casing to ~5,000 m/s at 1.0 km depth. The direct velocity measurement at the bottom of casing suggests the upper 300 m contains an average velocity of 2,800 m/s. This

Figure 6-10. Mountain Home study area topographic map with seismic line and cross section locations, water and exploration well locations, and geologic map for the southern portions of the study area (Jenks et al., 1998).

velocity is consistent with near surface basalt layers that appear in nearby boreholes and are mapped on the surface (e.g., Jenks et al., 1998). The sediment-dominated zone between 0.4-0.7 km depths derived from paleo-lake Idaho (Wood, 1994) is consistent with relatively the measured seismic velocities. Due to the required smoothing filter, the seismic velocities for the thin volcanic rock interbeds within this zone are likely underrepresented. Below 0.9 km depth, we observe higher seismic velocities consistent with a zone dominated by basalt.

Removal of the downgoing VSP seismic energy using a median subtraction filter highlights (upgoing) reflections from seismic boundaries at depth (Figure 6-11b). Reflections projected back to direct first arrival travel time indicate that many velocity (and reflecting) boundaries tie to sediment interbeds both at and below VSP depths. A corridor stack (Figure 6-11c), produced by doubling of the travel time of these filtered result, simulates a surface source and receiver to compare with surface seismic reflection profile. Two key seismic boundaries at 750 m and 890 m depth represent the top of volcanic layers and suggest these boundaries can be imaged with surface seismic techniques.

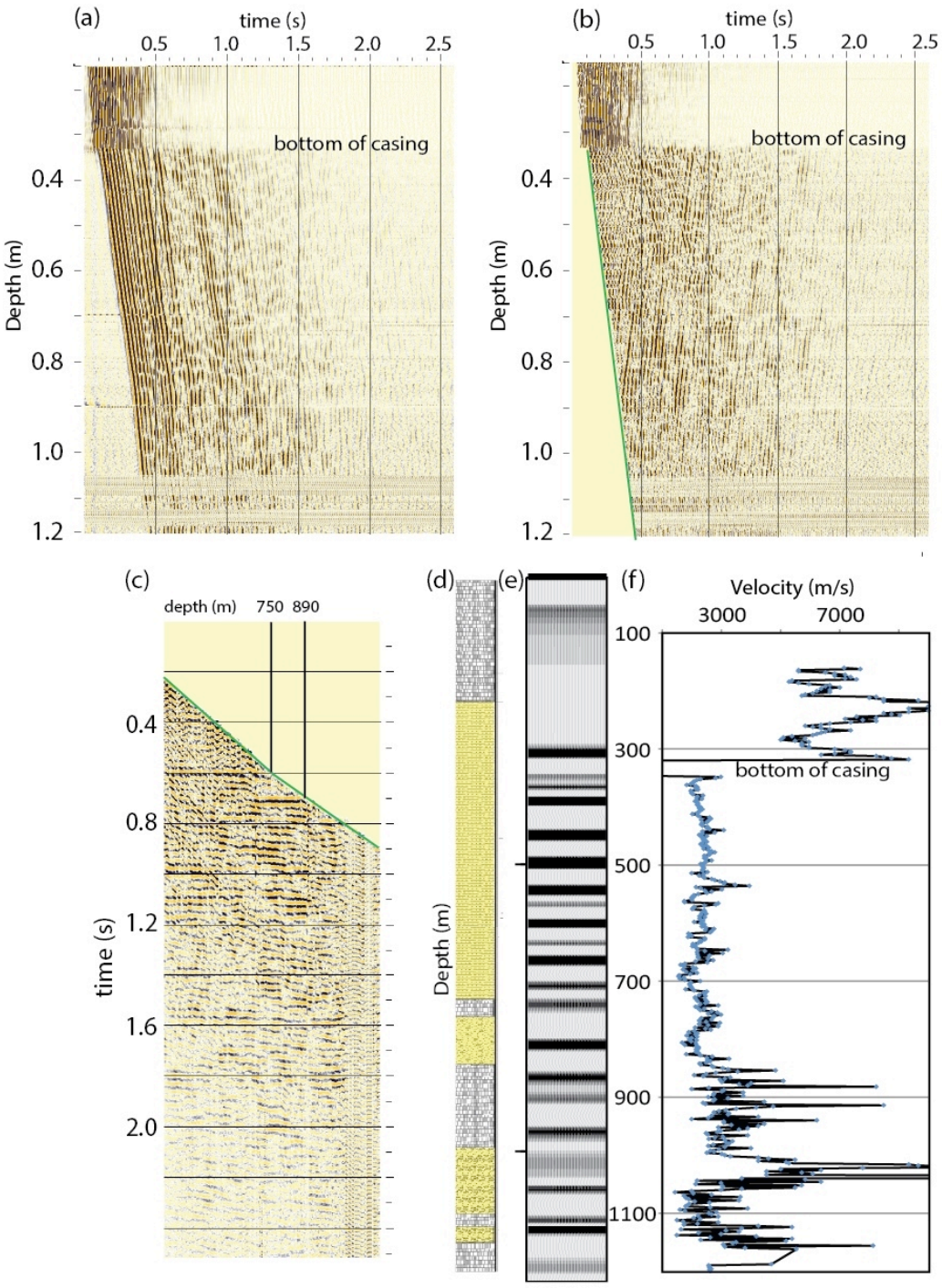

Figure 6-11 (a) Vertical component VSP from the Mountain Home borehole to emphasize direct downgoing arrivals. (b) Downgoing arrivals were removed through signal processing to emphasize reflected (up going) arrivals. Note that casing extends to ~310 m depth and interferes with first arrival (c) Corridor stack in two-way travel time is used to tie VSP results to surface seismic results. (d) Borehole log from Mountain Home well. (e) Synthetic seismogram derived from interval velocities measured on (a) (f) Interval velocity log derived from first arrival picks showing low velocities associated with lake sediments and higher velocities associated with basalt layers.

Mountain Home Surface seismic results

Seismic reflection results show high amplitude arrivals and diffractions at near-surface depths, consistent with surface and near surface basalts (Figure 6-12). Below this shallow layer, a relatively transparent reflection zone appears. At depths from 600 m to more than one km, a high amplitude reflector matches the depth of the Tertiary basalt top, where basalt and sediment interbeds are noted to more than 3 km depth (Figure 6-13; Arney et al, 1982). A large step in the basalt surface appears immediately south of the CJ Strike reservoir that may be fault related or a flow boundary. Data quality south of the Snake River was higher quality compared to the area to the north. We attribute this change to different surface conditions. Whereas we acquired seismic data on dry desert roads with poor seismic coupling to the north of the river, saturated farm fields located south of the Snake River provided an ideal coupling environment for both source and receiver. This result emphasizes that saturated materials that contain seismic velocities more similar to the shallow volcanic rock sequence reduce scattering and energy trapped in near surface layers.

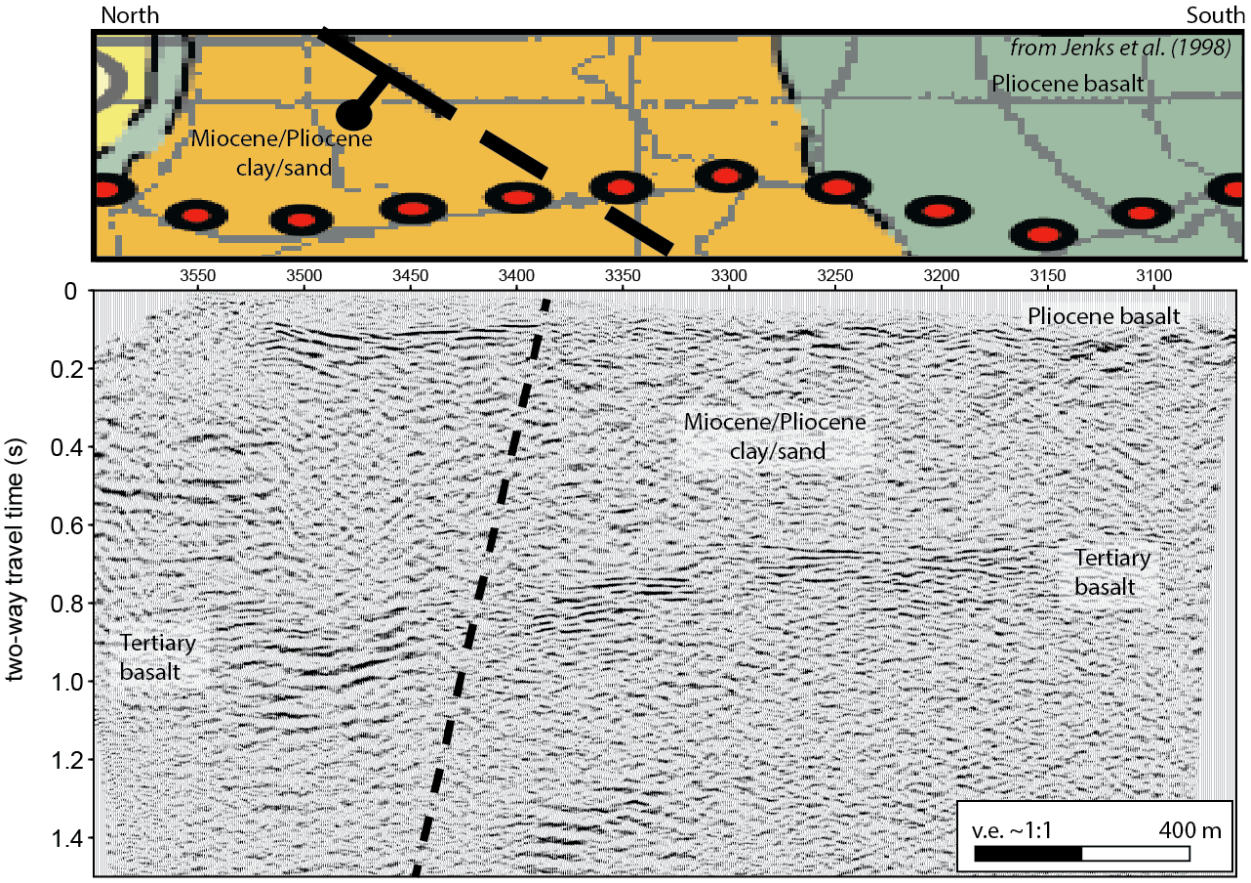

Figure 6-12. Seismic reflection results from the Mountain Home area, south of Strike Reservoir. Pliocene clay and sand dominate the section, with dense reflections from younger Pliocene basalts and younger Pliocene to Miocene basalts.

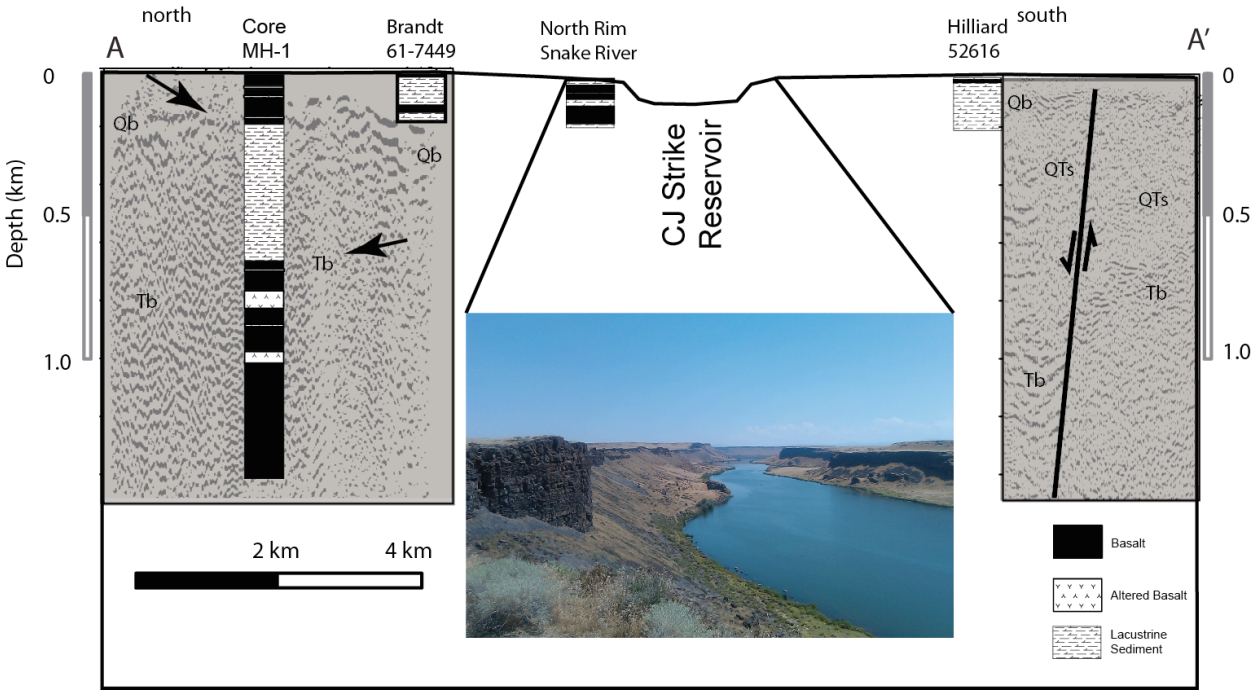

Figure 6-13. Seismic reflection results from the Mountain Home area. Two p-wave seismic profiles were acquired to characterize surface (Quaternary) basalts, near-shore lacustrine sediments related to paleo Lake Idaho, and underlying Tertiary basalts. Although lake sediment reflections are sparse (due to the homogenous nature of the sediments), a reflector between 0.6-1.0 km depth matches the depth to the top of the Tertiary basalt sequence.

SUMMARY

Surface and borehole seismic data show seismic imaging in the Snake River Plain sequence of volcanic rocks is possible, but requires a focus on detailed processing and acquisition design. VSP results show increasing seismic velocities with depth within the volcanic rock sequence and suggest low seismic attenuation at relatively low frequencies and large velocity contrasts are present. However, our results suggest that a small vibroseis source is capable of imaging to geothermal target depths at these sites. Surface seismic images show these large velocity contrasts are imaged, but data quality diminishes with increasing depth. High fold to obtain wide angle coverage is necessary and high frequency attenuation suggests a focus on lower frequency acquisition will provide improved results. The potential for large static effects need to be addressed in processing and with an accurate velocity model tied to borehole information, improved seismic imaging may be achieved with prestack migration methods.

CHAPTER 7:

SLIM HOLE CORING AND DRILLING OPERATIONS

Chris Delahunty and Dennis Nielson
DOSECC Inc., Salt Lake City, Utah

John Shervais
Utah State University, Logan, Utah

ABSTRACT

A deep core drilling project focused on the geothermal properties and development of the Snake River Plains area of southern Idaho was commissioned and started in the fall of 2010. Slim-hole coring was selected as the most cost effective means to accomplish the project goals. Three locations were chosen with target depths as follows: Kimama 1524m (5000 ft.), Kimberly 1829m (6000 ft.), and Mountain Home 1524m (5000 ft.). These depth objectives were exceeded for all three hole. A continuous core sample was produced and down-hole temperature was measured while drilling. Total core produced was 2034 m at Kimama (including sidehole core), 1745 m at Kimberly, and 1670 m at Mountain Home. Core recovery (length core recovered/ length of section cored) was 99.86% at Kimama, 100% at Kimberly, and ~96% at Mountain Home. Low recovery at Mountain Home was due to the poorly consolidated sediments found in much of the upper section. We conclude that the use of small diamond coring drill rigs to produce slim holes (<6" diameter) for geothermal exploration and geothermal resource confirmation is clearly an effective and cost-efficient approach.

Introduction

Geothermal environments pose unique challenges for reservoir assessment and production drilling. For assessment purposes, coring presents the advantage of observing reservoir lithologies, hydrothermal mineralogy and fluid inclusions, fracture character as well as offering the opportunity to measure down-hole temperature **(**Hulen and Nielson, 1995; Nielson *et al.*, 1996; Nielson *et al.,*1998). In addition, the cost of core drilling is much lower than production well drilling, and coring can be done to the depths of production wells (Nielson, 2001). This has led many companies to conduct core drilling prior to bring in the more expensive production rigs. However, there are few papers that document operating experience and costs as well as the scientific benefits of coring.

The Hotspot Project was designed to evaluate three different geothermal environments in the Snake River Plain (Shervais *et al.* 2012). The effect of fresh water aquifers on high heat flow from this large magmatic province is well established (Blackwell, 2011). Because of this, deep coring was necessary.

The coring of three geothermal holes took place from September of 2010 through October of 2011. The sites were chosen to evaluate three different geothermal environments: the axis of the eastern SRP, the southern margin of the SRP and an axial area on the western SRP. These holes were located at Kimama, Kimberly, and Mountain Home Air Force Base. All core drilling was performed by DOSECC Inc. (Drilling Observation and Sampling of the Earth's Continental Crust) of Salt Lake City, Utah. Additional air rotary services were performed by Eaton Drilling and Pump Services of Wendell, Idaho, and under Idaho well drillers license 026. An Atlas Copco CS-4002 coring rig was the primary drilling platform used throughout the project shown in Figure 7-1. All work done by Eaton Drilling and Pump Service was accomplished with a Ingersol-Rand T3W air rotary drill rig using down hole hammers (Figure 7-2).

Geothermal test wells in the State of Idaho must meet all State of Idaho Well Drilling and Construction Standards, in accordance with the Idaho Geothermal Resource Act. Well design, well drilling, and well construction in the State of Idaho are administered by the Idaho Department of Water Resources. Basic requirements include a surface conductor set to 40' depth, installation of a blow-out preventer if bottom hole temperatures exceed 100ºC, and 0.25" thick steel casing set to 10% of total depth, with a 1" cement annulus. On our first hole (Kimama) we met this by widening the HQ-size hole after coring. This proved time consuming and expensive; on subsequent holes we used a water-well driller to rotary drill a hole to 10% depth for casing.

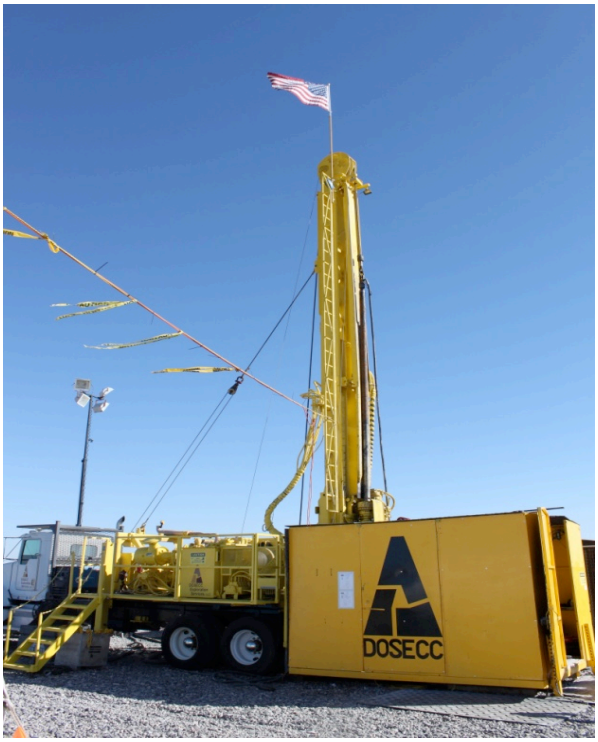

Figure 7-1. DOSECC CS-4002 core drill rig.

Figure 7-2. Eaton's T3W air rotary drill rig.

KIMAMA (42°50'21.56"N 113°47'47.66"W)

The Kimama site is located approximately 20 miles North of Burley, Idaho in the abandoned township of Kimama. There is access to the site on gravel roads, and it is seasonally dry and dusty in a loess covered basaltic field shown in Figure 7-3. The Kimama site was initially chosen for a 10,000 foot well that would document a cross section of the entire basalt and underlying rhyolite section. Because of the high costs for drilling such a deep hole, it was decided to split the drilling into a 5000 foot section at Kimama and a comparable section at Kimberly to pick up the rhyolite. Ultimately, a suitable site was located and leased in order to accomplish the drilling goals. Site preparation at Kimama consisted of clearing brush, installing a 3.5' x 3.5' x 3.5' concrete box as a mini-cellar in order to fit the choke and kill ports under the well head, and still allow the annular preventer to fit under the foot clamp of the CS-4002 drill rig. Next a woven geo-fabric was installed over a 100' x 100' area bounding the dirt access road. Engineered soils and aggregates were dispersed over the geo-fabric in order to stabilize the surface on the 4 foot deep loess that covered the site (Figure 7-4).

Figure 7-3. Drill site in Kimama Idaho, with water well installed.

Figure 7-4. Kimama site preparation.

Figure 7-5. Project Board.

Kimama Drilling/Casing Plan

The drilling and casing plan for the Kimama hole was driven by the requirements of the Idaho Department of Water Recourses (IDWR) under Idaho Code 42-238. The approved drill program was as follows and shown in Figure 7-6:

Drill a 10-5/8" hole to 38 fbs, and install a 7-5/8" casing cemented with a neat cement pressure grouted bottom up. Then drill a continuous 3.830" diameter HQ-Core from 38 fbs to 1000 fbs. Log the upper 1000 feet. A 6-1/2" rotary hole opener bit would be attached to the string and hole would be opened to 1000 feet. Install 1000 feet of 4-1/2" 0.25" wall HWT threaded casing cemented with a neat cement pressure grouted bottom up. Continuous 3.830" diameter HQ Core to 5000 fbs. Set temporary casing and drill 3.032" diameter NQ Core if needed. Run geophysical logs in the lower 4000 feet of the hole. Install 5000 feet of 2-3/8" tubing to TD and allow the well to equilibrate. Monitoring bottom hole temperature every 24 hours. Plug and abandon the hole with neat cement slurry installed by a tremie pipe.

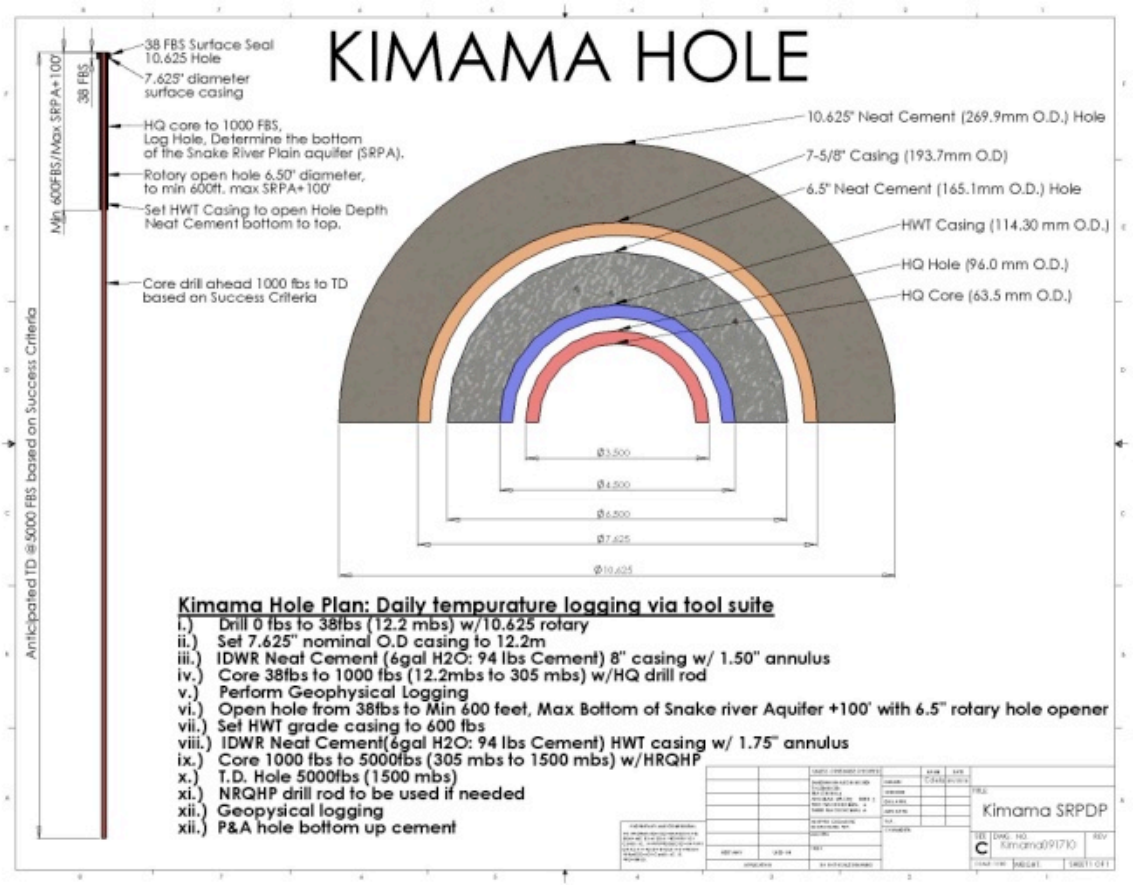

Figure 7-6. Kimama Hole Plan to 5000 feet.

Kimama Drilling History

The Kimama hole has IDWR well tag D0057001 on permit number 59752, granted to Utah State University Department of Geology. It was determined by IDWR that the use of blow out prevention equipment would not be necessary until bottom hole temperatures exceeded 100^{o}C. We preformed temperature logging every 100 fbs (Nielson *et al.* 2012). The Kimama hole was spudded on September 26, 2010. We drilled without returns the entire hole since the basalts were too fractured for lost circulation material or cement plugs to work. Despite the lost circulation, drilling went smoothly through multiple basalt, clay, and sand zones, through the water table at 260 fbs until October 3, 2010 where at 688 fbs we had a collapse of a sand zone that caught the string. The rods were worked through October 4, 2010 when the decision was made to reduce to NQ diameter to the 1000 fbs mark. NQ core was terminated at 1097 fbs mark and tripped out. We recovered 647 feet of HQ rods by cutting the string. The HQ rods were tripped in again to attempt drilling out the remaining steel. The hole was found to have collapsed at 647 fbs, and, in the clay and sand zones, the drill string moved off the original hole creating 1-B. Drilling progressed to 996 fbs and completed on October 12, 2010. The progress of the hole relative to budgeted time is shown in Figure 7-7.

The following day a 6-1/2” hole opener was installed and the opening procedure started. This activity was slower than anticipated, but progressed to 895 fbs. On October 23, 2010, we decided to run and cement the 4-1/2” casing at 895 feet. Pressure grouting of the 4-1/2” casing took place on October 23, 2010. HQ coring proceeded to a depth of 3887 fbs on November 23, 2010. At this point, we decided to reduce to NQ coring to increase the penetration rate. At this time, the equipment was winterized and shut down for Thanksgiving holiday. Drill crews reassembled on November 29, 2010, after a very harsh turn in weather shown Figure 7-8.

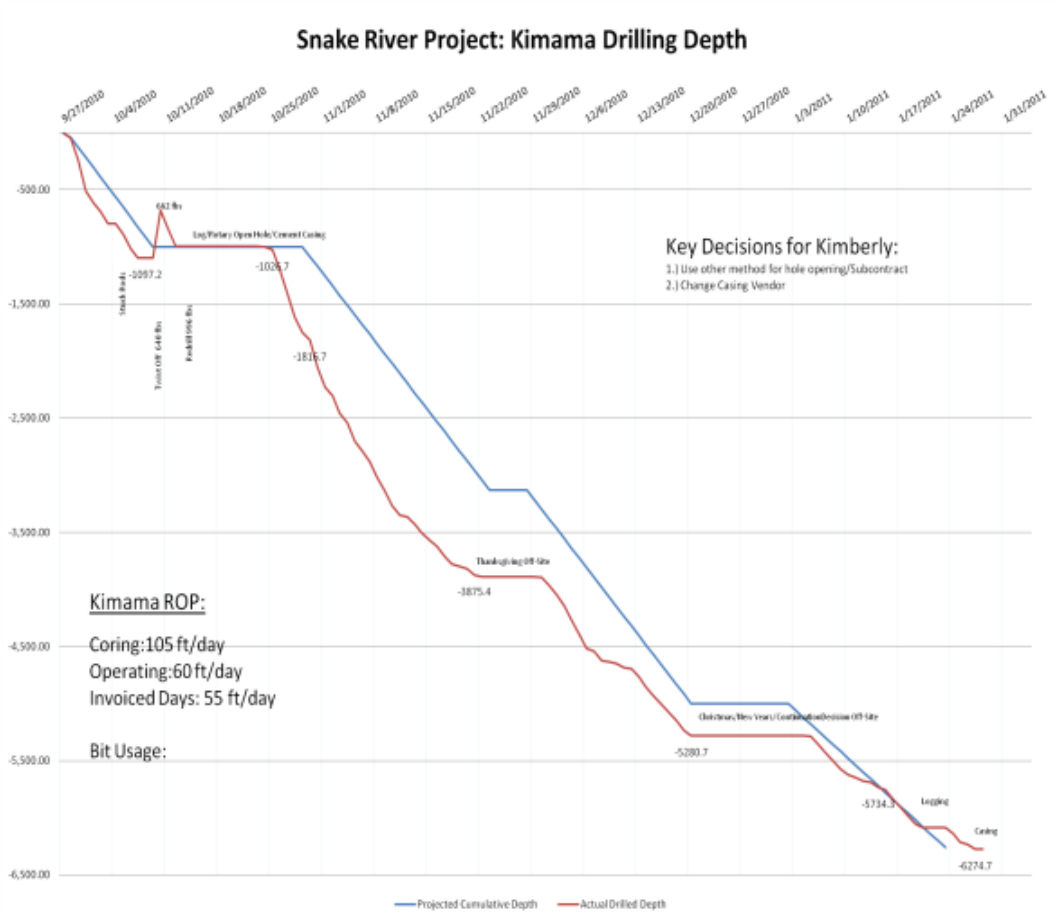

Figure 7-7. Kimama depth vs. time.

Figure 7-8. Kimama in winter

Drilling resumed on November 30, 2010 and reached a depth of 5000 fbs on December 16, 2010. Drilling to the original planned T.D. was accomplished on time and on budget. However, we were still drilling basalt, and the anticipated contact with rhyolite had not been intercepted. At the depth of 5280 fbs on December 20, 2010 the rhyolite interface had still not been reached. At that time, the project shut down for Christmas and New Year's in order to review budget and determine how much further our drilling budget could be stretched. After the Holiday break and budget review, it was decided that funds would be reallocated from the Kimberly hole and Kimama would be cored to a depth of 6000 feet.

Drill crews assembled on January 03, 2011 and coring proceeded to a depth of 6000 feet on January 19, 2011. The rhyolite interface had still not been intercepted. Again, after reviewing the budget, we continued coring to a total depth of 6275 feet on January 27, 2011 (Figure 7-9). The hole was completed in basalt.

A 2-3/8" liner was installed in the hole to total depth. There were two issues with the liner. First, we had planned to hang it in the hole , but it was landed and that was believed to have created a kink at 4622 feet. There was also a manufacturing issue that showed up when threading the liner. There was a visible non-concentricity in the pin and box ends making the inner diameter smaller. The tight inner diameter of 1.994" minus the non-concentricity would not allow tools to pass that point during temperature logging. The geophysical logging of the hole commenced on June 29, 2011 and lasted until July, 06, 2011. The casing was used as a tremie pipe, and Kimama was plugged and abandoned on October 12, 2011.

Figure 7-9. Kimama Core at TD 6275 fbs.

Kimama Results

Total Depth: 1-A 38-1097:	1059 feet / 322.8 m
1-B 662-6275:	5613 feet / 1711 m
Total footage Drilled:	6672 feet / 1912 m
Total core recovered:	6663 feet / 2031 m
Core Recovery:	6663/6672 = .9986 (99.86%)
Mud consumption:	$33.80 USD/ft. (Lost circulation at the onset of hole)
Bit usage:	$4.88 USD/ft
Total Days:	135.5 (Site Prep to demobilization, off site inclusive)
Days Offsite:	22 (Holidays and site reviews)
Days of Operation:	103.5
Days Drilling:	59.5
Days Ops not Drilling:	44
Days Standby:	10
ROP when coring:	105.4 ft/day
ROP While Operating:	60.6ft /day
ROP days invoiced:	55.3 ft/day
Max Bottom Hole Temp While Drilling:	59.3^{o}C

Results are shown actual time breakdown as in Figure 7-10. Operations time breakdown is shown in Figure 7-11.

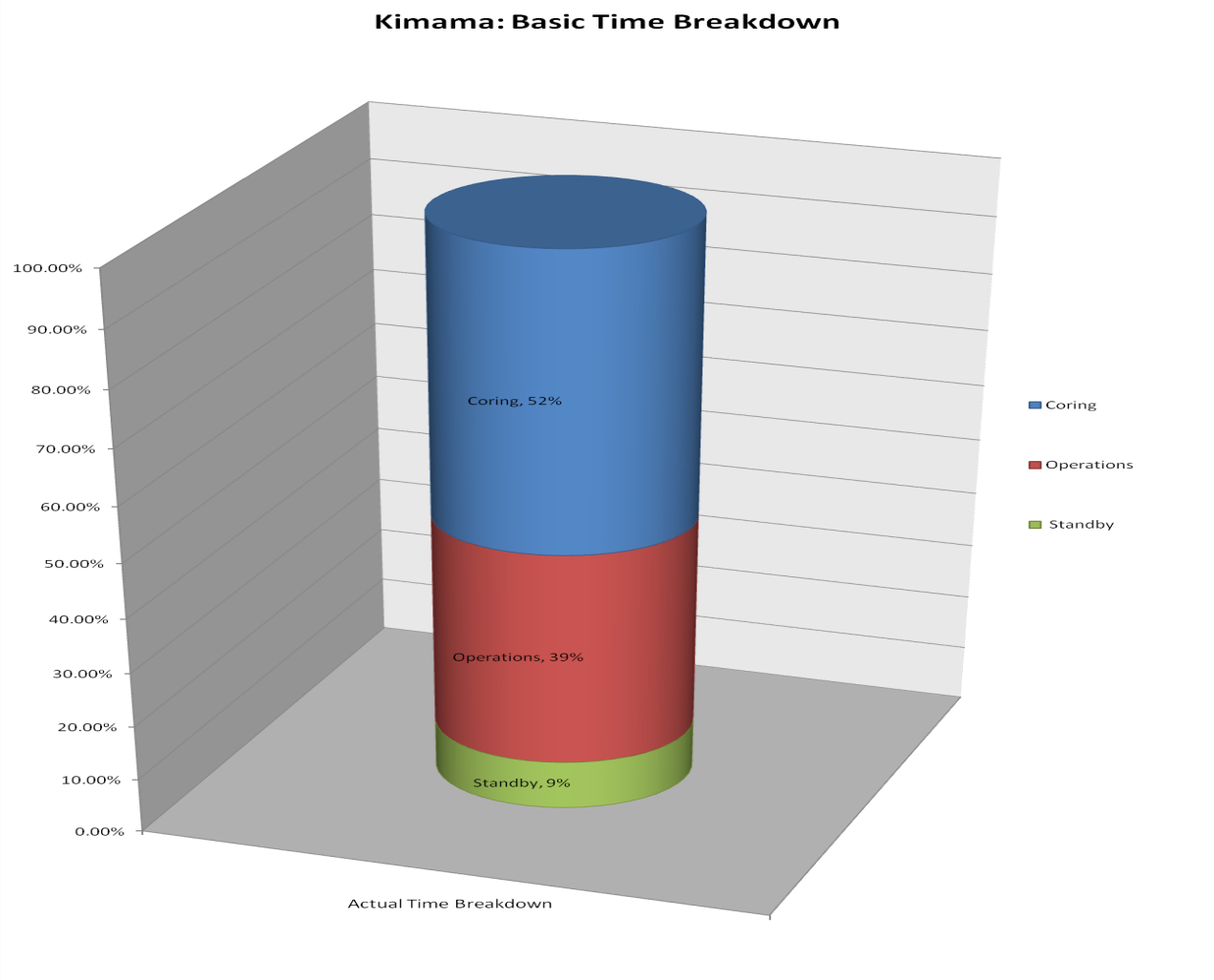

Figure 7-10. Kimama time Breakdown.

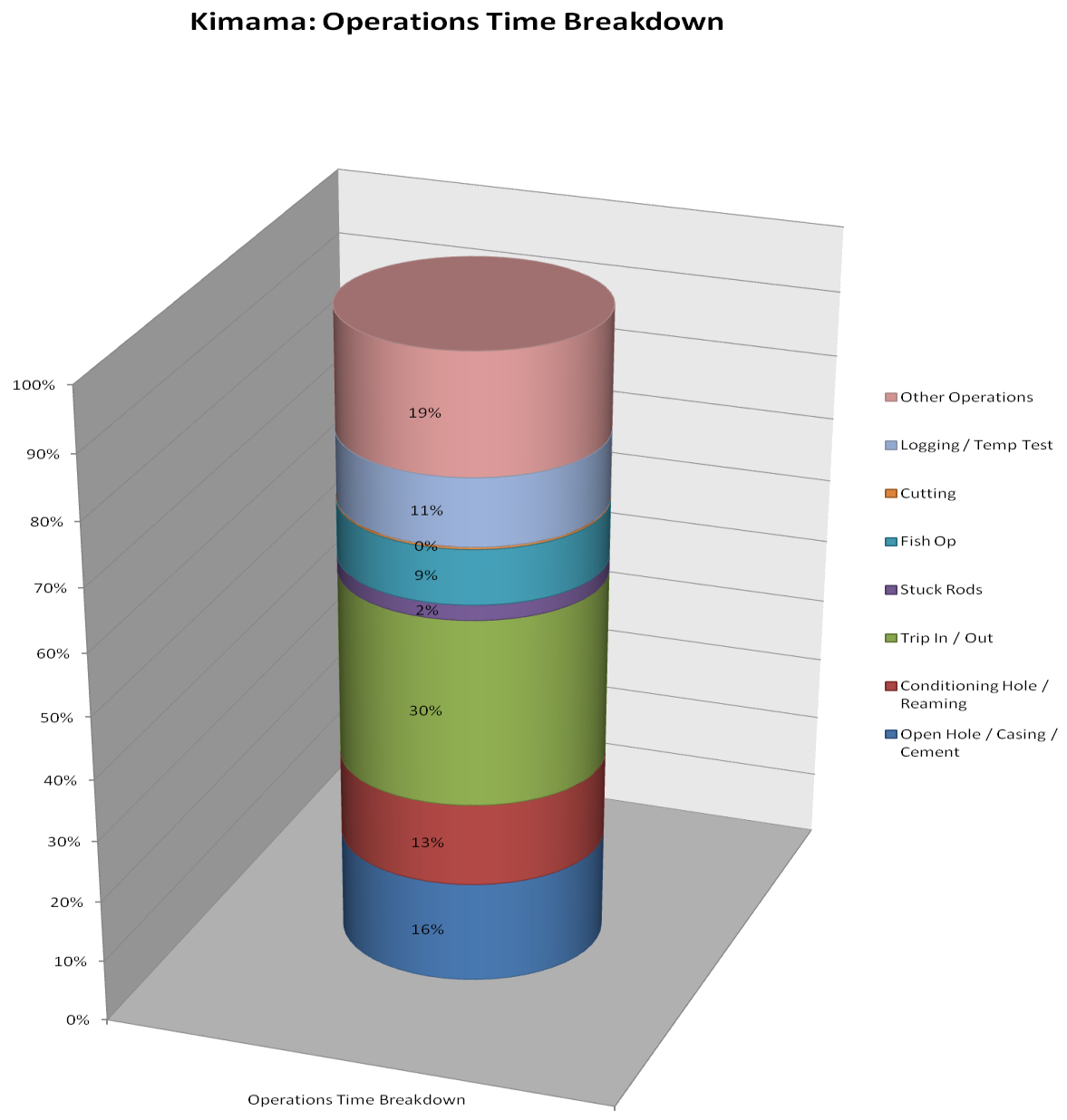

Figure 7-11. Kimama Operations Time Breakdown

Kimama Lessons Learned

In the course of drilling at the Kimama location a few lessons were learned. First, although the CS-4002 a great drill rig for coring, is not as effective at rotary drilling. A larger mud pump must be used in order to lift the cuttings at a suitable up hole velocity so that the bit does not re-work the cuttings continuously. This will help with the bit life and rate of penetration. On subsequent holes we decided to use a rotary company to drill and set the initial 4-1/2" casing to 10 percent of the hole depth or greater. Second, we decided to change liner vendors because of quality control problems with the threading. It is believed that this was a large factor in not being able to pass 4200 foot depth. In general, the liner did its job but the machining was crude. Third, we tried to core the upper portion of the hole with water only; this led to problems with hole stability in the loess sections that could not be adequately remedied by switching to mud. This was likely partially responsible for the hole going off-track in the 400-600 foot sediment layer, which resulted in the need to kick off into a new hole at 660 feet (Hole 1B). Lastly, we needed something better for loss of fluids. The upper 280 feet of the Kimama hole, above the water table, was so permeable that cement was not effective in plugging the lost circulation. Cement was pressure grouted on the back side of the 4-1/2" casing to ensure as good of a job as possible, but what should have been a four cubic yard cement job ended up consuming 50 cubic yards in order to close off the casing annulus.

Operations other than drilling or standby accounted for 39% of the time spent on site at Kimama (Figure 7-10). Much of this time (30% of operations) was spent tripping (Figure 7-11). Other operations that accounted for significant time were related to opening the hole for casing and casing, and other hole-conditioning operations (29% of operations; Figure 7-11). Much of this time would have been saved by using a rotary water-well rig to open the hole to 10% anticipated TD, as discussed above. Geophysical and temperature logging only accounted for 11% of operations time.

KIMBERLY (42°32'59.39"N 114°20'33.26"W)

The Kimberly drill site was located approximately 2 miles northeast of Kimberly City on US Highway 50, on property owned by the University of Idaho. This area is a semi-rural area with domestic residences within a quarter mile of the desired drill pad. This site had the convenience of access from a major road, with easy water access from city fire hydrants within a mile. As previously stated, the reason for drilling at Kimberly is that it lies on the margin of the Snake River plain, and has a relatively thin basalt cap that overlies known rhyolite.

Kimberly Drilling/Casing Plan

The original drilling and casing plan for the Kimberly hole is the same as the Kimama hole, with the exception that the original planned depth of the Kimberly hole was to be 6000 feet. The Kimberly hole drill plan is as follows and seen in Figure 7-12.

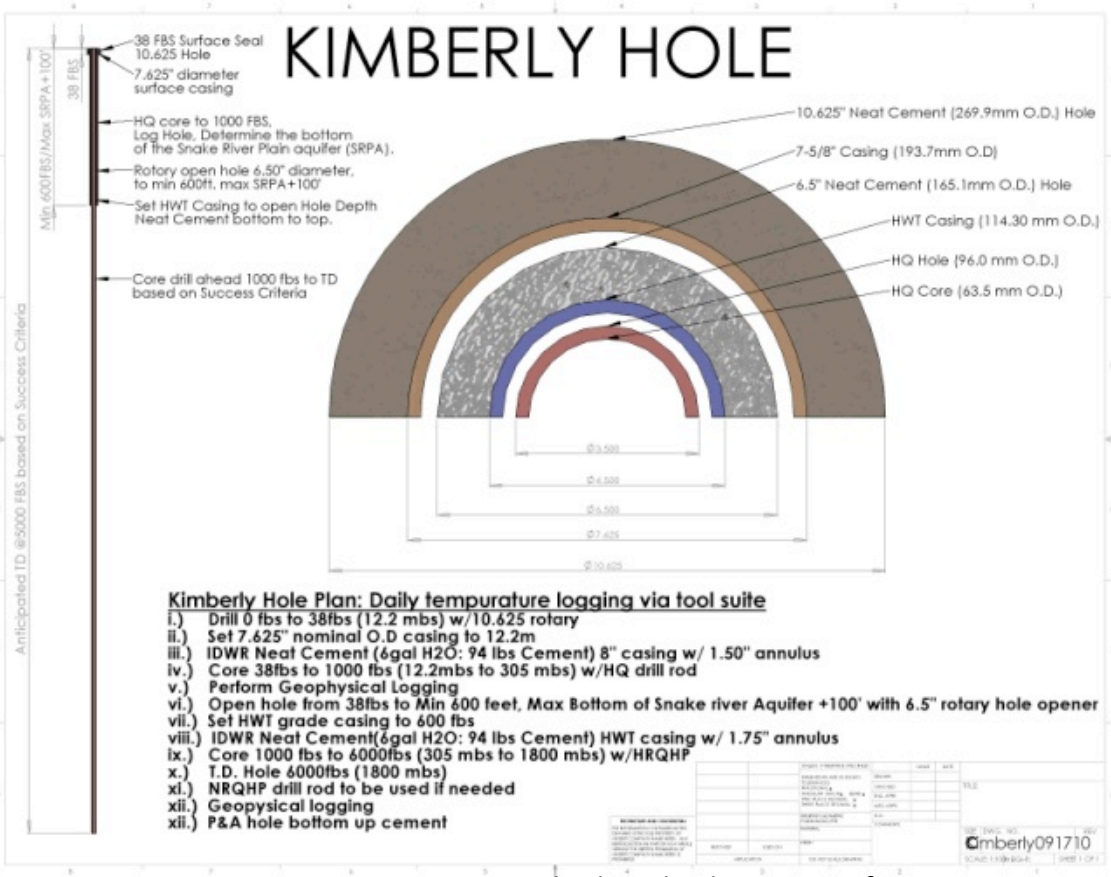

Figure 7-12. Kimberly Hole Plan to 6000 feet.

The IDWR-approved well design is as follows:

> *Drill a 10-5/8" hole to 38 fbs, Install a 7-5/8" casing cemented with a neat cement pressure grouted bottom up. Then drill a continuous 3.830" diameter HQ-Core from 38 fbs to 1000 fbs. Log the upper 1000 feet. A 6-1/2" rotary hole opener bit would be attached to the string and hole would be opened to 1000 feet. Install 1000 feet of 4-1/2" 0.25" wall HWT threaded casing cemented with a neat cement pressure grouted bottom up. Continuous 3.830" diameter HQ Core to 5000 fbs set temp casing and drill 3.032" diameter NQ Core if needed. Run geophysical logging in the lower 4000 feet of the hole. Install 5000 feet of 2-3/8" tubing to TD and allow the well to equilibrate. Periodic monitoring of the temperature, and ultimately plug and abandon the hole with neat cement slurry installed by a tremie pipe.*

On January 18, 2011 DOSECC Inc started clearing the site at the Kimberly and preparing a 100' x 100' drill pad. As it was middle of winter the soil was easy to move on in the morning and quite mucky in the late afternoon. The dirt road coming off of the University of Idaho's drive way to the drill pad also required geo-fabric and engineered soils as seen in Figure 7-13. This increased pad preparation costs as it was not expected that this section would need work. A concrete box was installed to serve as a mini-cellar for the well head and annular preventer, and reserve pits were dug.

Figure 7-13. Kimberly site preparation.

Kimberly Drilling History

Taking the lessons learned from the previous hole we decided that the core of the top 700 feet would be sacrificed in order to obtain a cased hole in a short amount of time so that the hole total depth could be accomplished within a budget that had been partially distributed to the previous hole. Two miles directly to the north of this site, the Snake River cut through the margin, and 300 ft of the overlying basalt can be seen. Being able to describe this without drilling made it easier to sacrifice the core. In this light Eaton Drilling and Pump Service was called out to air rotary a hole to 700 fbs. They spud Kimberly on January 26, 2011. The 12" hole was drilled to 40 fbs, and 8" casing installed and neat cemented in. Eaton then used an 8" hammer to drill to 703 fbs hitting the water table at 224 fbs. 703 feet of 4-1/2" x 0.25" wall threaded HWT casing was neat cemented in and Eaton was dismissed on January 31, 2011.

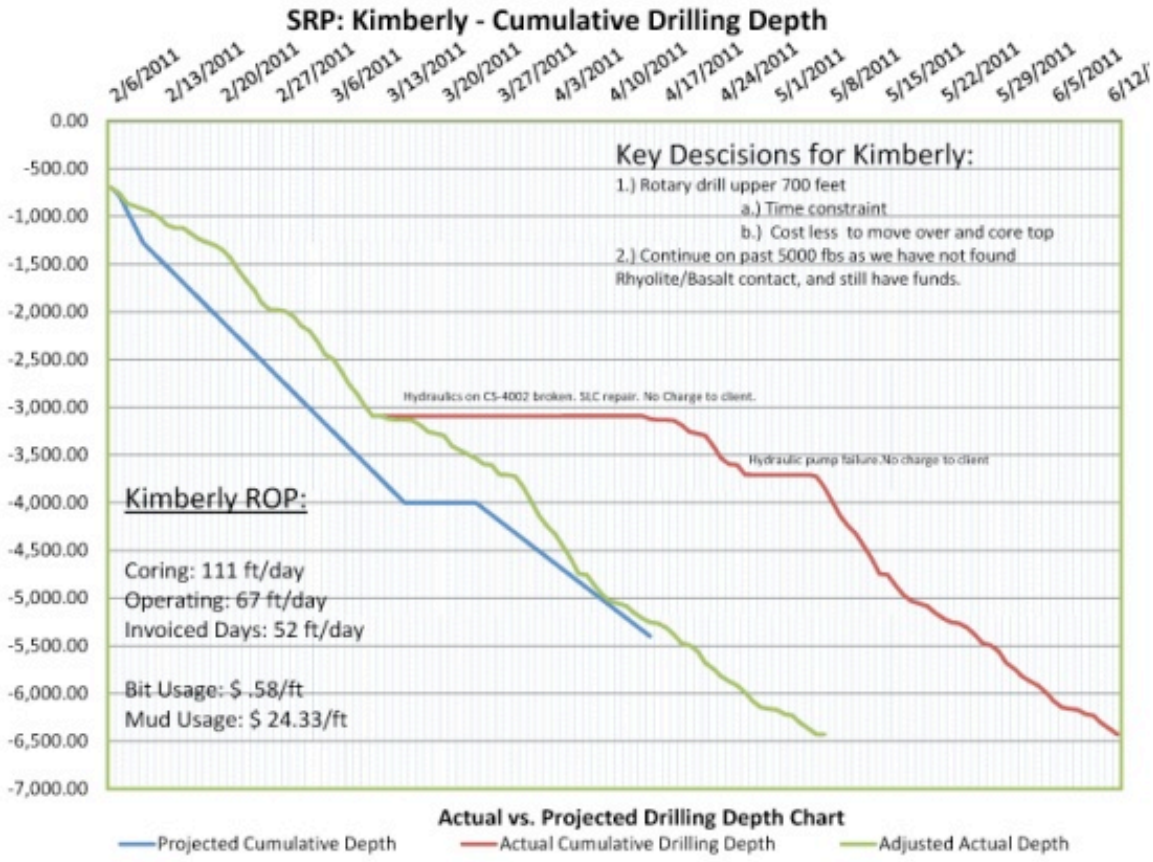

Figure 7-14. Kimberly depth vs. time and budget.

DOSECC Inc. then mobilized from the Kimama hole and proceeded to set up all equipment and was on the Kimberly site ready to drill out the casing on February 05, 2011. The progress of the hole relative to budgeted time is shown in Figure 7-14. We still drilled the entire hole with lost circulation as there was nothing that we used for LCM that would get or keep returns.

Drilling HQ from the onset we drilled to the 3091 fbs depth on March 11, 2011 with only minor issues and trips for bits. The lithology alternated between rhyolite (Figure 7-15) and basalt with two thick sections of silt, sand, and ash in the 875-950 and 975-1375 fbs levels.

Figure 7-15. Kimberly core at T.D. 6422 fbs.

Starting in late February of 2011 we noticed an issue developing with the feeding system of the CS-4002 drill rig. The head would drift down on its own once the main line break had been disengaged. This made it very difficult to control the feed rate and subsequently the weight on bit. The manufacturer could not diagnose the problem, and ultimately the repair was done by systematic replacement of parts, starting with the least expensive. After many pressure and load tests on the system, we determined that as unlikely as it may be the main feed cylinder was washed out and allowing the hydraulic bypass. At this point field repair was not possible. The Kimberly site was winterized and the CS-4002 was driven to Salt Lake City for repairs. Once the main cylinder was removed and inspected it was found that there was a crack that had developed in the main cylinder as seen in Figure 7-16.

Figure 7-16. Crack perpetuated from port through seal on piston.

The replacement cylinder was ordered, shipped and replaced. We were able to re-mobilize and drilling commenced in the Kimberly hole on April 13, 2011. With minor restart issues, hole conditioning and reaming to bottom core started out slowly but picked up until April 28, 2011 at 3709 fbs. The hydraulics became non-responsive and another inquest into issues started. We found that the primary pump failed and it is believed due to issues with the hydraulics system during the previous month. So a new pump was ordered and on May 5, 2001 was installed. At this point we decided to land the HQ rod as a temporary casing string and start coring NQ diameter in order to pick up time and depth in the budget. May 6, 2011 drilling started again and facing a large deficit in actual drilling days to budgeted, the crews got to work and in the following days up to the target depth of 5000 fbs were able to close the gap from 15 days over to just 4 days by May 18, 2011.

Upon arriving at the T.D. of 5000 fbs, we had not breached the formations underlying the rhyolites, and as there were still funds available the decision to drill ahead was given. Still using NQ we drilled to 6422 fbs by June 13, 2011 whereupon the rods became stuck. The hole was then completed at 6422 fbs (1958 m).

Extensive logging through the rods was started on June 15, 2011. When logging through the rods was completed a wireline cutting service was called out and the free point of the rods was measured and an chemical cut of the NQ rods was done at 6377 fbs on June 16, 2011. Open hole logging commenced while pulling the NQ rods out. After multiple tools were used the hole had become unstable at 6280 fbs. Multiple trips in and out with the NQ rods were made and each time the hole was unstable and would not remain open. Eventually tripping into the cut off NQ rods was not possible. Logging ceased on June 24, 2011 and 2-3/8" casing was run in the hole and crews tried to wash into the NQ rods up to June 28, 2011, including a trip to ream NQ to the cut interface. The casing was hung and its bottom was measured at 6270 fbs after tagging a bridge at 6280 fbs. The equipment was moved to Mountain Home and the drill rig went back to Kimama to do open hole logging there. Figures 7-17 and 7-18 show the time breakdowns for Kimberly.

Kimberly Results

Total Depth:	6422 feet / 1957 m
Total Footage Rotary Drilled:	703 feet / 214 m
Total Footage cored:	5719 feet / 1743 m
Total Core Recovered:	5727 feet (over 1.0 in certain zones with expanding clays)
Core Recovery - Cored Depth:	5727/5719 = 1.000 (100%)
Core Recovery - Total Depth:	5727/6422 = .8917
Mud Consumption:	$24.35 USD/ft. (Lost circulation at the onset of hole.)
Bit Usage:	$4.20 USD/ft
Total Days:	160.55 (Site Prep to demobilization, off site inclusive)
Days Offsite:	38 (Equipment related not billable)
Days of Operation:	122.5
Days Core Drilling:	57.7
Days Ops not Drilling:	38.8
Days Standby:	15.7
Days on DOSECC Onsite Repairs:	10.3
ROP when coring:	111.3 ft/day
ROP While Operating:	66.55 ft/day
ROP days invoiced:	52.41 ft/day
Max Bottom Hole Temp While Drilling:	59.3°C

Results are shown in basic time breakdown as in Figure 7-17; operations time breakdown is shown in Figure 7-18.

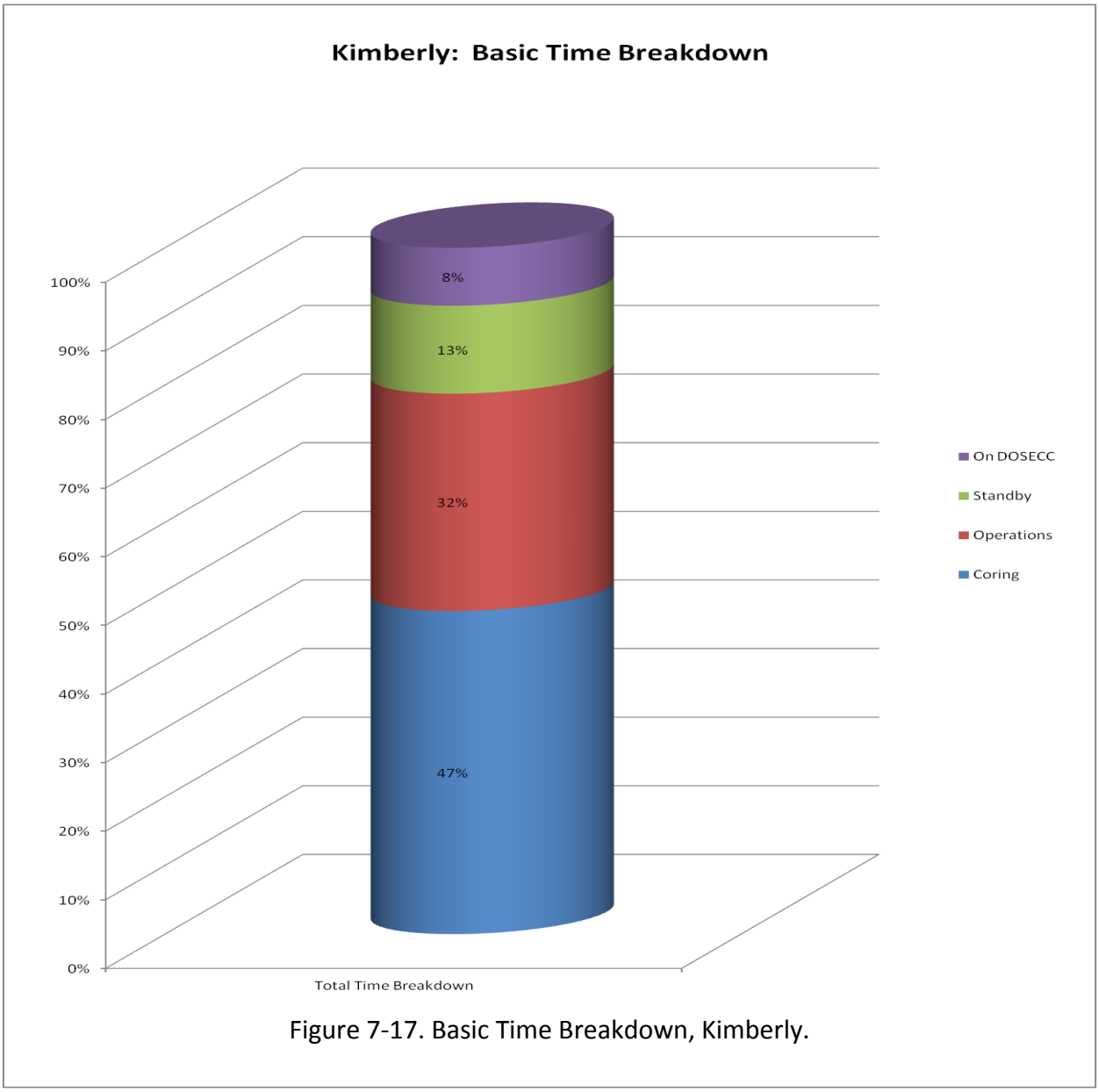

Figure 7-17. Basic Time Breakdown, Kimberly.

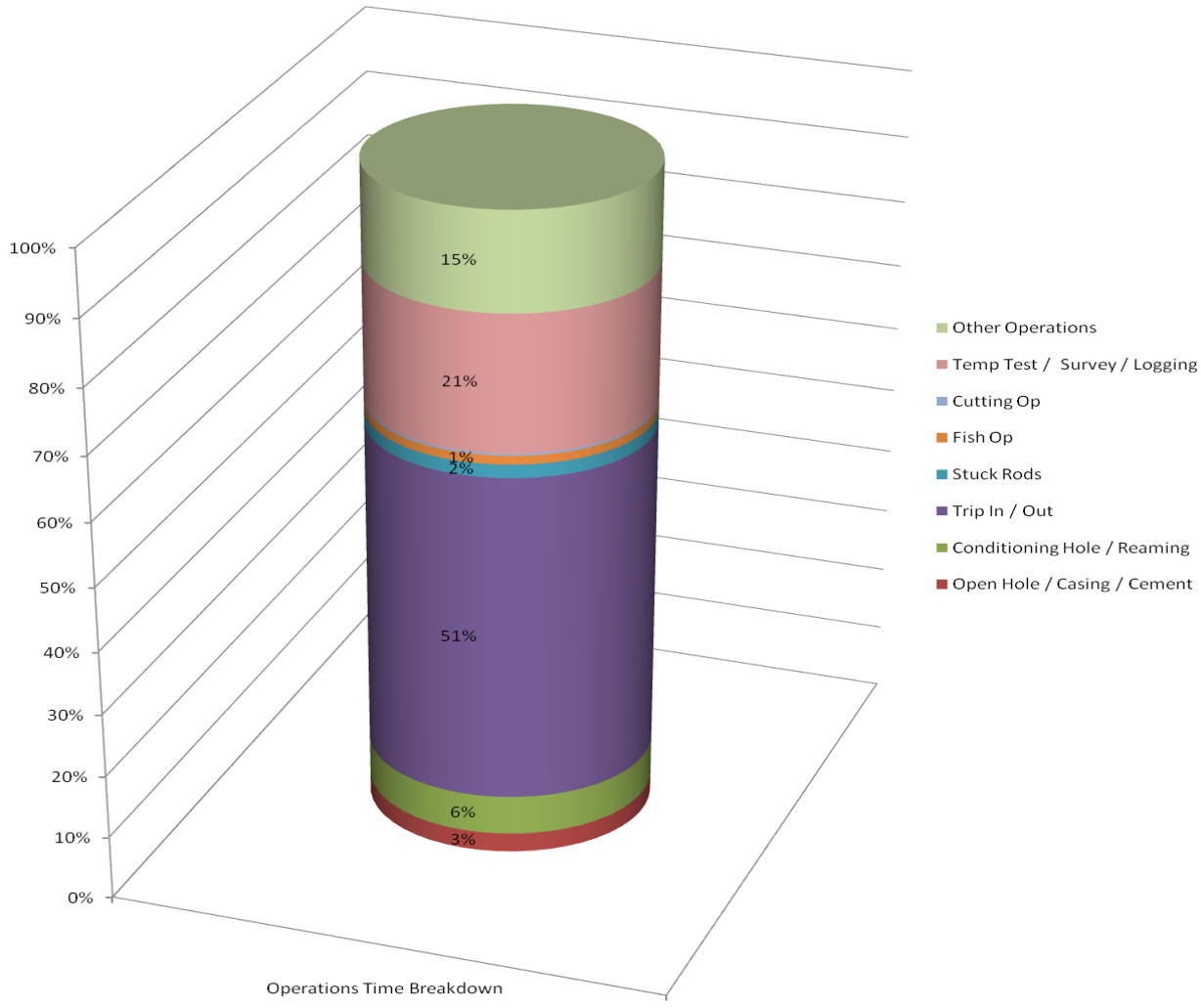

Figure 7-18. Operations Time Breakdown, Kimberly.

Kimberly Lessons Learned

Although the drilling went fairly well on the Kimberly site, we were plagued with a couple of long term drill health issues that made this particular site drag on 38 days longer than projected. Backwards analysis and observation of drilling procedures would indicate that high pressures can be formed inside the feed ram when drillers stop the head suddenly while fast feeding down in an open column. This was observed when drillers, waiting for a tool to latch, think it is caught on sand in the barrel and try to force it to seat and latch. Although no calculations or measurements have been done to verify if these actions are exceeding designed pressure rating of the feed ram, one can see that it is probably not good on equipment. In response, we implemented a procedure that helps avert such wear and tear on the feed system of our drill rigs. We also have a procedure to flush the entire hydraulics system after a major repair that involves any of 6 major areas: (1) Leveling Jacks/Mast Raise/ Mast Dump rams; (2) Head rotation motor, (3) Feed cylinder; (4) Main hoist motor replacement; (5) Wire line motor replacement; and (6) Any of the 3 pumps replacement. Lastly, in order to drill this area and make the hole cost effective, there needs to be a better LCM choice for the major fracturing that occurs in these upper basalts.

Only 32% of time on site at Kimberly was spent on operations other than drilling or standby (Figure 7-17). Again, much of this was trip time (51% of operations; Figure 7-18), with another 20% of operations time spent on geophysical and temperature logging. Conditioning, reaming, and casing the hole only accounted for 9% of operations time -- less than one-third of the time spent on these operations at Kimama.

MOUNTAIN HOME AFB (43° 4'11.57"N 115°53'34.61"W)

The Mountain Home MH-2 well site is located on the northwestern corner of Mountain Home Air Force Base, approximately 1⁄4 mile east of the Grandview gate. Our sponsor at this site was the 366th Civil Engineering Squadron Mission Support Group, who also prepared the drill site.

Drilling and coring was carried out using a Atlas Copco CS-4002 diamond drill rig with a rated depth capacity of 8400 fbs with NQ drill rod. Eaton Drilling drilled and set the surface conductor casing, and drilled and cased the upper 530-705 feet, using an Ingersoll-Rand air rotary rig. This allowed penetration of the upper part of the section quickly with a large diameter hole that could be cased to IDWR requirements for a geothermal test well.

The original drilling and logging plan for the well was worked out during the Snake River Scientific Drilling Project Technical Workshop held in Twin Falls in September 2009, which included personnel from DOSECC, ICDP, INL, and the U.S. Geologic Survey (USGS), and various universities involved in the project. Subsequently, meetings were held with DOD and MHAFB staff, INL scientists, and the "Project Hotspot" Drilling Team to discuss well construction and testing. The well was designed to be drilled in stages and logged between stages to accommodate the multiple engineering and scientific objectives of the project. A well schematic diagram prior the well being plugged and abandoned (P&A) is shown in Figure 7-19, and the drilling and casing plan is shown in figure 7-20.

In addition to satisfy the many technical objectives, the well design also had to meet all State of Idaho Well Drilling and Construction Standards in accordance with the Idaho Geothermal Resource Act. Well design, well drilling, and well construction in the State of Idaho are administered by IDWR. The well design was reviewed and approved by IDWR on June 1, 2011, with the specification that the well be properly decommissioned within one year of initiating drilling. Injection and/or production of geothermal resources were not authorized under the permit. On June 18, 2012, IDWR issued a six month extension on the drilling permit to allow the well to remain open for testing. The well was required to be decommissioned on or before December 23, 2012. The project met all the terms of the well drilling permit and its extension.

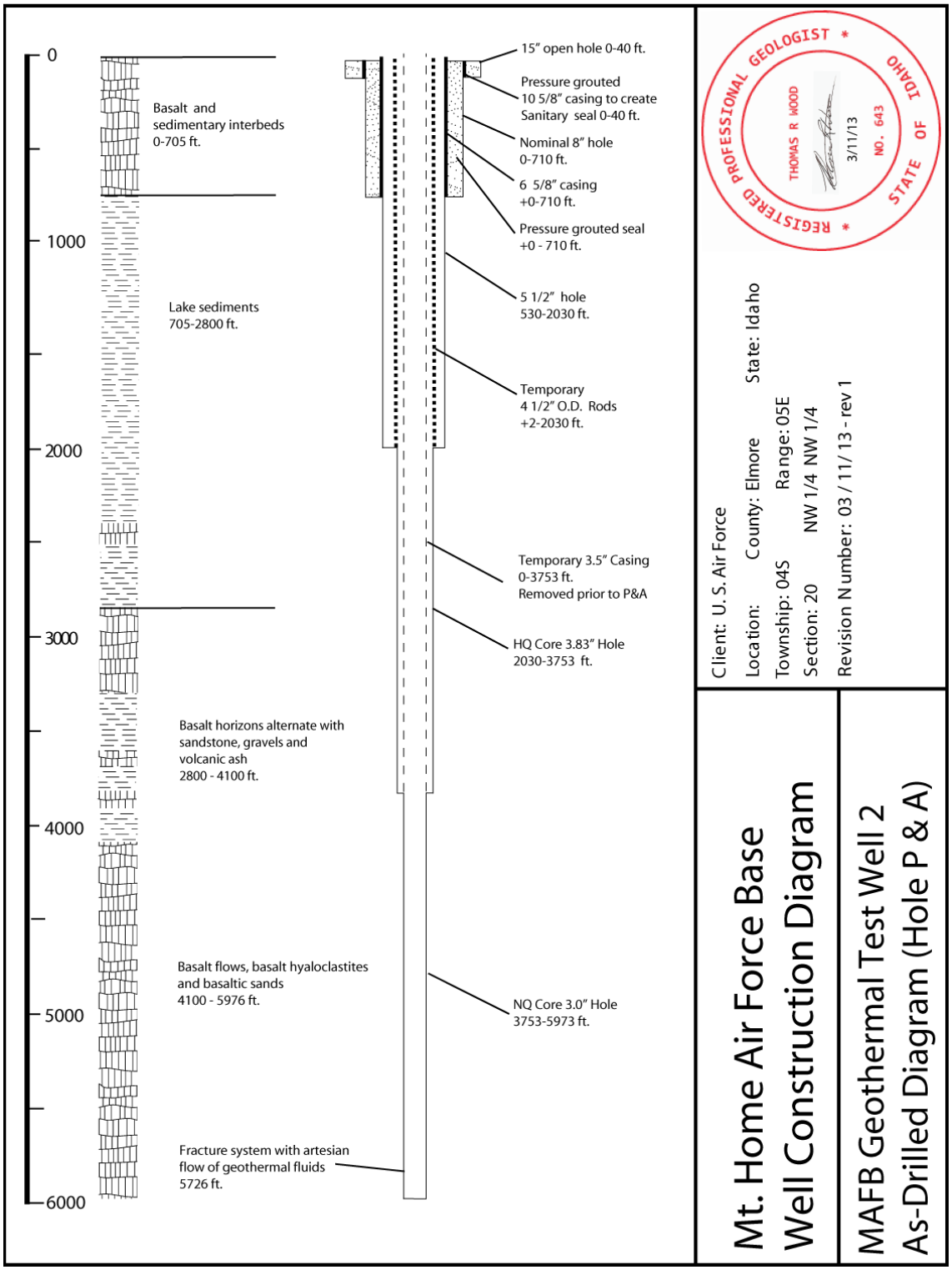

Figure 7-19. As-drilled well schematic (not to scale).

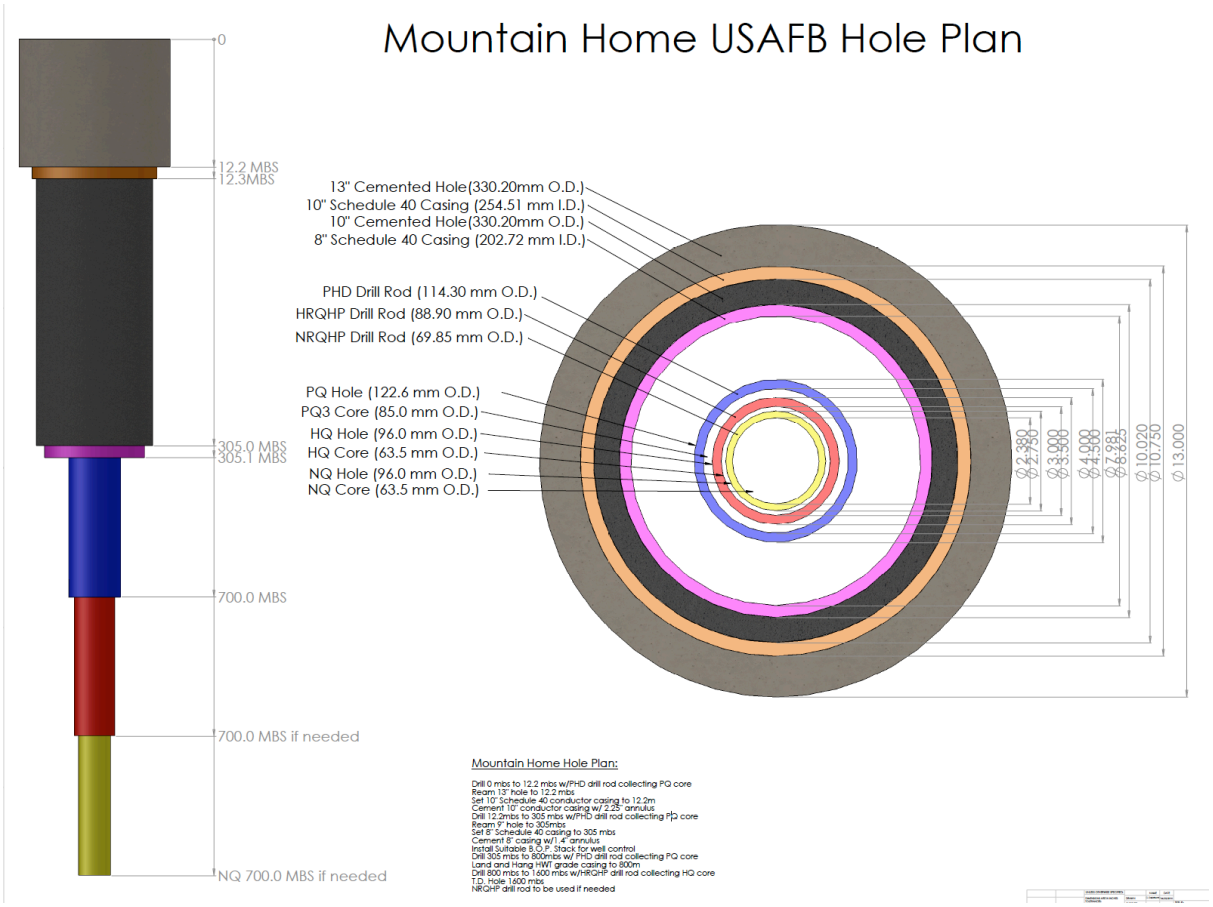

Figure 7-20. Drilling and casing plan for Mountain Home Well

Mountain Home Drilling History

Mountain Home test 2A on IDWR geothermal application 61-GR-08 was begun on June 24, 2011. Eaton Drilling and Pump Services drilled and set a 40-foot pressure grouted surface seal and then drilled to 530 feet below surface (fbs) through the basalt cap to the depth where the top of the lake sediments were expected to be based on other nearby well logs. DOSECC

Inc. moved on the hole and started coring from 530–705 fbs through massive basalt. Coring continued from 705–1967 fbs through sand and intermittent clay layers. At this depth the rods became stuck and drill crews worked for several days to free them. It was decided that it would be more cost effective to abandon this hole (MH-2A) and to start a new hole. The drill rod was cut above the stuck interval and retrieved for reuse. The new hole (MH-2B) was offset 20 feet from MH-2A. Eaton Drilling and Pump Services drilled and set a new 40-foot pressure grouted surface seal then drilled to 705 fbs through the basalt cap to the lake sediments. The CS-4002 Drill Rig was moved over the hole and DOSECC rotary drilled through the sediments to 2030 fbs. Upon reaching 2030 fbs in MHAFB test 2B and still in the lake bed sediment, the temporary

casing was landed to ease drilling difficulties. HQ core was drilled out the bottom of the temporary casing. HQ coring continued to 3753 fbs on October 29, 2011. NQ coring commenced after landing the HQ as a temporary casing string. Drilling was suspended over Christmas and New Year's from December 8, 2011 – January 15, 2012 to allow invoices to clear so that an accurate budget review could be performed. On January 15, 2012, the geophysical surveys began and lasted through January 22. NQ coring recommenced and advanced to 5640 fbs where lost circulation began to develop and at 5726 fbs on January 26, 2012 , water under artesian pressure flowed at 11 gal/min. Water sampling was performed and drilling continued using a heavy barite mud to balance the upwards pressure. NQ coring advanced to the total depth of the hole of 5976 fbs on January 31, 3012. The total depth of the hole was called due to budget constraints. Drilling progress at Mountain Home is shown in Figures 7-21 and 7-22.

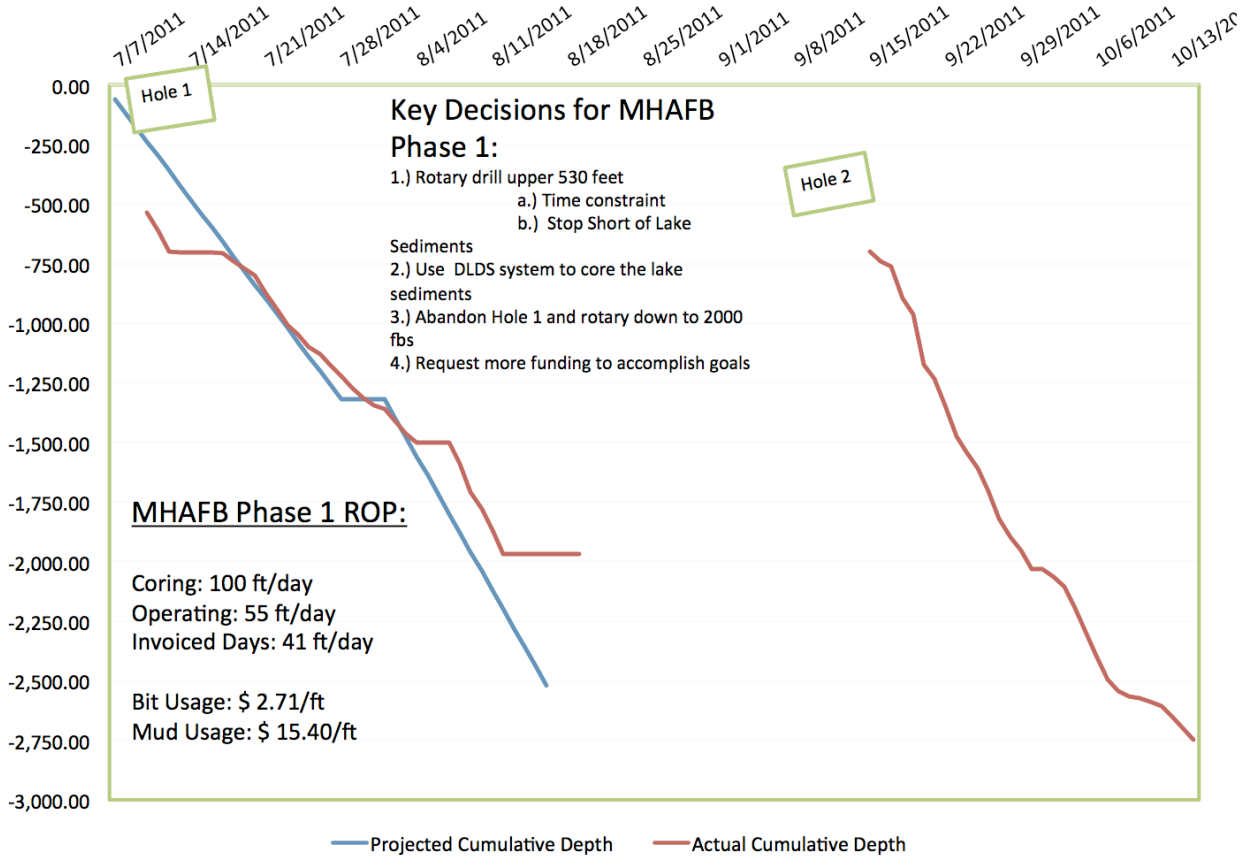

Figure 7-21. Drilling progress at Mountain Home AFB for Holes MH-2A and 2B (DOE-funded drilling operations).

Drilling operations funded by DOE at Mountain Home ceased on October 15, 2011, when the funds budgeted for drilling at this site were fully expended. At that time, ownership of the drill hole was turned over to the USAF, which provided funds for additional drilling as part of their "Green Energy" initiative. This additional drilling was referred to as "*Mountain Home Phase 2.*" At that time all onsite expenses were transferred to the USAF account, including support for all on-site science crews. Phase 2 drilling commenced on 16 October 2011, and continued to December 7, 2011. Drilling recommenced after completion of logging on January 22, 2012, and continued to January 29, 2012, as discussed above. Drilling progress for Phase 2 drilling is shown in Figure 7-19. Operational time breakdowns are depicted in Figures 7-23 through 7-26.

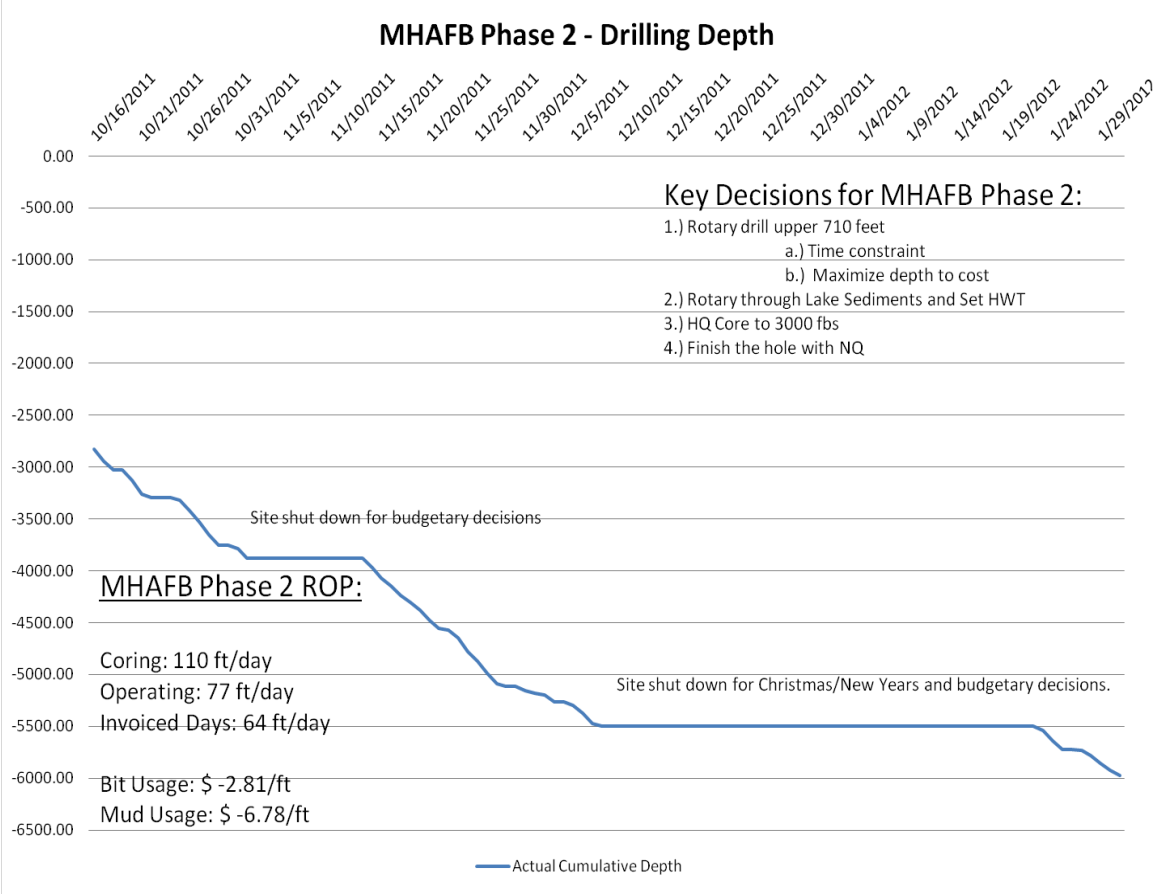

Figure 7-22. Drilling progress at Mountain Home AFB for Holes MH-2A and 2B (Phase 2: USAF-funded drilling operations, after completion of DOE-funded operations).

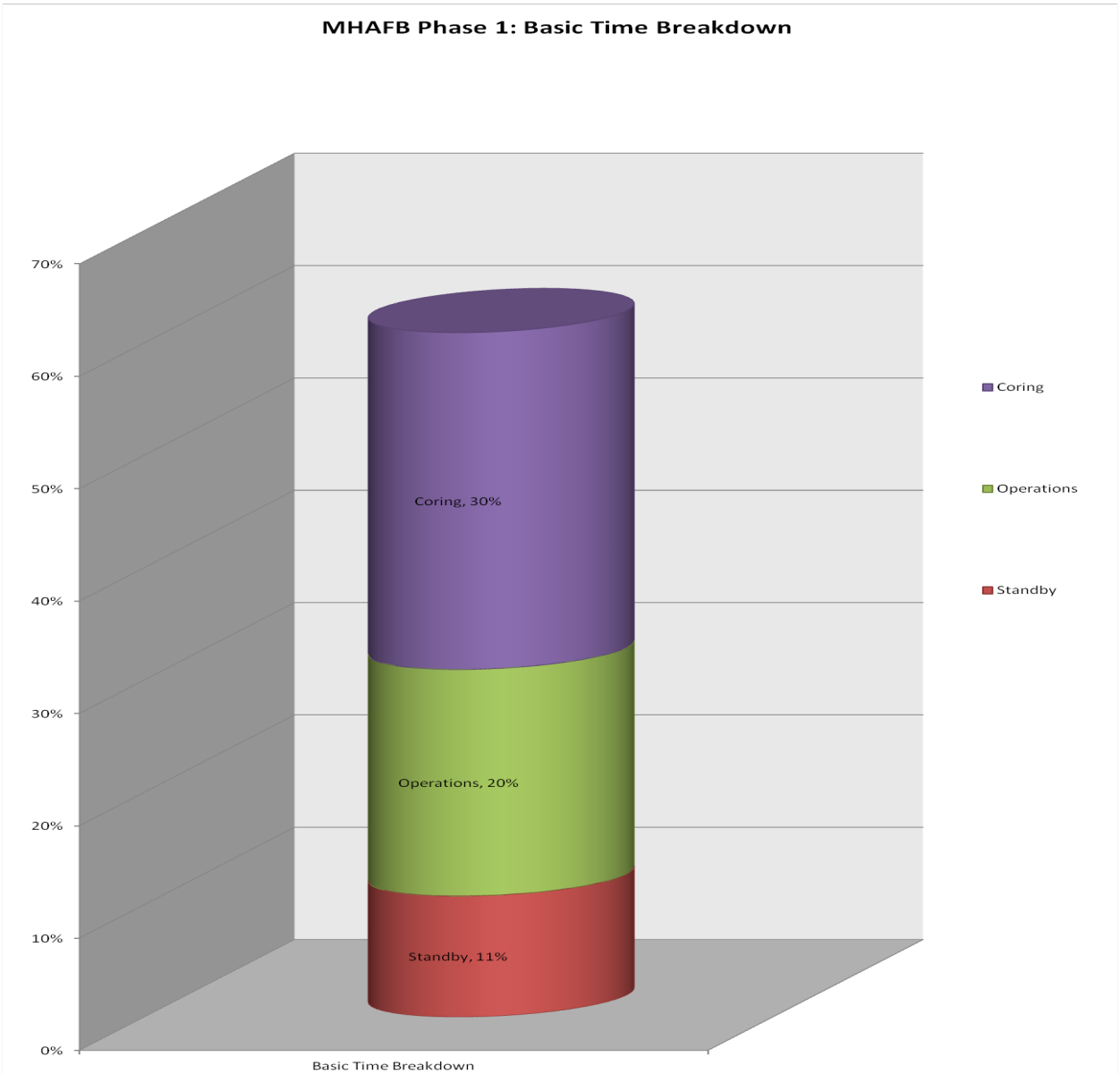

Figure 7-23. Basic Time Breakdown for Mountain Home, Phase 1 (DOE-funded)

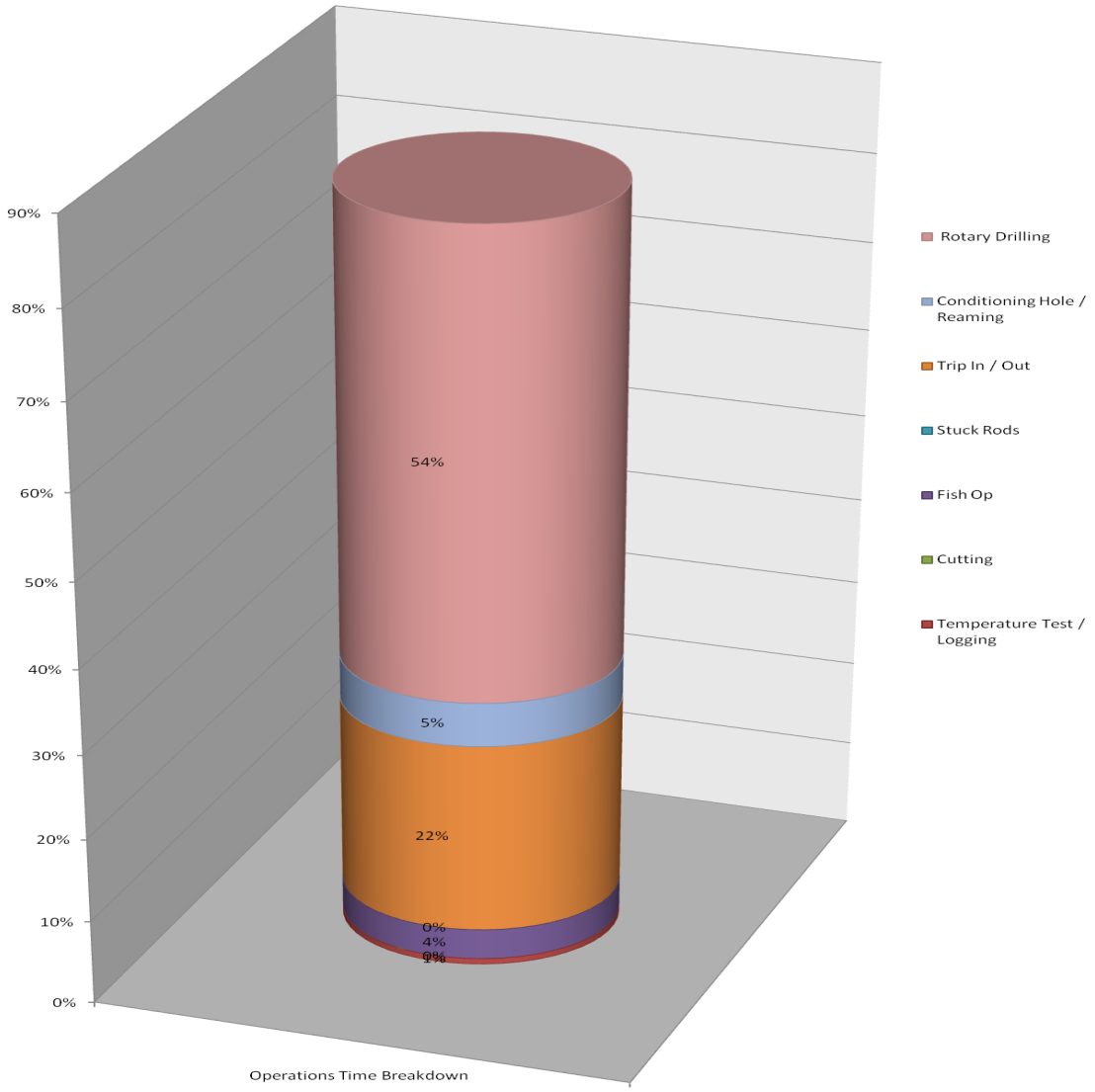

Figure 7-24. Time Breakdown for Operations, Mountain Home, Phase 1 (DOE-funded)

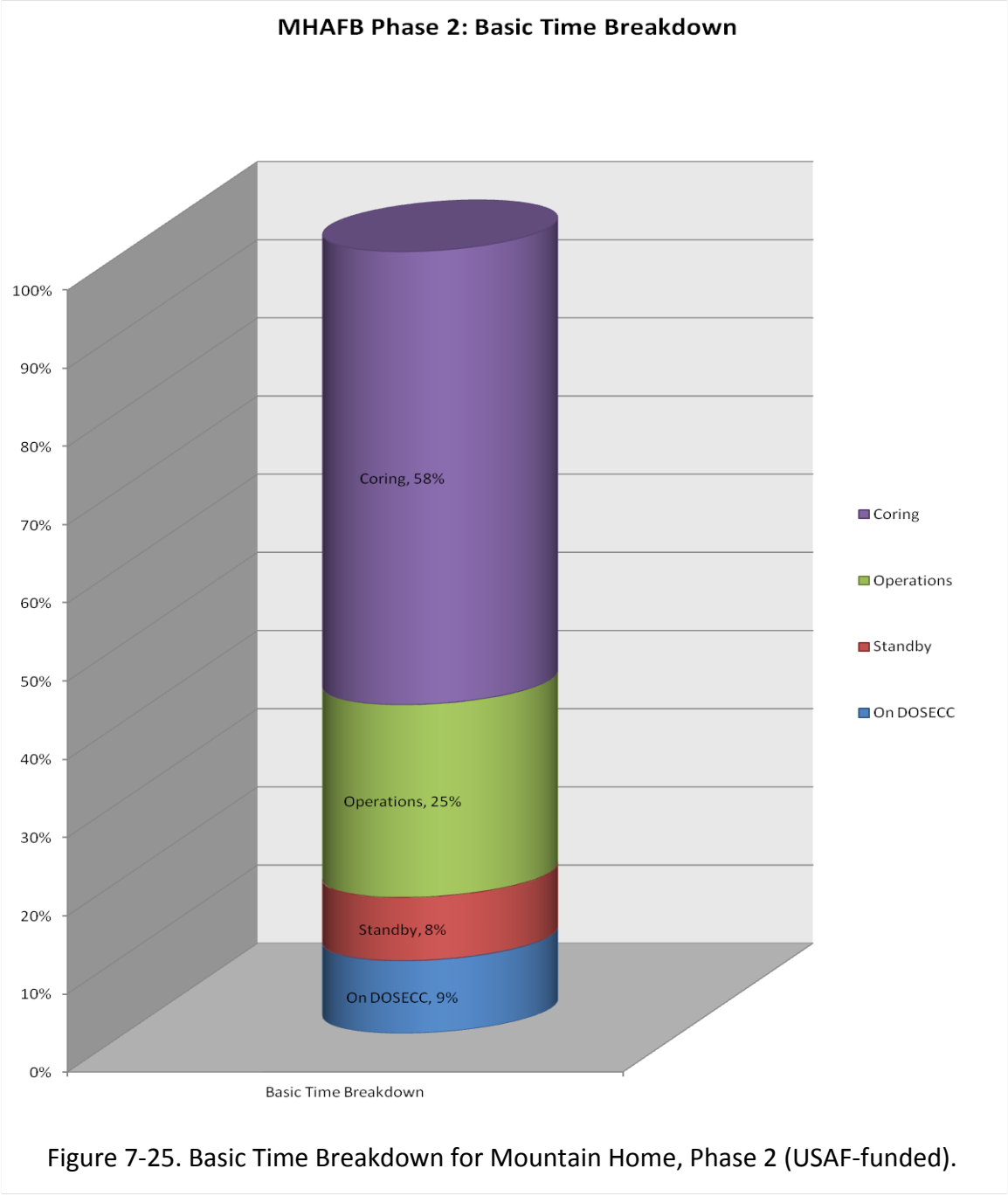

Figure 7-25. Basic Time Breakdown for Mountain Home, Phase 2 (USAF-funded).

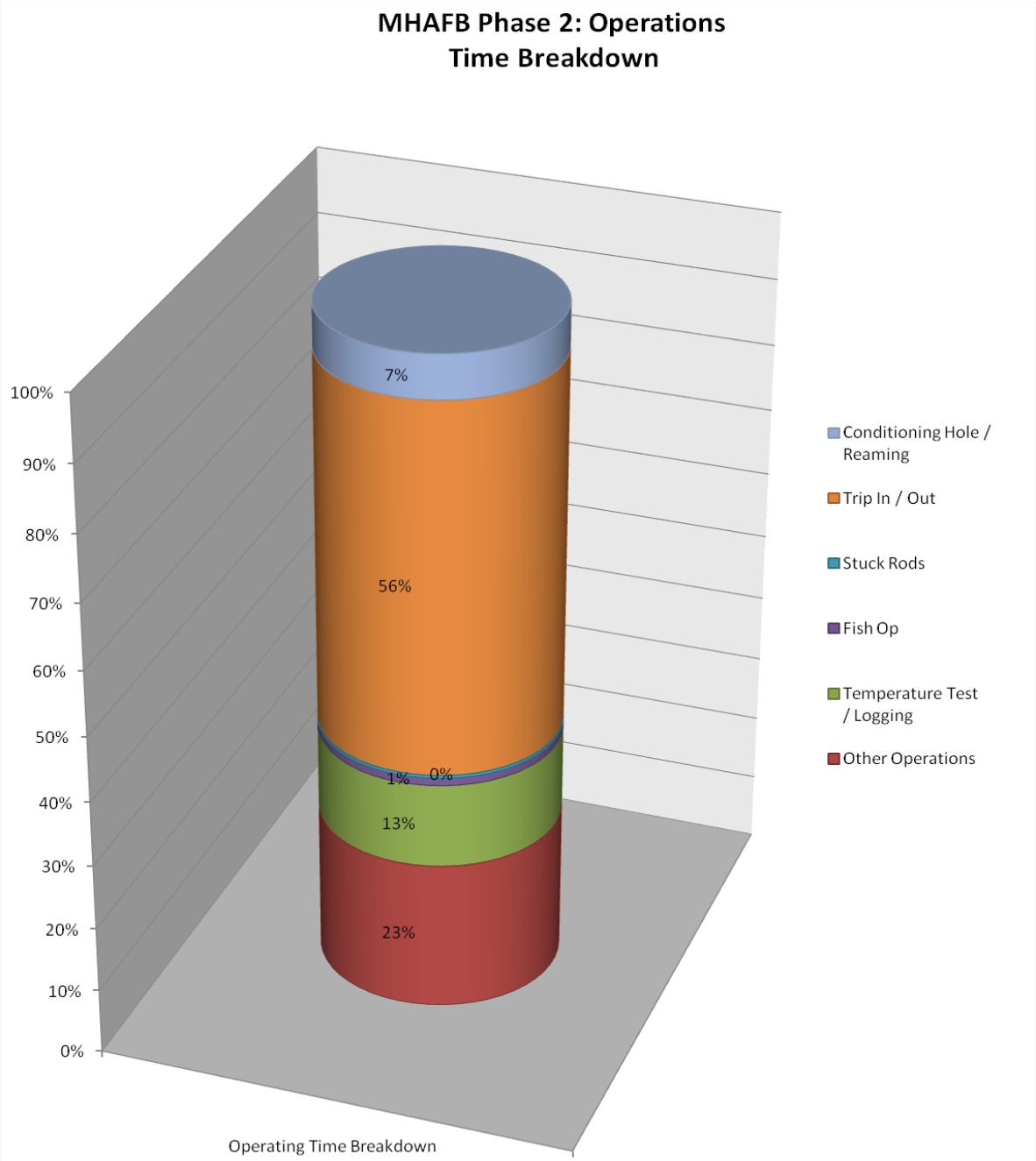

Figure 7-26. Time Breakdown for Operations, Mountain Home, Phase 2 (USAF-funded).

Plug and Abandonment of Mountain Home Wells

DOSECC, Inc., remobilized to Mountain Home on November 6, 2012, to P&A the hole. There was considerable discussion among the project team concerning the advantages of leaving the hole open as a monitoring well; however, the IDWR did not approve this option.

The CS4002 drill was set up on 11/07/12. The annular blow out preventer (BOP) was nippled up, and the 2-3/8” tubing was connected and 1500 feet of 2-3/8" liner was tripped into the hole. There was no upward flow of water from the hole. The liner was out of the hole by 15:00 on 11/08/12. The drillers then ran NQ rods in the hole and made temperature measurements with the DES temperature tool at 4200, 4800, 5600, 5720, and 5976 fbs, total depth (TD). No obstructions were encountered in the hole. Mud was circulated in the hole on 11/10/12 to reduce the bottom hole temperature in preparation for open hole logging. The NQ rods were withdrawn, and South West Exploration spent 11/11/2 and 11/12/12 logging the open hole.

The drillers then attempted to spear and retrieve the HQ rods that were landed at 3753 feet, on the morning of 11/13/12. However, the rods were stuck, so the drillers tripped out and ran in the rod cutter. Several attempts were made to cut and pull the HQ rod. The drillers were able to get the HQ rods cut and removed 3547 ft of HQ rod. An HQ bowen spear and NQ cutter were both lost with 1135 ft of NQ rod to the bottom of the hole while trying to cut and fish the rods. The drillers had the HQ rods out on 11/15/12 and tried to connect to the PQ rods. The PQ rods were in tight with barely any stretch. Three different attempts were made to cut the PQ at 1500, 1000, and 800 feet. All 3 attempts failed. The PQ rods were abandoned, and the NQ rods were tripped in to tremie cement. On 11/19/12, with a representative from IDWR present, the neat cement slurry was pumped down the tremie pipe to a depth of 4841 feet to the top of the NQ rod. In lifts of 1000 ft and volumes of 5 cubic yards, the hole was plugged with a total of 25 cubic yards of 15.5 lb/gallon neat cement. Cementing was accomplished by 11/19/12. The PQ casing was cut off 3 feet below grade, and the 3'x3'x3' cement cellar was filled with cement as a monument on instructions from USAF personnel. The equipment was rigged down on 11/20/12, and the site was cleaned, leveled and pits backfilled. A representative of the USAF approved the site, and all equipment was demobilized to Salt Lake City on 11/21/12.

Mountain Home Results

Total Depth:	MH-2A: 1967 / 599 m MH-2B: 5975 feet / 1821 m
Total Footage Rotary Drilled:	A: 503 feet / 153 m B: 2000 feet / 609 m
Total Footage cored:	5383 feet / 1641 m
Total Core Recovered:	5104 feet / 1556 m
Core Recovery - Cored Depth:	5104/5383 = 96.2%
Core Recovery - Total Depth:	5104/5975 = 85.4%
Mud Consumption:	$12.1 USD/ft.
Bit Usage:	$2.9 USD/ft
Total Days:	138
Days of Operation:	142
Days Core Drilling:	71
Days Ops not Drilling:	49.5
Days Standby:	21.5
ROP when coring:	111.0 ft/day
ROP While Operating:	66.0 ft/day
ROP days invoiced:	66.0 ft/day
Max Bottom Hole Temp While Drilling:	149^{o}C

Mountain Home Lessons Learned

Drilling in thick sedimentary sequences with diamond coring rig can present challenges in terms of hole stability. The simple HQ3 coring system (plastic liner in standard HQ core bit) performed better than the DOSECC lake drilling tools, which were used initially because we would be coring lake sediments. However, the well-indurated sediments and sedimentary rock responded well to standard diamond coring tools. Rotary drilling through the sediments (MH-2B) after failure of the first Mountain Home hole (MH-2A) proceeded more quickly than coring, but not as quickly as a larger oil-field rig using oil-field tubulars due to the nature of the diamond core drilling (thinner tubulars, high rpm, low bit weight) versus oil field rotary drilling (thick joints on tubulars, low rpm, high bit weight). In future holes in this area we would contract with an air rotary water well driller to go as deep as possible (~400 m) to set casing before beginning rotary or diamond coring with the diamond core rig.

OVERALL LESSONS LEARNED

The use of small diamond coring drill rigs, which are commonly used in mineral exploration for resource confirmation, to produce slim holes (<6" diameter) for geothermal exploration and geothermal resource confirmation is clearly an effective and cost-efficient approach. After subtracting logistical support and wireline logging costs (both direct payments to contractors that were paid through DOSECC, and the time needed to carry out the logging campaigns), the cost of our ~2 km deep slim holes was around $1M each. In one case, costs were inflated by hole failure, but in most situations hole stability was not a significant problem. The ability to drill ahead under lost circulation conditions is especially important, although it does result in increased mud costs. Because oil-field style rotary rigs must cure lost circulation before they can proceed to deeper levels, drilling through sections with high proportions of lost circulation, or sections with continuous lost circulation (e.g., Kimama) can take significantly longer and result in significantly higher costs. Even without lost circulation issues, rotary drilling with large oil-field style rigs will result in drilling costs that are 3x to 4x higher per hole than slim hole diamond core drilling. It was found that contracting with local water well drillers using air rotary rigs to drill the upper part of each hole and case it (~upper 300 m) was a cost effective way to complete the hole at lower cost and to comply with IDWR regulations for casing and cementing geothermal test wells (which require 0.25" thick steel casing with 1" cemented annulus to 10% of total depth).

CHAPTER 8:

BOREHOLE GEOPHYSICAL LOGGING

Douglas R. Schmitt[1], Madeline D. Lee[1], Lee M. Liberty[2], James E. Kessler[3], Jochem Kück[4], Randolph Kofman[1], Ross Bishop[1], John W. Shervais[3], James P. Evans[3], Duane E. Champion[5]

[1]Institute for Geophysical Research, Dept. of Physics, University of Alberta, Edmonton, AB T6G 2E1
[2]Center for Geophysical Investigation of the Shallow Subsurface, Boise State University, Boise, ID 83725-1536
[3]Department of Geology, Utah State University, 4505 Old Main Hill, Logan, UT 84322-4905
[4]ICDP Operational Support Group, Deutsches GeoForschungZentrum GFZ, Heinrich-Mann Allee 18/19, Potsdam, D-14473
[5]United States Geological Survey, 345 Middlefield Road, Menlo Park, CA 94025

ABSTRACT

Hotspot: The Snake River Geothermal Drilling Project was undertaken to better understand the geothermal systems in three locations across the Snake River Plain with varying geological and hydrological structure. An extensive series of standard and specialized geophysical logs were obtained in each of the wells. Hydrogen-index neutron and γ–γ density logs employing active sources were deployed through the drill string, and although not fully calibrated for such a situation do provide semi-quantitative information related to the 'stratigraphy' of the basalt flows and on the existence of alteration minerals. Electrical resistivity logs highlight the existence of some fracture and mineralized zones. Magnetic susceptibility together with the vector magnetic field measurements display substantial variations that, in combination with laboratory measurements, may provide a tool for tracking magnetic field reversals along the borehole. Full waveform sonic logs highlight the variations in compressional and shear velocity along the borehole. These, together with the high resolution borehole seismic measurements display changes with depth that are not yet understood. The borehole seismic measurements indicate that seismic arrivals are obtained at depth in the formations and that strong seismic reflections are produced at lithological contacts seen in the corresponding core logging. Finally, oriented ultrasonic borehole televiewer images were obtained over most of the wells and these correlate well with the nearly 6 km of core obtained. This good image log to core correlations, particularly with regards to drilling induced breakouts and tensile borehole and core fractures, allow for confident estimates of stress directions and/or placing constraints on stress magnitudes. These correlations will be used in core orientation to derive information useful in hydrological assessments, paleomagnetic dating, and structural volcanology.

INTRODUCTION

The Snake River Plain (SRP), Idaho, hosts potential geothermal resources due to elevated groundwater temperatures associated with the thermal anomaly Yellowstone-Snake River hotspot. Project HOTSPOT has coordinated international institutions and organizations to understand subsurface stratigraphy and assess geothermal potential. Over 5.9 km of core were drilled from three boreholes within the SRP in an attempt to acquire continuous core documenting the volcanic and sedimentary record of the hotspot: (1) Kimama, (2) Kimberly, and (3) Mountain Home (Figure 1-4). The most eastern drill hole is Kimama located along the central volcanic axis of the SRP and documents basaltic volcanism. The Kimberly drill hole was selected to document continuous volcanism when analysed in conjunction with the Kimama drill hole and is located near the margin of the plain. The Mountain Home drill hole is located along the western plain and documents older basalts overlain by sediment.

The following report covers the details of the logging process, the data collected, and preliminary discussion. The wireline logging was carried out overall between 2010 and 2012 and the principle aim was to identify porosity, fractures, drilling induced fractures, and lithological variations. A detailed discussion on the preliminary borehole geophysics results can also be found in Shervais et al. (2013). An ambitious borehole geophysics program was implemented to both support the geological interpretations and to provide additional information on modern day tectonic regimes in the Snake River Plain. The logs obtained include total natural γ−radiation (including some spectral γ logging for U, Th, and K contents), neutron hydrogen index, γ−γ density, resistivity, magnetic susceptibility and full vector magnetic field, 4-arm caliper (i.e., dipmeter), full waveform sonic, and ultrasonic borehole televiewer imaging.

METHODS

The neutron and γ–γ density logs employ radioactive sources. As such, and in the interest of minimizing any risk they would be lost in the open hole, both these were run in the drill string. While this precludes accurate quantitative assessment of density or hydrogen index, it does provide useful semi-quantitative comparisons for purposes of mapping the lithology. These data were acquired by the USGS (Twining and Bartholomay, 2011) and Century Geophysical in the upper and lower sections of Kimama; Co-log and SouthWest Exploration obtained a neutron logs in the Kimberly and Mountain Home core holes, respectively.

The neutron response is primarily sensitive to the density of hydrogen nuclei in the surrounding fluids, clays, and hydrous alteration products. As such, and somewhat unexpectedly, the relative neutron log intensity could indicate individual basalt flows primarily because of porosity and clay content differences between the dense massive basalt and the rubbly and sediment containing flow tops. This signal decays towards the top of the flow where

the higher porosity can contain more fluids and possibly hydrous minerals. The sediment layer, too, has higher porosity and contains clay minerals that produce a low neutron response.

Natural γ-ray radiation (NG) is produced by the decay of various isotopes of uranium, thorium, and potassium. The concentration of these elements is typically low in basalt except for horizons of "Craters of the Moon" type evolved basalts with high K_2O (>1wt%: Potter et al 2012). Spectral γ-logging (SG) through the thick rhyolites at Kimberly, however, gives wt% K concentrations of between 2.5% to 3.5% that contributes to a relatively high total response often in excess of 200 API units. In the basalt flows, the natural γ-ray log usually, but not always, was a strong indicator of sediments throughout the flows.

The electrical resistivity, measured by the lateral log, is high in the massive basalts due to their low porosity and lack of conductive minerals. The lateral log resistivity mirrors to some degree the neutron responses. The sediments are much more conductive.

The full-waveform acoustic log also displays interesting correlations with the lithology through this section. Through the massive basalt the traveltimes are short indicative of the high sonic log velocity through this zone. Strong S-waves also appear throughout the massive basalt. Careful examination of these records may even show the existence of split shear waves (e.g. the section between 1374 m and 1372 m) that is most probably caused by stress induced anisotropy around the borehole. Only the P-wave first arrival is seen within the sediment layer. However, no clear S-wave that can be unambiguously interpreted through the sediments.

A summary of the logs collected at each hole, along with the depths intervals sampled, is presented in Figure 8-1.

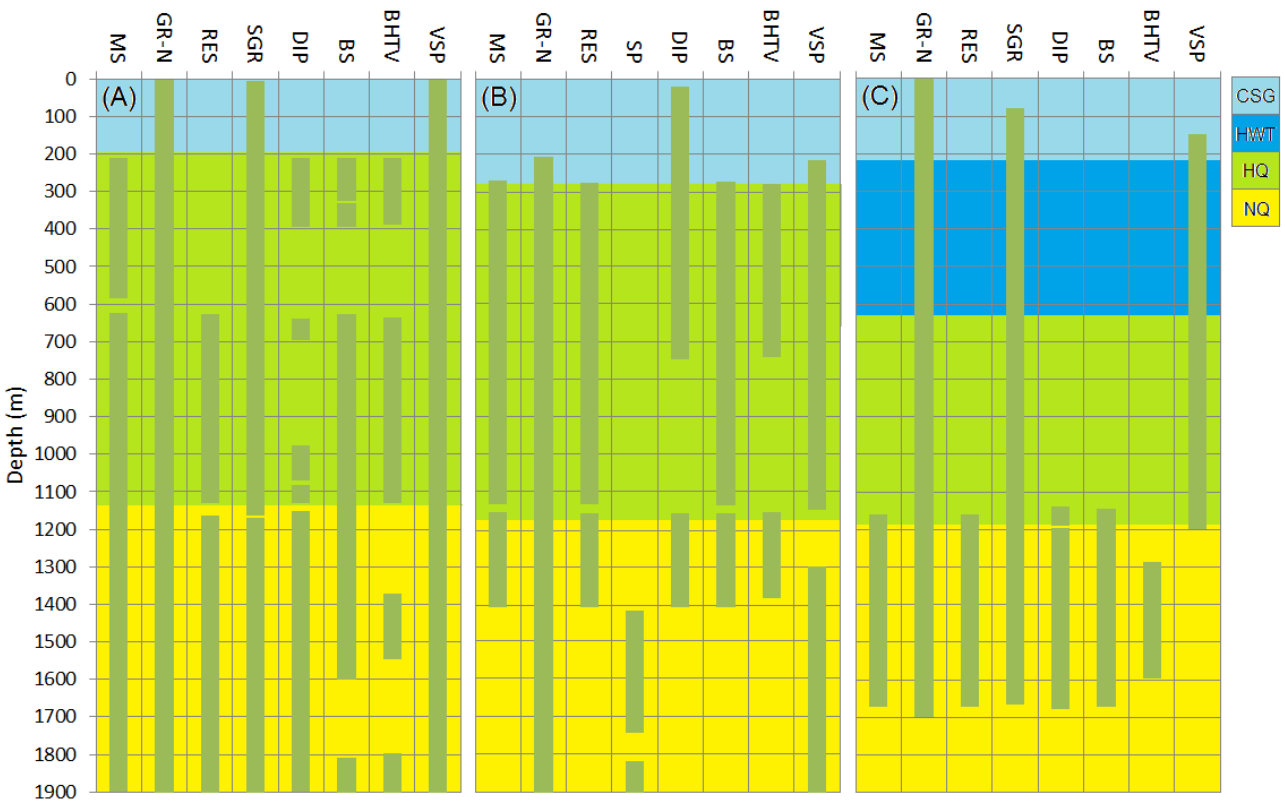

Figure 8-1. Log summaries for (A) Kimberly, (B) Kimama, and (C) Mountain Home. The measurements collected were: Magnetic susceptibility (Mag Sus); Radioactivity (GR-Neutron); Electrical properties (E logs); Spectral Gamma Ray (SGR); Sonic travel time and amplitude (Dipmeter); Acoustic properties (Sonic); Borehole Televiewer (BHTV); Spontaneous potential (SP); Drill log diameter (3 arm caliper); Vertical seismic profile (VSP). Drill log diameter is dependent on drill type: Coal Steam Gas (CSG), drill pipe (HWT), 75.7mm (NQ), and 96mm (HQ).

GEOPHYSICAL LOGS

Kimama Geophysical Logs

***Kimama*,** completed at a final depth of 1912 m, is sited on the axis of the Snake River Plain that blanketed with thick overlapping basalts originating from a series of vents. The important Snake River Plain Aquifer (*Hubbell et al.*, 1997) underlies the site. The aquifer is in part recharged by flow of water from the mountains to the north with the general underground flow to the SE with significant discharge into the Snake River. The flow of these fluids cools the aquifer zone resulting in the conductive heat transport zone being at substantial depth. The general lithology at Kimama consists of primarily of basalt flows interbedded with weak, wind-blown sediments deposited during volcanic hiatuses.

The upper part of the KImama drill hole was logged geophysically by the U.S. Geological Survey (*Twining and Bartholomay*, 2011). Wireline geophysical logs were made by the USGS in

two stages: first from surface to 300 m on 7-8 Oct 2010, then from surface to 761 m on 9-10 Nov 2010. Tools included gyroscope, gamma ray, neutron, and density logs run through drill string. The gamma ray logs document K-rich sediment interbeds, while the neutron and density logs distinguish lava flow stratigraphy, with massive water-poor flow interiors and more fractured, water-rich flow tops.

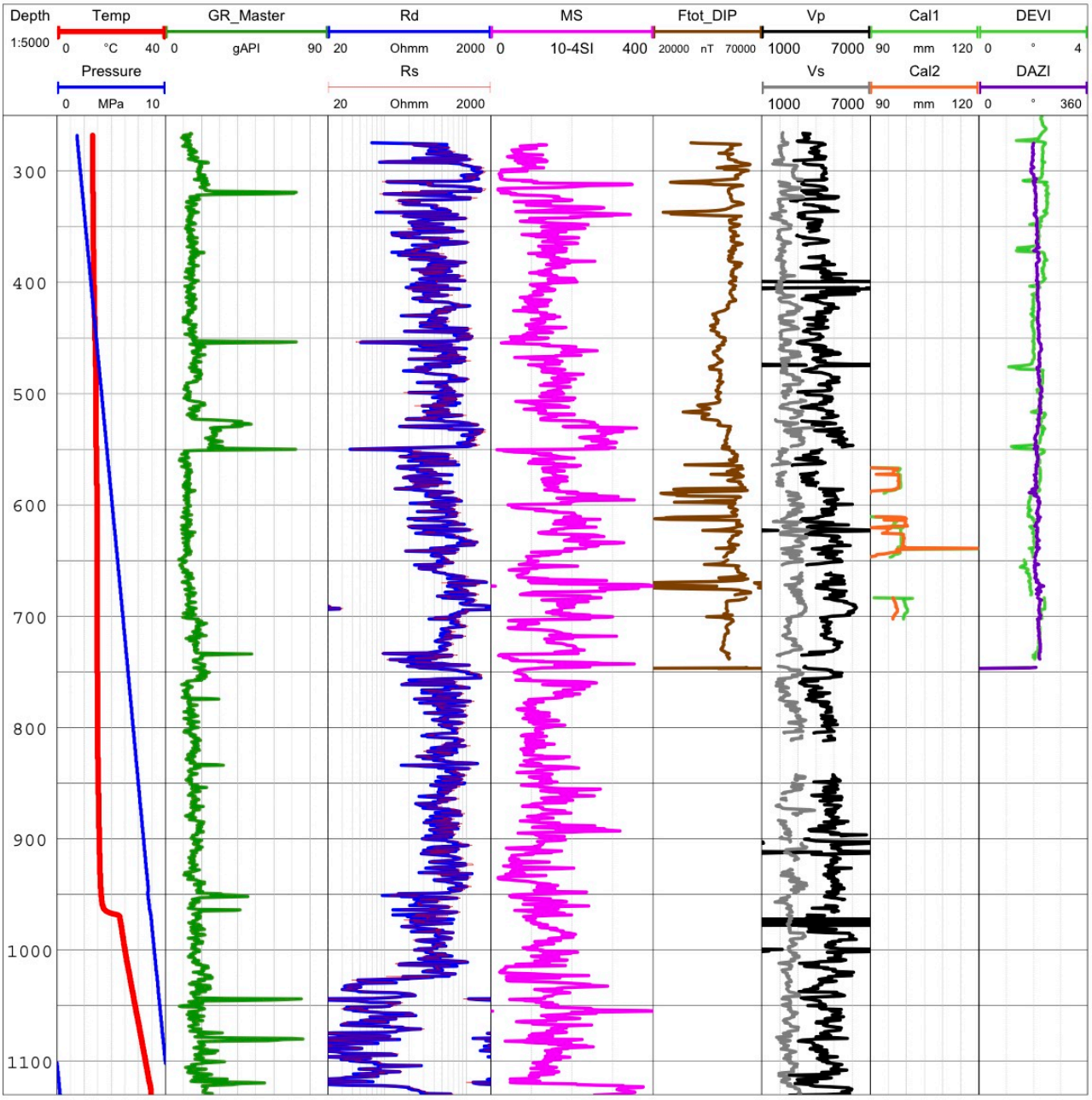

Figure 8-2. Composite plot of Kimama wireline logs run by Operational Support Group. From left: temperature and pressure, gamma, resistivity, magnetic susceptibility, dip meter, sonic, and caliper.

Wireline geophysical logs of the lower part of the Kimama drill hole were made by Century Geophysics in late January 2011. Tools included gamma ray and neutron through drill string (to 1854 m depth), and electric, magnetic susceptibility, sonic, 3-arm caliper, and televiewer image logs in the open hole from 1183 m depth to 1854 m depth, but tool failures due to high temperatures below 1402 m rendered the deeper logs unsuccessful. The one exception was quality magnetic log data, which was obtained to almost 1741 m depth. The N-GR log acted as a correction for the other logs. The gamma ray logs document K-rich sediment interbeds, while the neutron logs distinguish lava flow stratigraphy, with massive water-poor flow interiors and more fractured, water-rich flow tops.

Open hole geophysical logs at KImama were completed by the Operational Support Group in July 2011, limited to the upper part of the hole that were not logged by Century in January. The bridge at 1408 m prevented open hole logging below that depth, but the deeper levels were logged by Century in January. Open hole logs were attempted throughout the section below 1188 m depth (HQ drill string in place) but the drill hole bridged off at ~1432 meters so open hole logs were not possible below that depth. Data collected at during this logging campaign: included natural gamma, spectral gamma, magnetic susceptibility, electrical resistivity, borehole sonic, dip meter, and borehole televiewer logs. A vertical seismic profile of the KImama hole was carried out by the University of Alberta Group (Schmitt) using the OSG VSP geophone string and the University of Alberta vibroseis source discussed in Chapter 6).

The Kimama drillhole represents the central volcanic axis and consists mostly of continuous basalt except for a sediment layer in the top 200m and some loess-like sediment intercalations in the lower 300m. Borehole geophysics mainly identifies these sediment intercalations by an increase in GR and SGR. A total of 557 basalt flow units were identified by Potter et al. (2011) and a minimum of 30 basalt flow groups have been identified by geochemistry and paleomagnetics. These anomalies are corroborated by Potter's detailed description of the core. Table 2 includes both notable borehole geophysics anomalies and the lithology as described by Potter. The key indicators for massive basalt and individual basalt flows are: relatively high N due to variations in clay content and porosity between basalt flows; Acoustic logs as basalt has shorter travel times resulting in high sonic velocities; relatively high resistivity as massive basalts have a low porosity and lack of conductive minerals. Figure 8-3 shows a portion of the borehole logs where sediment intercalations within the basalt are identified with black arrows. These sediment intercalations have a relatively high GR, low RES, and are highly weathered. Electrical resistivity may also be an indicator of depth to water-saturated basalt and indicate the base of the Snake River aquifer. Below the aquifer the basalt porosity is sealed by restricted permeability and is estimated about 850m. This aquifer is associated with elevated temperatures relative to ground water, where the aquifer is approximately 15-17°C while the groundwater is 9°C.

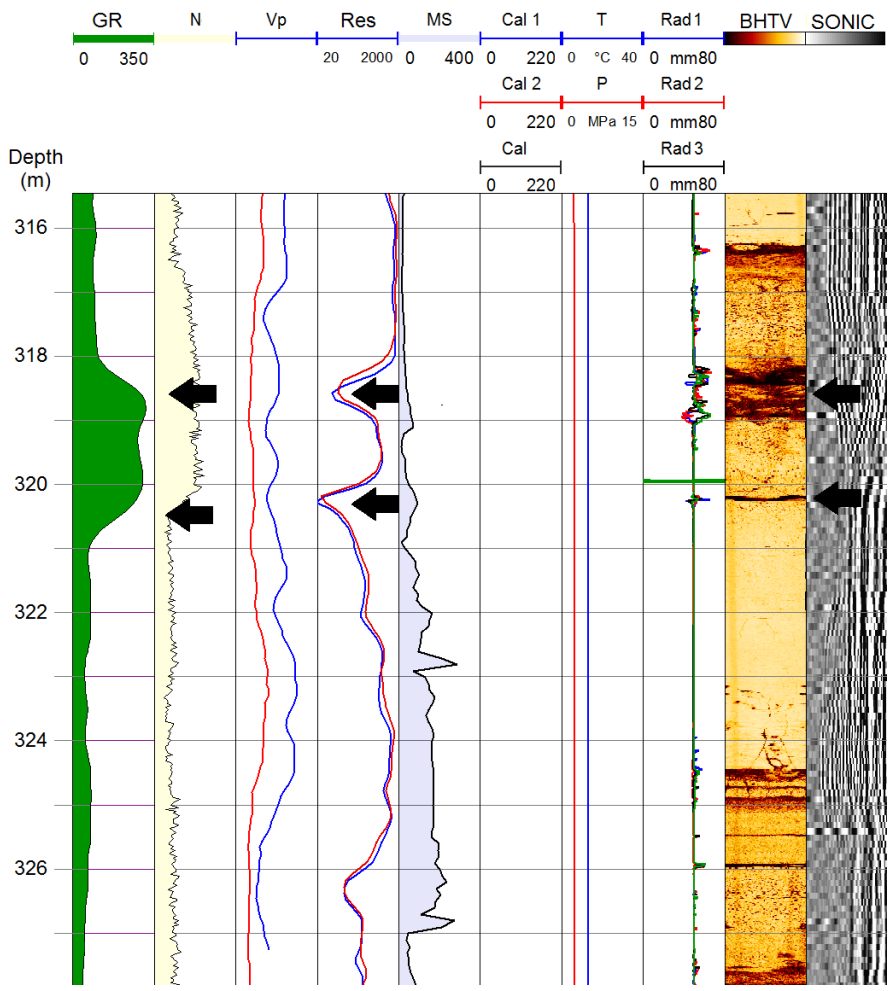

Figure 8-3. Portion of Kimama logs from 315.5m to 327.5m. Sediment intercalations have been indicated with a black arrow and are associated with relatively high gamma ray (GR) and neutron (N), a relatively low resistivity (RES), and are extremely weathered causing a loss of image in the borehole televiewer (BHTV) and longer travel times in borehole sonic (sonic).

Kimberly Geophysical Logs

Kimberley is in the Twin Falls region that is already well known for its low enthalpy geothermal resources. Here, the ground waters are recharged in the mountains to the south, seeps deeper into the crust where it is heated, then upwells forming an artesian system (*Street and deTar*, 1987). The lithology here does include a veneer of basalt and sediment interbeds above 430 m, but is then almost a completely rhyolite except for a few isolated and thin sediment zones to its total drilled depth of 1958 m. The maximum logging depth of Kimberly was 1900 m. The uppermost 214m was not cored as similar exposed area nearby at Snake River Canyon. The cemented cased section was 0 to 213m while HQ and/or NQ drilling pipes were used for casing during wireline logging.

The logging and borehole seismic program was carried out in June, 2011 upon the completion of drilling. A commercial operator (Colog, Denver) was contracted to carry out neutron and gamma logging through the drill strings on 15 June 2011. Flow rate logging was attempted once the NQ drill string was removed but was unsuccessful on account of the viscous drilling fluids remaining in the borehole. Additional logging was carried out by the Operational Support Group (OSG) of the International Continental Drilling Program (ICDP) 16-24 June 2011. Data collected at Kimberly: Total Natural Gamma Ray (GR); Spectrum Natural Gamma Ray (SGR); Magnetic Susceptibility (MS); Sonic (BS); Resistivity (RES); Caliper, orientation, and magnetic field (DIP); Borehole Televiewer (BHTV); Temperature (T).

Operational Support Group (OSG) of the International Continental Drilling Program (ICDP). OSG logs included telemetry, gamma ray (natural and spectral), dual laterolog electric, magnetic susceptibility, sonic, 4-arm caliper, dip meter, temperature, and borehole televiewer image logs (BHTV) in the open hole (Figure 8-4). A vertical seismic profile of the Kimberly hole was carried out by the University of Alberta Group (Schmitt) using the OSG VSP geophone string and the University of Alberta vibroseis source (Chapter 6). The lower sections of the borehole were drilled through a relatively homogeneous mass of rhyolite and this provided for a good quality borehole and, consequently, success with most of the logging operations. Although hole conditions precluded obtaining BHTV images along the complete well, that which was acquired was of high quality. The BHTV log correlates well against the boxed core photos through a ~0.6 m long section of the rhyolite core. This core material displays a series of open vugs that may also be seen in the corresponding BHTV images.

Kimberly drillhole location was designed to capture the transition zone between the basalt and rhyolite, which characterizes the central and eastern SRP. The main lithology of Kimberly is massive rhyolite lava, welded ashflow tuffs with basalt and sediment intercalations. These intercalations occur from 241 m to 424 m and thin altered ash interbedding from 600m to 612 m. There are no apparent flow contacts below 900 m. The sedimentary intercalations are identifiable through a relative increase in GR and SGR. The soft sediment layers are also more weathered resulting in a loss of image in the BHTV and a decrease in MS. The rhyolites are relatively featureless in the BHTV except for fractures filled with precipitate. Temperature logging was completed to assess the geothermal potential and measurements show a cool water aquifer from 400m to end of hole (1958m).

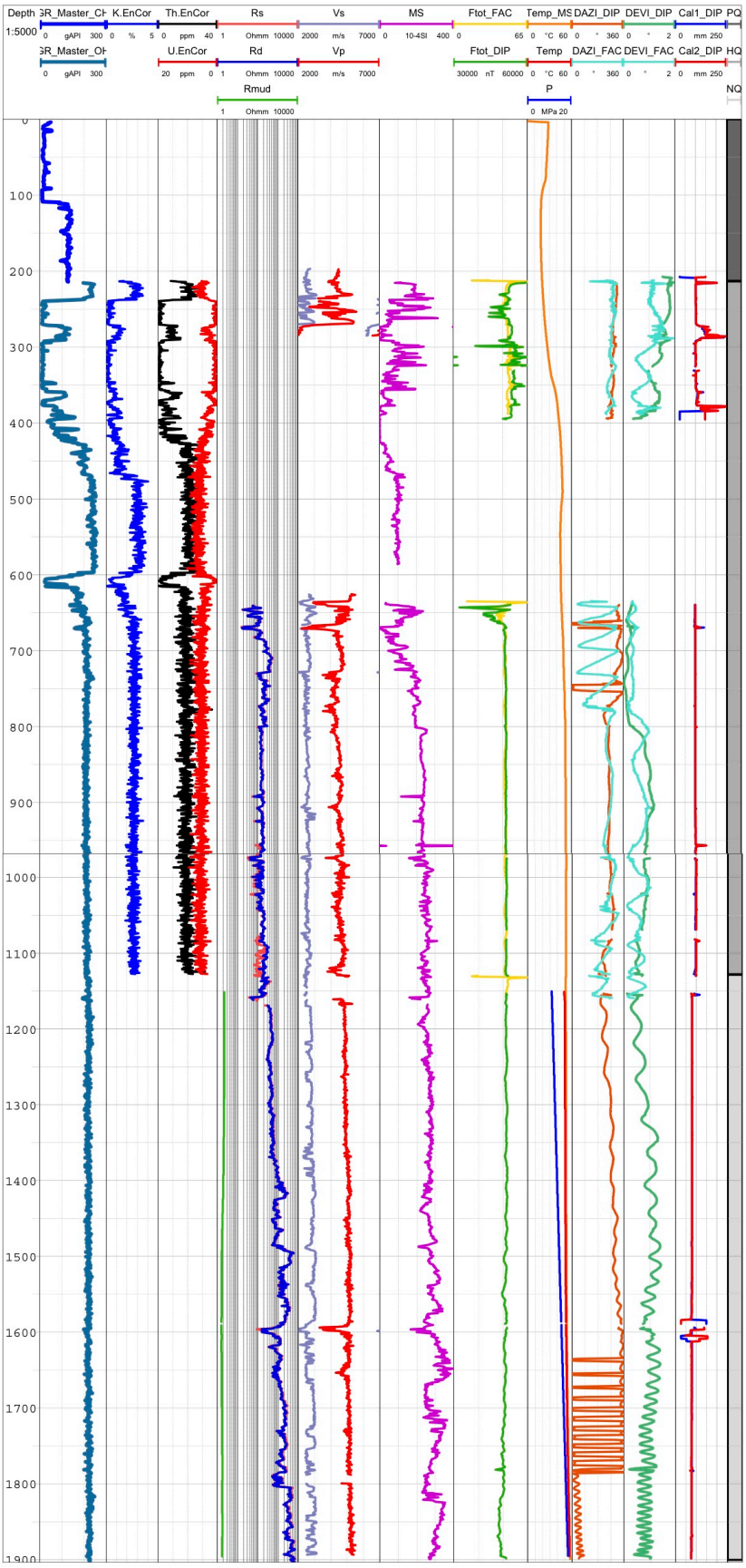

Figure 8-4. Composite plot of Kimberly wireline logs run by Operational Support Group. From left: temperature and pressure, gamma, resistivity, magnetic susceptibility, dip meter, sonic, and caliber.

Mountain Home Geophysical Logs

Geothermal resources in the Western Snake River Plain have been exploited for nearly 100 years, and as noted by *Shervais et al*. (2012) the main science driver for this well was to obtain new information about temperatures and fractures in order to evaluate the geothermal potential. The fractures at Mountain Home are of particular interest because at 1745 m coring intersected an artesian fracture zone sufficiently pressurized to produce flow of hot water to the surface (*Armstrong et al.*, 2012; *Lachmar et al.*, 2012; Chapter 12, this volume).

Logging was first carried out by the ICDP *Operational Support Group* 17-21 January 2012. The maximum drilling depth of Mountain Home was 1675m while the maximum logging depth was 1672m. The cemented PQ section was 0 to 619m, while HQ pipe was used 619 to 1166m, and NQ pipe was used 1166 to 1675m during wireline logging. Data collected at Mountain Home: included natural gamma ray (GR), spectral gamma (SGR), magnetic susceptibility (MS), borehole sonic (BS), resistivity (RES), dipmeter (DIP), temperature (T), and borehole televiewer (BHTV). Temperature and GR were acquired with drill string in place. The open hole logs (MS, RES, DIP, and BS) were restricted to 533m of the drill hole (NQ-size) between 1143m and 1676m (Figure 8-5). The upper portion of the hole was deemed too risky due to weak sediments, especially if the HQ rods and PQ-size casing were removed.

After completion of the first logging campaign, budgets allowed for additional core to be recovered and the hole was completed to 1821 m. At 1745 m, a fracture zone was intersected with free-flowing geothermal water (Chapter 11). A 2⅜" liner was then placed in the hole to allow for longer term temperature logging.

A second campaign of geophysical logging was initiated on 11-12 November 2012, carried out by SouthWest Exploration (SWEx). Cold water was circulated through the NQ drill string to cool the hole prior to logging and allow the use of logging tools in the higher temperature part of the hole. Temperature measurements were logged as of November 11 after the cold water failed to return to surface. This indicates that the formation was taking up the injected water. Natural-gamma and neutron logs were run through the NQ string from surface to 1693m after which the gamma instrument failed; the neutron instrument failed at 1371m. It is anticipated that potentially downhole temperatures had an effect as this tool is rated at 149°C. BHTV logging was planned to allow imaging of the artesian fracture at 1745 m, however, temperatures in the hole below 1500 m exceeded the thermal rating of the BHTV (120C). As a result, the tool was returned to 1286m to log back down to 1463m. In the end the fracture zone was not reached with geophysical logging during the second logging campaign.

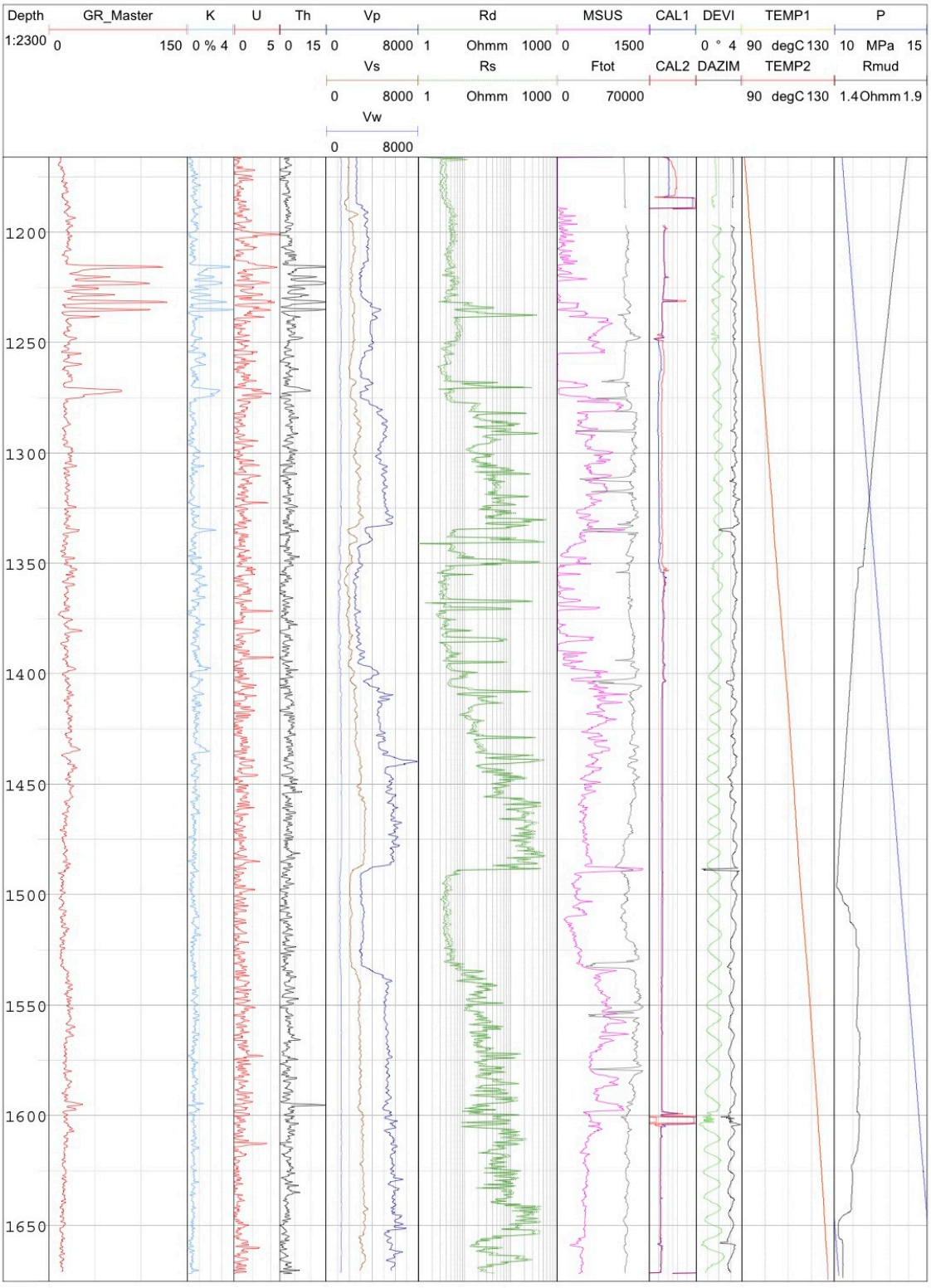

Figure 8-5. Composite plot of Mountain Home wireline logs run by Operational Support Group. From left: temperature and pressure, gamma, resistivity, magnetic susceptibility, dip meter, sonic, and caliber.

This drillhole represents the lacustrine sediments that overlie basaltic volcanism of the western SRP. The lithology consists mainly of basalt with sediment intercalations (0-215m) and a 739m layer of lacustrine sediments (mudstone). The lower portion of the hole consists of basalt flows, basalt hyaloclastites, and basaltic sands. These basalts are associated with a relative increase in MS and RES; similar to the geophysical anomalies associated with the basalt flows in Kimama. Numerous fractures and stress-related features are apparent in the high quality BHTV and the borehole reflections correlate with expected lithological changes. The lacustrine sediments generate peaks in GR and SGR and a loss of signal in the BHTV. Geothermal fluids were encountered at 1745m and associated with a fracture system. Temperatures at the bottom of the hole indicate elevated temperatures of 150°C when first encountered. Later measurements indicate 135-140°C due to downward cold water flow.

Figure 8-5 gives an interesting comparison between the P and S wave velocities and the electrical conductivity at Mountain Home. All three logs mimic each other's behaviour along the well. The large drop in resistivity between 1490 m to 1540 m depth is tracked by corresponding substantial decreases in the P and S wave velocity. The reason for this is not yet known but it may be related to alteration of the basalts as is seen in the retrieved core.

CORRELATION OF BORELOGS AND LITHOLOGY

Correlations observed between the wireline logs and lithologic logs based on recovered core document our ability to recognize lithologic variations in boreholes even in the absence of core. This is particularly important when rotary drilling is used and cuttings, which are not well-located within the borehole, provide the only indication of lithology. In this section we provide three examples, one from each site. Summaries of these correlations are presented in Tables 1 and 2 below.

At the Kimama site the neutron and natural gamma logs proved to be the most useful for recognizing lithologic variations within the borehole, with gamma log spikes corresponding to sediment interbeds and neutron log intensity varying within individual basalt flow units. Figure 8-6 displays a portion of the gamma, neutron, and density logs obtained by the USGS (Twining and Bartholomay, 2011) compared to lithologic logs based on core. As noted earlier, the distinct sawtooth pattern in the neutron log correlates perfectly with individual flow units in the basalts, where the massive flow interiors have low neutron absorption (high neutron recoil) and the shelly pahoehoe or rubbly flow tops (which contain higher interstitial water) have high neutron absorption (lower neutron recoil). This pattern allows us to recognize individual flow units in the logs, even at depth where flow boundaries are more difficult to recognize in core. In addition, not illustrated here, elevated gamma response from intervals that are not sedimentary (based on their neutron response) indicates the occurrence of high-K lava flows.

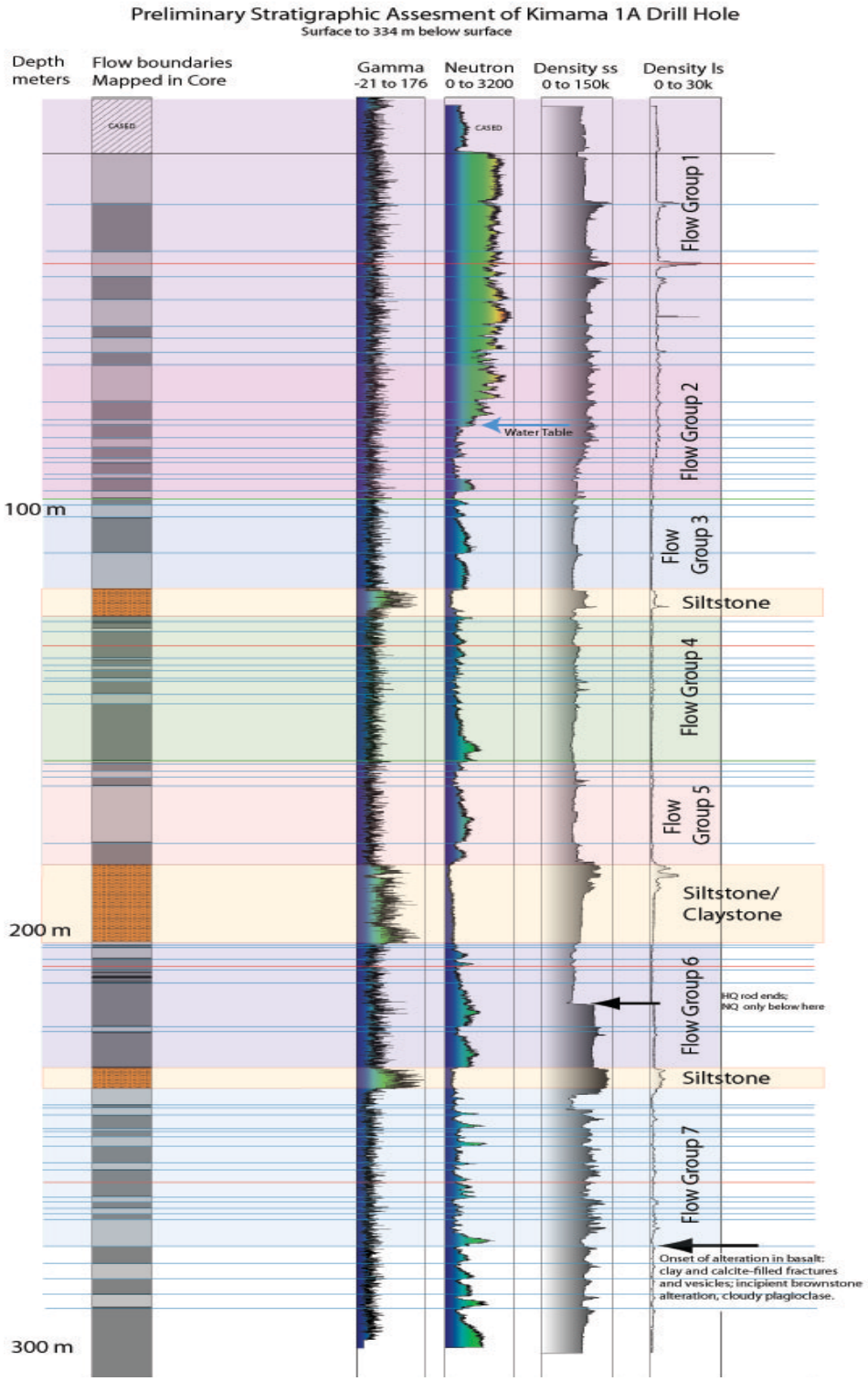

Figure 8-6. Stratigraphy of Kimama drill hole 1A compared to gamma, neutron, and density logs from USGS (Twining and Bartholomay 2011). Note correlation between neutron log saw-tooth pattern and logged basalt flows based on core.

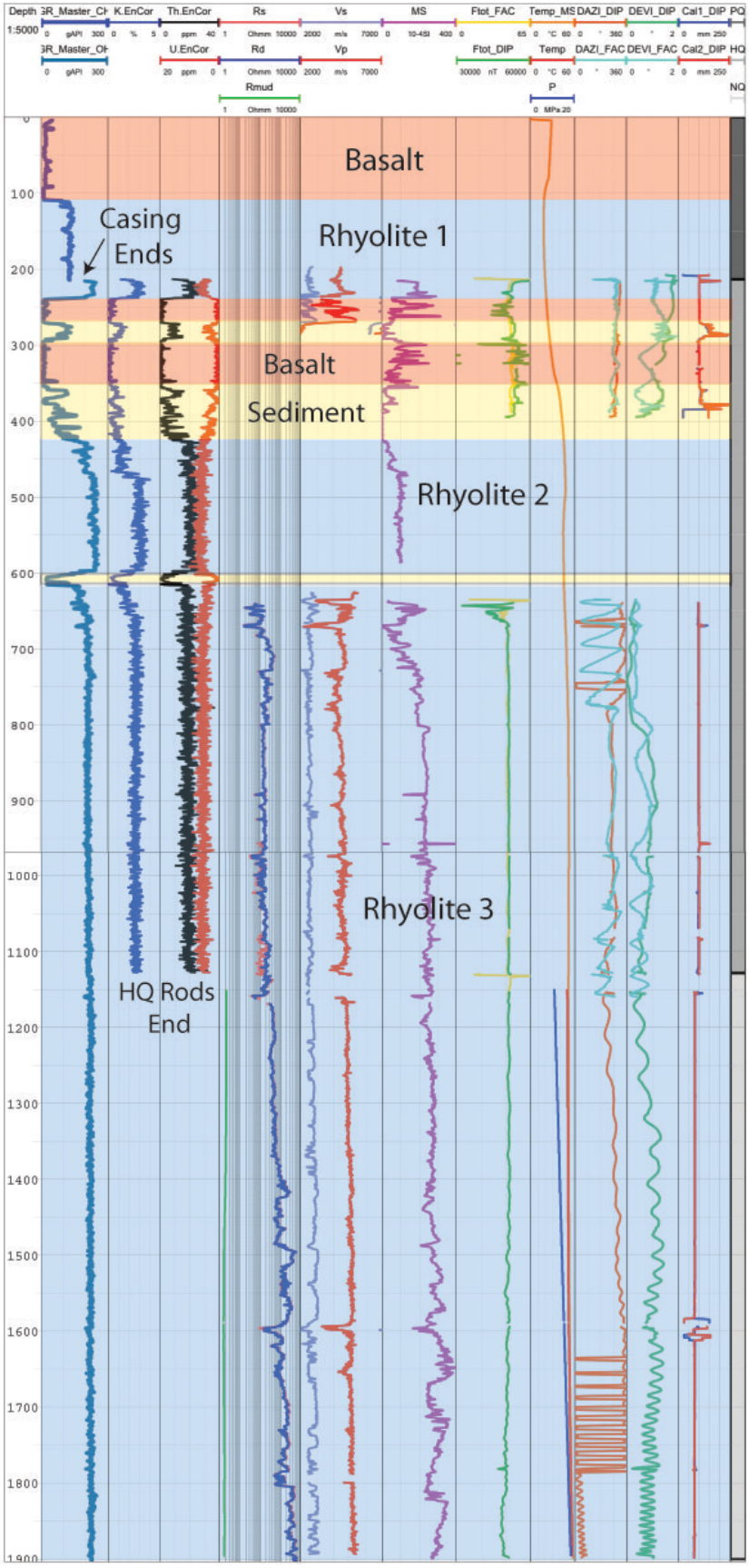

Figure 8-7. Stratigraphy of the Kimberly site compared to lithologic variations with depth. Prominent breaks occur in natural gamma at the upper basalt-rhyolite contact (imaged through the cemented casing) and at the end of the cemented casing string. Rhyolite ash flow sheets have the highest GR signals (high K, Th, U) while sediment horizons are generally lower and more variable. The Rhyolite 3 layer is remarkably uniform lithologically and in its wireline response, except for variations in sonic logs between 600-700 m depth; this corresponds to thermal anomaly which indicates influx of cold water along fractures.

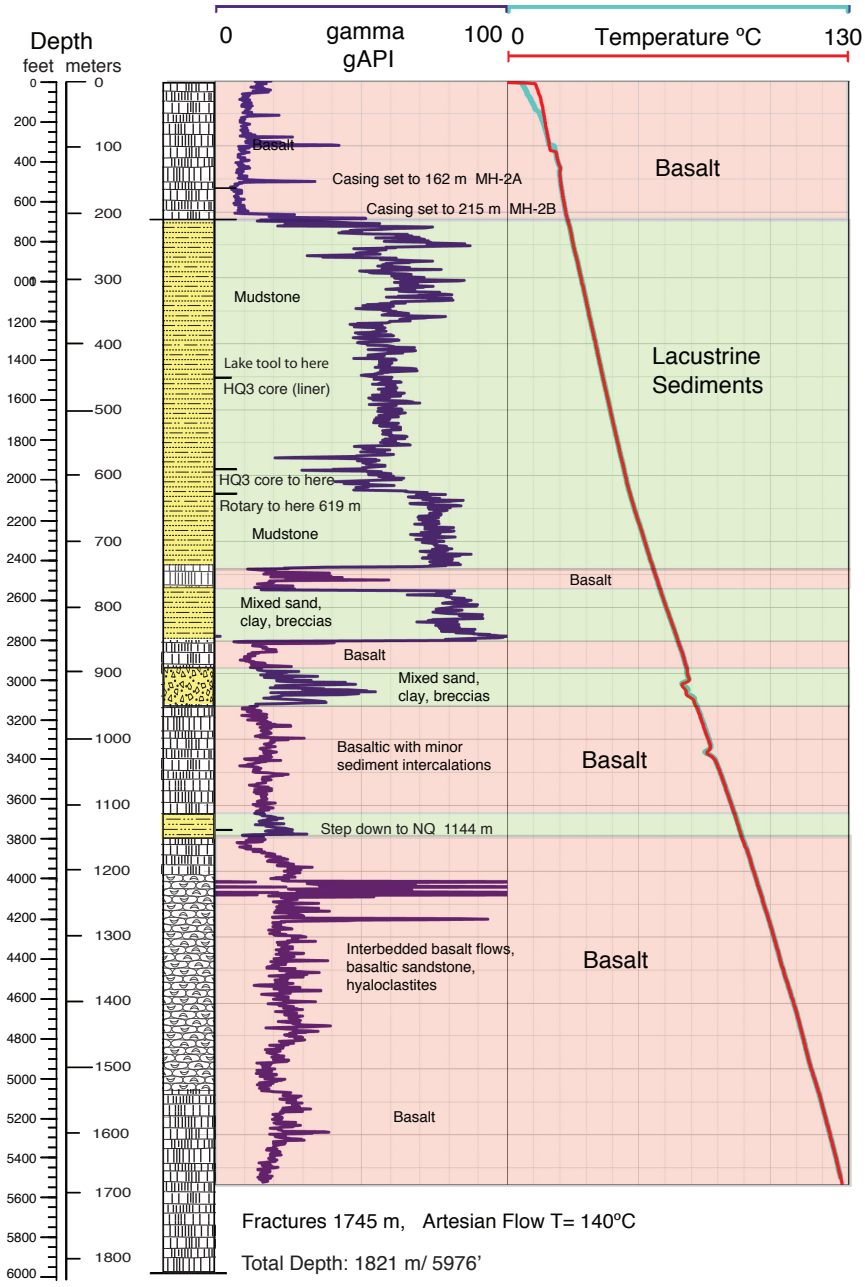

Figure 8-8. Correlation of wireline logs with lithology at Mountain Home. Intercalated basalt and sediment layers highlighted by gamma signals (high = sediment). Casing was cemented to 215 m, which corresponds to the basalt-sediment contact, prior to logging by OSG. Variations in basalt below 1150 m depth result from variable compositions of basalt hyaloclastites and basaltic sandstones. Detailed comparisons of rock strength with sonic, magnetic, and other logs are in progress.

At the Kimberly site the natural and spectral gamma logs, and sonic logs proved to be the most useful for recognizing lithologic variations and fractures within the borehole (Figure 8-7). Rhyolite ash flow sheets have the highest GR and SG signals (high K, Th, U), while sediment horizons are generally lower and more variable. The rhyolite layers tend to be remarkably uniform internally, except for variations in sonic logs between 600-700 m depth; this corresponds to thermal anomaly which indicates influx of cold water along fractures.

At the Mountain Home site, gamma log spikes corresponding to sediment interbeds within the basalt sequence. Figure 8-8 displays the natural gamma and temperature logs obtained by OSG compared to lithologic logs based on core. More detailed comparisons of other wireline logs (sonic, resistivity, magnetic susceptibility) with rock mechanical properties are in progress.

SUMMARY

An extensive series of geophysical logs and borehole seismic experiments have been carried out at all three drill sites, summarized below in Figures 8-9, 8-10, and 8-11. The logs have already been of use in locating sediment interbeds and even highlighting the finer scale structure of the basalt flows. Interpretation of the image logs is of the greatest priority in order to learn more about the natural fracture systems and the in situ states of stress. Further, the image logs will allow much of the core to be oriented; this information will be of use for refined paleomagnetic analyses and should find use in deducing the directions of the basalt flows and rhyolite deposition. Current ongoing work focuses on correlating mechanical properties of recovered core with measured borehole properties to better understand the relationship between borehole logs and what they represent. This work is being carried out by graduate students at Utah State University and the University of Alberta.

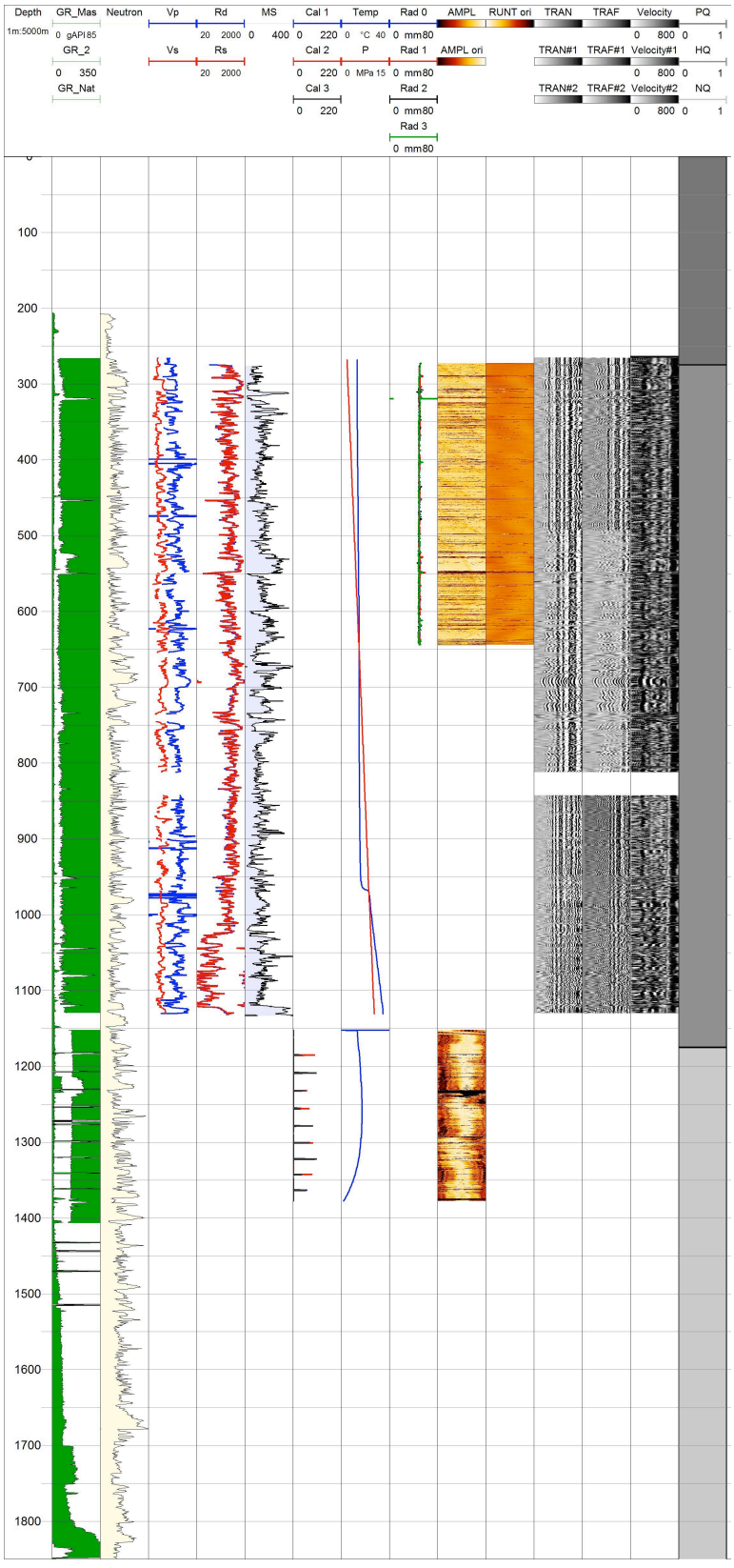

Figure 8-9. Composite wireline logs for the Kimama site, including BHTV and VSP logs.

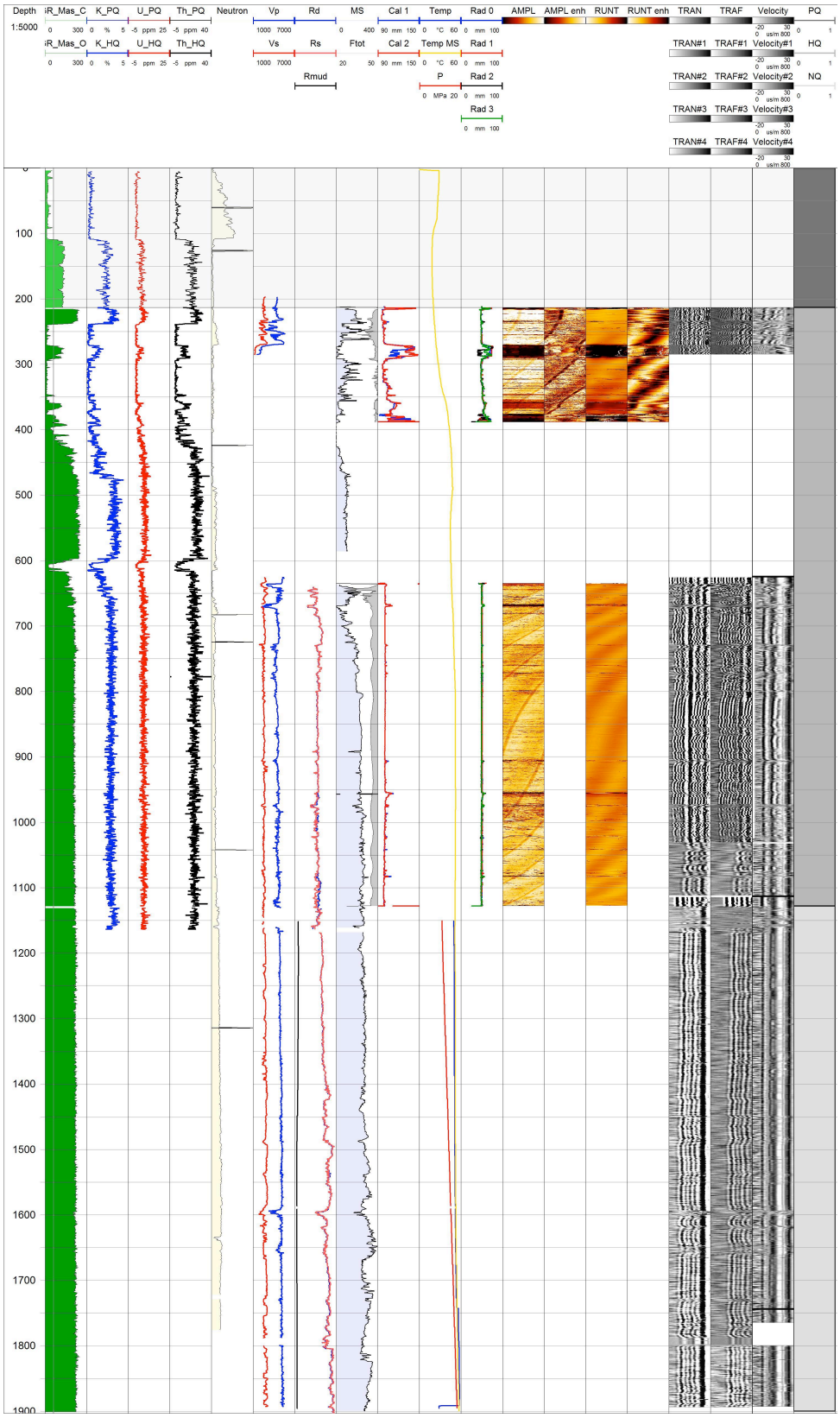

Figure 8-10. Composite wireline logs for the Kimberly site, including BHTV and VSP logs.

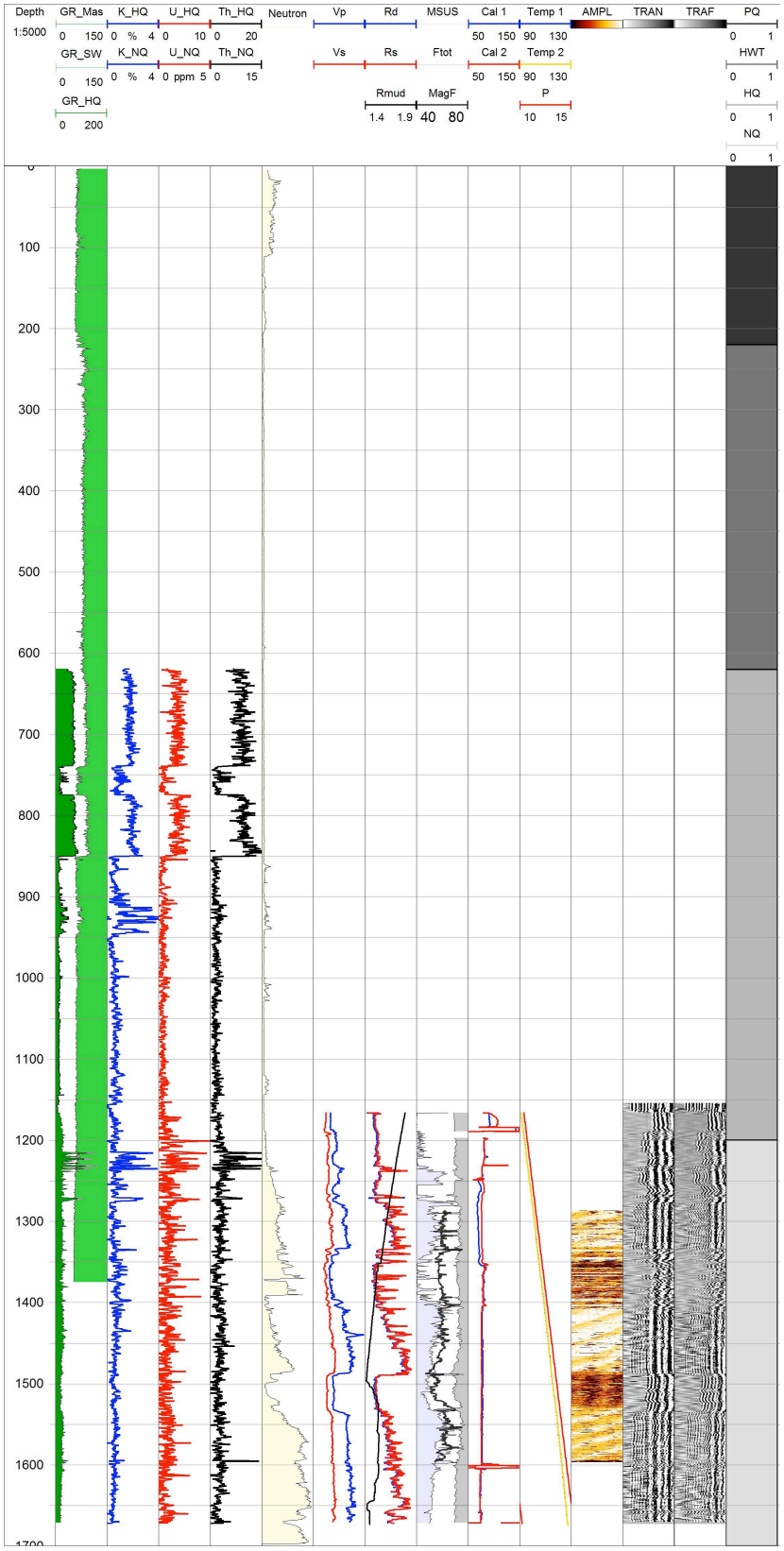

Figure 8-11. Composite wireline logs for the Mountain Home site, including BHTV and VSP logs.

Table 1. Lithologic log of Kimberly borehole based on wireline geophysical response.

Start (m)	End (m)	Thickness (m)	Lithology	Description
0	109	109		Dec GR, SGR; Inc N; Basalt
109	214	105		Inc GR, SGR; Dec N; Rhyolite
214	240	26		Inc GR, SGR; Dec MS; Rhyolite
240	271	31		Dec GR, SGR; Basalt
271	292	21		Inc GR, SGR, cal, rad, BHTV; Dec MS; Sedimentary layer
292	346	54		Dec GR, SGR, cal, Rad, BHTV; Inc MS
346	349	3		Inc GR, SGR, cal, rad, BHTV; Dec MS; Sedimentary layer
349	355	6		Dec GR, SGR, cal, Rad, BHTV; Inc MS
355	370	15		Inc GR, SGR, cal, rad, BHTV; Dec MS; Sedimentary layer
370	377	7		Basalt
377	605	228		Inc GR, SGR; Rhyolite
605	616	11		Dec GR, SGR; Mudstone, Sandstone, Ash
616	667	51		Inc GR, SGR - Stable until EOH; Rhyolite
667	671	4		Dec MS; Inc cal, rad, BHTV, BS; Fractured rhyolite
671	728	57		Rhyolite
728	731	3		Dec MS; Inc cal, rad, BHTV, BS; Fractured rhyolite
731	772	41		Rhyolite
772	773	1		Dec MS; Inc cal, rad, BHTV, BS; Fractured rhyolite
773	799	26		Rhyolite
799	800	1		Dec MS; Inc cal, rad, BHTV, BS; Fractured rhyolite
800	891	91		Rhyolite
891	892	1		Dec RES, MS; Rhyolite
892	905	13		Rhyolite
905	910	5		Inc cal, rad, BHTV, BS; Fractured rhyolite
910	950	40		Rhyolite
950	955	5		Inc cal, rad, BHTV, BS; Fractured rhyolite
955	975	20		Rhyolite
975	977	2		Inc cal, rad, BHTV, BS; Fractured rhyolite
977	1082	105		Rhyolite
1082	1084	2		Inc cal, rad, BHTV, BS; Fractured rhyolite
1084	1595	511		Rhyolite
1595	1601	6		Dec RES, MS; Inc BS; Rhyolite
1601	1634	33		Rhyolite
1634	1639	5		Dec N; Rhyolite
1639	1800	161		Rhyolite

Table Legend

Inc: Increasing, Dec: Decreasing, GR: gamma ray, SGR: spectral gamma ray, N: neutron, RES: resistivity, MS: magnetic susceptibility, BS: borehole sonic, BHTV: borehole televiewer, Cal: caliper.

Table 2. Lithologic log of Mountain Home borehole based on wireline geophysical response.

Start (m)	End (m)	Thickness (m)	Lithology	Description
0	111	111		Steady GR until 200m; Inc N; Basalt
111	200	89		Inc N; Basalt
200	739	539		Inc GR; Dec N; Lacustrine sediments (mudstone)
739	774	35		Dec GR, SGR; Basalt
774	851	77		Inc GR, SGR; Mixed sand, clay, breccias
851	853	2		Dec GR, SGR; Basalt
853	855	2		Inc GR, SGR; Sediment
855	907	52		Dec GR, SGR; Basalt
907	950	43		Inc GR, SGR; Mixed sand, clay, breccias
950	1007	57		Dec GR, SGR; Basalt with small sediment intercalations
1007	1028	21		Inc N; Sediment intercalation
1028	1120	92		Dec GR, SGR; Basalt with small sediment intercalations
1120	1144	24		Inc N; Sediment intercalation
1165	1215	50		Dec GR, SGR; Basalt with small sediment intercalations
1215	1239	24		Inc GR, SGR, BS; 2m thick interbedding sediments in basalt
1239	1255	16		Inc MS, N; Basalt flow
1255	1268	13		Dec MS, N, RES; Inc BS; Basalt flow
1268	1271	3		Inc MS, N, RES; Basalt flow
1271	1273	2		Inc GR, SGR; Basaltic sandstone?
1273	1348	75		Inc MS; Basalt flow
1348	1391	43		Inc N; BSariable MS, RES; Highly fractured
1391	1485	94		Inc MS; Basalt flow
1485	1531	46		Dec MS, N, RES; Inc BS; Highly fractured
1531	1662	131		Inc MS, N, RES; Dec BS; Steady to EOH; Basalt

Table Legend

Inc: Increasing, Dec: Decreasing, GR: gamma ray, SGR: spectral gamma ray, N: neutron, RES: resistivity, MS: magnetic susceptibility, BS: borehole sonic, BHTV: borehole televiewer, Cal: caliper.

CHAPTER 9:

BOREHOLE THERMAL LOGGING

Dennis Neilson[1], David Blackwell[2], Zach Frone[2], John W Shervais[3]
[1]Drilling, Observation, and Sampling of Earth's Continental Crust, Inc, Salt Lake City, Utah
[2]Geothermal Laboratory, Southern Methodist University, Dallas, Texas, 75275
[3]Utah State University, Logan, Utah 84322

ABSTRACT

Temperature gradient measurements were made on three deep boreholes in southern Idaho: Kimama, Kimberly, and Mountain Home. Initial measurements were made while coring in order to monitor bottom hole temperatures. Temperature while coring measurements were made with a custom designed and built memory tool that was delivered with the inner core barrel and equilibrated for 30-40 minutes before drilling resumed; equilibrium temperatures were calculated using the recorded time-temperature curve and the F(α, τ) *method of Harris and Chapman(2007). Post-drilling temperature measurements, carried out after allowing time for thermal equilibration, were made with the SMU temperature tool, the OSG temperature tool, and a variety of commercial tools, depending on the bore hole. The Kimama site is characterized by a near isothermal gradient to 980 m depth (14-17ºC) followed by a steep conductive gradient of ~75C/km. The isothermal gradient reflects convective cooling by the Snake River Aquifer. The Kimberly site is characterized by a decrease in temperature from 0-100 m depth, followed by a rapid rise to 50ºC from 100-400 m depth. Below 400 m, temperatures are nearly isothermal (50-58ºC) to total depth at 1958 m, except for a slight cooling around 500-600 m depth (influx of cool water). The isothermal section at depth indicates convective mixing of water (flow through) even though major fractures are absent from core. The Mountain Home site is characterized by a steep conductive gradient of ~75ºC/km from the surface to total depth 1821 m, with an small spike around the fluid entry point at 1745 m depth. The conductive gradient at Mountain Home is attributed to the overlying sedimentary cover (lacustrine muds and silts) and altered basalt at depth, which prevent convective mixing of fluids. While both Kimama and Mountain Home exhibit steep geothermal gradients at depth (≥75ºC/km), only the Mountain Home site possess the fracture porosity needed at depth to produce geothermal fluids.*

INTRODUCTION

The Snake River Plain (SRP) magmatic province was formed by passage of the North American Plate over the Yellowstone mantle plume (Blackwell, 1989; Potter *et al.* 2011) producing felsic, caldera-related volcanism followed by voluminous eruptions of basalt. Compilations of subsurface temperature data (Blackwell, 1989) demonstrate high regional heat flow masked by the Snake River Aquifer. As a consequence, there has been little serious geothermal exploration within the center of the plain; although there are numerous springs and wells with low-temperature geothermal fluids, as well as the Raft River geothermal system, on the southern flanks of the SRP.

The Hotspot project was designed to investigate the geothermal potential of the SRP through coring and scientific evaluation at three sites (Shervais *et al.,* 2012). These sites are located at Kimama, north of Burley, in the center of the plain; at Kimberly near the southern margin of the plain; and at Mountain Home Air Force base in the central part of the western SRP (Fig. 1). Both the Kimberly and Mountain Home sites are located in areas that have warm wells and hot springs; whereas, the Kimama site has neither surface nor subsurface thermal manifestations (Mitchell *et al.*, 1980). Drilling activities for each of the holes cored by the Hotspot project are described in Delahunty *et al.* (2012).

TEMPERATURE WHILE CORING

Wire line coring offers a number of advantages over rotary drilling in the exploration for geothermal resources. It utilizes smaller rigs that can be operated at relatively low cost. Core samples can be analyzed for hydrothermal alteration and structural character. In addition, there is less thermal disturbance of the borehole compared to those drilled by rotary techniques.

Equilibrated temperature measurements are important for understanding the thermal regime encountered by a drill hole. However, temperature measurements during drilling can be very important in guiding an exploration drilling program. Our bottom-hole temperature measurements are based on the concept that slim-hole coring circulates lower fluid volume than rotary drilling, and the core stub at the bottom of the hole is the least thermally disturbed part of the hole. DOSECC designed a Bottom Hole Temperature Logger that is delivered to the bottom of the hole within the wireline core barrel. The temperature sensor extends out the bottom of the core barrel assembly and rests directly on the core stub. A temperature data logger records temperature as a function of time and is subsequently correlated with depth. The logger is allowed to remain in contact with the bottom hole for 20 to 30 minutes, and the resulting temperature build up curve is corrected using the $F(\alpha, \tau)$ method (Harris and Chapman, 2007). We use this correction to standardize the measurements at infinite time. However, the boreholes are not thermally equilibrated and retain the thermal impact of

drilling. That is, permeable zones that have taken drilling fluid show up as negative excursions on temperature gradient plots.

The measurement of bottom-hole temperature during the drilling process also allows the operators to address permit and potential safety issues in real time. In addition, temperature data is available even if access to the hole is lost. As we will show in the subsequent discussion, temperature data from other sources has been used to verify the measurements made by the Bottom Hole Temperature Logger. We principally use temperatures measured by the Operational Support Group (OSG) of the International Continental Scientific Drilling Program (ICDP). Their measurements are from a temperature sensor (PT1000) located within their magnetic susceptibility sonde.

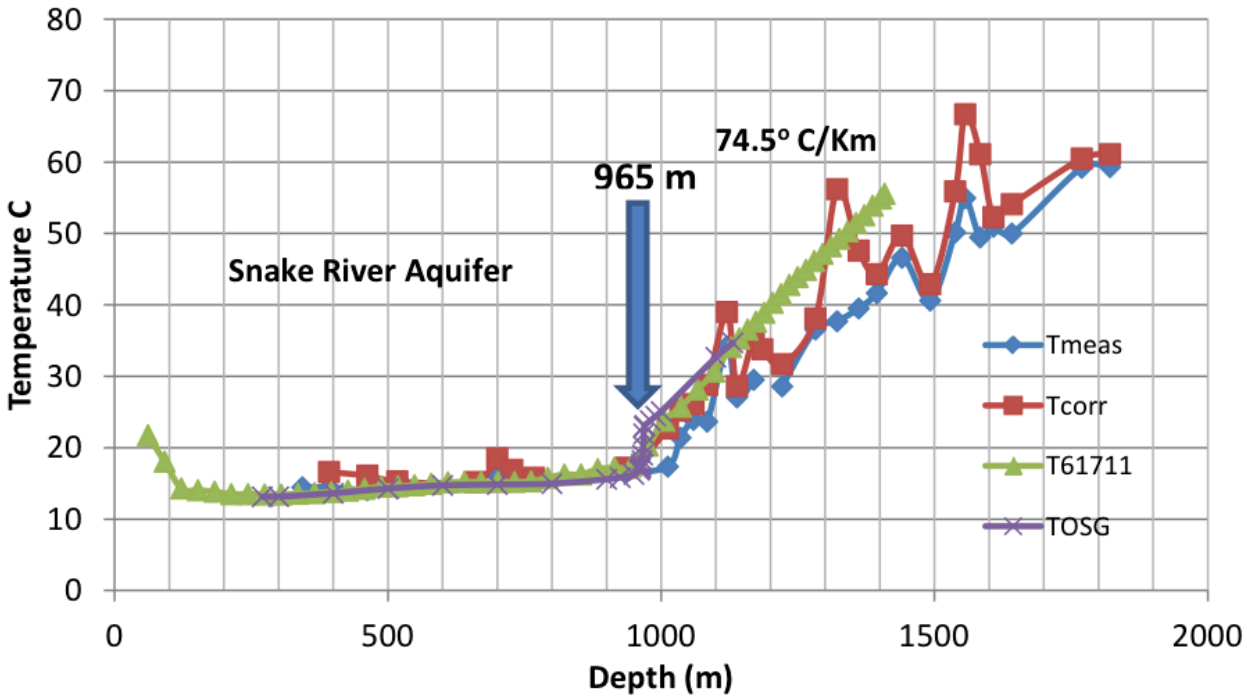

Figure 9-1. Temperature-depth curves for Kimama. Tmeas = measured high temperature with the temp while logging tool, Tcorr = corrected temperature using the F(α, τ) method, T61711 = equilibrated gradient using DOSECC logging tool, and Tosg = Operational Support Group temperature log. Post-drilling logs stop at 1408 m due to separated casing.

Kimama Thermal Logs

The Kimama hole was spud on 9/26/10 and reached a total depth of 1,912 m on 1/27/11. The temperature with depth profile measured while drilling was underway in the Kimama hole is shown in Figure 2. The graph shows the temperature measured while drilling (T_{meas}) as well as the data that was corrected using the F(α, τ) method (T_{corr}). The data show gradually increasing temperature from 13.5° to 17.4° C to a depth of about 965 m representing the Snake River Aquifer. Below this depth, a conductive temperature gradient is apparent. Lower temperature excursions on the T_{corr} curve represent zones of circulation loss causing formation cooling.

On 30 January 2011, a string of 2-3/8" casing was set to a depth of 1,912.4 m. The casing was capped on the bottom and filled with water in preparation for subsequent temperature measurements. DOSECC ran a continuous temperature log on 17 June, 2011 following 5.5 months of equilibration (T_{61711}). At that time, it was found that the casing was blocked at a depth of 1,408.7 m prohibiting the probe from extending to greater depth. When the casing was retrieved prior to plugging and abandoning, it was found that a casing connection was unscrewed at 1,408.7 m.

In May 2011, the Southern Methodist University Geothermal Laboratory's logging trailer (slick line winch) was brought to Idaho and a thermal log of the Kimama well (hole #1) was obtained to a depth of 1408 m (4620 feet) -- a deeper log was prevented by a separation in the casing. The SMU logging tool includes a gamma tool that allows correlation with the other logs. OSG performed logging on 29 June, 2011 to a depth of 1131 m, and their data are also plotted on Fig. 2 (T_{OSG}). The OSG and the DOSECC 6/17/11 data are similar. The T_{corr} data shows a similar temperature gradient, but higher temperatures suggest the final curves may be cooler than original formation temperature that may result from water flow between the casing and the borehole wall.

The temperature logs at Kimama (site #1) indicate isothermal conditions in the upper 965 m of the drill hole at 15-17ºC, corresponding to an unusually thick Snake River Plain aquifer (which is typically less than 300-500 m thick). The gradient becomes conductive below that with a slope of 74.5°C per km, projecting to a temperature of ~100ºC at 2 km depth.

Temperatures logs show that the upper 965 m comprise a nearly isothermal cold water aquifer with an average temperature of ~15ºC. This aquifer is nearly three times thicker than anticipated, based on deep drilling results from the Idaho National Laboratory site. The water temperature is ~5ºC warmer than in the SRP aquifer at INL or on the margins of the plain, documenting a large conductive heat source at depth. Below the aquifer temperatures increase significantly – up to 55ºC at 1555 m below surface – but these bottom hole temperatures do

not reflect equilibrium, being cooled by down flow of cold water from higher levels. Equilibrium measurements will be made after drilling is completed.

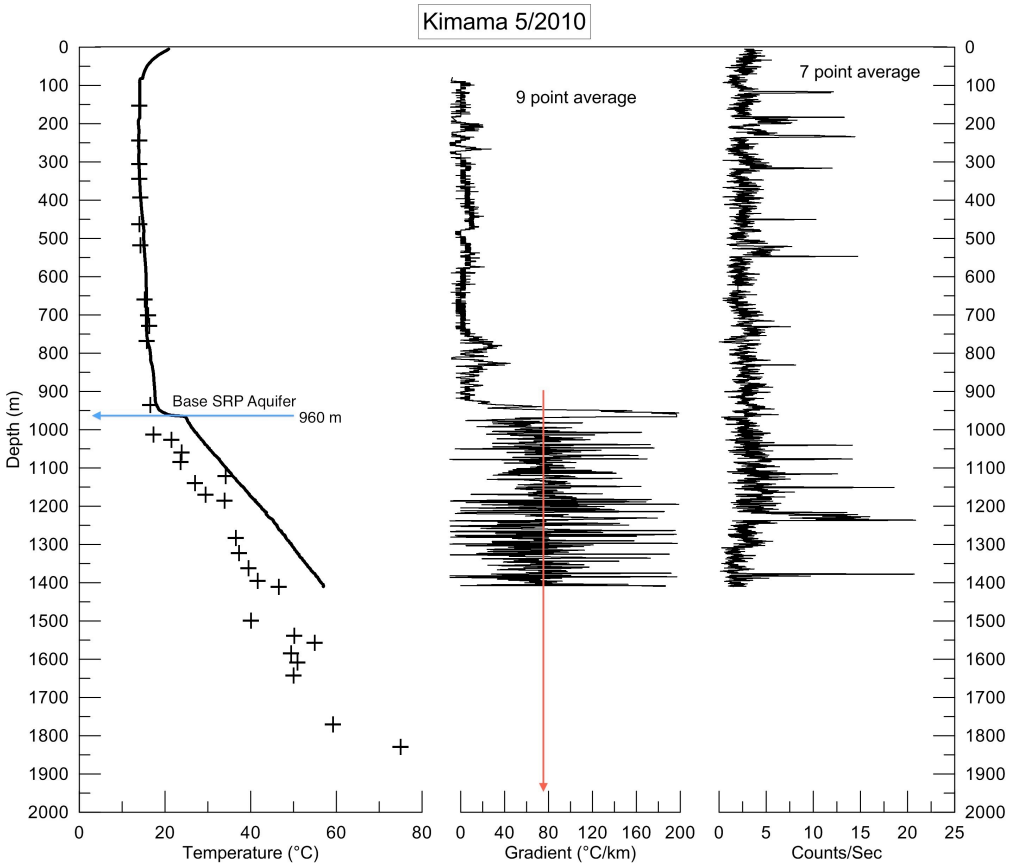

Figure 9-2. Thermal gradient log of the Kimama drill hole, by Southern Methodist University staff. Plus signs are DOSECC downhole tool (while coring).

Kimberly Thermal Logs

The hole at Kimberly, ID was started on 1/25/11 and reached total depth of 1,958 m on 6/13/11. This hole is located between two areas where there are numerous warm water wells, Twin Falls to the west and Artesian City to the southeast (Mitchell *et al.*, 1980). Open-hole logging took place before casing (2-3/8") was set to a depth of 1,911 m on 6/27/11. Caving in the lower part of the hole during the open hole logging prevented the casing from being set to total depth. Figure 9-3 shows the bottom-hole temperature measurements (T_{meas}) and corrected temperatures (T_{corr}). Subsequent temperature measurements were conducted by OSG on 6/20/11 and by DOSECC on 10/13/11 (T_{101311}). The OSG log shows that there was rapid thermal recovery of the hole above 800m. Temperature in the hole below 800 m remained relatively constant with temperature from 50°C at 739 m to 57.4°C at 1,911 m.

SMU performed a thermal gradient log in May 2010, while drilling was shut down for rig repair, when the hole was about 1100 m deep (Figure 9-4). Drilling had ceased about 4 weeks before, so conditions were at least partially equilibrated. The SMU is basically the same as the OSG log, but has more fine scale detail in the temperature variations because it was logged more slowly than the OSG tool. The included gamma log allows us to locate this within the section with great precision. The overall pattern is nearly isothermal, with minor excursions to lower temperature caused by cold water influx.

The temperature gradient at the bottom of the hole is 18.2°C/km. To our knowledge, this well is the deepest exploration of a low-temperature geothermal system. If there is subsurface continuity with the Twin Falls and Artesian City areas, this represents a very large energy source. In the lower part of the hole, the temperature measurements while coring are very similar to the equilibrated temperatures. They also demonstrate the effect of formation permeability above 800 m.

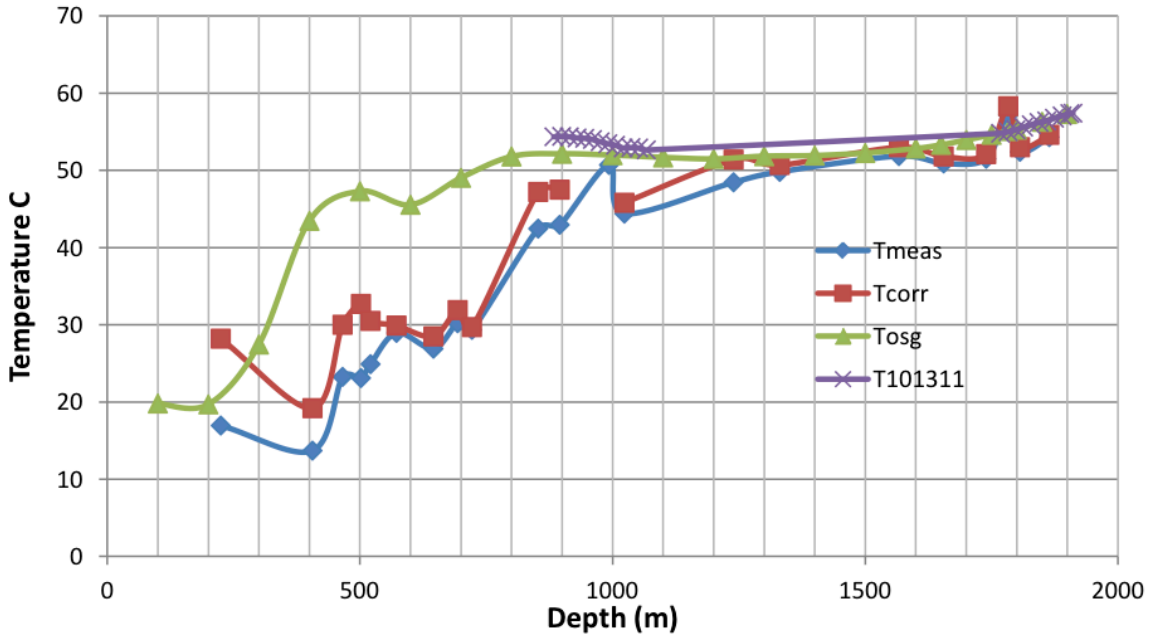

Figure 9-3. Temperature-depth curves for Kimberly drill hole. Tmeas, Tcorr, and Tosg as in figure 9-1. T101311 is DOSECC tool log.

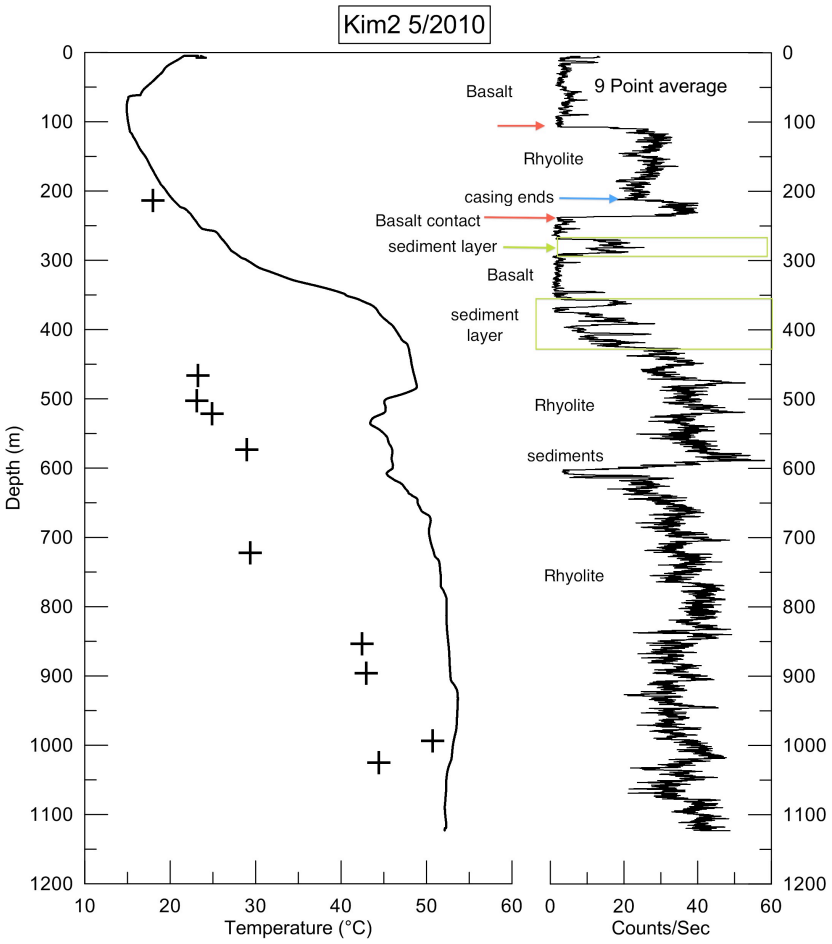

Figure 9-4. Thermal gradient log and gamma log of the Kimberly drill hole, by Southern Methodist University staff. Log was run during rig repair in May 2010, and does not extend to TD.

Mountain Home Thermal Logs

MH-2 reached total depth of 1821.5 m on 2/4/12 and was subsequently cased to a depth of 1818.0 m. Figure 9-5 shows the bottom hole measurements recorded as the drilling progressed along with the corrected temperatures. During the coring, mud returns were established at 1500 m. They were subsequently lost at 1745 m where artesian flow to the surface was also encountered. Our bottom hole temperature probe shows a corrected temperature of 149.4° C at 1,745 m and 1,772 m. However, this temperature exceeds the limit of our probe, and the data was extrapolated from the buildup curve.

In 1986 a geothermal test well (MH-1) was drilled at Mountain Home AFB to a depth of 1,342 m (Lewis and Stone, 1988; Armstrong *et al.,* 2012). MH-1 had a maximum measured temperature of 93°C at 1,219 m. The Hotspot hole (MH-2) was located 4.7 km to the northwest of MH-1. The temperature depth measurements from MH-1 are shown in figure 9-5 and closely follow those from MH-2.

While the well was flowing, a temperature probe was suspended in the hole at 1355.1 m and measured 134.6° C. The flow at the surface through NQ pipe (60.3 mm inner diameter) was estimated at 42 liters/minute. In order to continue coring, the hole was treated with mud and lost circulation material that effectively stopped the artesian flow.

In April 2012, Pacific Process Systems, Inc. (PPS) recorded a continuous temperature and pressure survey in the 2-3/8" casing. These data have been corrected for ice point. The pressure data suggests the probe was hanging up in the casing below 1676 m. When the depth is corrected for the hydrostatic pressure, it yields a maximum temperature of 133.9° C at 1768.1 m. With a thermal gradient of ~75ºC/km, this implies a bottom hole temperature of 138ºC at 1821.5 m or a projected temperature of ~151ºC at 2 km depth (Figure 9-5).

The core from the flow zone encountered at 1745 m, suffered from poor core recovery and there were no clear indication of the character of the faults that cut the zone. In the course of this inspection, we identified hydrothermal breccias. These are typical jigsaw puzzle breccias whose voids have been partially filled by quartz + calcite (bladed) and include pyrite and chalcopyrite. A late filling of crystalline laumontite forms a coating but does not completely fill the voids.

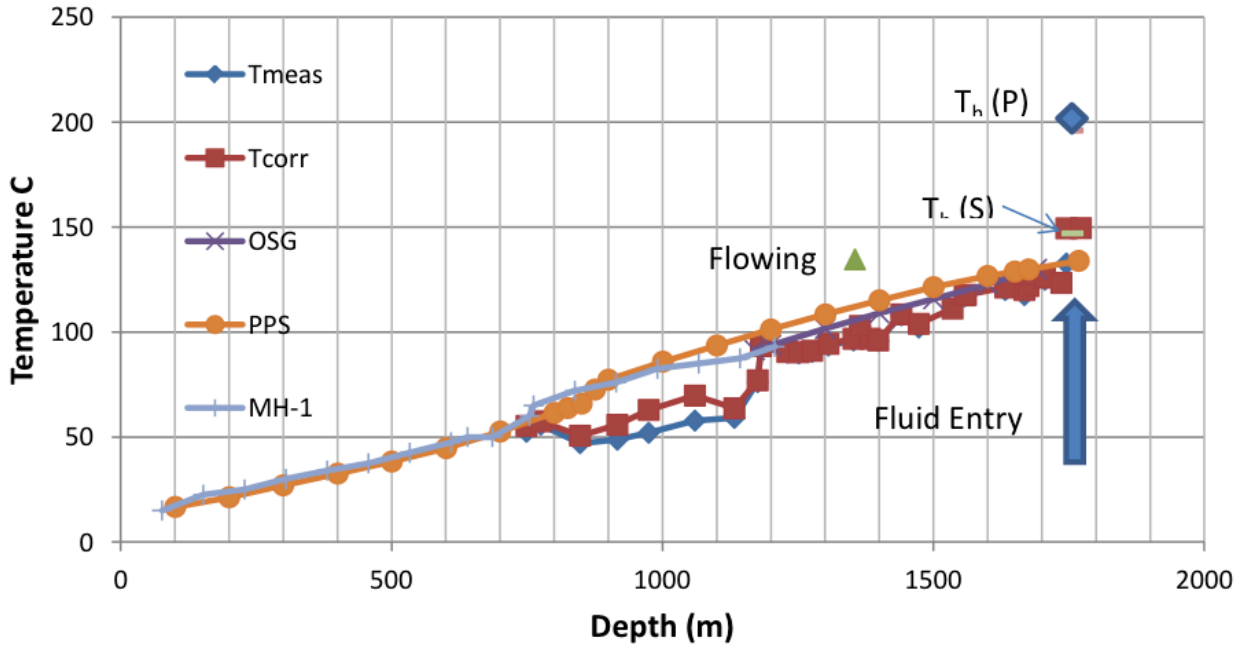

Figure 9-5. Temperature-depth curves for MH-1 and MH-2. Tmeas, Tcorr, and Tosg as in figure 9-1. PPS = gradient log by Pacific Process Systems; MH-1 is gradient for drill hole MH-1. T_h (P) and T_h (S) show primary and secondary fluid inclusion temperatures. The green triangle shows the temperature recorded in the hole while fluid was flowing to the surface. The location of the fluid entry at 1745 m is also shown.

Hydrothermal brecciation indicates that P-T conditions were along the boiling point curve (BPC). Therefore, we envision conditions as shown in Figure 9-5, which assume the depth is as observed and the hydrostatic is controlled by the present land surface elevation. This suggests temperatures of about 340°C with cooling to the present observed 134°C to 150°C. These temperatures are similar to current production temperatures at the Raft River geothermal system (Jones *et al.*, 2011).

The temperatures measured in MH-2, the presence of hydrothermal brecciation and the apparent size (4.7 Km strike length) implies that the system has a magmatic association. It is also important to state that the coring has just intersected the top of the geothermal zone. So, the lateral extent, depth and reservoir temperature has not been fully determined. The region around this site represents a prime target for further exploration.

CONCLUSIONS

The Hotspot project has sampled three different thermal regimes in the Snake River Plain (Figure 9-6). The Kimama hole showed that the Snake River aquifer was much thicker than previously thought. However, beneath the masking effect of the aquifer, high temperature gradients were encountered suggesting that electrical grade geotherrmal resources could be present, but their identification could be difficult. The Kimberly hole demonstrated that low-temperature resources along the southern flank of the SRP can have considerable depth. The overall architecture of this large low-temperature system deserves further investigation. Hole MH-2 at Mountain Home AFB in the central part of the western SRP has encountered the upper part of a high temperature geothermal resource that also remains to be fully evaluated. The temperatures measured at Mountain Home AFB are similar to current production temperatures at the Raft River geothermal system (Jones *et al.*, 2011).

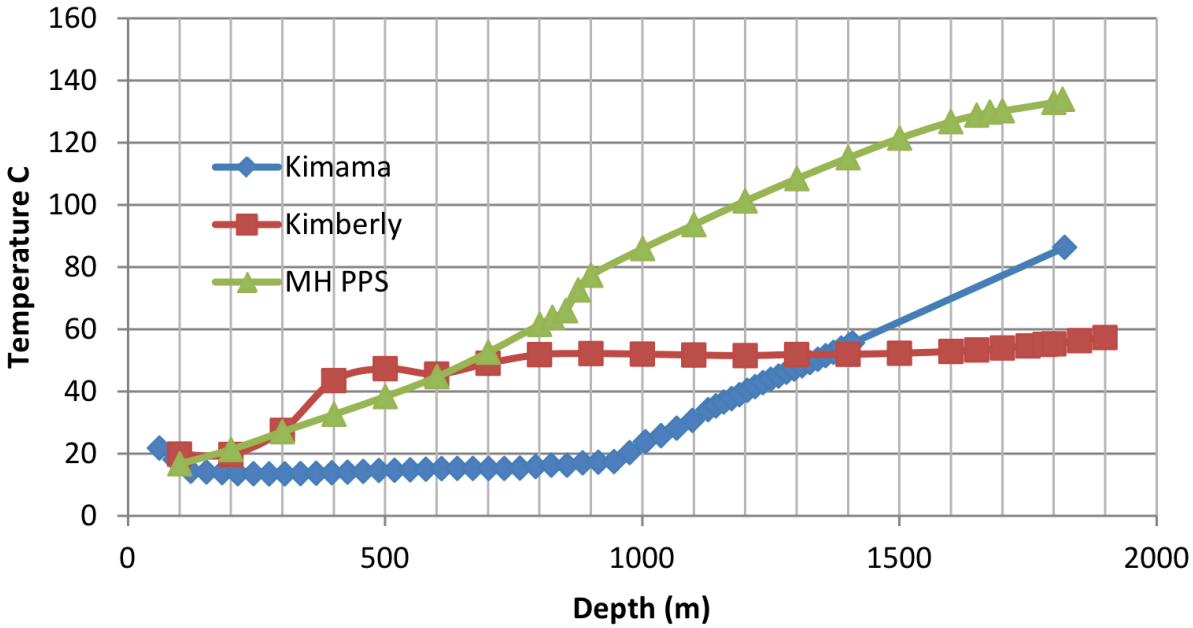

Figure 9-6. Compilation of temperature-depth curves for holes drilled on the Hotspot project. Note that the temperature gradient for the Kimama hole has been extrapolated to the total depth of the well.

CHAPTER 10:

LITHOLOGIC LOGGING AND STRATIGRAPHY

John W. Shervais, Katherine Potter
Utah State University, Logan, Utah

Eric Christiansen
Brigham Young University, Provo, Utah

Alexander Prokopenko
University of South Carolina, Columbia, South Carolina

ABSTRACT

In this chapter we summarize the core descriptions and present preliminary interpretations on the stratigraphy of the sections sampled. Each location is unique: the Kimama core sampled predominantly basalt with minor intercalations of sediment; the Kimberly core is largely rhyolite, with a thick sequence of basalt and sediment in the upper part of the hole; and the Mountain Home core is dominated by lacustrine sediments in its upper section (overlain by basalt), which transitions to basalt and basaltic sediments in the lower section. As a result, each site has distinct physical properties that contribute to their unique thermal gradient profiles, as we discuss later in this report.

Lithologic logging and stratigraphic analyses were carried out in two steps. Each core run was logged initially in the field by the Site Science team prior to photographed and boxed for shipment to the core laboratory at USU in Logan, Utah. Core logging manuals were prepared for the Site Science teams to ensure consistency in descriptions and completeness, with separate manuals for basalt core and rhyolite core. Detailed lithologic logging was carried out in the Core Lab at USU, with all data compiled and entered into the ICDP Drilling Information System database.

All three of bore holes drilled for this project were cored from the base of the casing to total depth; one hole (Kimama) was core from the base of the surface conductor. All of the core was logged for lithology and structure in order to document the stratigraphy at each site. The Kimama site consists almost entirely of basalt flows up to 50 m thick, comprising some 430 flow units. Sedimentary intercalations occur in the upper 200 m (dominantly silt and loess) and in the lower 230 m (fluvial sands and gravels). Basalts form a series of upward fractionation units, with several horizons of "Craters of the Moon" like high-Fe and high Fe-K lavas. Ar-Ar and paleomagnetic time scale ages document a bottom hole age of ~6.25 Ma, and an accumulation rate of ~335 m/Ma.

The Kimberly core consists almost entirely of rhyolite welded ash flow tuffs, with two sections of basalt+sediment in the upper 250-450 m of core. The oldest rhyolite ash flow is over 1300 m thick, suggesting accumulation within a subsiding caldera complex.

The Mountain Home site consists of an upper volcanic section of subaereal basalt (215 m thick) overlying a thick section of Pliocene-Pleistocene lake sediments that continue to ~850 m depth. From 850 m to total depth at 1821 m, the Mountain Home section comprises basalt lava flows and hyaloclastites, basaltic sandstone, and minor intercalated lacustrine silts. No age data are available yet for the Mountain Home or Kimberly sites, but previously published data suggest an age of 6.25 Ma for the uppermost rhyolite at Kimberly.

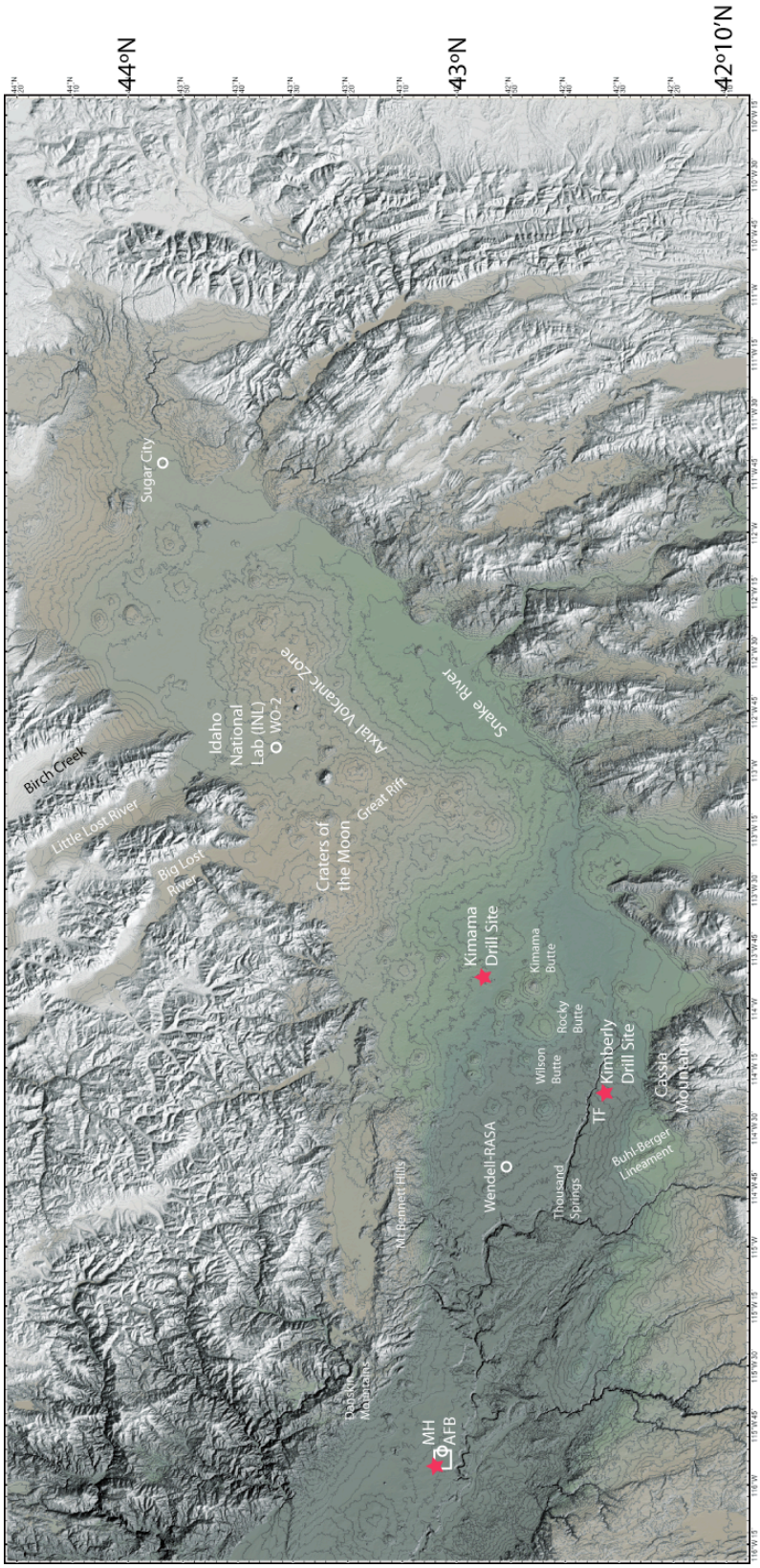

Figure 10-1. Topographic-relief map of southern Idaho showing location of the sites drilled for this project: Kimama, Kimberly, and Mountain Home. Also shown are selected prior deep drill sites (white circles) and major features of the Snake River Plain.

INTRODUCTION

Lithologic logging and stratigraphic analysis was carried out in two steps. Each core run was logged initially in the field by the Site Science team prior to being photographed and boxed for shipment to the core laboratory at USU in Logan, Utah. Core logging manuals were prepared for the Site Science teams to ensure consistency in descriptions and completeness, with separate manuals for basalt core and rhyolite core. Detailed lithologic logging was carried out in the Core Lab at USU, with all data compiled and entered into the ICDP Drilling Information System database. A complete description of core handling and logging procedures is presented in Appendix A.

In this chapter we summarize the core descriptions and present preliminary interpretations on the stratigraphy of the sections sampled. Each location is unique: the Kimama core sampled predominantly basalt with minor intercalations of sediment; the Kimberly core is largely rhyolite, with a thick sequence of basalt and sediment in the upper part of the hole; and the Mountain Home core is dominated by lacustrine sediments in its upper section (overlain by basalt), which transitions to basalt and basaltic sediments in the lower section. As a result, each site has distinct physical properties that contribute to their unique thermal gradient profiles, as we discuss later in this report. Drill site locations are shown in Figure 10-1.

KIMAMA

The Kimama site was strategically selected for its location along the axial volcanic high, a region of densely spaced volcanic centers aligned with the track of the Yellowstone hotspot. The Kimama drill core is thought to access the greatest thickness of erupted basalt and the most complete record of SRP-YP mafic volcanism. Previous drilling projects indicated about 1 km of Pliocene-Pleistocene tholeiitic basalt, interbedded with minor terrestrial sediments of eolian, fluvial, and lacustrine origin, overlying rhyolite volcanics (Doherty et al., 1979; Kuntz et al., 1992; Anderson and Liszewski, 1997). As seen in Figure 10-2, which compares a lithologic log of the Kimama drill hole to its companion deep holes along the central axis, Wendell RASA to the west and WO-2 to the east, basalt in the Kimama hole is 65% thicker than the basalt section in hole WO-2, and almost six times thicker than basalt encountered in Wendell RASA.

Preliminary investigations of Kimama drill core were based on borehole geophysical logs. Neutron and gamma logs correlate well with lithologic facies observations (Figure 10-3). Gamma logs document individual flow units as well as the depth and thickness of sedimentary interbeds. Neutron logs demonstrate the contrast between massive flow interiors and more porous flow tops. Wireline logs image 430 basalt flow units (0.1-50 m thick), grouped into at least 155 lava flows and 21 flow groups.

A combination of lithologic, geochemical, and paleomagnetic data suggest the presence of 430 basalt flow units comprising 144 lava flows, each erupted during a single episode of volcanism (decade scale). Basalt flows were recognized using volcanic facies observations based upon models for inflated pahoehoe lava flow emplacement (Chitwood, 1994; Self et al. 1998). Lava flows erupted from a single magma reservoir form a complex aggregate of flows termed flow groups (Welhan et al., 2002; Hughes et al., 2002b). Lava flow groups have areal dimensions of kilometers to tens of kilometers and are synonymous with lava fields, such as the Wapi and Hell's Half Acre lava fields (Welhan et al., 2002; Greeley, 1982). Kimama basalt flows are grouped into 35 basalt flow groups. Flow groups were identified using stratigraphic relationships and magnetostratigraphy, and have an average thickness of 48.6 meters. Intercalated eolian clay and sand, average thickness 6.1 meters, represent lulls in regional volcanic activity and show a relationship to polarity reversals representing thousands of years of time.

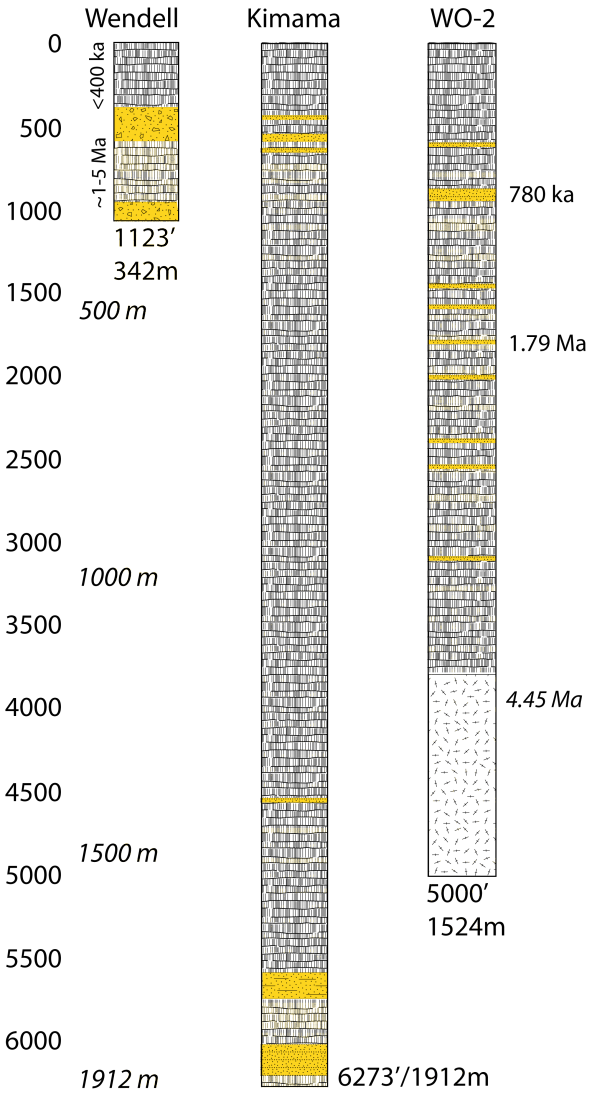

Figure 10-2. Scale comparison of the lithologic logs for Wendell RASA and WO-2 (INL site) compared to lithologic log for the Kimama drill site.

Paleomagnetic inclination was measured in over 1200 samples collected at 2 meter depth intervals by Duane Champion of the US Geological Survey. Twenty-one magnetic reversals were identified and correlated to dated paleomagnetic Chrons and Subchrons. Paleomagnetic dates provide an age framework for erupted Kimama basalts. Robert Duncan of Oregon State University analyzed five basalt lava flows for $^{40}Ar/^{39}Ar$ using incremental heating by broad-beam infrared laser. Flows sampled at 320 m, 454 m, 1155 m, 1284 m, and 1489 m provide reliable ages of 1.54 ± 0.15, 1.60 ± 0.13, 4.18 ± 0.58, 4.39 ± 0.30, and 5.05 ± 0.81 Ma respectively (Duncan, pers. commun. 2012). A linear fit to ages determined from $^{40}Ar/^{39}Ar$ and paleomagnetic analyses extrapolates a bottom hole age of 6.2 Ma and define a mean accumulation rate of 335 m/Ma (Champion, 2012; figure 10-4).

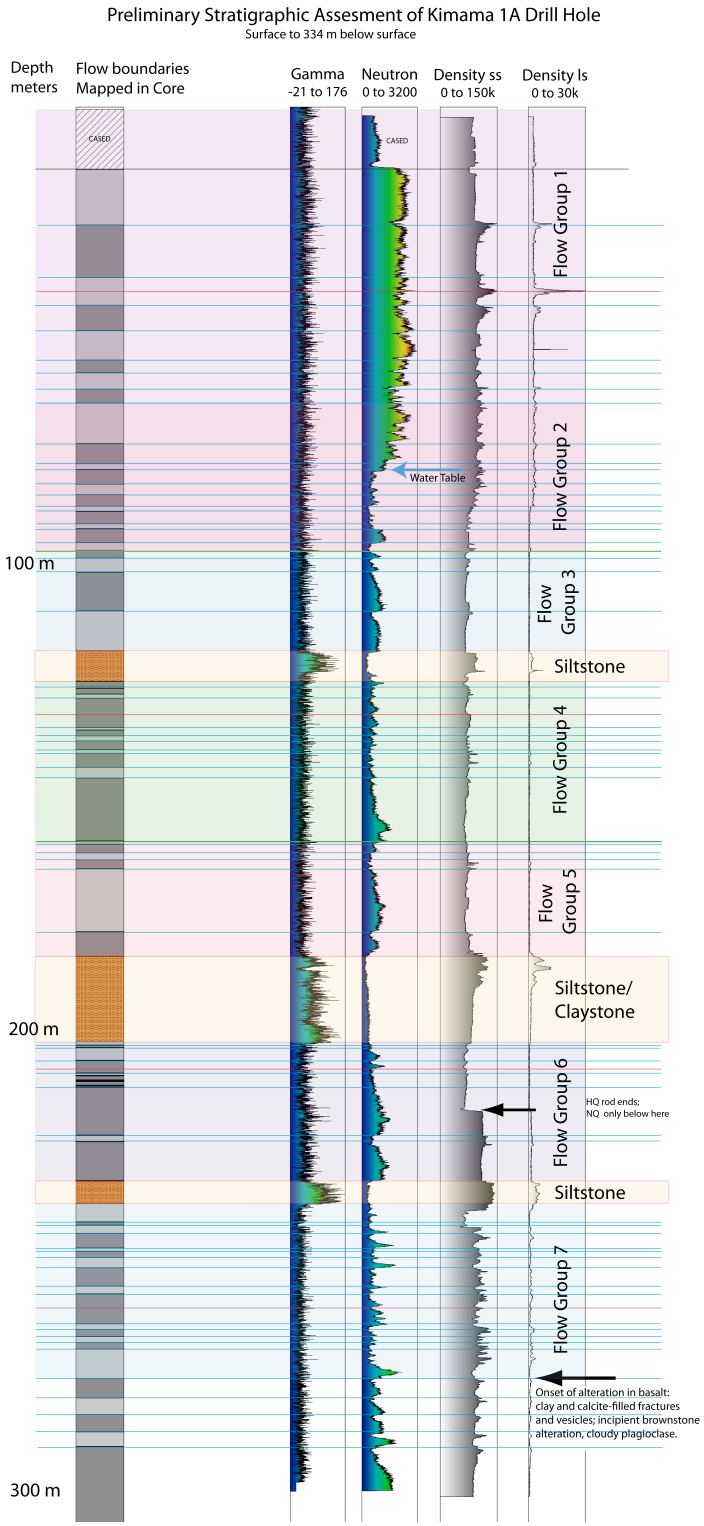

Figure 10-3. Stratigraphy of Kimama drill hole 1A compared to gamma, neutron, and density logs from USGS (Twining and Bartholomay 2011). Note correlation between neutron log saw-tooth pattern and logged basalt flows based on core.

Whole rock major and trace element data were measured in 270 basalts. Compositionally, the majority of Kimama basalts are olivine tholeiites. Geochemical composition plotted against depth demonstrates sequences of magma fractionation and recharge (i.e., Shervais et al., 2006). Upsection increases in Mg, Cr, and Ni signal an influx of primitive mantle-derived magma and depletion of LREE. Upsection increases in FeO*, K_2O, and Zr signal magma fractionation in closed system-reservoirs and enrichment in LREE.

Chemically evolved basalt flows were identified at five depths within the Kimama core. Evolved flows have elevated K_2O, FeO* and Zr. Two suites were identified. Flows at 350 m, 547 m, 1119 m, and 1138 m have elevated concentrations of TiO_2 and FeO* and low SiO_2 relative to Kimama olivine tholeiites. Evolved flows at 319 m and 1078 m have elevated K_2O and FeO* and SiO_2 similar to Kimama olivine tholeiites (figure 10-5). The high K_2O flows are compositionally similar to ferrobasalts erupted at Craters of the Moon National Monument, ~14 km to the northeast. The high TiO_2 flows are also compositionally similar to lunar maré basalts.

Radiogenic isotope chemistry, in conjunction with paleomagnetic stratigraphy, and $^{40}Ar/^{39}Ar$ geochronology, temporally constrain the mass proportions and flux of magma source components in Kimama basalts. We analyzed 15 basalt samples from a range of geochemical compositions and depths within the Kimama core for Nd, Sr, Hf, and Pb isotope ratios. Radiogenic Pb isotope values for Kimama basalts ranged from $^{206}Pb/^{204}Pb$ ~18.0-18.5, $^{207}Pb/^{204}Pb$ ~15.6--15.7, and $^{208}Pb/^{204}Pb$ ~38.5-39.0. Radiogenic Hf isotopes range from 0.282683--0.282745. Samples were processed and measured at the isotope geochemistry laboratory at San Diego State University. Previous studies identify isotopic variation and temporal correlation with distance from the Bruneau-Jarbidge caldera complex in the south central SRP to the Yellowstone Plateau. Temporal isotopic variation is attributed to a decreasing proportion of sub continental lower mantle/hotspot source and increasing lithosphere age from west to east (Hanan et al., 2008). Preliminary Pb and Hf isotope analyses for Kimama agree with models for E-W variation along the Snake River Plain-Yellowstone Plateau hotspot track.

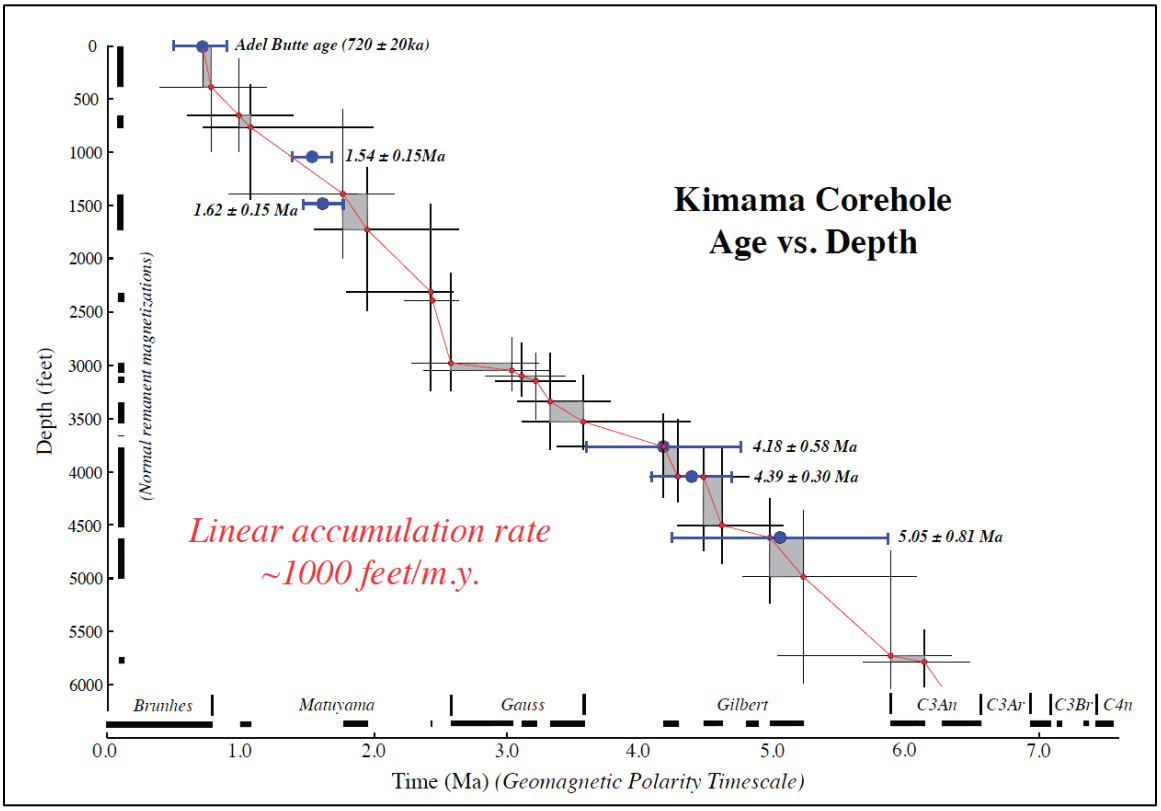

Figure 10-4. Accumulation rate of Kimama basalt lava flows: A linear fit to ages determined from $^{40}Ar/^{39}Ar$ and paleomagnetic analyses define a mean accumulation rate of 335 m/Ma and extrapolates a bottom hole age of 6.25 Ma.

Detrital zircons were recovered from two upward fining sandstone interbeds at 1842-1844 m and 1707-1748 m depth. Zircons were sampled from 1842 and 1844 m in the lower interbed and 1708, 1733, and 1749 m in the upper interbed. Zircon grains were analyzed for U-Pb and Hf isotopes using a high-resolution laser ablation inductively coupled plasma mass spectrometer (HR-LA-ICPMS) at the University of Arizona LaserChron laboratory. At the base, both interbeds contain mainly Miocene detrital volcanogenic zircons of the Yellowstone-Snake River Plain magmatic system (5 to 10 Ma). Higher sands contain successively older zircon groupings. Volcanogenic detrital zircons were ejected during caldera-forming eruptions in the central Snake River Plain, transported by eolian or fluvial processes, and deposited within the fluvial deposits shortly after their eruption. The presence of volcanogenic detrital zircons implies that the depositional age of the sediment intervals corresponds to the U-Pb age of youngest zircons in each unit (5.8 Ma and 6.2 Ma).

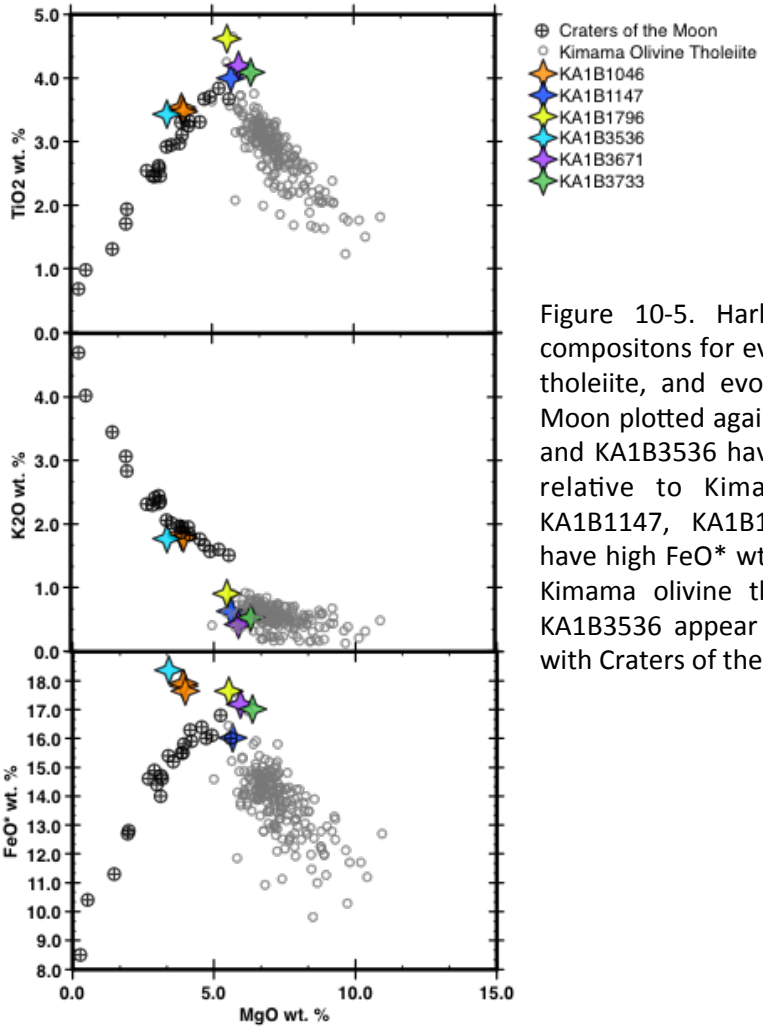

Figure 10-5. Harker Diagrams of major element compositons for evolved basalt flows, Kimama olivine tholeiite, and evolved lava flows of Craters of the Moon plotted against MgO wt. %. Samples KA1B1046 and KA1B3536 have high K_2O wt. % and FeO* wt. % relative to Kimama olivine tholeiites. Samples KA1B1147, KA1B1796, KA1B3671, and KA1B3733 have high FeO* wt. % and high TiO_2 wt. % relative to Kimama olivine tholeiites. Samples KA1B1046 and KA1B3536 appear to have compositional similarities with Craters of the Moon lava flows.

Kimberly

The Kimberly drill hole was designed to core the basalt-rhyolite section (Figure 10-6) of the Central Snake River Plain (Shervais et al., 2011). Regional Bouguer gravity anomalies and inferred pyroclastic flow directions in the Cassia Mountains suggest that the drill site lies on the southern margin of the Twin Falls eruptive complex, an immense Yellowstone-scale field inferred to underlie the Central Snake River Plain (Figure 10-1). The Kimberly site was selected to test the hypothesis that a caldera margin is in this area.

The Kimberly drill hole is dominated by thick sections of rhyolite lava and welded ignimbrite, with basalt-sediment intercalations between 241 m and 424 m depth (Figure 10-6) Preliminary examination of the drill core, chemical, petrographic, and O-H-isotopic analysis of selected samples, and the initial paleomagnetic measurements converge to suggest that there are three major rhyolite units in the Kimberly core. The upper two rhyolite eruptive units are provisionally interpreted to be viscous lava flows or sills based on the lack of eutaxitic fabric in core or thin section and the presence of contorted flow foliations and vitrophyric breccias. Both of the upper units have plagioclase, sanidine, and two pyroxenes, along with accessory zircon, apatite, ilmenite, and magnetite. In addition, the middle unit (Rhyolite 2) has dramatically resorbed quartz grains. The lower 1,340 m (Rhyolite 1 from 2,000 to 6,400 ft) has no apparent flow contacts or cooling breaks and may represent a single, thick ignimbrite. There are no indications of intrusive contacts or granophyric textures that suggest an intrusive origin, even in the deepest part of the core. The lower unit is eutaxitic with sparse lithic fragments and subhorizontal vapor-phase gashes. Phenoclasts are plagioclase, sanidine, two-pyroxenes, and Fe-Ti oxides, along with accessory zircon and apatite. It is chemically distinct in whole-rock composition from the upper units and very homogeneous throughout (Figure 10-7). Chemically, the lower unit is a low-silica rhyolite with high concentrations of Fe_2O_3 and TiO_2. Using new data collected as described below, we will test the hypothesis that this unit is a thick intracaldera deposit for one of the ignimbrites exposed in the Cassia Mountains.

Current data indicate that it most closely resembles the regionally extensive 10.1 Ma tuff of Wooden Shoe Butte (Perkins and Nash, 2002; Parker et al., 1996; and Ellis et al., 2010). However this is one of several large, petrologically and geochemically similar outflow ignimbrites as young as 8.6 Ma exposed in the mountains south of the Kimberly hole (e.g., McCurry et al., 1996; Wright et al., 2002, Ellis et al., 2010). Detailed volcanological, petrologic, geochemical, and paleomagnetic comparisons will be made between those sheets and Kimberly Rhyolite 1 to define a possible correlation.

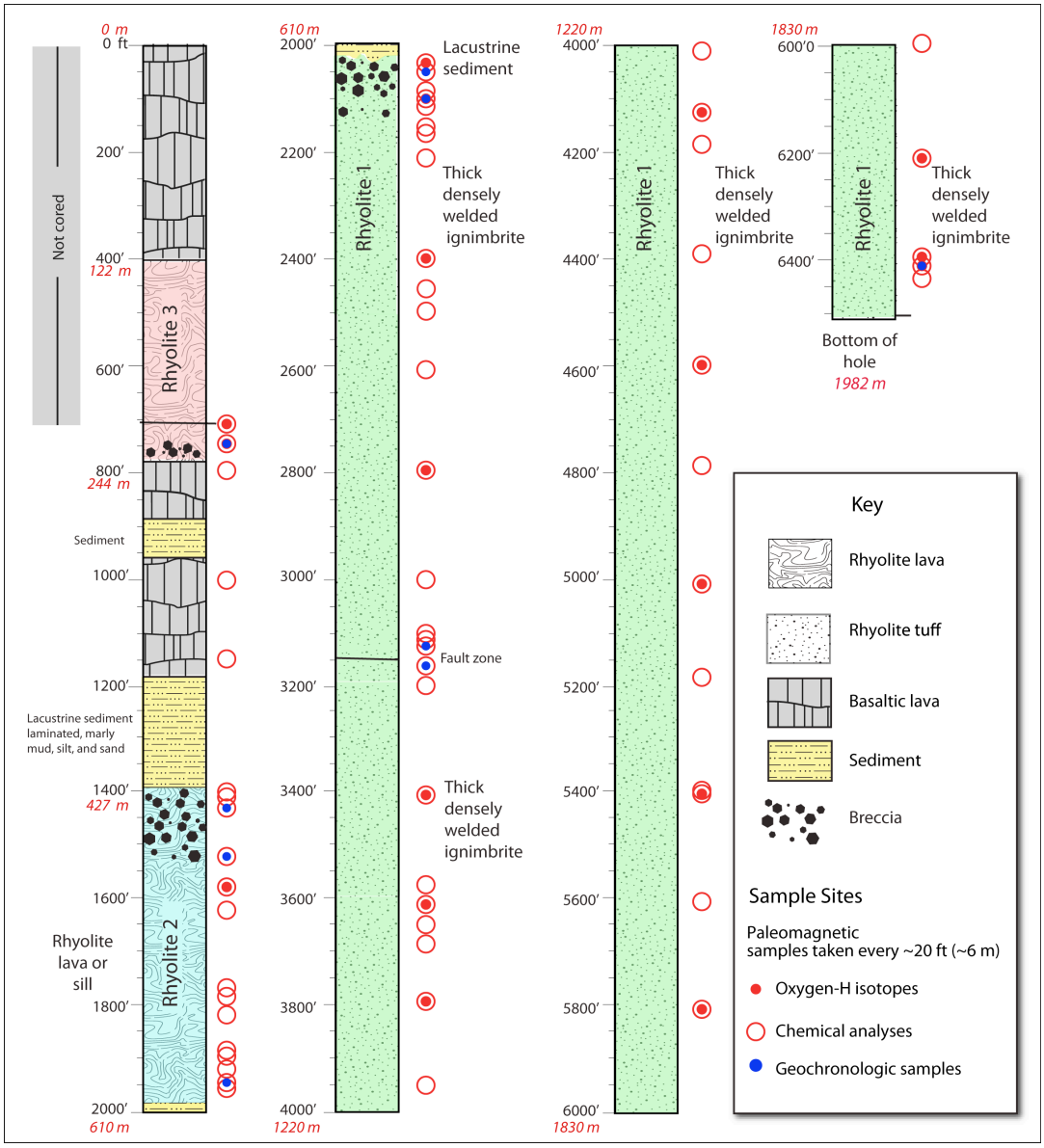

Figure 10-6. Lithologic log of the Kimberly section, compiled by Lisa Morgan and W.C. Shanks during drilling and supplemented with logging and interpretations by E. Christiansen, M. McCurry, M. Branney, T. Knott, and T. Bolte. All rhyolites have phenocrysts of plagioclase, alkali feldspar, 2 pyroxenes, magnetite, ilmenite, apatite, and zircon. Rhyolite 2 has quartz in addition to these other phases.

Preliminary O-H-isotope data reveal that the units in the core have large and systematic variations with depth: $\delta^{18}O$ from +1 to +9.8‰ and $\delta^{2}H$ from -140 to -180‰ (Figure 10-7 shows 19 whole rocks and 7 mineral separates). As expected for the Central SRP, magmatic $\delta^{18}O$ is low (<3‰; Bindeman, et al., 2007; Watts et al., 2010, 2011, 2012; Boroughs et al., 2005; 2012; Ellis et al., 2012) High whole-rock $\delta^{18}O$ values are for hydrated clay-altered rhyolite (5% H_2O) and the lowest values are for the fresh upper rhyolite lava and its feldspar phenocrysts. $\delta^{18}O_{feldspar}$ is

magmatic, unaffected by low-T alteration of the host groundmass (glass hydration or phyllosilicate generation). Quartz (higher than feldspar) and clinopyroxene (lower than feldspar) retain magmatic values and fractionations with feldspar. A petrogenetically important temporal decrease of $\delta^{18}O_{feldspar}$ (Figure 10-7) gives us additional leverage to explore the origin of the typically low $\delta^{18}O$ of rhyolite of the Central SRP. The data indicate a progressive recycling of more hydrothermally altered material into the magmas that erupted to form the rhyolites.

Chemically, mineralogically, and isotopically, all of the rhyolite in the Kimberly core is similar to other SRP rhyolites and dissimilar to older rhyolites like those erupted from the Challis volcanic field (52-48 Ma) to the north or to rhyolites from the Basin and Range province (<21 Ma) to the south and east.

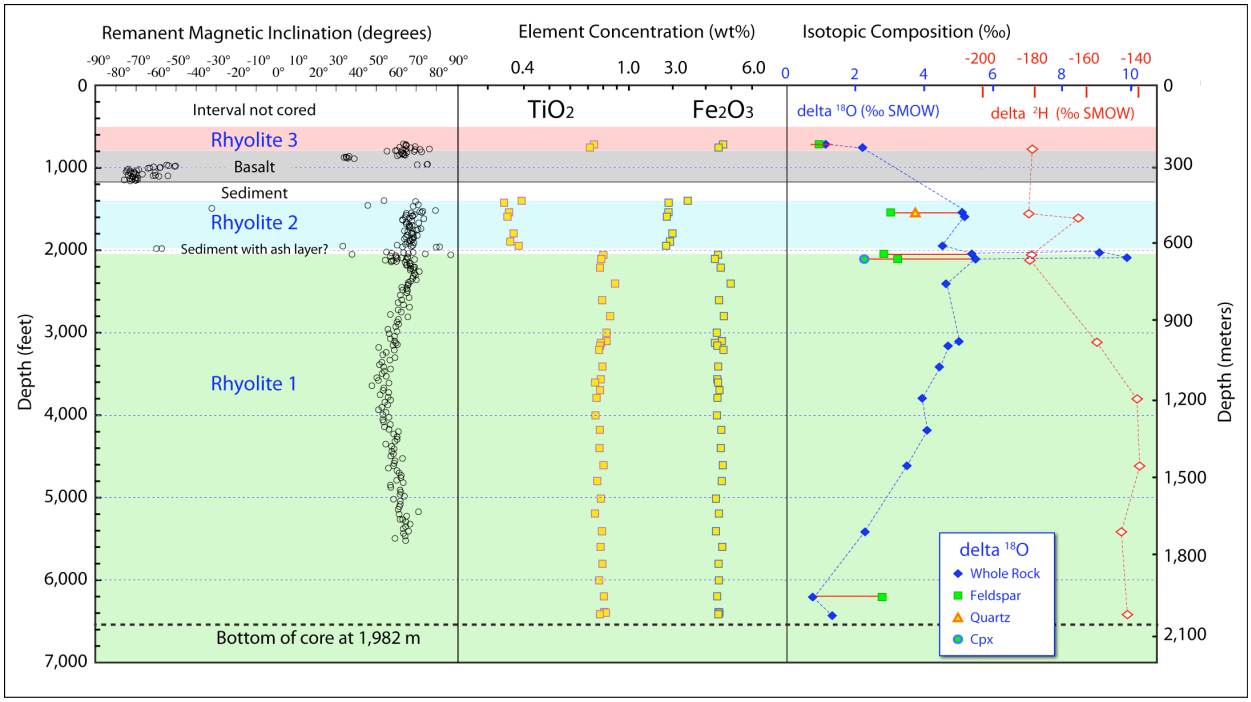

Figure 10-7. Paleomagnetic inclinations and composition of the rhyolites in the Kimberly core suggest there are at least 3 eruptive units in the core. Other units may be found during detailed logging and geochemical and paleomagnetic investigations. Oxygen and hydrogen isotopic compositions show that quartz, feldspar, and clinopyroxene have retained their magmatic values in spite of alteration of the groundmass. Feldspar (=magmatic) delta 18O ranges from 1‰ (in Rhyolite 3), to 3‰ (in Rhyolites 1 and 2). Note feldspar has same 18O in the upper and lower parts of Rhyolite 1, even though whole-rock O-isotope ratios systematically decline and H-isotope ratios increase with depth.

Mountain Home

Lithology of the Mountain Home site consists of an upper basalt unit with minor interbedded sediments 0-215 meters (0-705 feet), overly interbedded sands and clays, with minor gravels and thin basalt layers from 215-850 meters (705-2800+ feet). Coring the upper 215-599 meters was carried out with Lexan core barrel liners (HQ3) to facilitate sediment recovery. The lower section consists of basalt, altered basalt, and basaltic “sandstone”, likely derived from hydro-magmatic eruptions (Figure 10-8).

There are four major units below the upper basalt layer in MH-2A. Unit 1 consists of sand, sandy silt, and minor clay/gravel intervals (215-456 meters). Unit 2 is very fine sands (456-518 meters). The sediment is quite compacted and dense, not cemented to be "sandstone", but quite solid in the core. The entire unit is quite uniform, coarse lamination is apparent through the liner. Only thin intervals of this otherwise uniform sand unit consist of finer clayey silt (e.g., 492-495 meters). The bottom of this unit may be placed at 518 meters, where there is a shift to medium sand and coarse sand, all quite well sorted. Unit 3 consists of coarse sand, compacted but not cemented (518- 552 meters). Below 524 meters this coarse sand contains abundant basalt clastic grains, and there are three layers of basalt, each about 30 centimeters thick at 529, 543, and 545 meters (all depths are below rotary table, which was 2 meters above ground). At about 552 meters, there is a sharp change from coarse sands of Unit 3 to fine clayey silt, this is the top of Unit 4 (552-599 meters depth). Unit 4 is remarkably uniform - fine laminated clayey silt all the way to the bottom of Hole 1A.

Coring of the new drill hole, MH-2B, began on 1 October 2011, and was rotary drilled to a depth of 619 m, when coring was renewed. DOE funded drilling stopped at midnight on 15 October 2011, at total depth of 838 meters below the surface. Continued drilling, supported by the U.S. Air Force, reached a total depth of 1812 m. An artesian aquifer was encountered at 1745 m depth, with a temperature of ≥140C.

Lithologic units in cored interval of MH-2B (>619 m depth) include lacustrine sediments, altered basalts, and basaltic sandstones (Figure 10-12). Lacustrine sediments extend from 619 m to ~738 m depth, where a 30 m thick interval of basalt is encountered. This is followed by sedimentary intervals of mixed sand, clay, and breccia (768-853 m; 898-957 m; 1120-1155 m) alternating with basalt flows (853-898 m; 957-1120 m; 1155-1211 m). Below this is a thick section of basaltic sandstone or hyaloclastite, which extends from 1211 m to 1542 m depth (Figure 10-12). This greenish-black basaltic sandstone is composed of granular fragments of altered basalt, 1-3 mm diameter, that are tightly packed together form a rock that resembles basalt but is much less dense. Fracturing and mineral veins are rare.

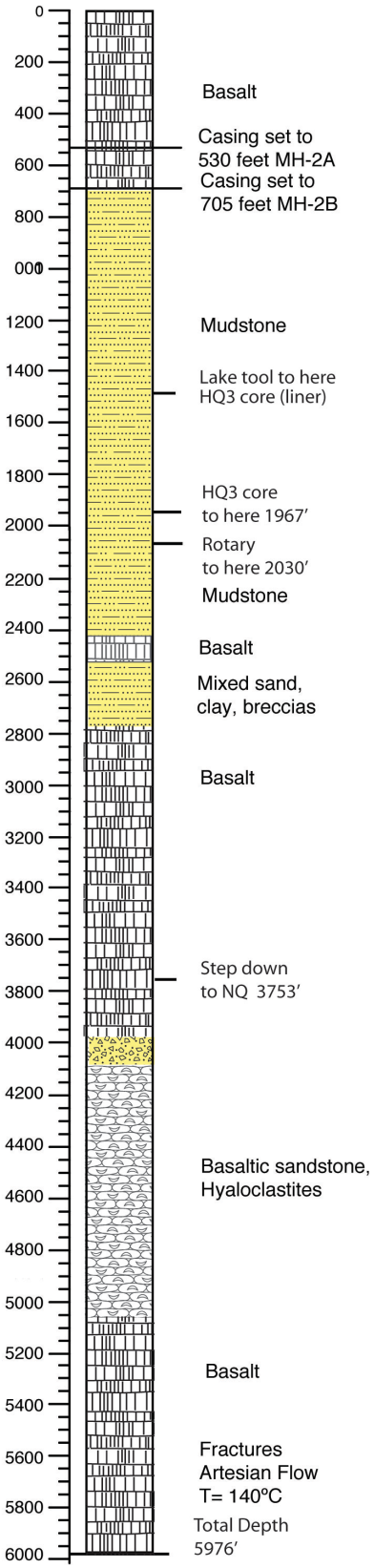

Below 1542 m the section consists of highly altered and mineralized basalt. Alteration phases include smectite, chlorite, calcite, and laumontite. Ore minerals include pyrite and chalcopyrite. Mineralized breccia is common, with calcite forming the dominant secondary phase cementing the angular fragments together. We infer that these are hydrothermal explosion breccias formed when the geothermal system was at a higher temperature than today, as documented by fluid inclusion temperatures in calcite.

Core recovery in the active flow zone of the geothermal system was less than 50%, indicating large aperture fractures that exceed the diameter of the NQ core samples.

Figure 10-8. Combined lithologic log for Mountain Home wells 2A and 2B. Depth in feet. Below upper basalt (700’ thick), ~2100’ of lacustrine sediment with minor basalt intercalations. From 2800’ to 4000’ is largely basalt, followed by basalt hyaloclastites (volcanic breccias) and basaltic sandstone (~4000’-5000’). Lower 900’ is hydrothermally altered basalt.

CHAPTER 11:

LOW TEMPERATURE AND HYDROTHERMAL ALTERATION

Christopher Sant[1], Jeff Walker[2], Joseph Wheeler[2], John W. Shervais[1]

[1]Utah State University, Logan, Utah

[2]Vassar College, Poughkeepsie, NY

ABSTRACT

Low temperature and hydrothermal alteration of wallrock in geothermal areas produces mineral assemblages that reflect ambient temperatures and pressures during geothermal alteration of volcanic rocks and volcanogenic sediments. These mineral assemblages allow us to reconstruct the thermal history of the rocks and their response to elevated temperatures.

We have carried out detailed X-ray diffraction analysis of phyllosilicates in the Kimama and Mountain Home drill cores. The Kimama core is characterized by the onset of groundmass smectite alteration at about 963 m depth, which corresponds to an inflection in the thermal gradient from essentially isothermal (~16ºC) and convective, to conductive with a steep gradient of ~75C/km below 980 m depth. We infer that the onset of smectite alteration seals fracture and microfracture porosity below 980 m, which thus forms the effective base of the Snake River aquifer.

The Mountain Home drill core contains a 50m thick zone of corrensite (R1 mixed-layered chlorite/smectite) at around 1750 m overlain and underlain by smectite-bearing alteration assemblages. The top of the corrensite zone corresponds to a region of increased fracturing and hot water under artesian pressure, suggesting that the corrensite is related to the increased fluid flow, and/or the composition the hydrothermal fluids at that depth. The Mountain Home Core allows the study of whether the transition from smectite to corrensite is continuous (involving intermediate random interstratifications of different percentages of chlorite and smectite layers) or discontinuous, changing from discrete smectite to discrete corrensite with no intermediate phases.

INTRODUCTION

A detailed understanding of the clay minerals formed by hydrothermal alteration will document the thermal history of the water that comprises this system. X-ray diffraction spectrometry is the primary method used by mineralogists to identify and quantify clay mineral analyses. Because clay minerals are typically very fine grained, and may form interlayered structures with other phyllosilicates, optical and micro-analytical methods are less useful than for other mineral species. Clay minerals form typically at low temperatures and pressures from pre-existing high-temperature phases (e.g., feldspar, pyroxene, or glass), but the types and structures of the clay minerals are themselves controlled in part by formation temperatures and circulating hydrothermal fluids. The transition in structural order-disorder from low to higher, and from simple clays to mixed layer clay or mixed layer phyllosilicates, is also a function of formation temperatures and fluids.

ANALYSIS OF CLAY MINERALOGY AT KIMAMA

Samples were collected from the Kimama drill core every 45 meters, for a total of 42 samples throughout the depth of the borehole. Ten additional samples were taken from splits prepared for whole rock XRF analysis, between the depth interval from 917 to 1,038 meters. These samples were chosen because preliminary analysis showed that this interval contained the transition from basalts with relatively fresh groundmass to basalts with clay in the groundmass. Finally, eighteen samples were collected from vesicles using the picks and dental tools method. In all, seventy samples were examined for this study.

Data Acquisition and Methodology

Samples were powdered using standard methods. Bulk whole rock powders were scanned to determine overall mineralogy and to detect presence or absence of clay minerals. Clay separates were prepared for detailed clay analyses using gravity settling. Each clay separate slide goes through a three-step treatment process, with an X-ray diffraction run after each step. Step one consists of being exposed to room temperature atmosphere. Step two consists of exposing the samples to ethylene glycol vapor at 60°C for 24 hours. Step three consists of heating the sample to 500°C for two hours.

X-ray diffraction analyses at Utah State University were carried out on a PANalytical X'Pert Pro X-Ray Diffractometer (XRD). Twenty-two randomly oriented whole-rock powders were analyzed with scanning parameters of 2° 2Θ/min from 3 to 33°, 1° slit size, and 20 mm window; all scans were run using CuKα radiation at 45kV and 40mA. Clay separates were analyzed at 0.25° 2Θ/min with 0.5° slit size and a 10 mm window. Four samples (1234, 1396, 1676, and 1798 m) were analyzed at Vassar College using a Seimens D-5000 theta:2-theta diffractometer

at 40kV and 30mA with a 0.5° slit size. Samples were run with a 0.02 step size at 1° 2Θ per minute from 0° to 35° 2Θ.

Results of Analysis of Mineralogy Data

Whole-Rock Powders

Twenty-two whole-rock powders were analyzed using X-ray diffraction. None of the samples above 963 m have clay peaks present (Figure 11-1). Between 963 m and 1,038 m, about half the bulk rock samples display prominent clays peaks. All samples below 1,038 m have a low-angle clay peak present below 10° 2Θ.

Nine samples were selected for clay separate analyses. Random powder mounts and oriented clay mounts were analyzed at both Utah State University (USU) campus and at Vassar College. All of these samples were taken below 1,038 m because that is the approximate location where clays become abundant enough to collect a sufficient clay for X-ray analysis. Four representative samples are discussed here (Figure 11-2).

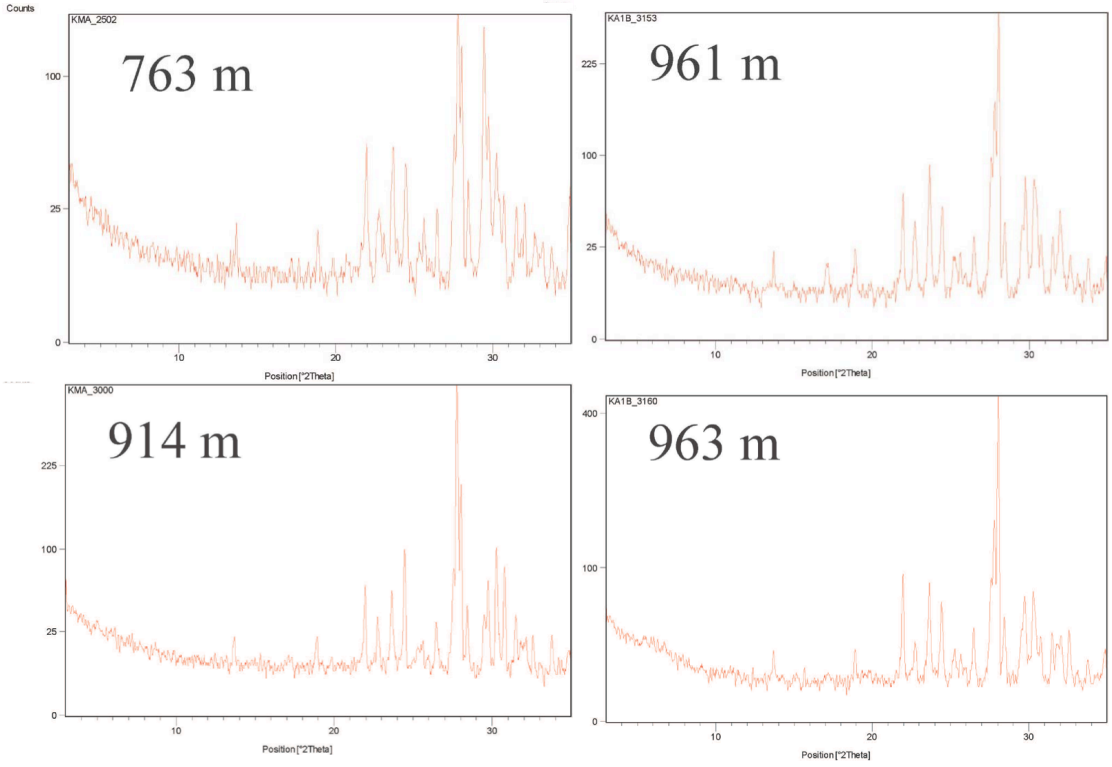

Figure 11-1. Whole rock X-ray diffraction scans for clay peaks reveal no significant clay alteration in samples above 965 m depth.

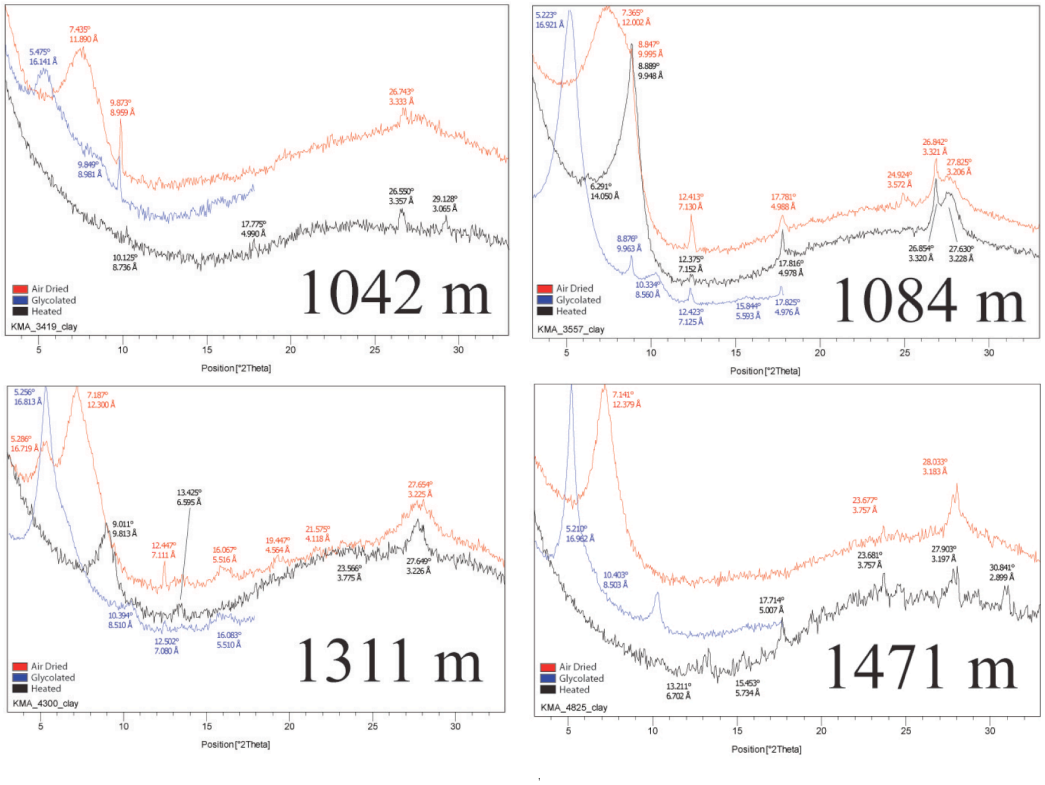

Figure 11-2. X-ray diffraction patterns in low 2-theta range for samples below base of aquifer. Prominent clay peaks in all. Scans 1042 m and 1471 m are dioctahedral smectites, scans at 1084 and 1311 m depth are trioctahedral smectites.

Sample 1042 m is from a non-authigenic sedimentary interbed. This sample is not a classic smectite example, but does contain smectite derived from surface sediments. Sample 1084 m is from a vesicular section of a basalt flow; it is an example of authigenic Fe-rich smectite. Sample 1311 m is from a massive section of a basalt flow that was fractured and then sealed with mineralization. This sample contains smectite in the matrix of the whole-rock as opposed to only in vesicle fillings. Sample 1471 m is from vesicle fillings. This clay is the same brown hue as sample 1042 m that was sampled from a sedimentary interbed. The data show much the same results as in sample 1042 m, suggesting it is a non-authigenic smectite that infiltrated the flow.

Clay Mineral Structural Modeling

Smectite clay minerals with different defect-free distances were modeled using the NEWMOD software with the objective to determine the degree or quality of crystallinity of the smectite clay. We modeled one type of clay with two slight variations. Both clays modeled are a glycolated Fe-rich dioctahedral smectite. The only difference between the two models is the amount of defect broadening, or the value of N. The first sample modeled, with low values of N, was modeled with a mean N of 1 (no perfect staking) and high N of 5. The second sample modeled uses higher values of N, with a mean value of 2.5, and a high value of 12.

The low-N model has a broader, less intense peak with a *Full Width Half Maximum* (FWHM) value of 1.5° 2Θ. The sample modeled with low values of N look very similar to sample 1234 m, suggesting that sample 1234 m contains an Fe-rich dioctahedral smectite. The high N model has a high narrow peak with a FWHM ratio calculated as 0.7° 2Θ. The sample modeled with high valued of N looks very similar to sample 1798 m, suggesting that sample 1798 m is a Fe-rich dioctahedral smectite with a larger defect-free distance than sample 1234 m.

The implications of defect broadening are very apparent in the FWHM measurements. A decrease from a mean of 2.5N to a mean of 1N more than doubles the peak width at half the max height from 0.7° to 1.5° 2Θ. Clays with a high degree of crystallinity (high N) are found deeper in the hole, and likely represent higher ambient temperatures than less crystalline clays. Measuring the FWHM ratios and also using a visual peak width comparison, this modeling technique can help determine the crystallinity quality, and thereby give some indication of temperature at the time of formation.

DISCUSSION: KIMAMA

Three main observations highlight the base of the aquifer on the axial volcanic zone of the Snake River Plain. The first signs of alteration occur around 960 m depth when clays first begin to appear as vesicle linings. The color of the core remains a light grey color, then a sudden color change occurs at 1,020 m depth. The color changes from light grey to green due to alteration, the vesicles begin to be filled with clay and other minerals, including hydrothermal minerals such as zeolites. Second, the temperature log data exhibits a major change in the geothermal gradient in the Kimama borehole at 960 m depth. The geothermal gradient changes from 4.5 to 75.5 °C/km indicating that the aquifer is not present below 960 m. Third, the mineralogical data suggest that smectite clay appears in the basalt groundmass just below 960 m. The presence of clay in the basalt groundmass causes pore spaces to be clogged and the smectite clay provides an explanation for lack of convective transport below 960 m.

We suggest, based on these data, that the base of the aquifer on the axial volcanic zone of the SRP at Kimama is ~960 m below the surface. Compared with estimated depths of 500 m or less at the INL (Smith, 2004), the thickness of the aquifer on the axial zone at Kimama is much greater than previously suspected. The major boundary between unaltered basalts and altered basalts begins at 960 m. It is at this depth which the temperature inflection is located, when smectite clay begins to clog the pore spaces in the rock, and secondary mineralization begins to occur. Below 1,020 m the basalts show signs of alteration such as a color change, vesicle filling, and other secondary mineralization, along with prominent smectite peaks in clay separates (Figure 11-3).

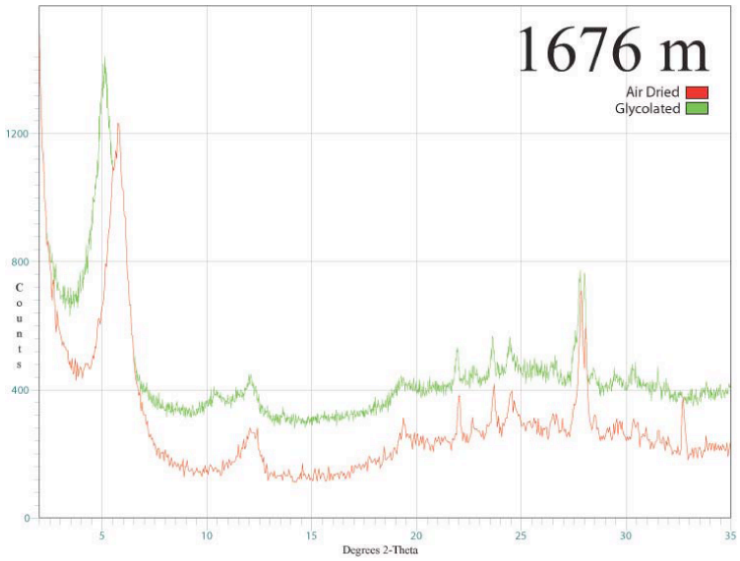

Figure 11-3. Prominent clay pattern in XRD scan of clay separate from 1676 m depth.

Dioctahedral clays are commonly found in sedimentary rocks and form from the weathering of K-feldspars. Dioctahedral smectites, with increasing temperature, convert to illite. The included models suggest that two of the samples (1234 and 1798 m) that do not have a heated smectite peak are dioctahedral smectite. Therefore, it can be assumed that all samples that contain smectite peaks in the air-dried and glycolated lines, but do not have a heated peak at 10 Å are dioctahedral smectites. The samples 1042, 1234, 1471, 1676, 1798, and 1829 m may be interpreted as dioctahedral smectites. Samples 1042 and 1234 m were samples a short distance from sedimentary interbeds so it is expected that they are dioctahedral.

Trioctahedral clays are derived from the weathering of mafic minerals such as pyroxene, olivine, and basaltic glass. With increasing temperature and pressure trioctahedral clays convert to chlorite instead of illite. X-ray diffraction data reveal that sample 1396 m is a trioctahedral smectite. Sample 1396 m has a heated clay peak, whereas, the dioctahedral samples do not. Therefore, we assume that all the samples with a 10 Å peak in the heated line are trioctahedral. The samples 1084, 1311, and 1396 m may be interpreted as trioctahedral smectites.

Johnston (1983) suggests that above 90° C smectite begins to become unstable and converts to illite. No mixed-layer clays of smectite/illite or smectite/chlorite were observed. Therefore, the temperatures since the formation of the present smectite clays present in the basalt has remained below 90° C. This is consistent with observed temperature gradient in the Kimama well, which projects to a bottom hole temperature of about 90-92ºC.

ANALYSIS OF CLAY MINERALS IN MOUNTAIN HOME 2A-2B

The Mountain Home drill core contains a 50 m thick zone of corrensite (R1 mixed-layered chlorite/smectite) at around 1750 m overlain and underlain by smectite-bearing alteration assemblages. The top of the corrensite zone corresponds to a region of increased fracturing and hot water under artesian pressure, suggesting that the corrensite is related to the increased fluid flow, and/or the composition the hydrothermal fluids at that depth. The Mountain Home Core allows the study of whether the transition from smectite to corrensite is continuous (involving intermediate random interstratifications of different percentages of chlorite and smectite layers) or discontinuous, changing from discrete smectite to discrete corrensite with no intermediate phases. *Discontinuous and continuous models suggest different hydrothermal regimes, and discerning between them will help to decipher the history of the hydrothermal system.*

Data Acquisition and Methodology

X-ray diffraction analyses were performed at Vassar College using a Bruker Θ:Θ diffractometer at 30kV and 10mA with a 0.6° incident beam slit size. Samples were routinely run with a 0.1 step size and a count time ranging from 1 to 4.0 sec/step from 2° to 35° 2Θ. Twenty-two samples from between 750m and 1800m (2460-5900 feet) depth were analyzed as randomly oriented <250 μm powders. From these, 8 were chosen to create <2μm oriented-grain mounts to be Ca-saturated, and analyzed air-dried and after exposure to ethylene glycol vapor at 60°C for 24hr. The oriented-grain diffraction patterns were modeled using the computer software NEWMOD to ascertain stacking sequence, layer composition, and degree and nature of disorder.

Data Analysis

Preliminary results indicate that from 760 m to 1750 m depth (~2500-5800 feet), the predominant tri-octahedral clay mineral is smectite, most likely saponite, that increases in diffracting domain size with depth. From 1750 m to 1800 m depth (~5800 to 5900 feet) the predominant clay mineral is corrensite, a 50:50 R1 mixture of chlorite:smectite (C/S). Below 1800 m, smectite is again present. Eight samples were selected for further study: 2 smectite-rich samples above the corrensite zone, one smectite-rich sample below it, and 5 in or near the corrensite zone. The <2um fraction was separated, saturated with Ca^{2+} using 0.1N $CaCl_2$, and analyzed in oriented powder mounts both air-dried, and solvated with ethylene glycol. The patterns were modeled with NEWMOD to study the nature of interstratifications, as well as changes in diffracting domain size.

Results of Analysis of Clay Minerals

The isolated occurrence of corrensite in a smectite-dominated alteration assemblage is shown in the representative random powder XRD analyses in Figure 11-4. Diffraction patterns of oriented mounts studied after calcium-saturation and glycolation are shown in Figure 11-5.

The shallowest two samples (Figure 11-5; 762 m and 1650 m) have one major low angle peak at ~16.9Å indicating the presence of smectite. Between 1752m and 1793m, however, the presence of the peak at ~30Å indicates the presence of corrensite. The deepest of these samples (1793m) is pure corrensite, whereas the others have both corrensite and smectite, and there is a suggestion that the amount of smectite (estimated by the size of the smectite shoulder at ~17Å relative to the adjacent corrensite peak) decreases with increasing depth. Pure smectite again dominates the clay fraction below the corrensite zone (sample 1807 m).

These trends match the random powder results (Figure 11-4) but also show that the corrensite zone is complicated by the coexistence of corrensite and smectite. The sharp peak at ~9.5Å in sample 1752 m is interpreted to laumontite.

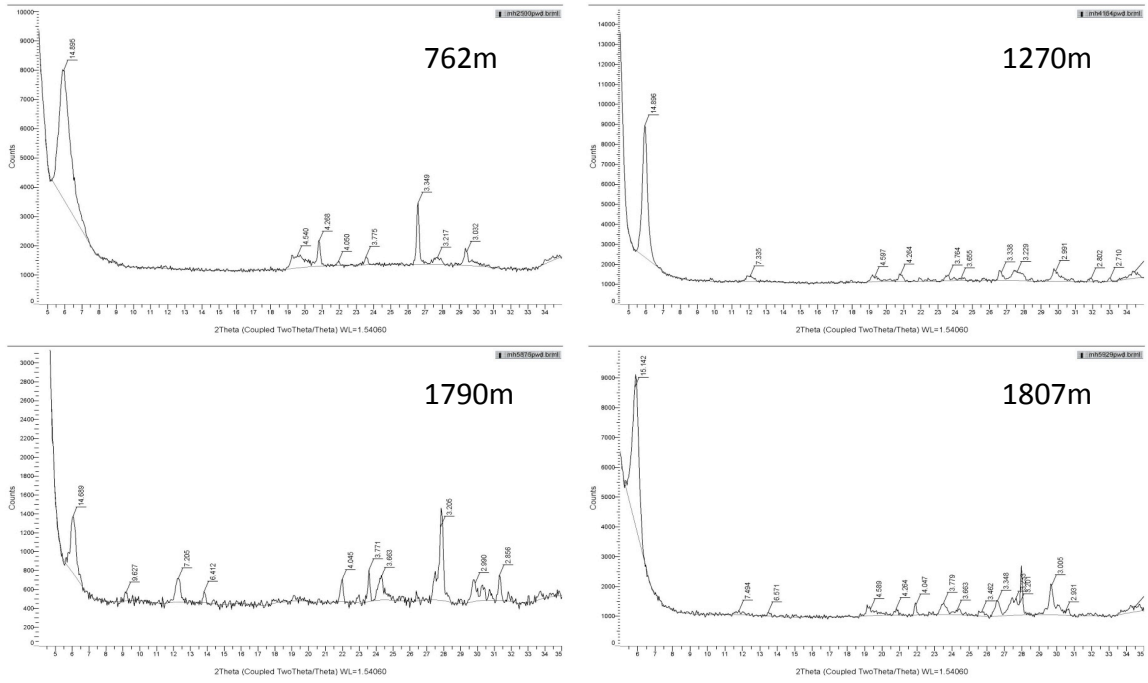

Figure 11-4 Four representative diffraction patterns for random powder mounts. 762m, 1270m, and 1807, all indicate smectite. 1790m is different and the pattern suggests corrensite.

Of the three samples that are pure smectite (762m, 1555m, and 1807m) the sharpness of the ~17Å peak increases with depth. NEWMOD-modeled changes of Full Width at Half Maximum (FWHM or β) show that the mean defect-free distance (δ) of the smectite increases with depth from 1.5 unit cells near the surface to 10 unit cells at the bottom of the core (Table 11-1).

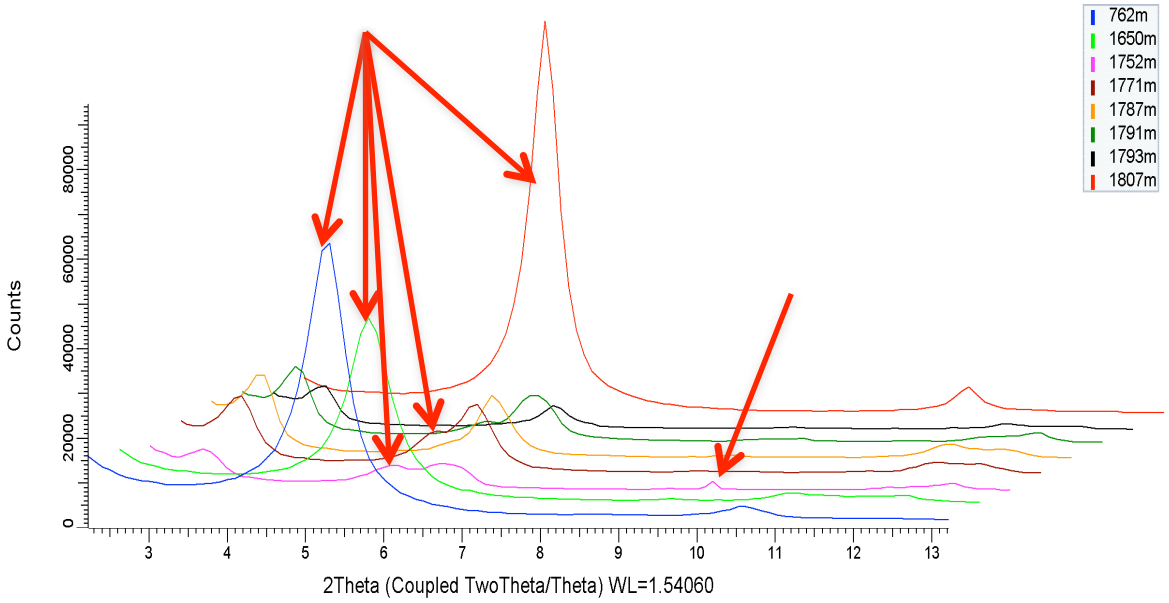

Figure 11-5a Smectite and laumontite peaks in MH-2b core

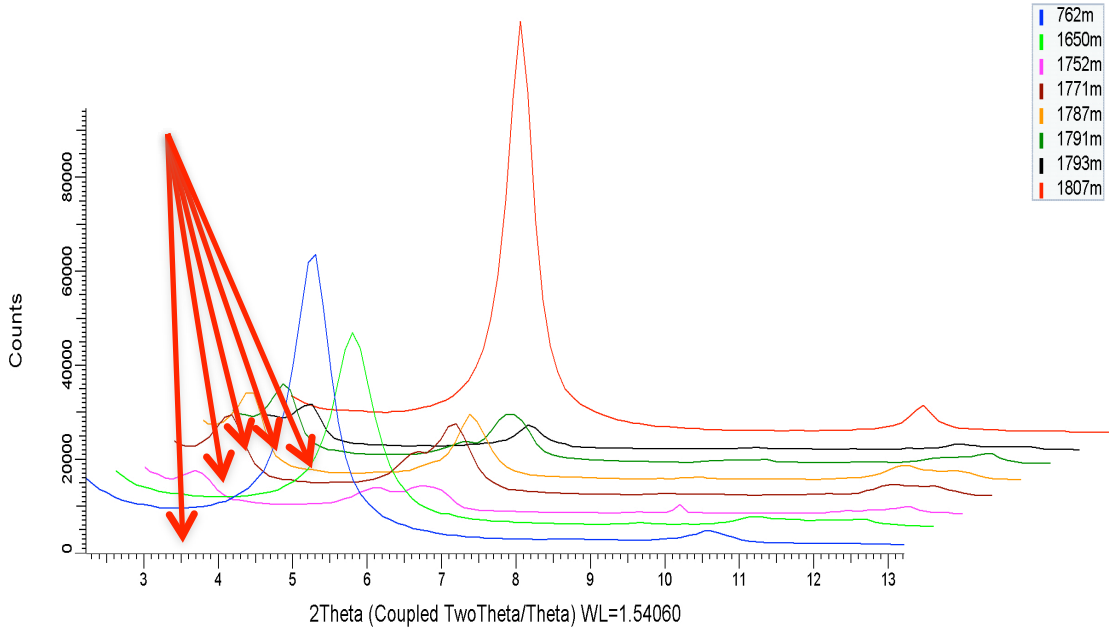

Figure 11-5b. Corrensite peaks in MH-2b core.

X-ray diffraction studies of vein fillings done at Utah State University and the University of Utah have also documented the occurrence of the Ca-zeolite laumontite at ~1750 m depth, as clear, sparry crystals coating fracture surfaces in large aperture open vugs, underlain by the C/S phase corrensite. The occurrence of laumontite implies temperatures of <200-220ºC. This is consistent with fluid inclusion data from calcite that document an early high-temperature inclusion group (T≈195ºC) and a later low-temperature inclusion group (T≈160ºC).

Depth (m)	Measured FWHM	Modeled ð	Modeled FWHM
762	1.26	1.5	1.26
1555	0.281	7	0.28
1807	0.241	10	0.24

Table 11-1 Modeled and measured FWHM (β) and defect-free distance (δ). With depth the measured value of smectite β increases. The model of this increase has a corresponding increase for δ values.

DISCUSSION

Formation of Smectite

The occurrence of smectite throughout the core may be a result of different processes acting at different levels in the section. Smectite may be a weathering product of the volcanic rocks formed by exposure to the atmosphere in the interim between eruption of lava flows. In hyaloclastic beds, volcanic glass may transform to smectite at low temperatures by palagonitization (Drief and Schiffman, 2004) or biological processes (Walton, 2008). Whereas smectite in the deepest samples could be formed by low-temperature mechanisms, its proximity to the artesian zone suggests that may be a high-temperature alteration product formed from super-saturated fluids in a zone of high fluid:rock ratio (Rigault et al., 2010).

Continuous vs Discontinuous Smectite to Corrensite Transition

The data show an abrupt appearance of the d_{001} corrensite peak at ~31Å, with a corresponding basal series of peaks. This peak will not appear unless an ordered (R1) interstratification of 14Å chlorite layers and 17Å smectite (glycol) layers is present. If R0 C/S formed as a precursor to the corrensite, we would expect to see a change in the broadening of the smectite (001) peak as chlorite layers randomly interspersed in the smectite break up the diffraction continuity of the crystallite. Instead, FWHM values decrease and modelled defect-free distances increase with depth for smectite, suggesting the formation of larger smectite diffracting domains. These results suggest that the transformation of smectite to corrensite in the MH-2 core is, in general, a discontinuous process with few or no intermediate, randomly interstratified phases.

Corrensite-forming Reactions and Conditions

The reaction of smectite to form less expandable minerals such as corrensite or chlorite can be initiated in volcanic rocks at threshold temperatures as low as 150°C (Robinson et al., 2002). However, the continuous or discontinuous progression of the reaction depends not simply on temperature, but also on the various factors that control reaction kinetics such as thermal gradient, grain size, fluid:rock ratios, and nutrients available in the hydrothermal fluids. Of these factors, fluid:rock ratios and nutrient availability appear to be most important in other geothermal areas (Robinson et al., 2002). In addition, because kinetic factors are so important to this reaction, time is also an important variable in assessing reaction progress (Rigault et al, 2010).

In the trioctahedral clays, rapid transformations favor discontinuous, equilibrium reactions from smectite to corrensite to chlorite. Such rapid transformations occur in fracture-dominated hydrothermal systems with high porosity and permeability in which warm fluids advectively transport the nutrients necessary for the reaction. If fluid and nutrient transport is primarily diffusive, as is the case in unfractured host rock where the primary pathways are along grain boundaries, then a continuous, disequilibrium reaction with intermediate random mixed-layered chlorite/smectite, is favored (Robinson et al, 2002).

If the MH-2b core is interpreted according to this scenario, the corrensite zone occurs in a zone of high fluid flow (artesian water at 145°C) in which the smectite to corrensite transformation began when the rocks reached the threshold temperature, and proceeded rapidly due to the abundant nutrient-rich water. The decreasing relative amounts of smectite in the corrensite zone result as smectite is transformed to corrensite at different rates governed by the increase in temperature with depth within the corrensite zone. In other highly fractured zones at shallower levels in the core the water was too cool, and temperatures have never been high enough to initiate the smectite to corrensite transformation.

Because the corrensite zone is primarily found within a zone of fractures that are mostly plugged by secondary mineral crystallization, an alternate explanation is also possible. Rigault et al. (2010) point out that the occurrence of different clays in some hydrothermal systems depends on whether hot fluids are able to achieve equilibrium with the host rock. For instance, areas with high permeability and high fluid/rock ratios are associated with a discontinuous transformation whereas continuous sequences are associated with low permeability and low fluid/rock ratios, implying that the rate of mineral growth is controlled by the amount and the character of fluids present during crystallization as well as the temperature (Dekayir et al. 2005, Schmidt and Robinson 1997, Shau and Pecor 1992).

Rigault et al. (2010) note that hydrothermal waters can become supersaturated with the nutrients necessary to crystallize smectite. Boiling of these fluids will cause crystallization of abundant meta-stable smectite in the host rock regardless of the temperature. If crystallization of the smectite fills the fractures in the rock, sealing them against further fluid flow, then the smectite will transform to corrensite and eventually to chlorite over time as hydrothermal activity changes to a depth-dependent geothermal gradient. This would explain the observation that most of the corrensite in the MH-2b core appears to be concentrated in a zone where fractures have been plugged by secondary mineral crystallization, although the bottom hole temperatures are not high enough to be in the range generally expected for simple thermal metamorphism of smectite to corrensite.

It is intriguing to note that preliminary fluid inclusion studies of calcite crystals from the bottom of the well found equilibration temperatures of nearly 200°C for primary inclusions and closer to 150°C for secondary inclusions, so temperatures may have been significantly higher in the past, and have cooled as the circulating hydrothermal waters have been cooled by mixing with meteoric water.

The presence of laumontite in the upper part of the corrensite zone does little to constrain the temperatures since laumontite is thought to form at temperatures as low as 50°C (Boles and Coombs, 1977); some surface waters in basaltic terranes in Iceland are saturated with laumontite (Arnorsson and Neuhoff, 2007). Experimentally it is stable up to 350°C before it transforms to wairakite (Jove and Hacker, 1997).

CONCLUSIONS

The clay analysis suggests that alteration temperatures in the lower volcanic section (and in the volcanogenic sediments) in both cores were at or above temperatures indicated by the thermal gradient measurements; that is, temperatures in the lower 2800 feet of the Kimama drill hole exceeded 75ºC, and ranged as high as 140ºC at TD. The occurrence of corrensite (layered C/S) and laumontite at ±5740 feet in the Mountain Home drill core (within and below the artesian fracture zone) implies somewhat higher temperatures associated with the geothermal fluids – 140ºC to 150ºC. As noted above, these temperatures are consistent with the fluid inclusion data from calcite, which document an early high-temperature inclusion group (T≈195ºC) and a later low-temperature inclusion group (T≈160ºC). A more detailed assessment of clay mineralogy may help document fluid thermal histories more fully, as well as which rocks were most affected (and thus saw the highest temperatures).

Notes: X-ray diffraction analyses at Utah State University were carried out on a PANalytical X'Pert Pro X-Ray Diffractometer (XRD). The software programs associated with the XRD are the PANalytical X'pert Data Collector, version 2.0b, published February 27, 2003, and the PANalytical X'Pert HighScore, version 2.2.0, published January 02, 2006. The Data Collector is used to collect the raw data from the XRD, and HighScore is used to refine and interpret the data from the XRD readings. All scans were run using CuKα radiation at 45kV and 40mA. Clay separate scans were analyzed using scanning parameters of 0.25° 2Θ/ min with 0.5° slit size and a 10 mm window. Each clay separate sample was run after each stage of a three-stage treatment process. The first stage is exposure to room temperature atmosphere and it is run from 3° to 33° 2Θ. The second stage of the treatment subjected the samples to ethylene glycol vapors at 60°C for 24 hours and then run in the XRD from 3° to 18° 2Θ. Due the volatility of ethylene glycol, after about one hour the sample begins to change thickness which could cause inaccurate results. For this reason, glycolated samples were only run for one hour, from 3° to 18° 2Θ. Stage three consisted of heating the samples to 500°C for two hours, then cooling and running them from 3° to 33° 2Θ.

CHAPTER 12:

HYDROLOGIC STUDIES

Thomas Lachmar, Thomas Freeman, John W. Shervais
Utah State University, Logan, Utah

ABSTRACT

Three exploratory coreholes were drilled at Kimama, Kimberly and Mountain Home on the Snake River Plain, Idaho, as part of the Snake River Geothermal Drilling Project to evaluate its geothermal potential. We used chemical data from five water samples that were collected from the three coreholes (one each from Kimama and Mountain Home, and three from Kimberly) in seven geothermometers (chalcedony: Fournier, 1977; quartz: Fournier, 1977; Na/K: Fournier, 1979; Na/K: Giggenbach, 1988; Na-K-Ca: Fournier, 1981; Na-K-Ca-Mg: Fournier and Potter, 1979; and K^2/Mg: Giggenbach, 1988) to estimate reservoir temperatures at depth. Three of the water samples were also analyzed for the stable isotopes deuterium and oxygen-18, and two samples were analyzed for carbon-13. Temperature log data from the coreholes were used to calculate geothermal gradients.

INTRODUCTION

Understanding geochemical aspects of deep fluid flow in geothermal systems are critical to assessing the volume and quality of the geothermal resource and its potential for power production. The temperature of groundwater and thermal waters is a direct indication of potential energy available for power generation, with warm groundwater reflecting thermal input from below. Thermal spring or well water may reflect actual water temperatures at depth within the geothermal system, or lower temperatures caused by mixing of cool meteoric water with deep-seated thermal waters. The affect of mixing with cooler surface waters can sometimes be mitigated by using chemical geothermometers, which calibrate dissolved cation concentrations with the equilibration temperatures of water with common mineral assemblages (e.g., feldspar, quartz, chalcedony). It is also possible to use the isotopic composition of water to determine its origin, e.g., heated meteoric water versus equilibrated formation waters.

In this chapter we review the chemical composition and thermal state of waters sampled from each of the three deep wells, and discuss the implications of these data on geothermal exploration in southern Idaho.

SAMPLING

Kimama

The Kimama corehole was sampled in July 2011, about 6 months after completion of the well. One water sample was obtained from this hole at a depth of 1,070 m (3,510 ft) on 3 July 2011 by the Operational Support Group (OSG) from Geo Forschungs Zentrum (GFZ). This sample was designated as KA-1. A sample was also collected from the shallow water-supply well at the Kimama drilling site on 3 July 2011 and labeled KA-W. The total depth of the water supply well is about 90 m (300 ft), and it has an electric submersible pump. The pump was turned on and the sample was taken directly from the spigot.

Kimberly

The Kimberly corehole was sampled in June 2011, about 1 month after completion of the well. Three water samples were obtained from this hole on 21 and 22 June 2011 using a Foerst Kemmerer-type mechanical sampler. The first sample was collected directly below the casing at 1,160 m (3,800 ft) and designated as KB-38. Another sample was taken around 1,585 m (5,200 ft) and labeled KB-52. The third sample (KB-63) was from the bottom of the hole at approximately 1,920 m (6,300 ft).

Mountain Home

The Mountain Home corehole was sampled on 26 January 2012. A flowing artesian zone was encountered in this hole at a depth of approximately 1,745 m (5,726 ft). This zone flowed at 12 to 18 gallons per minute, and it was allowed to flow for about 12 hours before it was sampled on 26 January 2012. This sample was designated as MH-5726.

CHEMICAL ANALYSES

All six of the water samples were analyzed in the field at the time of sampling for temperature, electrical conductivity, salinity, pH and alkalinity. A YSI Model 30 temperature-conductivity-salinity meter was used to measure those three parameters. An Orion Model 230A pH meter was used to measure the pH, and a Hach Alkalinity Test Kit Model AL-AP MG-L was used to measure the alkalinity in units of mg/L. The results of the field analyses are presented in Table 13-1.

The six water samples were analyzed for Al, As, B, Ba, Ca, Cd, Cl, Co, Cr, Cu, Fe, K, Mg, Mn, Mo, Na, Ni, P, Pb, S, Se, Si, Sr and Zn at the Utah State University Analytical Laboratory (USUAL). In addition, duplicates of the Mountain Home were analyzed by ThermoChem Labs, Santa Rosa, California, and the Vet Diagnostic Lab, USU. The analytical results for the major ions (Ca, Mg, Na, K, Cl, SO_4 and SiO_2) are presented in Table 13-2. In addition, the KA-W, KA-1 and MH-5726 samples were analyzed for deuterium and oxygen-18, and the KB-52 and MH-5726 samples

were analyzed for carbon-13. The deuterium and oxygen-18 analyses were performed by the Stable Isotope Ratio Facility for Environmental Research (SIRFER) at the University of Utah in Salt Lake City, and the carbon-13 analyses were performed by Geochron Laboratories, a division of Krueger Enterprises, located in Billerica, MA.

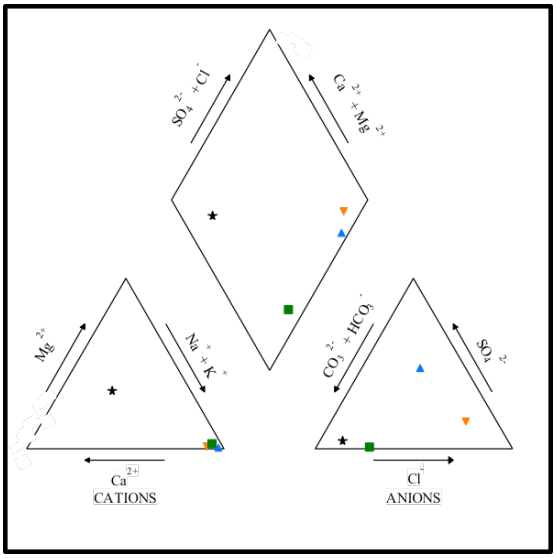

★	KA-W
▼	KA-1
■	KB-63
▲	MH-5276

Figure 12-1. Trilinear (Piper, 1944) plot of water samples.

RESULTS

Geochemistry

Four of the six water samples have been plotted on a trilinear (Piper, 1944) diagram (Figure 12-1). The sample from the shallow water-supply well (KA-W) is Ca-Mg-bicarbonate water, as is typical of water in the Snake River Plain aquifer. The dominant cation for all five of the samples from the three coreholes is sodium. However, the dominant anion is different for each of the three holes. The Kimama sample (KA-1) is Na-chloride water. All three of the Kimberly samples, which have very similar chemical compositions and thus only one sample (KB-63) was plotted on Figure (12-1), are Na-bicarbonate waters. The Mountain Home sample (MH-5726) is Na-sulfate water.

The results of the chemical analyses for the water samples obtained from the three coreholes were also used in geothermometric techniques proposed by Giggenbach (1988). The first technique divides geothermal waters into three main groups, fully equilibrated, partially equilibrated and immature, depending on the ratios of the Na, K and Mg concentrations. The resulting triangular diagram is known as a Giggenbach plot. A Giggenbach plot of the six water samples is shown in Figure 12-2A. The KA-W sample plots in the lower right-hand corner. The KA-1 sample and all three of the Kimberly samples plot on the line dividing partially equilibrated and immature waters near the lower right-hand corner of the diagram. The Mountain Home samples plot between the fully and partially equilibrated waters near the center of the diagram,

and lie along a 150ºC isotherm; the spread in their positions results from differences in Mg concentration. We suggest that the ThermoChem analysis (MtnHomeB) is the most reliable because they specialize in analyzing thermal waters for the geothermal industry.

The second technique used by Giggenbach (1988) is to characterize geothermal waters by plotting their relative chloride, sulfate and bicarbonate concentrations. Neutral chloride, acid and soda springs waters are the three broad classification types, and plot in the upper third, lower left-hand third and lower right-hand third, respectively, of the triangular diagram. The six water samples have been plotted on such a diagram in Figure 12-2B. The KA-W sample and all three of the Kimberly samples plot in the lower right-hand third of the diagram, and thus are soda springs waters. The KA-1 sample plots near the line dividing the neutral chloride and acid waters, and the Mountain Home sample is acid water as it plots squarely in the middle of the lower left-hand third of the diagram.

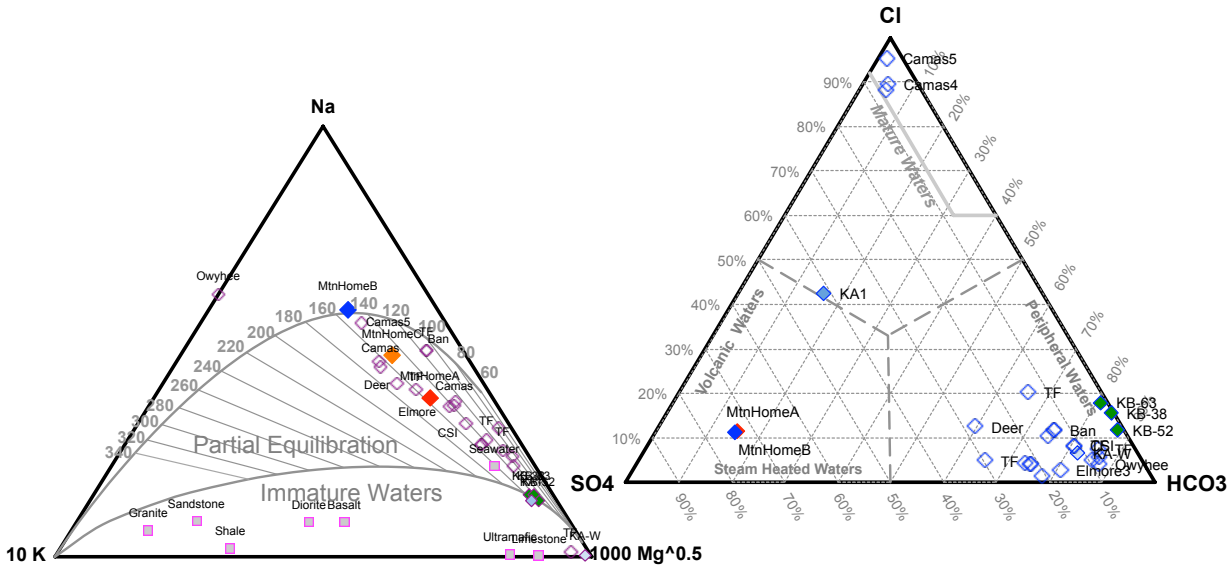

Figure 12-2. (A) Giggenbach (1988) plot of water samples. (B) Water samples plotted on chloride, sulfate and bicarbonate triangular diagram (Giggenbach, 1988). Filled diamonds: This report, pale blue = KA-1, Teal = Kimberly, red, orange and dark blue = Mountain Home. Unfilled diamonds: other thermal water samples from southern Idaho (TF: Twin Falls, Deer: Deer Flat, Ban: Banbury Hot Springs, Camas: Camas Prairie, Elmore: hot spring in Elmore County, Owyhee: hot spring Owyhee Mountains). Plots from Powell and Cummings spreadsheet, 2010.

Isotopic Compositions

The results of the isotopic analyses for deuterium, oxygen-18 and carbon-13 are presented in Table 13-3, and the results for deuterium and oxygen-18 are plotted on Figure 12-4. The Global Meteoric Water Line (GMWL; Craig, 1961) is also plotted on Figure 12-4. The KA-W and KA-1 samples plot very near the GMWL, and thus very likely are meteoric waters.

The Mountain Home samples plot well off the GMWL and appear to lie on a mixing line with volcanic waters. Consequently, the water in the Mountain Home corehole most likely is not meteoric water and probably is significantly older than the water in the Kimama hole.

The KA-1 and KB-52 water samples were analyzed for carbon-13. As is displayed in Table 13-3, the delta C-13 values for these two samples are -10.5 and -10.2, respectively. The result for the KB-52 sample is highly suspect, since the sample was taken only eight days after the total depth of the hole was reached and the sample was obviously contaminated with grease and drilling mud. However, the KA-1 sample was collected more than five months after the total depth of the hole was reached, and the sample appeared to be uncontaminated by drilling mud or grease. This sample displays a moderately heavy delta C-13 value, suggesting that it has been affected by dissolution of carbonate species. This is consistent with observations of secondary carbonate minerals in vesicles, vugs and fractures in the core.

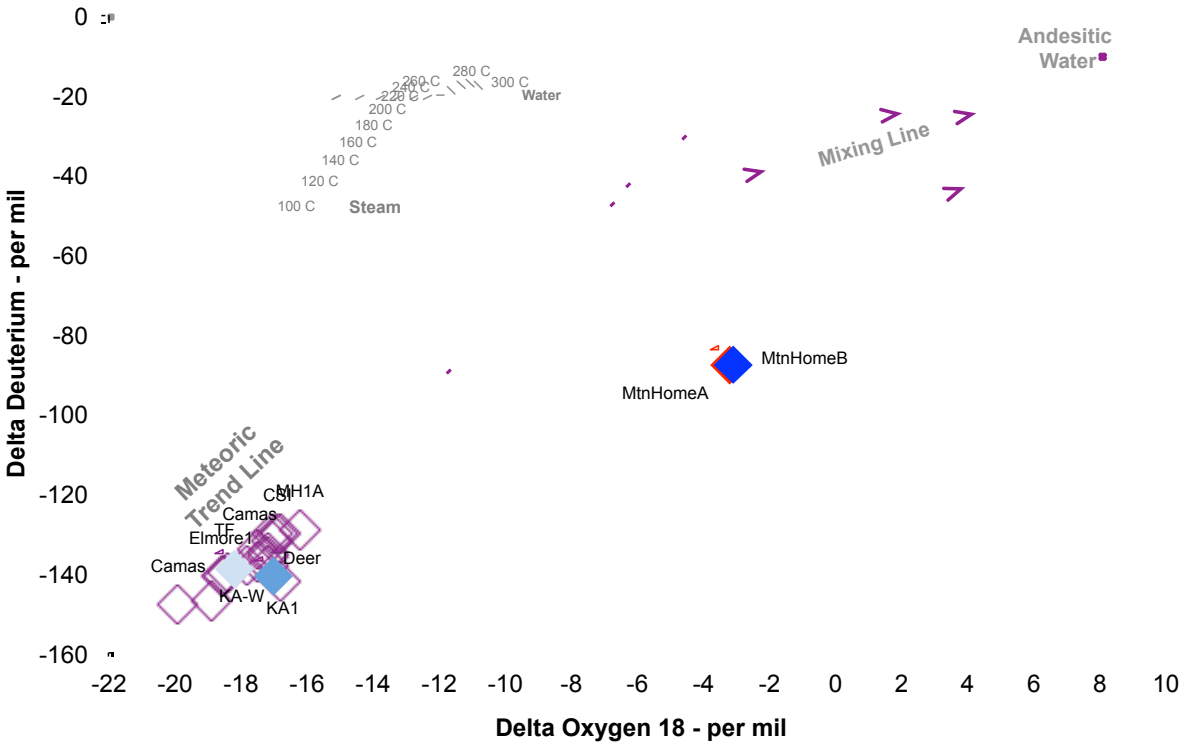

Figure 12-3. Plot of deuterium (^{2}H) and oxygen-18 (^{18}O) relative to the global meteoric water line (GMWL). Symbols as in Figure 12-2; MtnHomeA and MtnHomeB independent analyses of MH-2 water from two separate samples. Note that all thermal waters in southern Idaho, with the exception of Mountain Home MH-2 water, plot on the global meteoric water line. Duplicate samples from Mountain Home fall on a mixing line between meteoric water and juvenile volcanic water. Plot from spreadsheet of Powell and Cummings, 2010.

DISCUSSION

Measured Temperatures

Temperature gradient logs of all three wells are discussed in Chapter 9 of this report, with the results summarized here. The Kimama site exhibits a nearly isothermal gradient from the top of the Snake River Aquifer to about 960 m depth, with an average temperature of about 16^0C. There is a sharp transition at 960 m depth to a conductive gradient with a slope of ~75^0C/ km, and a projected temperature of ~100^0C at 2 km depth (Figures 9-1 and 9-2). The KImberly site cools with depth initially, then gradually warms to about 50ºC at 450 m depth. Incursions of cooler water cause another, small negative trend, followed by an increase to about 50-58ºC below 700 m depth, with a bottom hole temperature of 57.3^0 at 1,953 m. This gradient is nearly isothermal from 700 m to 1953 m depth, a range of over 1200 m with no significant increase in temperature (Figures 9-3 and 9-4). In contrast, the Mountain Home site is characterized by a steep conductive gradient of ~75^0C/km from the surface to total depth, with a projected bottom hole temperature of about 136^0C at 1812 m depth (Figure 9-5). This is less than the observed temperature of 149^0C taken with the DOSECC bottom hole tool in the artesian flow zone.

Geothermometry

Seven geothermometers were used to estimate reservoir temperatures at depth. The seven geothermometers are: (1) chalcedony (Fournier, 1977), (2) quartz (Fournier, 1977), (3) Na/K (Fournier, 1979), (4) Na/K (Giggenbach, 1988), (5) Na-K-Ca (Fournier, 1981), (6) Na-K-Ca-Mg (Fournier and Potter, 1979), and (7) K^2/Mg (Giggenbach, 1988). All were calculated with the Excel spreadsheet of Powell and Cummings (2010), and the results are shown in Table 13-4.

The geothermometry results for the KA-1 sample support the idea that the Kimama area actually has good geothermal potential despite the low bottom-hole temperature, but that the Snake River Plain aquifer suppresses temperatures. Six of the seven geothermometers predict equilibrium temperatures above 125^0C, with quartz and the Giggenbach Na/K geothermometers giving the highest estimates, while the K^2/Mg geothermometer is much lower than all of the others (82^0C). Of the four remaining, the Na-K-Ca geothermometer probably provides the most reliable results, with an estimate of 113^0C. The Mg corrected temperature is much lower (21^0C), and is not consistent with ambient water temperatures at depth; this may result from mixing with higher Mg waters from the overlying aquifer.

All three of the Kimberly samples provide similar geothermometer results. Quartz and Na/K (Fournier 1979) equilibrium temperatures are ~120-135^0C, while Na/K (Giggenbach 1988) and Na-K-Ca (Fournier 1981) equilibrium temperatures are ~130-155^0C (Table 13-4). The high Mg concentrations in these samples results in K^2/Mg temperatures that are low (73-81^0C) but still higher than observed water temperatures, whereas the Mg-corrected Na-K-Ca temperatures

are all negative. Since the water samples are drawn from quartz-saturated rhyolites, we suggest that the quartz thermometer results reflect the most likely reservoir temperatures. The observed lower temperatures in the Kimberly hole (50-58^{0}C) are proposed to result from mixing with lower temperature ground water.

All of the Mountain Home samples (which represent three analyses of the same sample by different laboratories) have similar high equilibration temperatures, mostly in the 132-138^{0}C range (Quartz Fournier, Na/K Fournier, Na-K-Ca Fournier, Na-K-Ca-Mg Fournier-Potter). These temperatures are generally lower than the temperatures measured within the well at the artesian flow zone, and must in this case reflect minimum equilibration temperatures. The Na/K temperatures of Giggenbach (1988) are higher (150-154^{0}C), whereas the K^2/Mg temperatures range from a high of 154^{0}C (MH5726B) to a low of 119^{0}C (MH5726A), in direct response to the measured Mg concentrations. As noted in Powell and Cummings (2010), analytical laboratories that normally work with groundwater samples may not provide reliable Mg analyses at the very low concentrations observed in some geothermal waters. As a result, we propose that the ThermoChem analysis (MH5726B) provides the most robust results for Mg concentration, and thus for any thermometers where highly precise Mg concentrations are critical. Note that all of the analyses for Mg in MH5726 are below 0.2 ppm (0.02 to 0.16 ppm), highlighting the need for extremely precise analyses that are specifically targeted for geothermal fluids.

CONCLUSIONS

Mountain Home has the strongest indicators of future geothermal potential, with the highest measured water temperature, the highest equilibrium temperature estimates, and the highest geothermal gradient for the entire well (75^{0}C/km). As seen in the Giggenbach plots (Figure 12-2), all of the Mountain Home analyses lie along a 150^{0}C isotherm (Figure 12-2A), supporting calculated equilibrium temperature of 150-154^{0}C, and consistent with the projected bottom hole temperature at the flow zone when it was first encountered (Chapter 9: Thermal Logging). Further, the Mountain Home thermal water is a unique sulfate-dominated water (Figure 12-2B), unlike the much more common bicarbonate waters that characterize other thermal systems in Idaho.

The isotopic composition of the Mountain Home thermal water indicates that it is not meteoric water; in fact, it is isotopically distinct from all other hot spring and thermal well waters in southern Idaho. Its composition lies on a tie-line between mid-latitude meteoric water and juvenile or equilibrated volcanic waters (Figure 12-3). *All* other thermal waters in southern Idaho plot on or adjacent to the meteoric fractionation line. *This suggests that the Mountain Home geothermal play may be more comparable to high enthalpy volcanic systems than to fault-controlled low enthalpy systems*.

Kimama – sitting on the axial volcanic high – also appears to have good geothermal potential. Although the maximum recorded temperature was only 59.3^{0}C at 1400 m depth, the equilibrium temperature estimates are only slightly lower than Mountain Home. The observed geothermal gradient below 960 m of 75^{0}C/km is also comparable to the thermal gradient at Mountain Home (Chapter 9). The Snake River Plain aquifer suppresses the gradient in the upper portion (0-960 m) of the Kimama well to only 5.5^{0}C/km, giving a seemingly false impression that the geothermal potential is poor. Further exploration along the volcanic axis in the central SRP must target areas where the SRP aquifer is thin, in order to minimize the depth drilled through isothermal conditions, and maximize the temperature at total depth. This will likely require the use of more detailed resistivity surveys, which give a good estimate of aquifer thickness (Lindholm, 1996). Kimama isotopic properties indicate that it is meteoric water, which is apparently heated from below by conductive heat transfer.

Kimberly has a maximum recorded temperature of only 57.3^{0}C at total depth (1957 m), and the lowest equilibrium temperature estimates. This site is south of the Snake River, and is thus not affected by the Snake River aquifer, as noted by Street and deTar (1987). Nonetheless, the near isothermal gradient in the Kimberly well requires convective heat transfer by flowing water. The enormous thickness of this warm water system (over 1500 meters, from about 450 m depth to total depth) implies an extremely large warm water thermal system that may underlie the entire Twin Falls warm water district (from Kimberly to Banbury Hot Springs). While this system is not hot enough to produce electricity, it had tremendous potential for direct use applications.

Table 12-1. Field measurements for water samples.

Sample	Temperature (^{0}C)	Conductivity (microSiemens)	Salinity (ppt)	pH	Alkalinity (mg/L)
KA-W	15.8	336	0.2	7.71	160
KA-1	28.8	1060	0.5	8.17	120
KB-38	23.3	2970	1.5	7.60	1100
KB-52	15.6	1765	0.9	7.72	950
KB-63	17.7	2568	1.3	7.83	850
MH-5726	31.3	870	0.4	9.59	100

Table 12-2. Results of chemical analyses for water samples (all values in mg/L).

Sample	Ca	Mg	Na	K	Cl	SO_4	SiO_2
KA-W	25.0	12.7	16.5	3.60	13.1	22.1	60.9
KA-1	21.1	3.21	284	10.3	315	306	158
KB-38	24.7	10.1	562	17.9	204	7.29	94.5
KB-52	15.4	5.43	363	9.38	128	14.1	71.6
KB-63	23.8	9.33	541	13.2	189	13.8	76.7
MH-5726A	8.71	0.16	288	9.02	74.8	4778	196
MH-5726B	9.64	0.02	313	9.11	76.7	508	101
MH-5726C	11.15	0.07	314	9.25			100.8

Table 12-3. Results of isotopic analyses of water samples (all values are per mil).

Sample	Delta D	Delta O-18	Delta C-13
KA-W	-149	-18.2	N/A
KA-1	-141	-17.0	-10.5
KB-52	N/A	N/A	-10.2
MH-5726A	-88	-3.2	N/A
MH-5726B	-87.61	-3.086	NA

Table 12-4. Results of geothermometer calculations (all values in ^{0}C). Temperatures from Powell and Cummings (2010) spreadsheet.

Sample Name	Chalcedony Fournier 1977	Quartz Fournier 1977	Na/K Fournier 1979	Na/K Giggenbach 1988	Na-K-Ca Fournier 1981	Na-K-Ca-Mg Fournier-Potter 1979	K^2/Mg Giggenbach 1988
Kimama-1A	141	165	143	163	113	21	82
Kimberly 3800	107	134	135	155	141	-102	81
Kimberly 5200	91	120	123	143	121	-84	73
Kimberly 6300	95	123	120	140	128	-104	75
Mountain Home 5726A USU Analytic	105	132	134	154	132	132	119
Mountain Home 5726B Thermochem	111	138	130	150	136	136	154
Mountain Home 5726C VetLab	111	138	131	151	136	135	133

CHAPTER 13:

FRACTURE ANALYSIS

James A. Kessler
Utah State University, Logan, Utah 84322

Douglas R. Schmitt
University of Alberta, Edmonton, Alberta T6G 2E1

James P. Evans
Utah State University, Logan, Utah 84322

ABSTRACT

Three boreholes were drilled through the Department of Energy (DOE)/International Continental Drilling Program (ICDP) Project Hotspot: The Snake River Geothermal Drilling Project to assess the potential for geothermal energy development in the central and western Snake River Plain, Idaho: Kimama, (1,912 m), Kimberly (1,958 m) and Mountain Home Air Force Base (MHAFB) (1,821 m). A full suite of wireline borehole geophysical logs were run throughout the uncased sections of the boreholes, including acoustic velocity imaging (BHTV) logs for a 281 m interval in Kimama and a 301 m interval at Mountain Home. Thermal gradients in the Kimama and Mountain Home boreholes indicate the most promise for commercial geothermal energy development, so fracture analysis focussed on those two sites. Core and BHTV data were used to measure fracture density, intensity, orientation, aperture, and principal horizontal stress orientations. The fracture data provide information on the potential for flow of geothermal fluids, and these data may be related to surface faulting. Fractures at Kimama generally have small aperatures (~17 mm) which trend NW and dip to the NE. Large aperture fractures are more common at Mountain Home, with an inferred fracture aperture of >48 mm within the artesian geothermal zone. Fractures at Mountain Home form two sets, one of which parallels range front faults (NW). The fracture and stress data will be used to identify mechanical stratigraphy that will be the framework under which stress models and fracture models will be built to predict natural fracture development and fracture propagation during potential reservoir stimulation.

INTRODUCTION

Fluid recovery in both naturally fractured geothermal systems and enhanced geothermal systems (EGS) is often accomplished via fluid flow through connected fracture networks that convectively transports heat to the production well. Successful exploitation of geothermal resources relies upon effective characterization of fracture networks in fractured reservoirs. Fracture density, frequency, aperture, and orientation are measurable characteristics that affect fracture connectivity and permeability of a fracture network. Those characteristics are measured in both core samples and with wireline borehole geophysical instruments. Coring work for Project Hotspot recovered >99% of whole rock core from Kimama (1912 m) and Kimberly (1957 m), and >90% of whole rock core from the Mountain Home-2 borehole (MH2) to a total depth (TD) of 1,821 m. A full suite of borehole geophysical data was also collected from the boreholes.

The objective of the fracture analysis was to assess the potential for geothermal energy development through analysis of fracture permeability. Controls on fracture permeability include fracture density, cumulative fracture frequency, fracture orientation (azimuth/strike and dip), and fracture aperture. These data constitute the fracture stratigraphy and will be correlated to lithology and mechanical stratigraphy to determine if fracture development is dependent upon any aspect of lithological and/or mechanical properties.

METHODS

We measured fracture characteristics from core samples, and mapped fractures in acoustic televiewer logs collected in the Kimama and Mountain Home boreholes over the *zone of interest* (ZOI). Each fracture measured from core was identified as naturally occurring or drilling-induced. Naturally occurring fractures are identified by recognizing indicators that the fracture is open or was open at some time in the past. Typical indicators are oxidation on or around the fracture plane, presence of secondary mineralization that has sealed or partially sealed an open fracture, alteration of host rock, and/or slip indicators on the face of a fault. The presence of any one or more of these characteristics requires that the fracture was open at some time before the borehole was drilled. Data were analyzed with the program *FracMan®*.

In the Kimama borehole KMA-1B the ZOI includes the interval of the televiewer log from 281m (923 ft) to 735 m (2,412 ft). In the Mountain Home borehole MH-2B the ZOI includes the interval of the televiewer log from 1,287 m (4,223 ft) to 1,597 m (5,238 ft). Televiewer logs of the artesian fracture system at Mountain Home were not obtained because temperatures below 1600 m depth substantially exceeded that thermal limits of the televiewer tool. Fracture analysis was not carried out at Kimberly because the low thermal gradient made it unlikely to be a viable prospect. Since resources were limited, it was decided to focus on the two holes with high thermal gradients.

Particular morphologies can be identified that are indicative of drilling-induced fractures. Centerline fractures, petal fractures, petal-centerline fractures, core edge fractures, saddle fractures, and disking are indicative of fractures formed post-drilling as a result of the release of stress on the core or the redistribution of stresses around the borehole wall (see Figure 13-1; Schmitt *et al.*, 2012). Drilling-induced fractures occur in slightly different places in the core compared to the borehole wall due to the differences between the release of stress on the core sample and the redistribution of stresses around the borehole wall that concentrates compressive stresses in relation to the minimum and maximum principal stress directions.

Other induced fractures are identified separately from drilling induced and include those that are a result of the act of the drill bit on the core or handling after that the core is removed from the core barrel. These are identified through a lack of planar fracture or induced morphologies, beveled edges on subhorizontal fractures indicates the two pieces of core spun against each other while in the core barrel. All induced fractures have clean, fresh faces that lack any indication of exposure before drilling and handling.

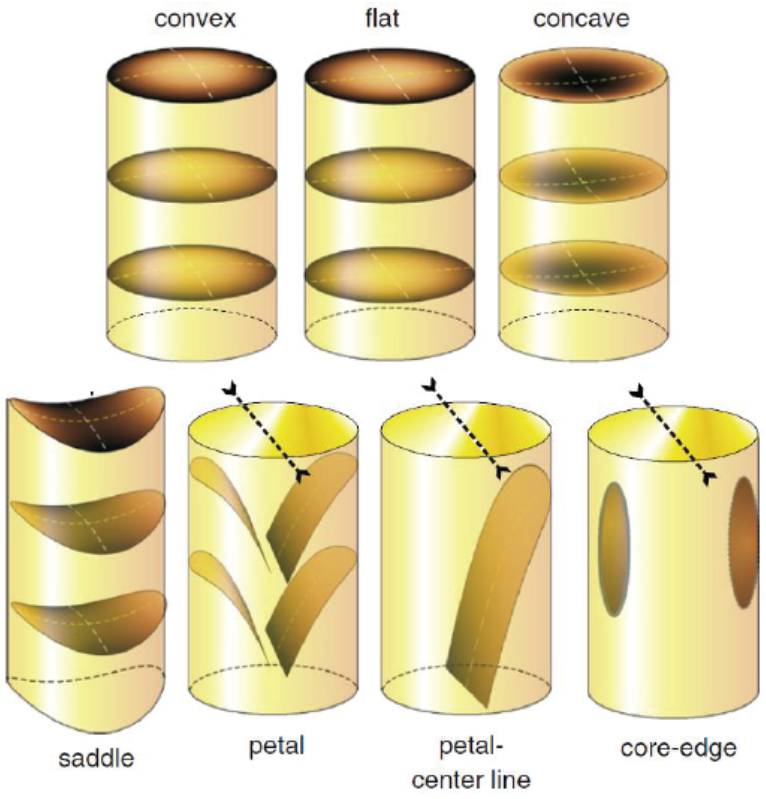

Figure 13-1. Drilling-induced fracture classifications as a result of tensile fractures in core (modified from Schmitt *et al.*, 2012).

Dip and aperture are measured in reference to the strike line of a fracture plane. The core is oriented so that the strike line is pointed vertically and the dip is measured with a digital protractor relative to horizontal. The borehole deviates little from vertical so is assumed to be vertical and the long edge of the core can be used as a reference to vertical. Aperture is measured with the core oriented the same way so that aperture could be measured perpendicular to the fracture faces and not at some apparent thickness at another location on the outside of the core. Aperture can only be measured in fractures that are closed or sealed. Some broken fractures can be fit together and the mineral fill is preserved enough to confidently measure aperture. Minerals observed to fill fractures include quartz, calcite, clays (chlorite and smectite), zeolite (laumontite), pyrite, and chalcopyrite.

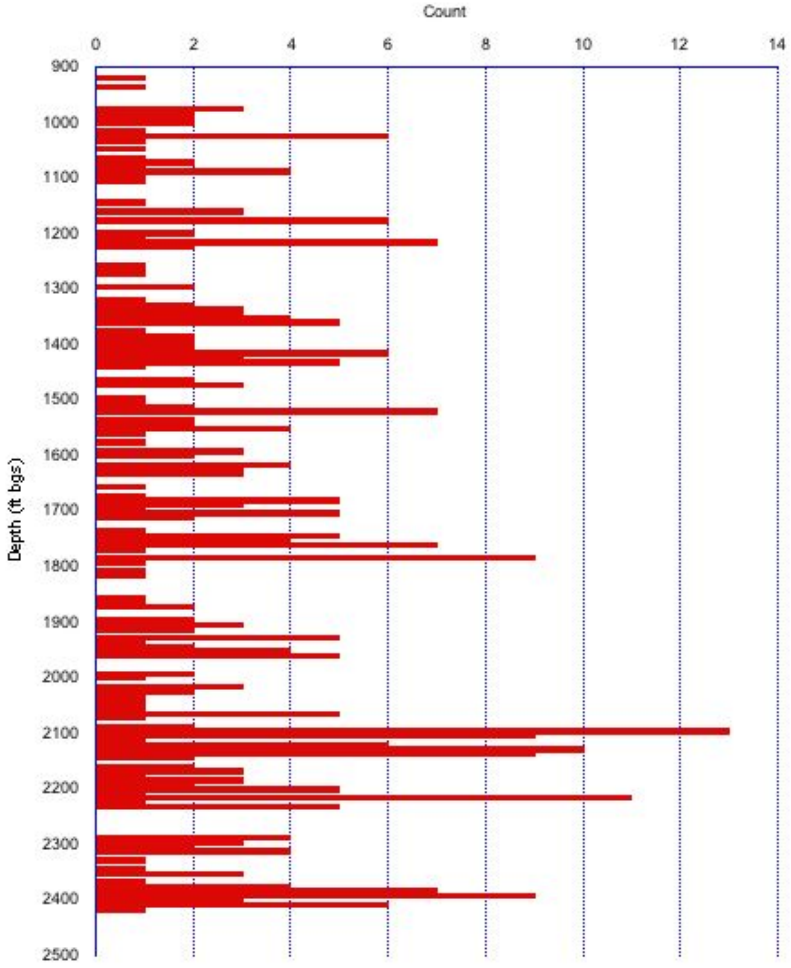

Figure 13-2. Fracture frequency distribution plotted as fracture density (# fractures/5 ft of borehole depth).

RESULTS

The spatial distribution of fracture density, cumulative fracture frequency, dip direction or strike, and dip angle will be used to define fracture stratigraphy and discrete fracture populations that can be correlated to lithology and mechanical stratigraphy. Fracture density distribution shows that fractures cluster with respect to depth in definable ways. We will use the distribution of the fracture population to define discrete zones along the depth profile of fracture densities. Those zones constitute fracture stratigraphy and are the framework under which we consider the distribution of other fracture characteristics and rock properties.

Kimama

The fracture density histogram (Figure 13-2) and cumulative fracture frequency curve (Figure 13-3) show us the pattern of fracture distribution with depth in KMA-1B. Most notable is a significant section of the borehole that lack fractures from ~686 m (2,250 ft) to ~701 m (2,300 ft). Thinner sections can be defined based on the presence of intense fracture populations or a lack of fractures. The data can be subdivided into as few as 4 fracture units or as many 20 or more, depending on what is most appropriate for the study. In this case, we will define the appropriate number to statistically correlate fracture stratigraphy with lithological units and mechanical stratigraphic units that are defined by the distribution of rock properties in the borehole.

Fracture aperture and orientation are intrinsically linked to fracture permeability. The distribution of apertures (Figure 13-4) shows that the majority of the fractures have small apertures that are ~17 mm. Large (> 20 mm) fractures and/or voids are present in the population of fractures. The large, standout voids are identified by visible gaps in televiewer data and by lack of core recovery in the drilling record. Core samples from large-aperture zones show significant high-temperature secondary mineralization. Large voids could be potential conduits for significant flux of hydrothermal fluid based on potential volume, if the voids are extensive enough. The presence of secondary mineralization is an indicator of previous hydrothermal fluid flow.

Fracture orientation is defined by strike and dip (Figure 13-5) and by the azimuth and dip angle of each fracture. The population of fracture data cluster in primary, secondary, and tertiary azimuth directions (Figure 13-6). The primary cluster dips generally in the NNE direction while the secondary cluster dips to the NW, and the tertiary cluster dips to the ESE direction. Dip angles are very consistent (Figure 13-7) and show that the majority of the fracture population over the ZOI dips between 40 and 80 degrees.

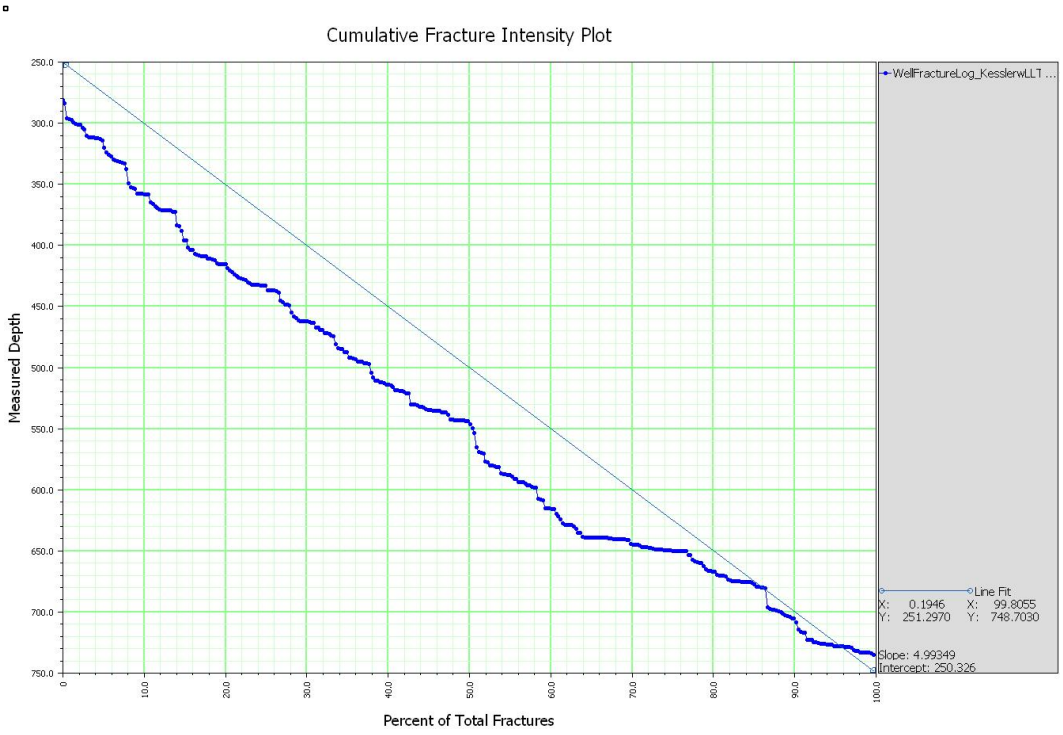

Figure 13-3. Fracture frequency distribution plotted as cumulative fracture frequency.

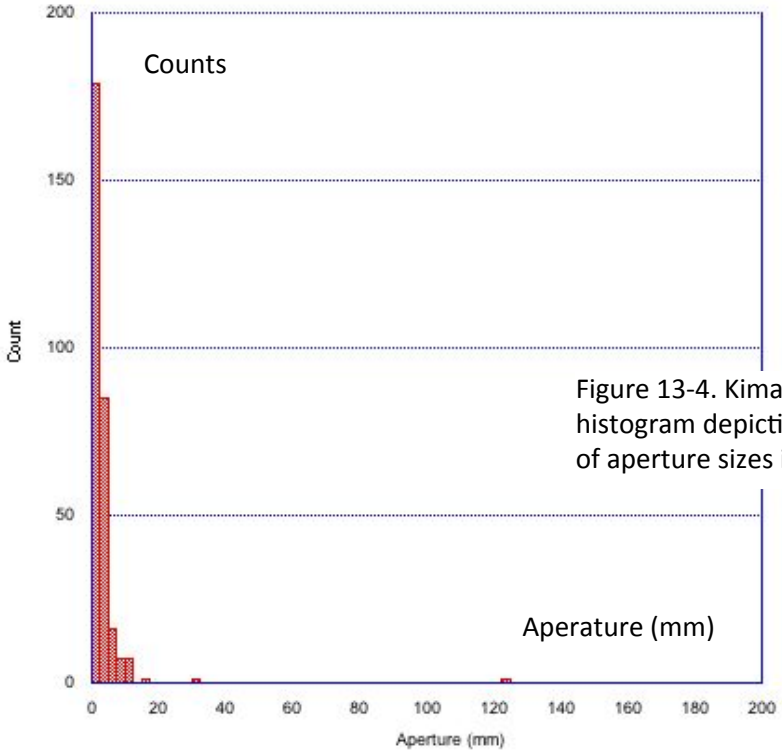

Figure 13-4. Kimama. Aperture histogram depicting the distribution of aperture sizes in the ZOI.

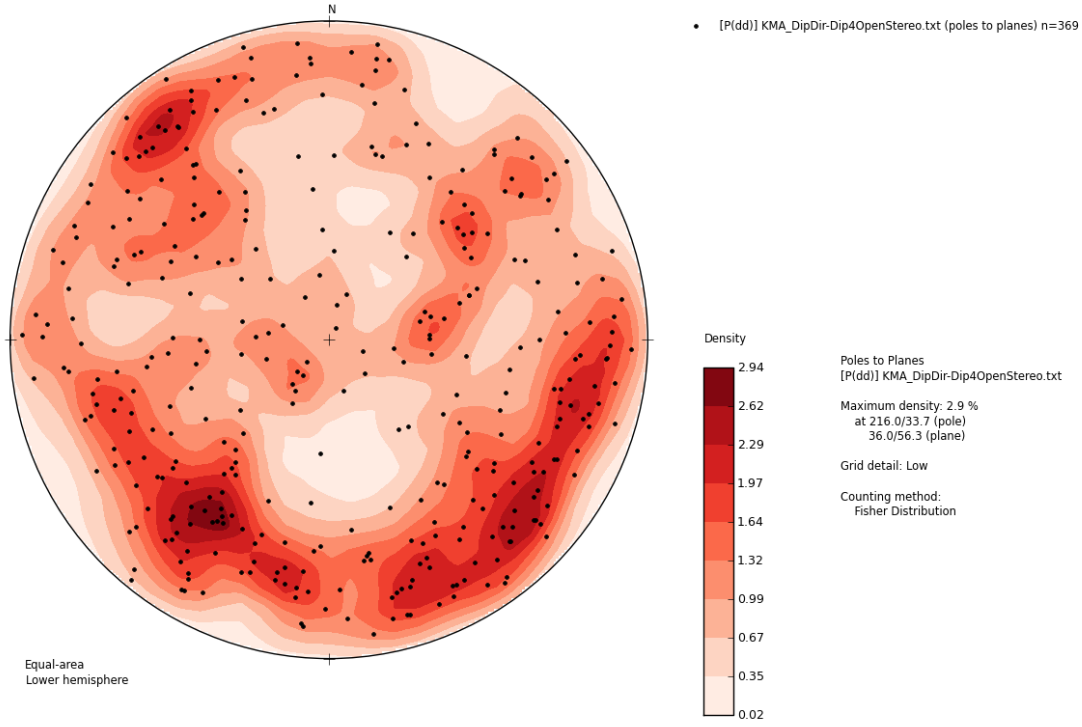

Figure 13-5. Kimama. Equal-area, lower-hemisphere stereonet plot of the poles-to-plane for fractures over the ZOI.

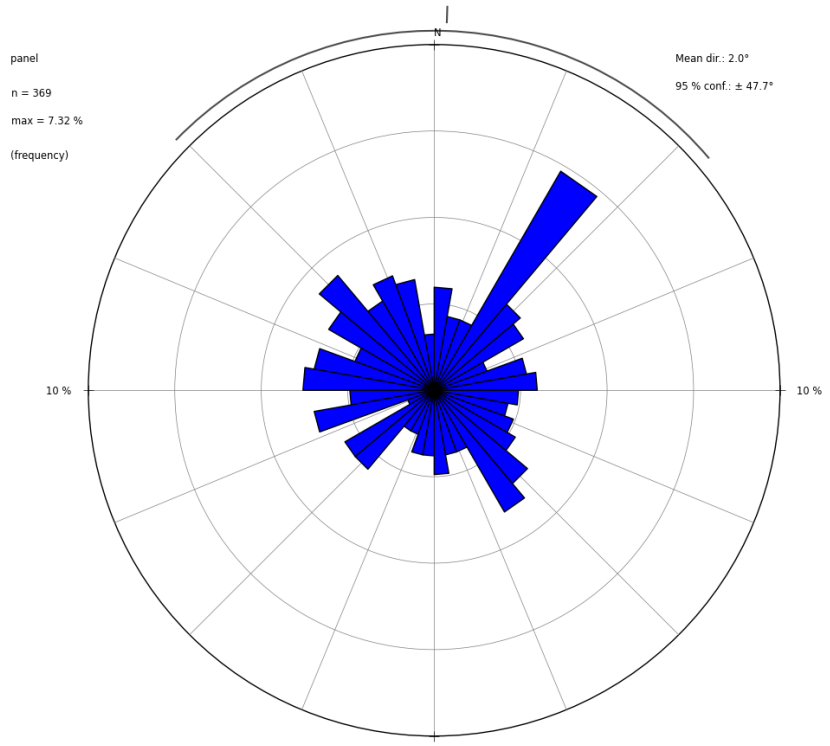

Figure 13-6. Kimama. Rose diagram depicting the distribution of fracture dip azimuths.

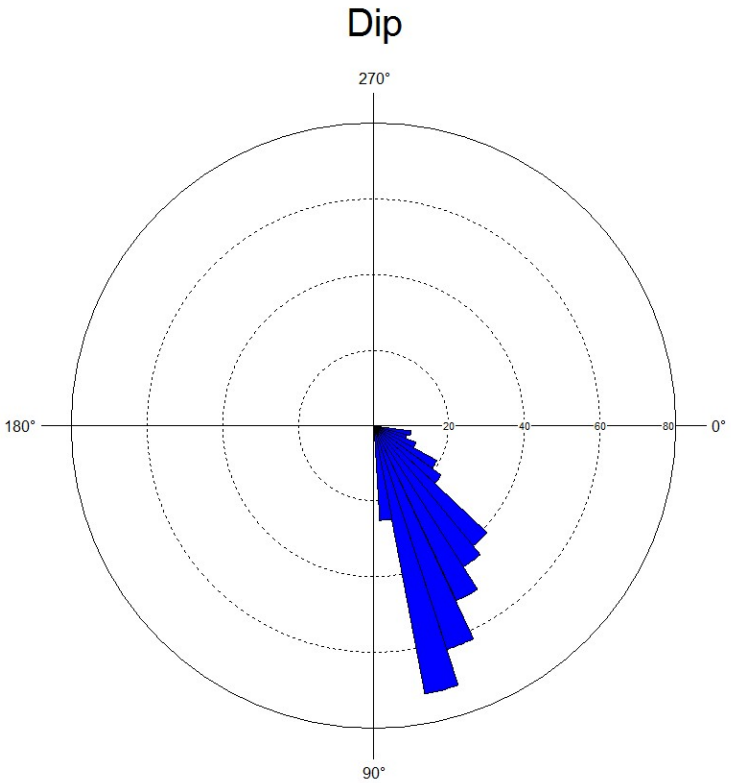

Figure 13-7. Kimama. Rose diagram depicting the distribution of dip angles from all fractures in the ZOI.Mountain Home.

Mountain Home

The fracture density histogram (Figure 13-8) and cumulative fracture frequency curve (Figure 13-9) show us the pattern of fracture distribution with depth in MH-2. Most notable are two significant sections of the borehole that lack fractures from ~1,349 m (4,425 ft) to ~1,384 m (4,540 ft) and ~1,481 m (4,860 ft) to ~1,532 m (5,025 ft). Thinner sections can be defined based on the presence of intense fracture populations or a lack of fractures in Figure 13-8. The data can be subdivided into as few as 5 fracture units or as many as 20 or more, depending on what is most appropriate for the study. In this case, we will define the appropriate number to statistically correlate fracture stratigraphy with lithological units and mechanical stratigraphic units that are defined by the distribution of rock properties in the borehole.

Fracture aperture and orientation are intrinsically linked to fracture permeability. The distribution of apertures (see Figure 13-10) shows that the majority of the fractures have small apertures that are <10 – 15 mm. Large (> 20 mm) fractures and/or voids are present in the population of fractures. The large, standout voids are identified by visible gaps in televiewer data and by a considerable lack of core recovery in the drilling record. Core samples from large-aperture zones show significant high-temperature secondary mineralization. Large voids could be potential conduits for significant flux of hydrothermal fluid based on potential volume, if the voids are extensive enough. The presence of secondary mineralization is an indicator of previous hydrothermal fluid flow. The largest of voids, those >40mm, are listed in Table 13-1. The large aperture fracture zone inferred at 1,745 m (5,725 ft) depth is inferred from the poor core recovery (<50%) and the occurrence of voluminous artesian flow from this zone. The aperture of >48 mm is inferred from the NQ core diameter (48 mm), assuming that aperture size exceeds core diameter in zones with <50% recovery.

Table 13-1. Depths and apertures of large voids in the ZOI, Mountain Home well MH-2.

Depth (m)	Depth (ft)	Aperture (mm)
1,328	4,356	47.6
1,347	4,418	113.0
1,396	4,581	95.4
1,407	4,618	88.7
1,534	5,032	43.4
1,745	5,726	> 48

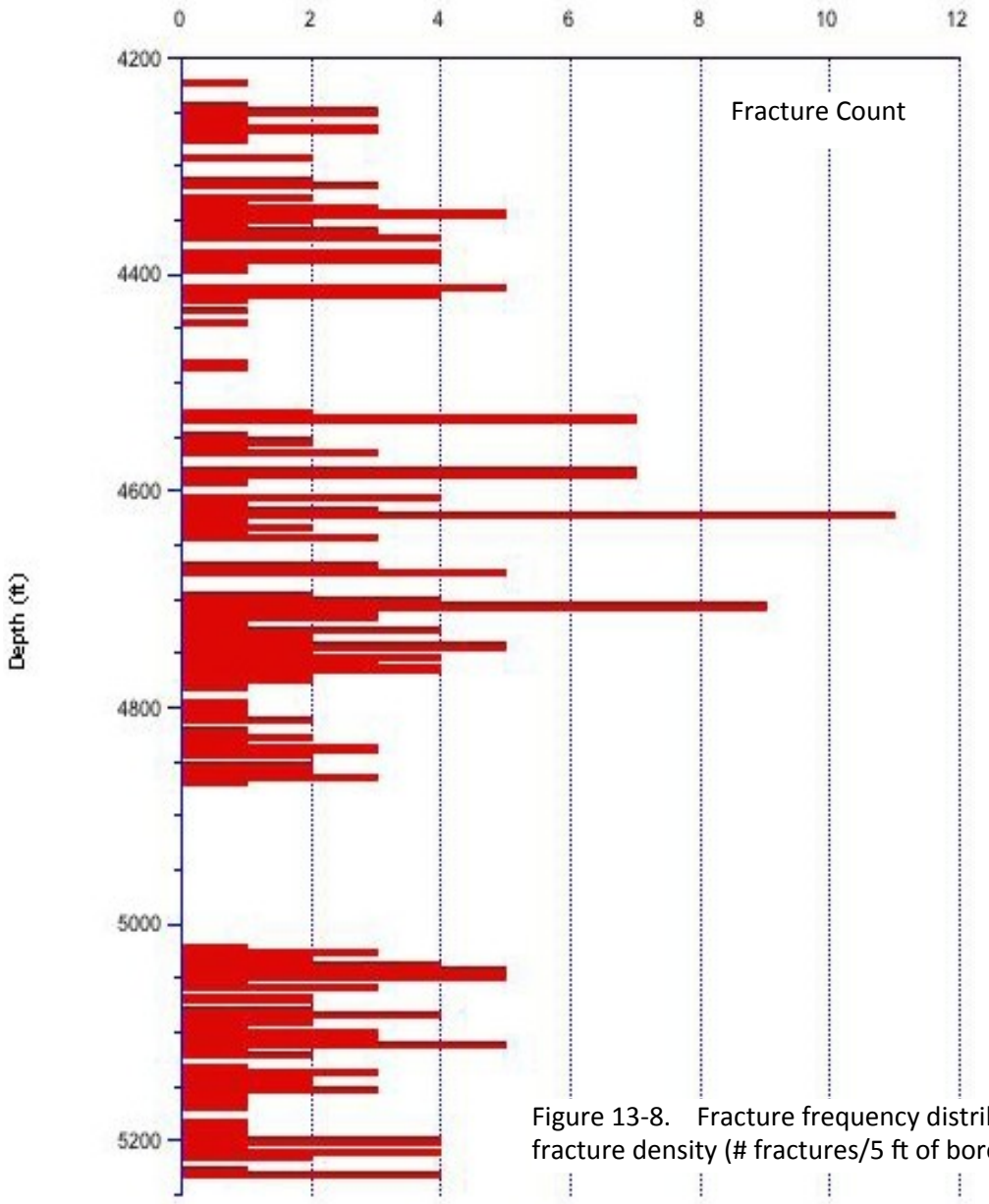

Figure 13-8. Fracture frequency distribution plotted as fracture density (# fractures/5 ft of borehole depth).

Fracture orientation is defined by strike and dip and plotted as a pole normal to the plane of the fracture (see Figure 13-11) and by the azimuth of dip direction and dip angle of each fracture. The population of fracture data cluster in primary, secondary, and tertiary azimuth directions (see Figure 13-12). The primary cluster dips generally in the NNW direction while the secondary cluster dips to the SSE, and the tertiary cluster dips to the WSW direction. Dip angles are very consistent (see Figure 13-13) and show that the majority of the fracture population over the ZOI dips between 40 and 80 degrees. Dip angles are consistent with the high normal range-front faults that bound the graben. However, while the dip angles are consistent, the orientations of the fractures vary from the regional geological structure.

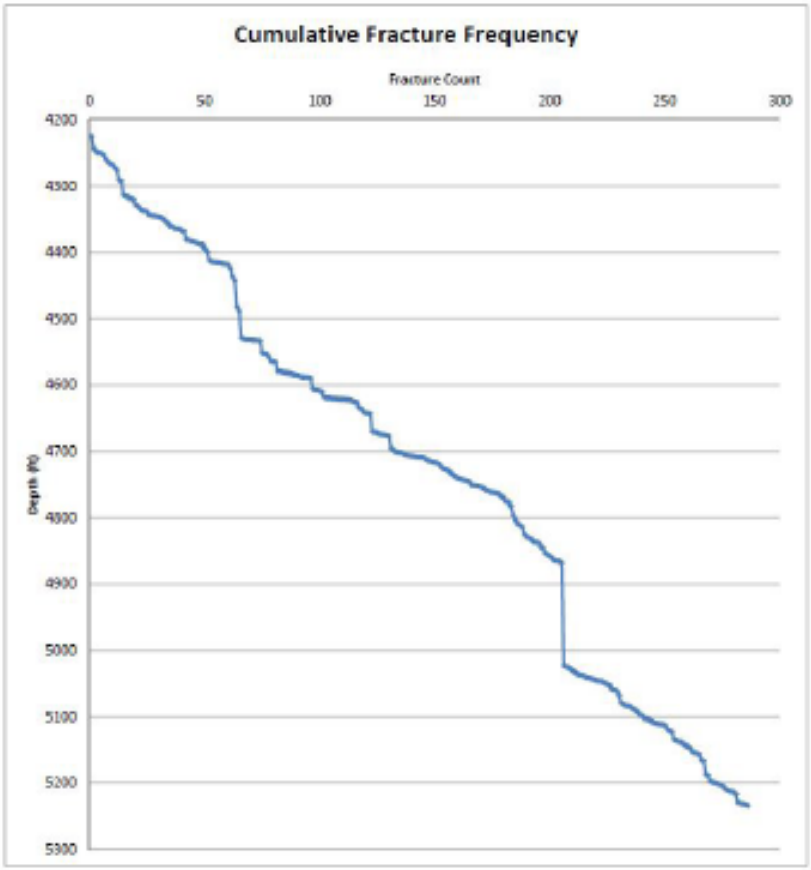

Figure 13-9. Fracture frequency distribution plotted as cumulative fracture frequency.

The range-front faults offset Miocene volcanic rocks and dip at high angles to the southwest and strike N55-60W. Quaternary faults are clustered in two sets oriented N85W and N60W (Shervais *et al.*, 2002). The primary cluster of fractures in the ZOI is oriented roughly N80W and dips at high angles to the NE. The secondary cluster of fractures strikes N45E and dips to the SE while the tertiary cluster strikes N30W and dips to the SW. The orientation of the primary cluster of fractures is oriented consistently with one set of Quaternary faults (N8085W), but dips in an antithetical direction. Slip indicators on many of the fracture surfaces may be oriented using televiewer data and might give insight into the reason for the inconsistency between the fracture population in the MH-2 borehole and the regional geological structures.

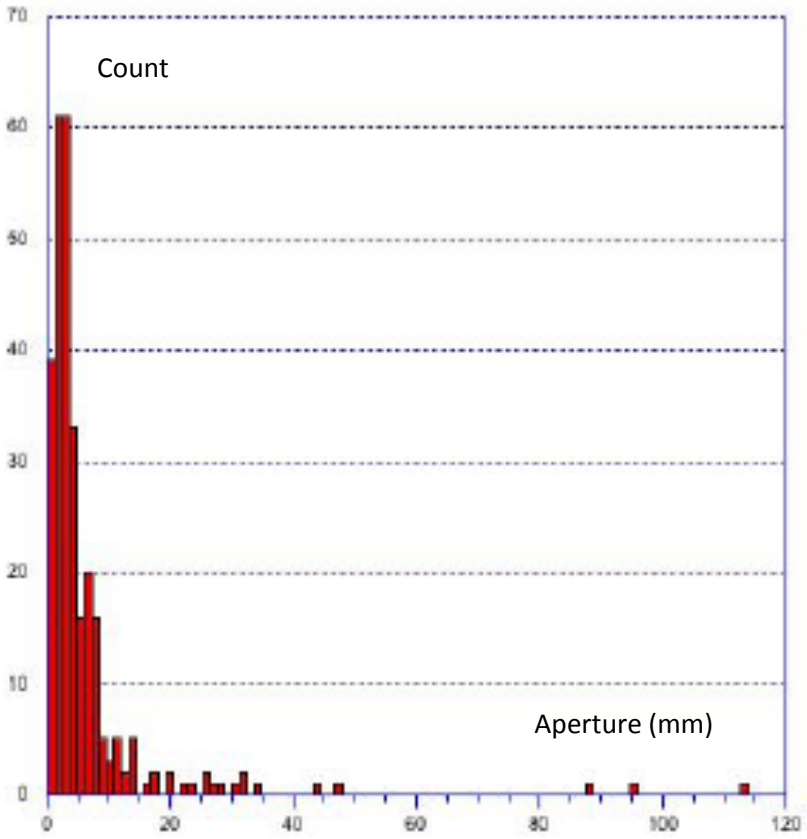

Figure 13-10. Mountain Home. Aperture histogram depicting the distribution of aperture sizes in the ZOI.

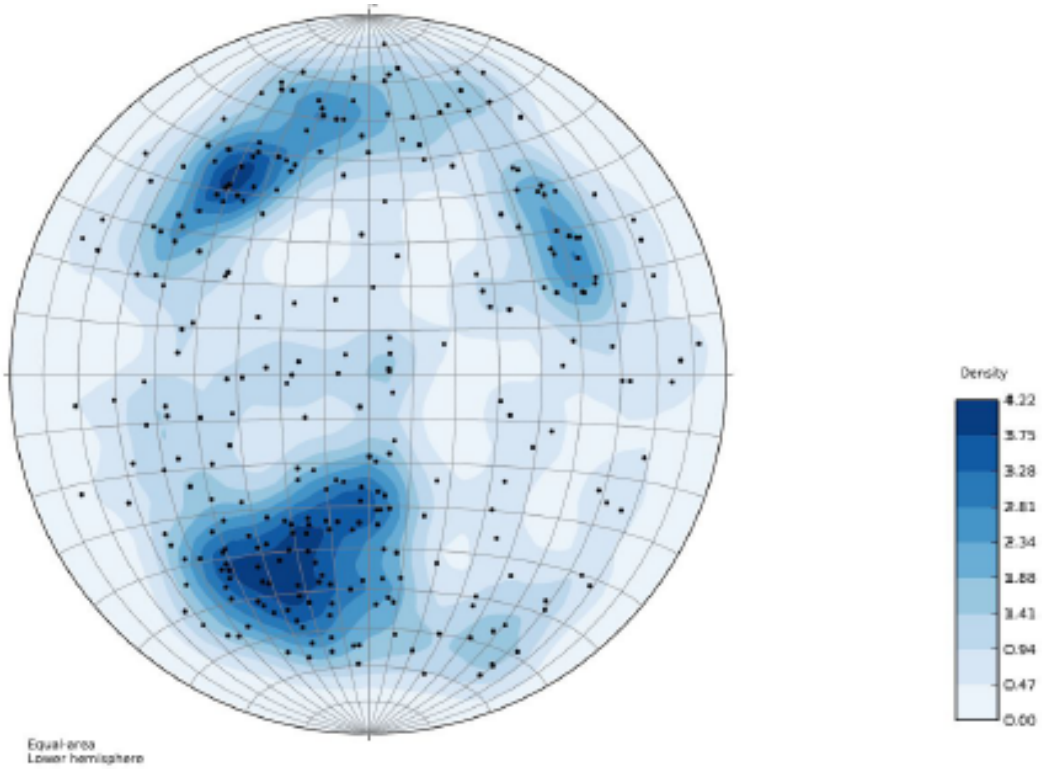

Figure 13-11. Mountain Home. Equal-area, lower-hemisphere stereonet plot of the poles-to-plane for fractures over the ZOI.

FUTURE WORK

The next phase of this project will be to conduct a stress analysis to determine the orientation and magnitudes of the three principal stresses (S_v, S_h, S_H). Principal stress orientations are identified from borehole breakouts and induced tensile fractures on the televiewer log. Dipole sonic data (V_s and V_p) and bulk density data, measured from core samples, are used to calculated Young's modulus (E) and Poisson's ratio (ν). Rock strength will be calculated from uniaxial compression strength (UCS) experimental data. Those data will be used to calculate the magnitudes of the principal horizontal stresses using the method from Zoback (2003). Vertical principal stress will be calculated using the relationship $S_v = \rho gh$. Where ρ is average density of the overburden, g is acceleration due to gravity, and h is depth of the ZOI. Mercury-injection porosimetry tests will yield porosity, permeability, and bulk density data. Those data along with the fracture data and results of the stress analysis will be used as spatial parameters and boundary conditions in a discrete fracture network (DFN) model using the industry-standard code *FracMan™*. The ultimate outcome of these analyses will be a quantitative assessment of fracture porosity in the rocks above the geothermal system, which will be important for the evaluation of the geothermal resource and its potential for energy generation.

Note: this research is the subject of a PhD dissertation by Kessler, which is in progress at the time of this writing. Further results will be published once this research is complete.

CHAPTER 14:

PROJECT MANAGEMENT AND REPORTING

John W. Shervais
Utah State University, Logan, Utah

ABSTRACT

Project management and reporting tasks were carried out by the Principal Investigator with the assistance of the Science Team (co-investigators), site Chief Scientists, the DOE Technical Review Team, Utah State University accounting staff, and a project manager hired specifically to for this project. Quarterly progress reports were prepared by the PI, and financial reports by USU accounting staff. Science and technical decisions were made by the PI in consultation with the Chief Scientist at each site, the Project Science Team, and the DOE Technical Review Team. DOE management was consulted on all decisions involving change of scope or revised drilling plans. Expenses were tracked on a bi-weekly basis except for drilling expenses when nearly hole completion, when expenses were estimated daily.

A Risk Management Plan was prepared as part of our Phase 1 report. This plan assessed potential risks involved in drilling and logging, their probability, and mitigations. This plan proved its value in several situations that arose, in particular the decision to abandon stuck rods in hole MH-2A and drill a new hole hole adjacent to it (MH-2B).

A project science meeting was held in April 2012 at Utah State University attended by the Science Team, Chief Scientists, project science staff, and range of participating scientists. This meeting included presentations on progress to date and plans for further study, as well as visits to the core processing and storage facilities to view the core and discuss future work and sample requests.

Reporting functions included Quarterly and Annual progress reports to DOE, presentations at DOE Peer Review events, presentations at scientific and professional meetings, and publications. Formal presentations were made at two Peer Review events, three annual meetings of the Geothermal Resource Council, and several meetings of the American Geophysical Union and Geologic Society of America. The PI Science Team also organized special sessions at several of these meetings.

INTRODUCTION

This work was organized by the Project Director/Principal Investigator (Shervais) and carried out by a consortium of universities, non-profits, and government agencies. Our organizational structure relied on a central core of co-investigators who managed studies and sampling within their area. All of the PI's and co-investigators had prior experience working with drill core and/or drilling projects, from the Snake River Plain, the Savannah River National Laboratory, ODP-IODP, Safod, Andrill, Finland, or lake drilling projects (Baikal-Qinghai-Great Salt Lake). As a result, the science team was well equipped for the challenge of this project. In particular, Shervais was PI on a multiyear DOE-funded study of legacy core from the Savannah River National Laboratory (Dennis et al 2004, 2003) and has carried out studies of existing core from the Snake River Plain (Shervais et al 2002, 2006; Hanan et al, 2008). All of the co-investigators have extensive research experience and publication records in their areas of expertise, and many have worked previously on international drilling projects.

MANAGEMENT STRUCTURE

The overall management structure is laid out in our organizational chart (Figure 14-1). *Shervais* was lead PI and Project Director, working in conjunction with a Science PI Group. The Chief Scientist at each drill hole represented the Site Science Crews for each location, and worked directly with DOSECC operations personnel to monitor drilling progress and made on-site decisions as needed. The Chief Scientists also interfaced with the Project Director and the Science PI Group when consultation was required for major decisions.

Quarterly progress reports were prepared by the PI, and financial reports by USU accounting staff. Science and technical decisions were made by the PI in consultation with the Chief Scientist at each site, the Project Science Team, and the DOE Technical Review Team. DOE management was consulted on all decisions involving change of scope or revised drilling plans. Expenses were tracked on a bi-weekly basis except for drilling expenses when nearly hole completion, when expenses were estimated daily. Financial tracking was especially important for cost share, in order to document that our project met its cost share requirements. Most of the cost share was contributed by the International Continental Drilling Program (ICDP), including support provided by their Operational Support Group (OSG) for geophysical logging and data base support. Additional cost share was provided by the participating universities.

It was also necessary to assure that USAF funds for additional drilling at Mountain Home were accounted separately from the DOE-funded project, and that there was not mixing of expenditures or effort at the drill site. This was handled largely by our USU Project Manager, who also handled purchasing, staff scientist schedules, and shipping (including international shipments to/from ICDP).

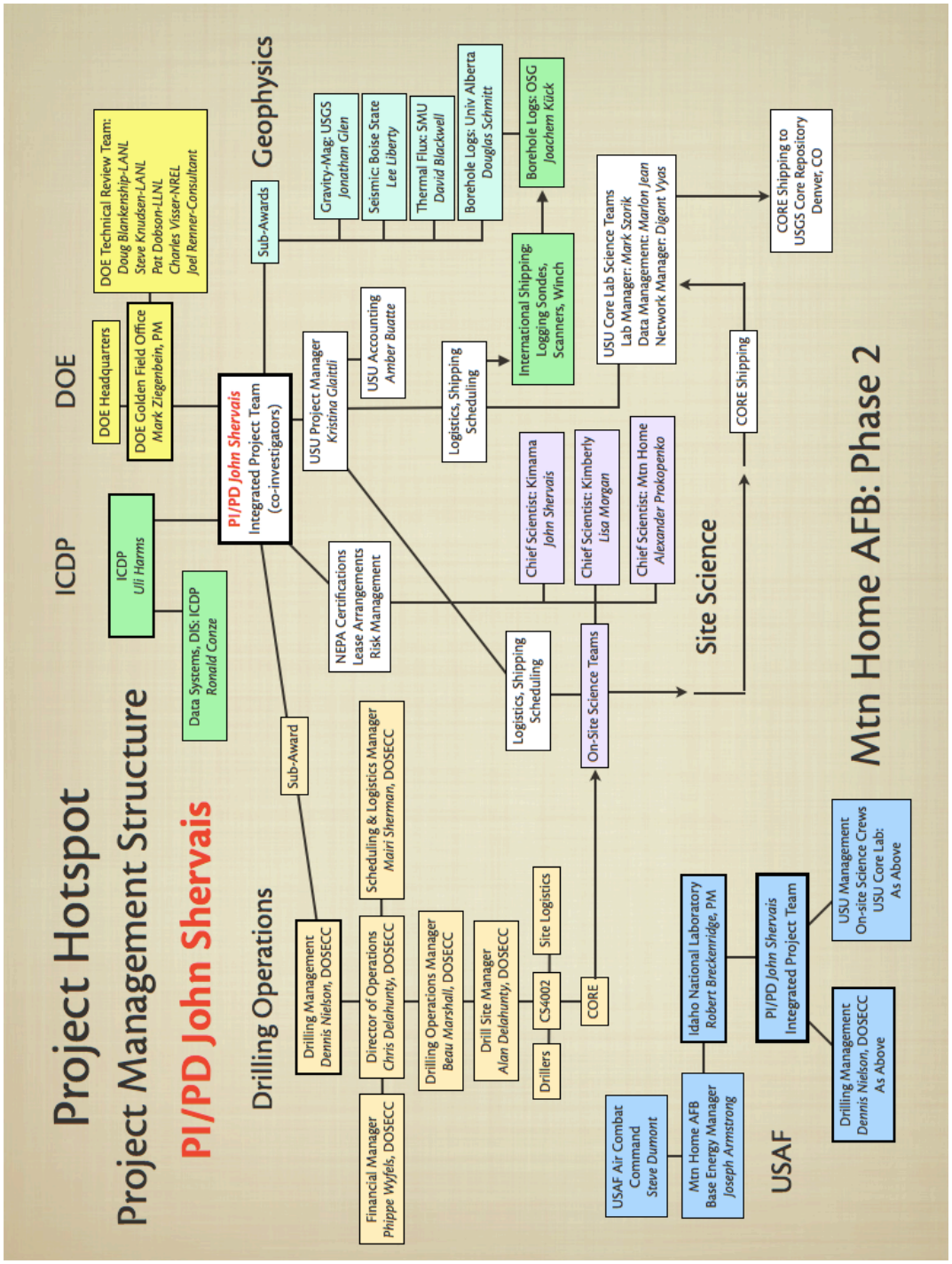

Figure 14-1. Organizational Chart for Project Hotspot. Boxes are colored coded by groups as follow: Yellow:DOE, Dark Green:ICDP, White:USU, Light Green:Geophysics subawards, Brown:Drilling subaward, Lavender:Onsite Science Teams, Blue:USAF "Phase 2 Mtn Home". Arrows show report lines and dependencies.

A Chief Scientist was designated for each hole, responsible for the on-site management of the drilling and making daily decisions. The Chief Scientist acted as the interface between the science team and the drill team, make daily decisions about the conduct of drilling activities, and manage activities of the on-site science team. The Chief Scientist varied on each hole: Kimama (Shervais, USU), Kimberly (Morgan, USGS), and Mountain Home (Prokopenko, USC). Shervais also oversaw the Core Logging Facility at USU, and was responsible for the distribution of samples to the participating scientists, following protocols established by the science team. This ensured that the initial core characterization was carried out thoroughly, and was coordinated among the different discipline-based projects. As the paleomagnetic and geochemical stratigraphy emerged, he coordinated the selection of samples for radiometric dating (Ar-Ar). Core and drilling related data were uploaded into the ICDP Drilling Information System database, so that all data produced from the project, including core logs, chemical and isotopic analyses, magnetic polarity data, and age data, are fully archived. Transfer of data into the National Geothermal Database system is in progress.

The Organizational Chart presented in Figure 14-1 is color-coded to distinguish different groups and organizations. Dependencies and hierarchies are shown by black lines and arrows. Boxes are colored coded by groups as follow:

1. Yellow: Department of Energy, including Headquarters, Golden, CO, Field Office, and the Technical Review Team. Our direct report was to Golden Field Office for general management issues and finances, but all three groups participated in conference calls during active drilling operations. The Technical Review Team were consulted on all important drilling-related decisions and provided valuable insights into risks involved.

2. Dark Green: International Continental Drilling Program (ICDP) provided a large fraction of the cost share ($1.1M), as well as technical support in the form the Drilling Information System (a database for managing all drilling and core related data) and the Operational Support Group, which provided a wide array of geophysical slim-hole logging tools and the personnel and wireline-winch to acquire the logs.

3. White: Utah State University (USU) was the prime awardee and responsible for overall project management and finances. In addition to PI Shervais as Project Director, Kristina Glaittli acted as Project Manager, responsible for coordinating staff, purchasing, travel, and logistics for movement of core and equipment (including shipment of geophysical logging tools from Germany to the U.S.). The Project Manager also interfaced with the USU Accounting Office and with subawardee business offices, and tracked billing to the appropriate accounts within the project. Also shown in white is the USU Core Lab and its

staff, who processed core after it was shipped to USU, and entered lithologic logs, scans, and high-resolution photographs into the Drilling Information System database.

4. Lavender: The Onsite Science Teams were all USU employees (except for two of the Chief Geologists) who accepted core from the drillers on site and processed it it prior to shipment to USU. The onsite crews logged each core run, boxed and photographed core, and prepared the core boxes for shipment to the USU Core Lab. They also reported to the PI on daily progress, issues during drilling, and on any interesting or unusual aspects of the core.

5. Light Green: Geophysics subawards, which included high-resolution gravity and magnetics (USGS, Glen), borehole geophysical logging (University of Alberta, Schmitt), surface seismic surveys (Boise State University, Liberty), and thermal logging (Southern Methodist University, Blackwell). Schmitt coordinated and supervised borehole logging by the ICDP Operational Support Group (OSG) and by commercial logging companies (primarily for neutron logging, as radioactive source tools are impossible to transport internationally). Additional borehole logging at Kimama was provided by the USGS from the Idaho National Laboratory, at no cost, because this site lies within their area of interest (Twining and Bartholomew, 2011).

6. Brown: Drilling subaward to the U.S. Continental Drilling Consortium "DOSECC" (Drilling, Observation, and Sampling of Earth's Continental Crust). DOSECC maintains a continental scientific drilling facility which includes a range of drill rigs and tools. They also maintain a complete project management system that tracks and allocates their resources, and provides detailed billing information, a Drilling Operations Director (frequently onsite), a Drilling Operations Manager (onsite), a Site Manager (on site), and a highly trained staff of drillers who specialize in collecting core. The DOSECC President (Nielson) has over 20 years experience in geothermal research and was a key partner in the project.

7. Blue: USAF funding for "Phase 2 Mountain Home" drilling. This project was distinct from the DOE-funded project, and commenced after termination of DOE-funded operations at the Mountain Home AFB site. This project, in collaboration with the Idaho National Laboratory, assumed ownership of the Mountain Home site and deepened the DOE-funded test well to assess geothermal potential on the base. As required by DOE, these projects were separated by a "bright line" financially, such that funding for all onsite operations were transferred to the USAF account upon termination of DOE-funded drilling (note that there are no linkages between these two projects shown in the organizational chart).

RISK ANALYSIS

As part of our Phase 1 Report to DOE we performed a risk analysis for Phase 2 drilling operations. The results of the that analysis are summarized in Table 14-1. Fourteen areas of potential risk were identified and ranked as having a Low, Moderate, or High probability, along with potential mitigations or corrective actions. Eight of the 14 areas of potential risk were actually encountered on at least one of the three holes drilled; these eight areas are highlighted by italic in the table. The Kimama site encountered severe *lost circulation* issues that could not be cured using LCM, and resulted in *excessive mud utilization*. We were able to drill ahead, but considerable resources were expended on the excessive mud use. The Kimama hole also had stability issues in a thick loess layer at ~150 m depth, which caused us to recenter the drill string in the washed-out sediment layer and re-core a section about 120 m long. The new hole (Kimama 1B) was straighter (less horizontal wander) than the initial hole (1A) and resulted in better long term core results. Inclement weather was also an issue but failed to halt drilling more than briefly.

The Kimberly hole encountered similar issues with *lost circulation, excessive mud use*, and *hole stability* in a sedimentary interbed, but these issues were less of problem than at Kimama. A *stuck rod* required hiring a contract chemical rod cutter. We did encounter a *major equipment failure* at Kimberly, however, with a cracked seal in the hydraulic system of the CS-4002 that required us to shut down drilling operations for over 4 weeks so the rig could be returned to Salt Lake City for repairs. The probability for such a failure was considered to be low, but the nature of the failure (cracked main seal in the hydraulic system) required extensive trouble-shooting. We were able to deal with this issue by standing down the drill crew, and by returning the site science crew to USU to work in the Core Processing Lab.

Our greatest challenges occurred at the Mountain Home site. Although this site had little to no lost circulation or excessive mud use, we did encounter *hole cave-in, stuck pipe, fish in the hole,* and *eventually, geothermal fluid entry*. Our first encounter with stuck pipe was overcome by fishing out the central core bit on the alien drill system, using a Bowen spear welded to NQ drill rod, as the wireline did not have sufficient strength to free the inner core rods. This allowed us to continue to ~700 m depth, where stuck drill rods forced us to abandon the hole and begin a new hole 7 m from the original (MH-2B). This was rotary drilled to 700 m, then cored with few problems until 1745 m, where we encountered geothermal fluid entry. After taking water samples, artesian flow was killed with weighted mud an drilling continued.

Minor hole stability issues prior to logging were dealt with by re-drilling and cleaning out the holes, and by logging out the bottom of the drill string in sections. At Mountain Home, the upper temporary casing strings (HQ) could not be removed, so no open hole logging was performed in the upper, cased section.

Table 14-1. Risk analysis matrix for Phase 2 drilling operations.		
RISK FACTOR	**PROBABILITY**	**MITIGATION, CORRECTIVE ACTION**
Drilling Equipment Failure	Low	Spare Parts Inventory, Nearby Mechanical Services Mechanical inspection/upgrade prior to Mobilization
Availability of Drilling Services	Low	Water well services in Burley and Twin Falls; Core Services and Supplies in Salt Lake
Land Owner Relations	Low	Very Good relationship with land owners
Lost Circulation	High	Cure lost circulation using LCM and cement through planned cased section (surface to 600 feet). >600 feet open hole; lost circulation cure if cuttings buildup using LCM and cement.
Hole cave in	Moderate	LCM and cement to cure stability as above. Potential to reduce from HQ to NQ
Penetration Rate Lower than Planned	Moderate	Revise budget; Reduce from HQ to NQ
Stuck Pipe	Moderate	Work pipe; reduce to NQ
Fish in Hole	Low to Moderate	Bowen spear and Junk basket on site. Cement fish and kick off (wedge) if cost is scientifically warranted
Hole stability - open hole logging	Low to Moderate	Clean out bridge; redrill. Log out bottom of drill rod in depth increments
Hole stability - temperature logs	Low to Moderate	Set pipe
Geothermal fluid entry	Moderate	Casing prepared for pressure control as above. BOP equipment on site and standby. Daily logging of bottom hole T
Excessive Mud Utilization	Moderate	Cure lost circulation as above. Water well on site
Inclement Weather	High	Winterized Rig; Good Paved and Gravel Roads
Permitting	Low	Permits currently in place

Figure 14-2. Decision Flow Line for Risk Response.

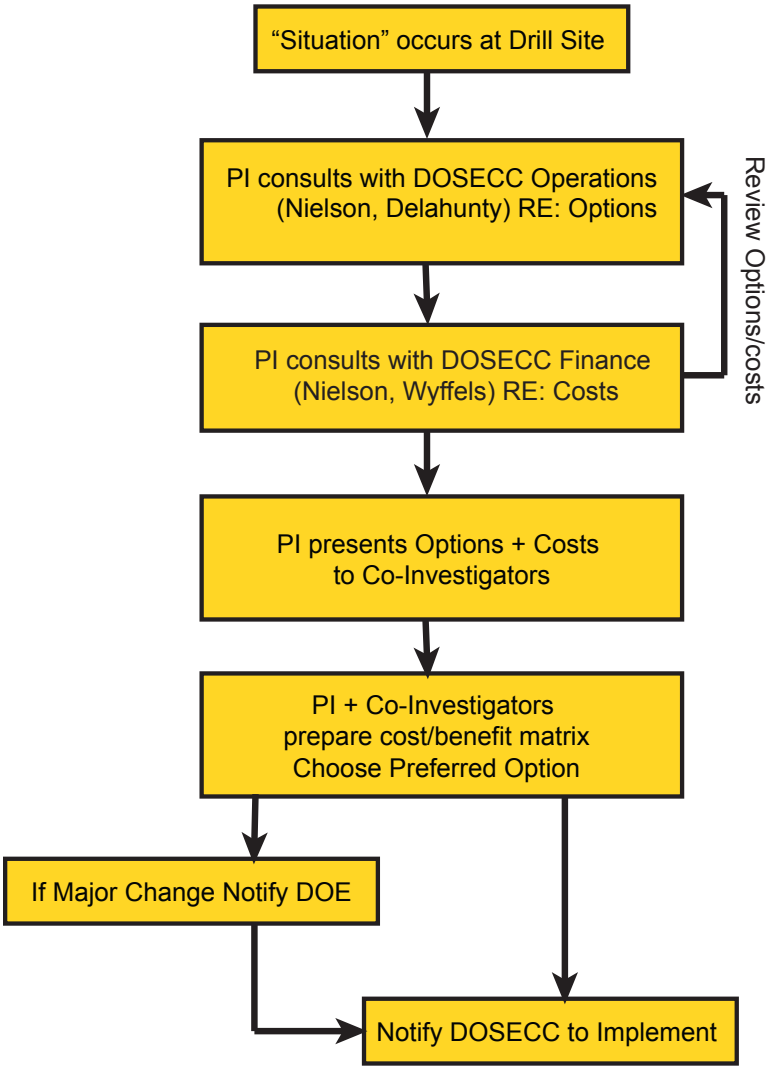

One issue that was not anticipated and did affect our operations at the Mountain Home site was the lack of high temperature logging tools, especially the borehole televiewer tool. This tool is critical for viewing and measuring fracture orientations and apertures in the borehole walls, especially in the entry zone for geothermal fluids. Unfortunately, NQ-sized borehole televiewers are not available commercially. In addition, commercially available NQ-size gamma and neutron tools are only reliable to about 70-75ºC, a temperature that was exceeded in the lower parts of both the Kimama and Mountain Home holes. If slim hole diamond drilling is going to play an important role in geothermal exploration, the development of more robust slim hole tools is critical.

It seems clear from this assessment that not all risk can anticipated, and that some low probability events may occur despite best efforts to avoid them. Nonetheless, a clear and detailed assessment of potential risk is critical to the success of any complex project such as this. By anticipating the risks it more likely that resources will be in place to mitigate or correct the problems that do occur. More important is the role of a decision tree for dealing with both anticipated and unanticipated issues that endanger the success of the project.

As part of our Phase 1 Report, we prepared a decision tree or flow line for risk response (Figure 14-2) that was used on multiple occasions, as discussed above. This decision tree involved a feed back loop that considered possible responses to risk events and the financial impact of these responses, so that the most cost effective solutions could be identified along with the more technically effective solutions. In all cases, solutions requiring a significant realignment of resources were discussed with the Golden, CO, Field Office and the Technical Review Team prior to implementation, and many proposed solutions were modified as a direct result of these consultations.

APRIL 2012 SCIENCE MEETING

The lead PI organized a project science meeting in April 2012 that was attended by 27 senior scientists from 14 universities, 2 Federal agencies (USGS, DOE/INL), and one non-profit NGO, 6 graduate students, and 7 staff geologists/geoscience technicians. There were 26 formal presentations on various aspects of the drilling and science, several extended discussions of completed work and future directions, and two extended visits to the core processing and storage facilities to view core and plan sampling activities. This meeting brought together almost all of the collaborating scientists involved in this project, to summarize what had been accomplished to date, what needed to be done, and how to obtain resources for further work. It was the first opportunity for all to review much of the geophysical data (including borehole and surface studies: gravity, magnetics, seismic) and to see the core from all three holes. Of particular importance was the opportunity to discuss relationships between the core, physical parameters of the drill sites obtained from borehole logs, and regional stuctures and correlations based on surface geophysics.

Based on discussions at this meeting, several new funding initiatives are moving forward to support more in depth study of the core and the geophysical logs. These include focused studies on the volcanic rocks, Ar-Ar age determinations, detrital zircons from sediment interbeds, hydrothermal alteration of the core and its implications for geothermal resources, experimental studies of volcanic rocks, and efforts to tie stratigraphy in the core to regional structure and stratigraphy using age dates, petrography and geochemistry of the units, and secular variation in the paleomagnetic orientations.

Table 14-2. List of talks and speakers at the April 2012 Science Meeting.		
Project Overview, Goals, 2006 Workshop	John Shervais	Utah State Univ.
Drilling Summary: What We Did, Why We Did It, Lessons Learned	Chris Delahunty	DOSECC
Finances: What it Cost, Projected vs. Actual, Time Lines	John Shervais	Utah State Univ.
DOSECC Downhole Temp Tool & Its Use During Hotspot	Dennis Nielson	DOSECC
Kimama: Stratigraphy & Basalt Geochemistry	Katie Potter	Utah State Univ
Kimama: Petrography of Primitive Basalts	Richard Bradshaw	Brigham Young Univ
Wendell-RASA: Kimama's Little Brother	Marlon Jean	Utah State Univ
Kimama: Paleomagnetic Stratigraphy	Duane Champion	USGS
Kimama: Clay Alteration	Chris Sant	Utah State Univ
Basalt Alteration: Future Studies	Tony Walton	University of Kansas
Isotopic Studies of SRP Basalts	Barry Hanan	San Diego State Univ
Experimental Petrology of SRP Basalts	Pyro Piersol	Univ of Idaho
Kimberly Overview: The Rhyolite Hole	Lisa Morgan	USGS
The Univ Leicester Rhyolite Project, Central SRP	Mike Branney	Unive of Leicester
Experimental Petrology of SRP Rhyolites	Francois Holtz	Univ of Hanover
Physical Properties Magmas: Future Directions	Cristina de Campos	Univ of Munich
Kimberly: Rhyolite Future Directions	Eric Christiansen	Brigham Young Univ
High Resolution Gravity & Magnetic Surveys, Snake River Plain	Jonathan Glen	USGS
Seismic Imaging through Volcanic Rocks of the Snake River Plain, Idaho for the ICDP Project Hotspot	Lee Liberty	Boise State Univ
Borehole Geophysical Logging: Overview and Preliminary Results	Doug Schmitt	U of Alberta
Fracture Analysis & Borehole Logs, Kimama	James Kessler	Utah State Univ
Mountain Home: Overview & Future Research	Alexander Prokopenko	Univ South Carolina
Mtn Home Lake Sediments: Preliminary Results	Anders Noren	UMN LacCore
Mtn Home Water Chemistry	Tom Lachmar	Utah State Univ
Mtn Home Air Force Base Geothermal Development	Tom Wood	INL
Current NSF Proposal: Overview	John Shervais	Utah State Univ
DIS System & Its Use in Future Research	Ronald Conze	ICDP
Core Viewing: USU Core Lab - On Campus and Nibley center	Staff	USU

REPORTING FUNCTIONS

Reporting functions included Quarterly and Annual progress reports to DOE, presentations at DOE Peer Review events, presentations at scientific and professional meetings, and publications. Formal presentations were made at two Peer Review events, three annual meetings of the Geothermal Resource Council, and several meetings of the American Geophysical Union and Geologic Society of America. The PI Science Team also organized special sessions at several of these meetings. A complete list of presentations and publications may be found in Appendix B, and are summarized in Table 15-3 below.

Table 15-3. Presentations, Publications, Abstracts	
Presentations	
Geothermal Resource Council	9
Geological Society of America	4
American Geophysical Union	11
Other Groups (Invited Presentations)	5
Total	***29***
Publications	
Geothermal Resource Council	10
Scientific Drilling Journal	2
Geosphere	1
USGS Circular	1
Total	***14***
Abstracts	***15***

CHAPTER 15:

CONCEPTUAL MODEL FOR GEOTHERMAL RESOURCES IN SOUTHERN IDAHO

Dennis Nielson
DOSECC, Inc. Salt Lake City Utah

John W. Shervais
Utah State University, Logan, Utah

ABSTRACT

The Snake River Plain (SRP) is part of the largest heat flow anomaly in the US. It is characterized by thick sequences of young flood basalts that erupted following the passage of the Yellowstone plume. However, apart from the obvious hydrothermal systems in the Yellowstone caldera, only a few small high-temperature hydrothermal systems are known, and these are located on the margins of the province. This observation is consistent with conventional wisdom that suggests basaltic provinces are poor targets for geothermal exploration because the low viscosity of basalt results in rapid flow to the surface along narrow conduits rather than forming shallow magma chambers that are large enough to support high-temperature fluid convection. Nonetheless, high temperature fluids found in slimhole test well MH-2 at Mountain Home Air Force Base document the occurrence of an active geothermal system. Water chemistry and fluid inclusions also document high temperatures (140-195°C) and chemical equilibrium with basalt. We propose that heat is provided by a complex of Layered Mafic Intrusions (LMI) that underlie the axial portion of the SRP, roughly delineated by the gravity high. While individual intrusions have limited heat capacity, the intrusion of multiple LMI sills into the same crustal levels will heat the surrounding country rock and prepare the ground for future intrusions.

INTRODUCTION

The Snake River Plain (SRP) volcanic province is part of the largest heat flow anomaly in the US (Blackwell and Richards, 2004). The SRP lies north of the Basin and Range province, which hosts active geothermal systems in northern Nevada and central Utah. It is subdivided into eastern (ESRP) and western (WSRP) segments that have different structural orientations and geologic histories. The ESRP represents the track of the Yellowstone hotspot – a deep-seated mantle plume that has remained relatively fixed in space as the North American plate moved to the southwest (Smith et al., 2009). As the plate moved over the plume, a number of large silicic caldera complexes formed through melting of continental crust. As the magma chambers beneath these calderas solidified and were able to sustain brittle fracturing, basalts were able to reach the surface and form the extensive lava flows that are seen today (Figure 15-1). In the ESRP relatively young felsic volcanics occur east of the Great Rift (e.g., Big Southern Butte), but none are found west of the rift (~W113.5º).

The WSRP lies to the north of the presumed plume track and is controlled by northwest-trending structures that are distinct from the Basin and Range faulting and probably related to reactivation of Cordilleran structures. No rhyolite volcanism younger than 9 Ma is present. Resurgent basalt volcanism (900-200 ka or less) formed long after the plume passed, driven by back-flow of plume material to the West. This resurgent basalt volcanism is plume-derived and postulated to be associated with delamination of subcontinental lithospheric mantle (Shervais and Vetter, 2009).

Although the SRP demonstrates young volcanic activity that is both widespread and voluminous, there has been relatively little geothermal exploration. We believe that this is the consequence of the lack of hot spring activity (except on the margins of the province) and the largely basaltic nature of the volcanism. Basaltic terrains are not generally considered to be viable exploration targets for high-temperature geothermal systems. Smith and Shaw (1975) pointed out that basalt is channeled rapidly from depth to the surface through fractures forming dikes that cool rapidly. In contrast, rhyolitic magmas commonly form chambers in the shallow crust and are therefore more capable of providing a larger and longer-lived heat source for hydrothermal circulation.

However, there are well documented hydrothermal geothermal systems in areas of basaltic volcanism without associated rhyolites. The south eastern rift of Kilauea Volcano on the island of Hawaii hosts the Puna geothermal system. Active extension and dike intrusion provides a continuous source of basaltic magma. Teplow et al. (1994) document a dacite melt intersected by injection well KS-13 at depth of 2480 to 2488 m in the Puna field. Although there are no exposed flows of dacitic composition, the authors speculate that this dacite has differentiated from basalt. They have calculated that the magma intersected by drilling had a temperature of

about 1050° C, and on the basis of thermal arguments, they suggest a body with a minimum circular dimension of 1 km and a thickness of at least 100 m.

Another well documented geothermal system specifically related to basaltic volcanism is located on the Reykjanes peninsula in Iceland (Fridleifsson et al., 2014). The character of the heat source has yet to be determined, but it is hypothesized to be either a sheeted dike complex or a major gabbroic intrusive body. Drilling in the Krafla field, where there is young rhyolite volcanism, intersected magma of rhyolite composition. Petrologic studies have shown that the magma was formed through the partial melting of altered basalt (Elders et al., 2011; Zierenberg et al., 2013).

Worldwide, the most extensive hydrothermal activity related to basaltic volcanism is the venting (Black Smokers) associated with submarine spreading centers. The hydrothermal activity occurs in narrow zones above axial magma chambers (Alt, 1995). A common feature of the above examples of active hydrothermal systems related to basaltic heat sources is the presence of a high-level magma chambers that have sufficient volume and longevity that it can sustain convective circulation. As the above examples also show, more felsic melts may be formed through partial melting or differentiation, and these rocks may not be exposed at the surface.

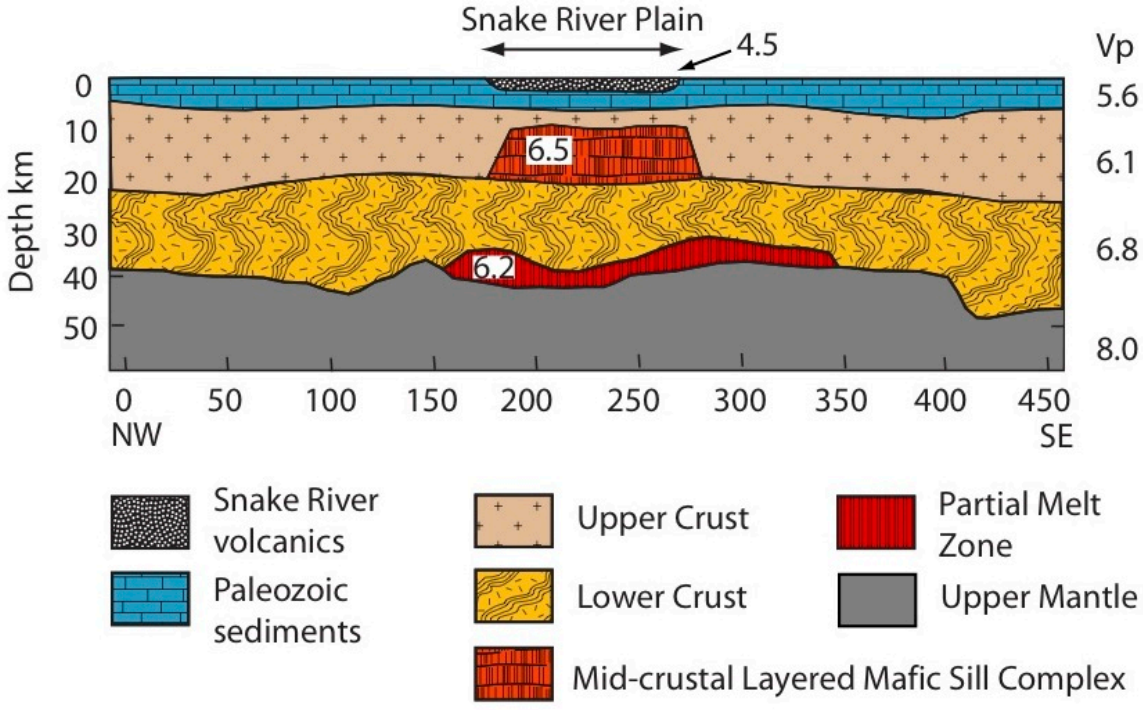

Figure 15-1. Interpretive cross section of the eastern Snake River Plain based on passive seismic deployment at right angles to the central volcanic axis. The mid-crustal sill complex is recognized by its high seismic velocity relative to the adjacent lower upper crust.

EASTERN SRP GEOTHERMAL SYSTEM

Thermal resources in the central SRP are distinct from other known systems, and require a new conceptual model that is fundamentally different from these systems. These differences have important implications for future exploration. The basic observations that pertain to the SRP overall include:

1. A lack of young felsic volcanism; relatively young felsic volcanics occur east of the Great Rift (e.g., Big Southern Butte), but none are found west of the rift (~W113.5º).

2. The occurrence of young basaltic volcanism throughout the region, with vents as young as 2,000 in the Great Rift-Craters of the Moon field, and large shield volcanoes as young as 100,000 years west of the rift.

3. Documentation of a mafic sill or sill complex in the mid-crustal region beneath the eastern-central SRP by seismic methods (e.g., Peng and Humphries, 1997; Figure 15-1).

4. Geochemical evidence for a layered mafic sill complex beneath the eastern SRP, based on fractionation-recharge cycles in basalt flows sampled as drill core (Shervais *et al.*, 2006; Figure 15-2).

5. The Graveyard Point Sill, exposed near the southern margin of the western SRP, documents a single layered basaltic sill up to 160 m thick (White, 2009); this confirms the existence of such sills inferred from seismic data and lava chemistry.

6. Further support for this sill complex comes from olivine gabbro xenoliths in basalt from Sid Butte, which lies just a few km west of the Kimama drill site (Matthews, 2000). These xenoliths have modes and compositions appropriate for basalt fractionation at mid-crustal levels (ol-plg-cpx) and suggest that basalts found on the surface were processed through this sill complex.

7. The highest heat flows are observed along the axial volcanic zone in the central plain, but only in deep drill holes which completely penetrate the ubiquitous Snake River Aquifer (which we have shown may be up to 1 km thick). Thermal gradients below the aquifer are 75-80ºC/km, on par with the highest observed gradients in the western SRP (this study).

8. Similarly, the highest groundwater temperatures are found in wells along the axial volcanic zone (McLong et al 2002; Smith 2004). In addition, groundwater becomes progressively warmer from east to west (down flow gradient), consistent with heating from below by a significant heat anomaly (e.g., Blackwell et al, 1990).

9. The central-eastern SRP is transected by a few “volcanic rift zones”, such as the Great Rift, that appear to represent the surface manifestation of deep-seated dikes (Kunz et al 1992).

10. The central-eastern SRP transects Basin-and-Range structures at a high angle, and lacks a bounding fault system similar to the range front faults of the western SRP.

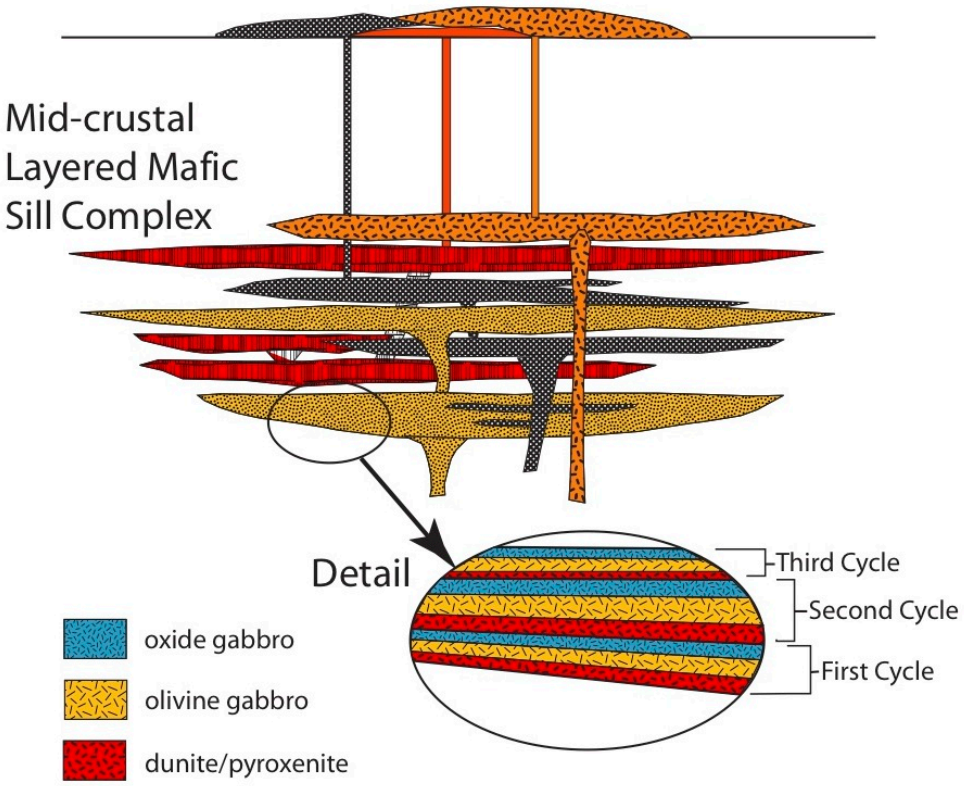

Figure 15-2. Schematic diagram of the mid-crustal sill complex as a layered mafic intrusive complex, based on upwardly zoned fractionation cycles and recharge cycles in basalts sampled by core in hole WO-2, INEL. After Shervais et al., 2006.

These observations require a basalt-driven system that is both long-lived and hot, similar to that in the Mountain Home area. In contrast to the western plain, however, the central (and eastern) plain is not affected by the same stress fields found in the western SRP graben. Although Basin-and-Range faults intersect the central SRP at a high angle, they do not appear to cross the plain, and seismicity is essentially absent beneath the plain (e.g., Smith and Sbar, 1986). It has been proposed that the stresses which lead to Basin-and-Range faulting north and south of the central SRP are accommodated by dike injection within the plain (Parsons et al 1998). This is supported by the occurrence of transverse “volcanic rift zones” which cut the plain in places, most notably the Great Rift (Kunz et al 1992).

CENTRAL SRP GEOTHERMAL SYSTEM CONCEPTUAL MODEL

We propose that the Central SRP Geothermal System derives its enthalpy from a layered basaltic sill complex in the middle to upper crust (Figure 15-2). As noted above, basalt-driven systems in Iceland and Hawaii are associated with relatively short-lived basaltic dikes that cool quickly; in contrast, the SRP basaltic sill complex is long-lived because (a) each individual sill is ~100-200 m thick, and (b) the intrusion of multiple sills into the same level of crust pre-heats this crust, minimizing heat loss from subsequent intrusions. These characteristics appear to apply to all thermal systems in the Snake River Plain, west or east, and are a direct function of heating by a plume-derived mantle anomaly that has thermally eroded the underlying lithosphere (Shervais and Hanan, 2008). A schematic diagram of the central SRP geothermal system is shown in Figure 15-3.

In contrast to the western SRP, the central SRP lacks the faults that provide conduits for heated fluids and allows that to gather in fracture systems. As a result, heat transfer above the layered sill complex, and below the Snake River aquifer, is largely through conduction. This is documented by our thermal gradient measurements at the Kimama site, which lies on the axial volcanic zone. Groundwater within the aquifer at Kimama has been heated to over 17ºC, from its initial temperature of ~8ºC (this study; Smith 2004). As noted by Blackwell et al (1992), this requires a substantial thermal flux from below.

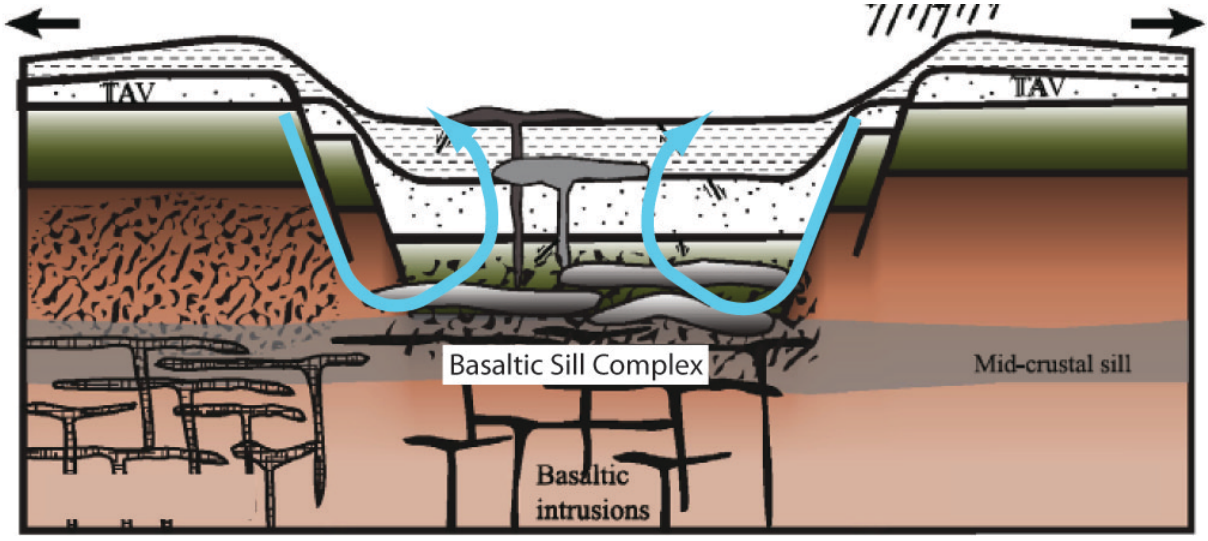

Figure 15-3. Generalized conceptual model for eastern SRP. Deep circulation of water along caldera margin or range-front faults; water is heated by basaltic sill complex (cooling of melt plus latent heat of fusion released upon crystallization) and reequilibrates with the basalts isotopically. Upflow of fluids limited by lack of internal faults, but may be accessed by deep drilling.

MOUNTAIN HOME GEOTHERMAL SYSTEM

The geothermal system discovered at Mountain Home Air Force Base (MH AFB) lies within the SRP volcanic province, which is generally thought to represent the track of the Yellowstone hotspot – a deep-seated mantle plume which has remained relatively fixed in space as the North American plate moved to the southwest (Smith et al., 2009). It also lies north of the Basin and Range province, which hosts active geothermal systems in northern Nevada and south-central Utah. However, the western SRP, where Mountain Home is found, does not sit on a presumed plume track (as represented by the SRP and the absolute motion vector for North America), and it is distinct from the Basin and Range in its structures and location.

The western SRP near Mountain Home hosts a basaltic volcanic system with eruptions as young as 200 ka (thousand years), and potentially even younger. Basaltic terrains are generally not appreciated as hosts for high-temperature geothermal systems. Smith and Shaw (1975) remarked on the idea that basalt is channeled to the surface through fractures and does not form high-level magma chambers, whereas rhyolitic magmas commonly form chambers in the shallow crust and are therefore more capable of providing a long-lived heat source for hydrothermal circulation. The question becomes: How do we account for an active geothermal system in a basaltic volcanic province that lacks shallow felsic intrusions and basin and range-type structural controls? The basic observations listed include:

1. The lack of young felsic volcanism anywhere in the western SRP; all of the felsic volcanic rocks are >9 Ma in age, too old to represent a heat source for an active geothermal system.

2. The occurrence of the MHAFB resource near the axis of the western SRP graben, over 30 km from the range front faults on the northern side of the graben, even farther from those on the southern margin (Shervais *et al.*, 2002).

3. The occurrence of young basaltic volcanism throughout the region, with vents as young as 200 ka or less (Shervais *et al.*, 2002; White *et al.*, 2002; Shervais and Vetter, 2009).

4. Documentation of a mafic sill or sill complex in the mid-crustal region beneath the western SRP by seismic methods (Pakiser and Hill, 1967).

5. The Graveyard Point Sill, exposed near the southern margin of the western SRP, documents a single layered basaltic sill up to 160 m thick (White, 2009); this confirms the existence of such sills inferred from seismic data and lava chemistry.

6. High-resolution gravity mapping by the USGS confirms the presence of an ~EW trending gravity high that lies at an oblique angle to the axis of the WSRP; this gravity high has been interpreted as a horst block, and may be cored by a mafic sill complex (Shervais *et al.*, 2002; 2013). The alignment of this gravity high is approximately parallel to a fault system mapped north of Mountain Home, which lies at an oblique angle to the range front fault system (Shervais *et al.*, 2002).

7. Water chemistry, isotope chemistry, and fluid inclusion data support relatively high fluid temperatures (140-195°C), and geothermal water that is in equilibrium with mafic volcanic rocks. Note that the MHAFB artesian geothermal waters are the only geothermal waters that do NOT sit on the meteoric fractionation line in D-O isotope space.

8. The Mountain Home geothermal system is currently active, although it was formerly at higher temperatures.

These observations require a basalt-driven system that is both long-lived and hot, and which is tapped by a stress field that is oblique to the stress responsible for the range front faults and opening of the western SRP graben.

MOUNTAIN HOME GEOTHERMAL SYSTEM CONCEPTUAL MODEL

We propose that the Mountain Home Geothermal System derives its enthalpy from a layered basaltic sill complex in the middle to upper crust, as in the central and eastern SRP. Unlike basalt-driven systems in Iceland and Hawaii, which are associated with relatively short-lived basaltic dikes that cool quickly, the SRP basaltic sill complex is long-lived because (a) each individual sill is ~100-200 m thick, and (b) the intrusion of multiple sills into the same level of crust pre-heats this crust, minimizing heat loss from subsequent intrusions. It has long been known that basaltic sills tend to pond at levels of neutral buoyancy, and that subsequent sills will cluster near this level, at or just above previously intruded sills.

Conduits for heated fluids are provided by faults that trend essentially parallel to the long axis of the gravity high, which is interpreted to represent an uplifted horst block (Figure 15-4). The location and orientation of these faults are thought to be controlled by the distribution of sill complex within the crust: crust modified by sill complex intrusion will tend to act as a rigid block during strain, localizing strain along its margins. Because the horst block lies near the axis of the western SRP, these conduits conduct fluid upwards far from the range front system.

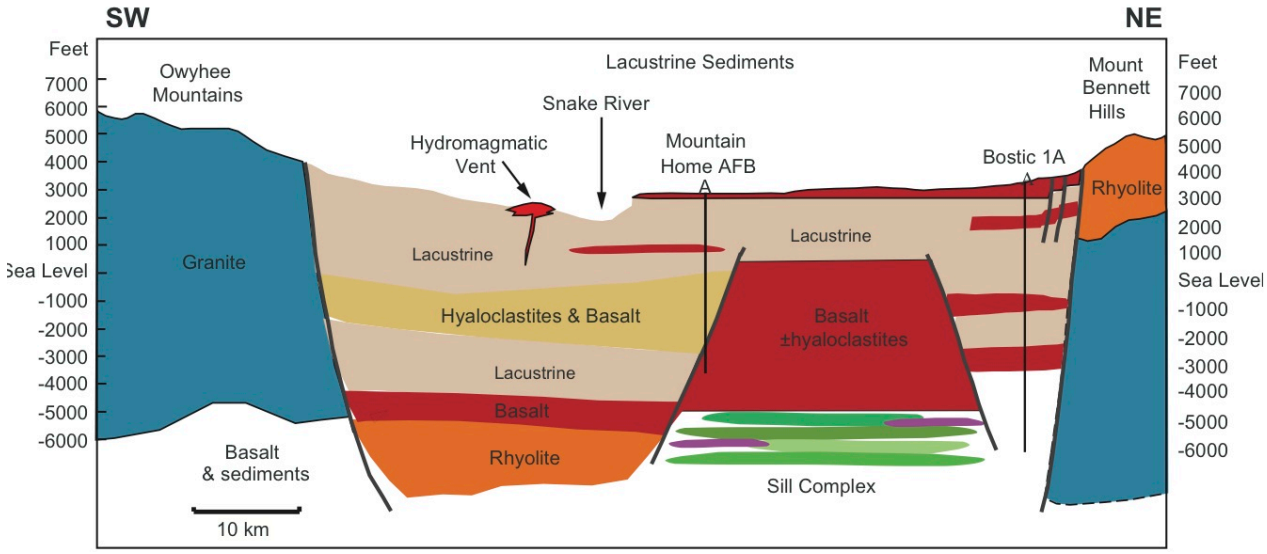

Figure 15-4. Generalized conceptual model for western SRP. Deep circulation of water along range-front faults; water is heated by basaltic sill complex (cooling of melt plus latent heat of fusion released upon crystallization) and reequilibrates with the basalts isotopically. Upflow of fluids along bounding faults of the hörst block may be accessed by deep drilling.

IMPLICATIONS FOR EXPLORATION STRATEGIES IN SOUTHERN IDAHO

The implications of this new conceptual model for geothermal resource exploration in the southern Idaho/SRP region are significant, because this model differs greatly from models that have proved successful elsewhere. First, the highest heat flux appears to occur along or near the central axis of the SRP (Shervais *et al.*, 2011). This is consistent with a heat source that is thickest near the axis, and thinner towards the margins. Further, the long-lived nature of this heat flux, and its continued flux long after the active plume has moved to the northeast (relative to the lithosphere), requires the slow release of heat from a cooling pluton, or in this case, sill complex representing multiple intrusions of basaltic melt. Second, the dominance of a nearly EW gravity high (horst block) beneath the western SRP, which appears to be bordered by a younger set of similarly oriented faults, implies that water heated by this source may be conducted into the upper crust by the boundary faults near the valley axis – and not along its margins.

If our model is correct, then geothermal resource exploration in the western SRP should focus on locations which are far from the range front faults, and that are also located over the steep gravity gradients that mark the margins of the gravity high/horst block. The dominant exploration tool will likely be high-resolution gravity mapping, coupled with seismic surveys and resource confirmation by a program of slim hole drilling and coring.

The apparent lack of faulting at depth within the central SRP means that normal fracture-controlled fluid transfer is unlikely to occur (in contrast to the situation at Mountain Home). As a result, development of thermal resources in the central SRP will need to rely heavily on artificially-stimulated fractures to form an enhanced geothermal system (EGS). In addition, the tremendous thickness of the Snake River Aquifer under parts of the central SRP will make drilling deep enough to encounter sufficiently hot rocks (200-300ºC) problematic, unless steps are taken to avoid the thickest portions of the aquifer. This would be best accomplished by using electrical resistivity surveys to document locations where the aquifer is thin. The best candidates at this time are sites north or south of the volcanic axis, where published resistivity surveys document a thin, basalt-hosted aquifer interbedded with lacustrine sediments, and areas near the Great Rift, which represents Holocene volcanism and thus likely overlies a young high-level magma chamber.

Future exploration should focus on a systematic approach that considers all available data within the context of a formal play analysis based on the conceptual model presented here. This will ensure that all potential resources are evaluated consistently, and with formal risk assessment applied quantitatively across prospects.

CHAPTER 16:
ECONOMIC ANALYSIS OF THE MOUNTAIN HOME GEOTHERMAL RESOURCE

Greg Mines
Idaho National Laboratory, Idaho Falls, Idaho

ABSTRACT

An economic analysis of the Mountain Home geothermal system was performed to assess power generation costs for the geothermal system discovered by Mountain Home AFB well MH-2. This analysis was performed using DOE's Geothermal Electricity Technology Evaluation Model (GETEM). Using reasonable assumptions for the size of the system and number of wells required to develop it, and using observed and equilibrium water temperatures, we calculate that a 14 MW power plant could generate power at an estimated cost of 11-15 cents per kilowatt-hour. This cost is comparable to other geothermal systems, although still higher than power generated by natural gas at this time. This calculation does not take into consideration the cost benefit of "secure power" for the USAF, or potential subsidies available to a commercial partner.

INTRODUCTION

An analysis was performed to assess the power generation costs from a resource that was postulated based on the Mountain Home Air Force Base Well MH-2. This analysis was performed using DOE's Geothermal Electricity Technology Evaluation Model, or GETEM. This model was developed for the DOE Geothermal Technologies Office to estimate representative power generation costs from geothermal energy. Though intended to provide a more generic assessment of power generation costs, it can be used to make a preliminary assessment of generation costs at a specific site.

The model estimates capital and operating costs based on the input provided to define a specific scenario. The scenario defined for the Mountain Home resource was based on the following assumptions which were inputs to the model:

Resource—Based on the exploratory well drilled, a resource is expected at a depth of 6,250 ft that would have a fluid temperature of 155°C.

Project Basis—At the expected resource temperature it is probable that a binary power plant would be utilized. For this conversions system, GETEM assumes that the plant will be air-cooled. For the evaluation, it is assumed that the resource will have 4 producing wells; each having a flow rate of 1,250 gpm. This flow approximates that from geothermal wells at similar depths in Idaho. It is assumed that the project would operate for 30 years.

Exploration—The exploration costs that are estimated by the model are those costs incurred in finding a potential resource. For the Mountain Home scenario, it is assumed that one well is drilled at a cost of $831K, with $50K allotted for activities not directly associated with drilling. This cost is low relative to what one might expect to encounter geothermal exploration, as a number of the sites that are explored do not produce an indication of a potential resource.

For the Mountain Home scenario, it is assumed that the exploration phase takes ~ 1.5 year with a discount rate (cost of money) of 30% applied to the costs incurred during this phase.

Confirmation—The costs that are estimated for the confirmation phase of a project development are for those activities needed to confirm the commercial potential of the resource. This typically requires drilling multiple wells that demonstrate the ability for the resource to provide some fraction of the total production capacity needed for the project. As with the exploration phase, in typical geothermal developments, not all locations that have a potential resource will be able to demonstrate commercial potential.

For the Mountain Home scenario, it is assumed that it will be able to demonstrate the necessary commercial potential. This will be done by drilling 2 successful production wells that will demonstrate half the total production capacity. Because not all wells drilled will necessarily be successful, a drilling success rate of 60% is used. The cost for each well drilled during this phase is $3,390K per well. This value is ~20% higher than the costs drilled when the well field is completed. The higher cost is used to reflect the effect of a learning curve when drilling multiple wells within a given field.

The confirmation phase at Mountain Home was assumed to take 1.5 year with a discount rate of 30% applied to costs incurred during this phase. The expectation is that once the commercial potential of the resource is shown, that the developer will be able to secure the funds to complete the project at lower discount rates.

Well Field Completion—Once the commercial potential of the resource is confirmed and funds secured to complete the project, the well field will be drilled out. During this phase a drilling success rate of 80% is assumed. To complete the well field, the remaining 2 production wells are drilled along with 2.7 injection wells and 0.9 unsuccessful wells. The capital costs for this phase are based on a cost of $3,325K for each well drilled. A cost of $200K per successful production and injection well is included in the capital cost estimate for the surface piping and equipment between the well and the power plant. A duration of 1.5 years is allowed to complete the field, with a discount rate of 15% applied to the costs incurred during this project phase.

Geothermal Pumping—The model calculates the geothermal pumping power needed based on a well configuration, the flow rate per well, well depth and fluid temperature, and a productivity/injectivity index defined by the user. For Mountain Home, a productivity index of 2,500 lb/hr per psi, or ~5.5 gpm per psi was assumed. The injectivity index was assumed to be the same as the productivity index. The estimated geothermal pumping power for both production and injection was slightly less than 1.4 MW electrical.

Power Plant—The model sizes the binary power plant based on the total flow from the production wells. Correlations are embedded in the model that relate the cost of the power plant to the amount of 'net' power that is produced from a given flow rate – plants that produce more power cost more. A trade-off is performed between the plant cost and the amount of power produced until the generation cost is minimized (effectively the total capital project cost in terms of $/kW is at a minimum as well). The relationship between cost and performance assumes that each plant is custom built for the specific site and application. If a user has a cost and level of performance for a specific plant, those values can be input to the model and used in estimating the generation costs.

The power plant construction is assumed to occur in parallel with the completion of the well field, with 1.5 years to design and construct. A discount rate of 7% is used for this project phase; this value is lower than that assigned to completing the well field because there is assumed to be less risk associated with the plant than with drilling the wells. For Mountain Home, it was assumed that 0.5 mile of transmission line would be needed and its cost is included in the total project capital cost.

The optimal plant size the model estimated was ~14.5 MW. After deducting the geothermal pumping power requirements, the project would produce ~13.1 MW of power for sale. The estimated cost of the plant (including transmission) is ~$45.2M, or ~$3,115 per kW.

Operating and Maintenance Costs—The maintenance cost portion of the annual operating and maintenance (O&M) costs are determined as a % of the capital cost estimates (typically 12%). The model estimates maintenance costs for the geothermal production pumps based on pump size and setting depth. Operation costs are based on the plant size and the type of plant. The model also includes estimates for royalties, and taxes and insurance. For the Mountain Home scenario, it is assumed that there are no royalties. For the Mountain Home scenario evaluated the annual O&M costs are estimated to be ~$2.96M.

Other—The estimated generation cost for the Mountain Home scenario assumes that the utilization factor for the plant during the first year of operation is 95% - this means the plant MW-hr of power produced would be 95% of what would be produced if the plant operated at the design output for the entire year (8,760 hrs). This factor takes into account both the effect of the varying ambient temperature throughout the year as well as the down time for maintenance. For Mountain Home it is assumed that the resource temperature declines at a rate of ~0.5°C per year. The effect of this declining temperature on power production is estimated and included in determining the generation costs.

The estimated generation costs include a 15% contingency for all capital costs, a 5 year MCRS depreciation schedule, and does not include the impact of any renewable incentives.

Estimated Costs

Table 16-1 summarizes the estimated capital costs, operating costs, and power output for the potential Mountain Home project based on the approach and assumptions described. Those costs are shown in the 2nd column (1st column of values).

Table 16-1. Estimated costs for the potential MHAFB geothermal project.

NUMBER OF WELLS	4	4	3
Cost per Well	$3,325K	$2,500K	$2,500K
Flow per Well	1,250 gpm	1,250 gpm	1,667 gpm
Total Flow to Plant	5,000 gpm	5,000 gpm	5,000 gpm
Power			
Plant, net	14,504 kW	14,190 kW	13,897 kW
Sales	13,129 kW	12,812 kW	11,863 kW
Capital Costs (with contingency)			
Exploration	$956K	$719K	$719K
Confirmation	$16,232K	$12,248K	$12,248K
Well Field Completion	$26,323K	$20,733K	$14,504K
Power Plant	$51,937K	$47,193K	$46,863K
Permitting	$288K	$288K	$288K
Total Capital Costs	$95,736K	$81,180K	$74,619K
Annual O&M Costs	$2,962K	$2,689K	$2,576K
GENERATION COSTS	12.73¢/kW-HR	11.44¢/kW-HR	11.31¢/kW-HR

Two other possible scenarios are given in the last two columns. These scenarios are based on the well costs being ~25% lower and the effect of increasing the flow per well and reducing the number of wells required to produce the same flow rate to the power plant. Note that the power output from the plant differs for the 3 scenarios even though the flow rate is constant. This is the effect of the model varying the plant performance and cost to produce the minimum generation cost. For the 3rd scenario, the geothermal pumping power increases by ~50% because of the increased flow per well. This decrease in sales is offset by the reduced well field costs. The net effect is a small reduction in the generation cost.

Summary of Economic Assessment

A preliminary evaluation of the potential generation cost at Mountain Home suggests that this cost would be between 11 and 13 cents per kW-hr, provided the assumptions made were realized. Because the model produces generic estimates for costs of power and the considerable uncertainty in the costs associated with finding and developing a commercial resource, it is probable that the actual costs could be 2 to 4 cents higher or lower than this estimate. Also this estimate does not include the effect of any federal or state incentives for renewable power production nor does it quantify the energy security benefits, which would lower the generation cost.

If the project were to proceed, the generation costs will be greatly dependent upon the resource that is found. Important resource characteristics that will impact the generation costs include its temperature and productivity. Higher temperatures allow more power to be produced from the well field, while increased productivity will allow the geothermal pumping power to be decreased or more flow produced for a given level of pumping power. For the defined Mountain Home scenario, if the fluid temperature ended up at 170°C with no change in productivity, the estimated sales would increase to ~15 MW with a generation cost of ~10.8 cents per kW-hr. Conversely if the temperature decreased to 140°C, the sales would decrease to ~10.9 MW and the generation cost would increase to ~15.7 cents. For the scenario defined for Mountain Home, reducing the Productivity/Injectivity Index by 50% would lower the generation cost to 11.7 cents, while doubling the value would increase the generation cost to 15.1 cents. The temperature and resource productivity are parameters that are inherent to the resource; their definition is critical to the confirmation phase, which would be the next step in developing the Mountain Home resource. The cost evaluation did not consider the benefit of an on-base source of “secure power.” This objective has be identified by the Air Force but placing a value on it is problematic at this time.

CHAPTER 17:

SUMMARY: GOALS AND ACCOMPLISHMENTS

John W. Shervais
Utah State University, Logan, Utah

ABSTRACT

Project Hotspot was designed to implement and assess a series of innovative approaches to geothermal exploration, to document best practices, and to evaluate the geothermal potential of the Snake River Plain volcanic province. Our Science/Exploration Goals and Objectives were: (1) to identify new geothermal resources in the undeveloped Snake River Plain region, (2) to characterize the thermal regime at depth in such a way as to further exploration goals in more focussed efforts, and (3) to document specific exploration methods and protocols that can be used effectively in these terranes. Our project has been a significant success in all three areas.

First, we have thoroughly documented three distinct geologic and geothermal regimes in the SRP, each of which has it's own character and geothermal potential. The axial volcanic zone (Kimama site) is dominated by the Snake River Regional Aquifer near the surface, but thermal gradients are very high below that; resource development is possible but only in specific locations. The plain margins (Kimberly) have significant low temperature resources that are not sufficient for electricity generation, but have other potential uses. The western SRP has high geothermal gradients, an insulating layer of sedimentary rock, and basement structures that favor fracture development. This represents the best short-term exploration target.

Second, we document that comprehensive assessment of available geologic and geophysical data, combined with slim hole test wells, borehole geophysics, high resolution gravity and magnetic surveys, and in places, high resolution seismic surveys, represents the best innovative approach to geothermal exploration. This work is best undertaken in a systematic fashion that first compiles and integrates existing data, then adds new geologic and geophysical surveys as needed to fill in the knowledge gaps, and to extend the compilation geographically.

Third, we have discovered a new blind geothermal resource in the western SRP at Mountain Home Air Force Base, which will contribute to their quest for energy independence. This resource is extensive, and a preliminary GTEM model suggests that a 10 MW power plant is feasible. This discovery has led to the development of a conceptual model that will facilitate further exploration in the Snake River Plain, and in other basalt-dominated volcanic provinces.

INTRODUCTION

The overarching objective of our project, *Hotspot: the Snake River Geothermal Project*, was to test a range of innovative technologies and approaches to geothermal exploration, and to assess their impact on improving the success geothermal exploration, with special emphasis on the Snake River volcanic province. These approaches included slim hole exploratory drilling, surface seismic surveys, high resolution gravity and magnetic surveys, thermal gradient logs in the drill holes, vertical seismic profiles, borehole geophysics, stratigraphy of recovered core, hydrothermal alteration, water chemistry, and fracture analysis. We selected three sites for slim hole test wells based on three distinct settings within the SRP: axial volcanic zone (thick basalt accumulation, highest groundwater temperatures), plain margin (thin basalt over rhyolite calderas, high thermal gradients), and the western SRP (graben structure, buried gravity anomalies, thick sedimentary cover). Each setting presents unique challenges for geothermal exploration and geothermal potential.

OVERVIEW

In our Phase 1 Report to DOE we laid out a number of scientific goals and objectives, as well as criteria for the success of our drilling program, which comprises a large portion of our budget. Our *Science/Exploration Goals and Objectives* were:

(1) To identify new geothermal resources in the undeveloped Snake River Plain region, or failing that,

(2) To characterize the thermal regime at depth in such a way as to further exploration goals in more focussed efforts, and

(3) To document specific exploration methods and protocols that can be used effectively in these terranes.

Further, we defined our criteria for success by three standards applied to these goals:

(1) Our goal of identifying new geothermal resources in the Snake River Plain region will be successful if we are able to show that sufficiently high temperatures and hydraulic conductivities exist in areas we have identified for detailed study.

(2) Our goal of characterizing the thermal regime at depth in such a way as to further exploration goals in more focussed efforts will be considered a success if we are able to show in some detail how temperature and hydraulic conductivity vary within the SRP, for example, under the axial volcanic zone or within the proposed caldera ring complex.

(3) Our goal of documenting specific exploration methods and protocols that can be used effectively in these terranes will be successful if we are able to show that certain combinations of geologic and geophysical methods, with or without slimhole exploration wells, can be used to predict regions favorable for geothermal development.

The objective of drilling was to evaluate the character of geothermal activity beneath the Snake River Aquifer. Critical factors for success include: (1) documenting high heat flow and the character of heat exchange (conduction vs convection); (2) determining what controls fluid flow: regional faults, caldera structures, or both, (3) establishing whether there is a difference in the character in the central part of the plain (Kimama) *vs*. the margin (Kimberly); and (4) determining the character of the Twin Falls caldera.

Overall, we conclude that our project has met or exceeded all of these goals. Specifically, we have discovered a new geothermal resource in the western SRP that has been judged to be economically viable using the GTEM model (Chapter 16 of this report), and which has led to a new conceptual model for geothermal exploration in the SRP that points the way for discovery of more resources in the future (Chapter 15 of this report). In a broader sense, we have documented the thermal regime in each of the three settings discussed above, and have tested all of the approaches and techniques in these settings. These results will be discussed in more detail for each site below. Some general conclusions we can draw from our work include the following:

(1) A detailed, comprehensive and systematic compilation of existing data is critical to the success of any geothermal exploration project. These data define the best strategy for further exploration and minimize exploration costs by focusing resources on those areas that have the highest potential for success (Chapters 3 and 4).

(2) A thorough understanding of the regulatory environment in the area to be studied is critical to the success of any project. This includes NEPA requirements, cultural surveys, and drilling regulations specific to geothermal test wells. Regulatory requirements vary depending on the activity (e.g., drilling *vs*. seismic surveys), land ownership and control (Federal, State, County, Private), and will even vary depending on which agency controls the land (e.g., BLM *vs.* Forest Service). Failure to understand the regulatory environment can derail even a well-planned exploration champaign (Chapter 2).

(3) Surface-based seismic surveys with tight geophone spacing can successfully image heterogeneities in subsurface lithology in complex volcanic terrains, to depths of 1-2 km, but the resolution is probably not sufficient in most cases to identify potential drilling targets, even when sonic velocities are known from vertical seismic profiles in adjacent wells (Chapter 6).

(4) Surface-based seismic surveys in terrains that are dominated by thick sedimentary cover (e.g., the western SRP) are much more robust and capable of imaging basement structure, as well as variations in the stratigraphy and structures such as faults (Chapter 6).

(5) High-resolution gravity and magnetic surveys are extremely successful in defining basement structure in both the eastern and western SRP. The importance of filtering existing data by correcting station locations and elevations is also documented. The ability of high resolution gravity surveys to image basement structure, in particular, is one of the most important findings of our project (Chapter 5).

(6) Slim hole drilling is one of the most cost effective strategies for documenting subsurface stratigraphy, thermal gradients, thermal alteration history, water chemistry, and fracture porosity. Diamond core slim hole drilling is especially effective in complex volcanic terrains with extensive lost circulation; standard rotary drilling must cure lost circulation before proceeding, whereas diamond core drilling can proceed through lost circulation zones without stopping (Chapter 7).

(7) We found that drilling costs may be minimized by using air rotary water well drillers to drill the upper 10% of each hole and set casing (as required by Idaho geothermal drilling regulations) before beginning diamond core drilling. Many of the approaches discussed in this report depend on the existence of either core or the drill hole (Chapter 7).

(8) The availability of core (from diamond core drilling) is critical for detailed assessments of lithology, stratigraphy, alteration, and fracture analysis. These data are essential for understanding both the geothermal reservoir and its overlying seal (Chapters 10, 11, 13).

(9) The availability of deep slim holes (from diamond core drilling) is critical for obtaining borehole geophysical logs that define the mechanical, electrical, and magnetic properties of the rocks within and above the geothermal reservoir. In addition, bore hole televiewer logs can provide detailed images of fracture distribution and reservoir permeability, provided the tools used are designed to work at high temperatures (Chapters 8, 13)

(10) The availability of deep slim holes is critical for obtaining thermal gradients and water samples. These are essential for understanding the thermal structure, depth to potential geothermal resources, water chemistry and equilibration temperatures, and planning future drilling operations (Chapters 9, 12).

(11) Large project management practices are critical for the success of any large exploration effort. This includes a clear chain of command and responsibility, critical chain mapping and resource leveling, and risk analysis. Strict budget tracking and cost controls are also essential, and must be established during the early stages of a project in order to avoid cost overruns later (Chapter 14).

The overall success of our project points the way for future work that builds on this success to plan and execute geothermal exploration strategies which are cost effective and promise a high probability of success. In the following sections we examine each of the three settings we tested to discuss their relative potentials for further geothermal exploration.

KIMAMA

The Kimama drill site sits in the Axial Volcanic Zone of the SRP, and overlies the Snake River Regional Aquifer (SRRA). Groundwater temperatures imply a high heat flux and concentration of thermal energy beneath the axis of the plain. Our drilling plan called for a 1500 m deep hole, but the thickness of the SRRA and the basalt caused us to increase that to 1800 m depth. Our final depth of 1912 m resulted in part from continued drilling while we waited for delivery of the steel liner. The liner proved to be a problem, in that it was not properly machined and separated at ~1400 m depth. As a result, tools were unable to go below this depth after the liner was placed, limiting our subsequent logging campaign to the upper parts of the hole. Fortunately, we contracted for neutron and gamma logging through the drill string prior to setting the liner.

Our thermal gradient logs document a sub-aquifer gradient of ≥75ºC/km -- equal to the highest gradients observed within the SRP volcanic province. Nonetheless, the extreme thickness of the SRRA (almost 1000 m), with its essentially isothermal gradient (14-17ºC over 980 m, or ~3ºC/km) resulted in a projected temperature of ~92ºC at 2 km depth. To achieve temperatures sufficient for electrical production (~150ºC) would require depths of ~2800 m or more. Further, there is no indication of fracture permeability at this depth that would provide fluids for power generation. This means that an EGS would be required.

Surface seismic was able to image sedimentary interbeds at depth, but did not image any major structures in the basement, which likely lie below the depth of penetration achieved by our study. Gravity shows a prominent high that may represent the thick basalt accumulation rather than a basement high. If so, more likely targets would lie outside this gravity high, where basalts (and the SRRA) are thinner.

Our data show that the base of the SRRA is defined by the onset of groundmass smectite (clay) alteration in the basalts. Smectite crystallinity increases with depth, reflecting higher temperatures, but high temperature phases (*e.g., chlorite*) are not found, confirming the low temperatures observed currently.

Based on our assessment of the local geology, and on the conceptual model presented in Chapter 15, we propose that successful exploration in this area should focus on areas that are as close as possible to the youngest basalt volcanoes (i.e., Craters of the Moon and the Great Rift), and that have the potential for fine-grained sediments overlying the potential reservoir. These sites would lie slightly NW or SE of the axial volcanic zone (a topographic high), in the moat-like lows which border the axial high.

KIMBERLY

The Kimberly Drill site sits on the margin of the SRP, south of the Snake River and SRRA, and within the Twin Falls warm water district. The location was chosen to avoid a thick basalt cover, and to focus on the outer margin of the underlying Twin Falls caldera complex. Our drilling plan called for an 1800 m deep hole, but we altered that to 1500 m in order to drill deeper at Kimama. However, by contracting with a water well driller to air rotary drill the upper 213 m and set casing, we saved enough in our drilling budget to complete the hole at a final depth of 1958 m.

The Kimberly site was expected to produce high temperature water at the planned depths because of its location in the Twin Falls warm water district, where many wells with depths of 500-700 m produce water with temperatures of ~40ºC. What we discovered, however, was that the thermal gradient becomes essentially isothermal at 50-58ºC below 800 m depth (Chapter 9). This indicates a convective flux of warm water that overwhelms any sign of higher temperature fluids from below. This comprises an immense warm water resource that could be tapped for a range of passive geothermal applications, but the temperatures are too low for electricity production.

Our high resolution gravity survey suggests that the Kimberly site may sit just within the bounds of the Twin Falls caldera complex, rather than on the outer margin of the caldera as we concluded during our Phase 1 study. This would explain the extreme thickness of individual welded ash flow units (up to 1300 m thick) and the lack of significant fracturing or faulting. Selecting a site outside the caldera rim, within the outer zone of bounding faults, would alleviate this issue, but would place the site farther from the heat source, which underlies the axial volcanic zone. Our seismic surveys were able to image boundaries between overlapping flow packages (different volcanoes) as well as sedimentary interbeds, but did not penetrate through to basement.

Thus, while the margins of the SRP are often cited for their high heat flow based on shallow thermal gradient wells, it seems that conditions deeper in the section compromise heat transport to the surface. Previous work (e.g., Smith and deTar, 1987) propose that thermal fluids found in the Twin Falls warm water district originate in the mountains to the south; we concur with that conclusion. Further, our data on water chemistry shows that this water is heated meteoritic water that has not equilibrated with the volcanic host rocks.

MOUNTAIN HOME

The Mountain Home drill site was chosen as representative of geothermal exploration in the western SRP and because it sits on the southern margin of a prominent gravity high interpreted to represent an uplifted hörst block; the steep gradient along the margins of this block may represent the bounding faults. The specific site on Mountain Home AFB was chosen because an older exploration well drilled on the base in 1988 showed a high geothermal gradient (~75ºC/km); however, at 1342 m total depth, it was too shallow to intersect fracture porosity. A wildcat oil well NE of the base (Bostic 1A) documented a similar high geothermal gradient and was the focus of a hot dry rock study by Los Alamos in the 1980's.

Our high resolution gravity survey confirmed our interpretations of the positive gravity anomaly as an uplifted hörst block and of its southern margin as a bounding fault. Seismic imaging revealed a simple stratigraphy with reflective basalt flows interbedded with more transparent sediments, and in places we able to document fault offsets in the contacts.

Drilling through the overlying lacustrine sediments presented some challenges, which led to one collapsed hole at ~650 m depth (MH-2A) and required us to rotary drill an offset hole (MH-2B) 6 m east of our original. Nonetheless, the lacustrine sediments provided an excellent thermal blanket for the underlying heat, with a thermal gradient of ~75ºC/km from the surface to total depth, with minor excursions for the influx of cool or hot water. At 1745 m depth we encountered a free-flowing artesian geothermal system. Downhole temperature tools indicate an influx temperature of ~149ºC. Water samples show that the water is chemically equilibrated with volcanic rocks, and has an equilibrium temperatures of ~150ºC (Chapter 12). This thermal water is unusual because it is the only thermal water in southern Idaho that does *not* sit on the Global Meteoric Water Line (GMWL) in deuterium-oxygen isotope space, but reflects equilibration with volcanic rocks (Figure 12-3). It is also the only water that plots in the "steam heated/volcanic waters" field of the Giggenbach sulfate-chlorine-bicarbonate plot (Figure 12-2).

Investigations of alteration assemblages show that the dominant alteration product is smectite (clay) except around the hot water inflow zone, which contains corrensite (an interlayered chlorite-smectite phase) and laumontite, a Ca-zeolite. Other mineralization phases include pyrite, chalcopyrite, calcite, and silica. Calcite spar crystals contain at least two generations of fluid inclusions: a high-T set (~195-200ºC) and a lower T set (~150ºC) that corresponds to ambient conditions.

We have developed a conceptual model for the Mountain Home system that may be generalized to the entire SRP (Chapter 15) and an economic analysis using GTEM (Chapter 16) shows that Mountain Home represents a viable, electrical-grade resource that could be used to help the USAF meet its goals for energy independence.

CONCLUSIONS

This project has demonstrated that a comprehensive assessment of available geologic and geophysical data, combined with slim hole test wells, borehole geophysics, high resolution gravity and magnetic surveys, and in places, high resolution seismic surveys, represents the best innovative approach to geothermal exploration. This work is best undertaken in a systematic fashion that first compiles and integrates existing data, then adds new geologic and geophysical surveys as needed to fill in the knowledge gaps, and to extend the compilation geographically.

The value of low-cost slim hole drilling to exploration has been noted before, but our work shows that it is critical to success, and remains the most cost-effective way to confirm or deny the existence of viable resources once a geothermal play has been identified, but before expensive production wells are drilled. Slim hole diamond core wells provide stratigraphic and structural data, allow detailed assessment of alteration assemblages and fracture analysis of core, and can be used to obtain wireline geophysical logs that allow correlation of lithology, mechanical and electrical rock properties, and surface geophysical data.

REFERENCES CITED

Aki and Richards (1980) "Quantitative Seismology", vol. I, sec. 5.2. Information on the Bortfeld approximation is found in “Bortfeld, R. (1961) Approximations to the reflection and transmission coefficients of plane longitudinal and transverse waves. Geophys. Prosp., 9, 485-502

Arney, B.H., 1982, Evidence of former higher temperatures from alteration minerals, Bostic 1-A well, Mountain Home, Idaho, Geothermal Resources Council Trans., 6, 3-6.

Arney, B.H., F. Goff, and Harding Lawson Ass., 1982, Evaluation of the hot dry rock geothermal potential of an area near Mountain Home, Idaho, Los Alamos Nat. Lab Report LA-9365-HDR, 65 pp.

Arney, BH, Gardner JN, Belluomini, SG, 1984, Petrographic Analysis and Correlation of Volcanic Rocks in Bostic 1-A Well near Mountain Home, Idaho, Los Alamos Nat. Lab Report LA-9966-HDR, 37 pp.

Baker, SJ, and Castelin, PM, 1990, Geothermal resource analysis in Twin Falls County, Idaho, Part II; in Geothermal Investigations in Idaho, Idaho Dept. Water Resources, Water Information Bulletin No. 30, Part 16, 36 pages.

Bankey, V., Cuevas, A., Daniels, D., Finn, C.A., Hernandez, I., Hill, P., Kucks, R., Miles, W., Pilkington, M., Roberts, C., Roest, W., Rystrom, V., Shearer, S., Snyder, S., Sweeney, R., Velez, J., Phillips, J.D., and Ravat, D., 2002, Digital data grids for the magnetic anomaly map of North America: U.S. Geological Survey Open-File Report 02-414, U.S. Geological Survey, Denver, Colorado, USA. http://pubs.usgs.gov/of/2002/ofr-02-414/

Baranov, V., 1957, A new method for interpretation of aeromagnetic maps: Pseudo-gravimetric anomalies, Geophysics, 22, 359-383.

Baranov, V., and Naudy, H., 1964, Numerical calculations of the formula of reduction to magnetic pole, Geophysics, 29, 69-79.

Blackwell, D.D. and M. Richards. 2004. Geothermal Map of North America. Amer. Assoc. Petroleum Geologists, Tulsa, Oklahoma, 1 sheet, scale 1:6,500,000.

Blackwell, D.D., 1980, Geothermal-gradient and heat-flow data, pp. 23-29, in Preliminary geology and geothermal resource potential of the Western Snake River Plain, Oregon, eds. D. E. Brown, G. D. McLean, G. L. Black, and J. F. Riccio, Ore. DOGAMI Open File Rep. 0-80-5, Portland.

Blackwell, D.D., 1989, Regional implications of heat flow of the Snake River Plain, Northwestern United States, in Tectonophysics, v164, 323-343.

Blackwell, D.D., JL Steele and LS Carter, 1991, Heat flow patterns of the North American continent: A discussion of the DNAG geothermal map of North America, in D.B. Slemmons, E.R. Engdahl, and D.D. Blackwell eds., Neotectonics of North America, Geol. Soc. Amer. DNAG Decade Map Volume 1, 423-437.

Blackwell, DD, 1978, Heat flow and energy loss in the western United States, pp. 175-208, in Cenozoic Tectonics and Regional Geophysics of the Western Cordillera, Memoir 152, eds. R. B. Smith, and G. P. Eaton, Geol. Soc. Am., Boulder, CO.

Blackwell, DD, SA Kelley, and JL Steele, 1992, Heat flow modeling of the Snake River Plain, Idaho, Dept. of Geological Sciences, Southern Methodist Univ, US Dept of Energy Contract DE-AC07-761DO1570, 109 pp.

Blackwell, DD, Steele, J.L., and Carter, L.C., 1989, Heat flow data base for the United States, in Hittleman, A.M., Kinsfather, J.O., and Meyers, H., eds., Geophysics of North America CD-ROM, Boulder, Colo, Natl. Oceanographic and Atmospheric Adm., Natl. Geophys. Data Center.

Blakely, R.J., 1995, Potential theory in gravity and magnetic applications: New York, Cambridge University Press, 441 p.

Blakely, R.J., and Simpson, R.W., 1986, Approximating edges of source bodies from gravity or magnetic data, Geophysics, 51, 1494-1498.

Bonnichsen, B, and Godchaux, MM, 2002, Late Miocene, Pliocene, and Pleistocene geology of southwestern Idaho with emphasis on basalts in the Bruneau-Jarbidge, Twin Falls, and western Snake River plain regions, in Bonnichsen, White and McCurry, eds., Tectonic and magmatic evolution of the Snake River Plain volcanic province., Idaho Geological Survey Bulletin 30. Moscow, ID, United States. 2004., p. 233-312.

Bonnichsen, B., Leeman, W., Honjo, N., McIntosh, W., and Godchaux, M., 2008, Miocene silicic volcanism in southwestern Idaho: geochronology, geochemistry, and evolution of the central Snake River Plain: Bulletin of Volcanology, v. 70, no. 3, p. 315-342.

Bouligand, C., Glen, J.M.G., and Blakely, R.J., (in press, JGR), Distribution of buried hydrothermal alteration deduced from high resolution magnetic surveys in Yellowstone National Park.

Bouligand, C., Glen, J.M.G., and Blakely, R.J., 2009, Mapping Curie temperature depth in the western United States with a fractal model for crustal magnetization, J. Geophys. Res., 114, B11104.

Bradford, J., Liberty, L.M., Lyle, M.W., Clement, W.P., and Hess, S.S., 2006, Imaging complex structure in shallow seismic-reflection data using pre-stack depth migration, Geophysics, v. 71, p. B175-B181.

Brott, CA, DD Blackwell, and JC Mitchell, 1976, Heat flow study of the Snake River Plain region, Idaho, p. 195 pp., in Geothermal Investigations in Idaho, Idaho Dept. Water Resour., Water Info. Bull., 30 (8).

Brott, CA, DD Blackwell, and JC Mitchell, 1978, Tectonic implications of the heat flow of the western Snake River Plain, Idaho, Geol. Soc. Am. Bull., 89, 1697-1707, 1978.

Brott, CA, DD Blackwell, and JP Ziagos, 1981, Thermal and tectonic implications of heat flow in the eastern Snake River plain, Idaho, J. Geophys. Res., 86, 11709-11734, 1981.

Brown, DE, GD McLean, and GL Black, 1980, Preliminary geology and geothermal resource potential of the western Snake River plain, Oregon, Oregon Dept. Geol. Min. Indus, Open-File Rep O-80-5, 114p.

Brown, DW, 2000, A Hot Dry Rock Geothermal Energy Concept Utilizing Supercritical CO2 Instead of Water, Proceedings of the TwentyFifth Workshop on Geothermal Reservoir Engineering, Stanford University, Stanford, CA, Jan. 24–26, 2000, Paper SGPTR165.

Christensen, N. I., 1982, Seismic velocities. Handbook of physical properties of rocks, 2, 1-228.

Christensen, N.I., Fountain, D.M., Carlson, R.L., and Salisbury, M.H., 1974. Velocities and elastic moduli of volcanic and sedimentary rocks recovered on DSDP Leg 25: In Simpson, E.S.W., Schlich, R., et al., Initial Reports of the Deep Sea Drilling Project, Volume 25: Washington (U.S. Government Printing Office), p.357.

Christiansen, E., and McCurry, M., 2008, Contrasting origins of Cenozoic silicic volcanic rocks from the western Cordillera of the United States: Bulletin of Volcanology, v. 70, no. 3, p. 251-267.

Christiansen, RL, 2001, The Quaternary and Pliocene Yellowstone Plateau Volcanic Field of Wyoming, Idaho, & Montana, Geology of Yellowstone National Park, U.S. Geological Survey Professional Paper 729, 1-156.

Cooke, M., 1999, Petrology, Geochemistry, and Hydrology of basaltic volcanism, Central Snake River Plain, Idaho, M.Sc. Thesis, University of South Carolina, 1999.

Cooke, MF, Shervais, JW, Kauffman, JD and Othberg, KL, 2006a, Geologic Map of the Dietrich Butte Quadrangle, Lincoln County, Idaho: Idaho Geological Survey, Moscow Idaho, DWM-63 scale 1:24,000.

Cooke, MF, Shervais, JW, Kauffman, JD and Othberg, KL, 2006b, Geologic Map of the Dietrich Quadrangle, Lincoln County, Idaho: Idaho Geological Survey, Moscow Idaho, DWM-66 scale 1:24,000.

Cordell, L., and McCafferty, A.E., 1989, A terracing operator for physical property mapping with potential field data, Geophysics, 54, 621-634.

DeRaps, M., 2009, Basaltic volcanism: surface flows and core, Western Snake River Plain, Idaho, M.Sc. Report, Utah State University, 2009.

Embree, GF, Lovell, MD, and Doherty, DJ, 1978, Drilling data from Sugar City Exploration Well, Madison County, Idaho, USGS Open File Report 79-1095, columnar section, scale ca. 1:120, one sheet.

Finn, C.A., and Morgan, L.A., 2002, High-resolution aeromagnetic mapping of volcanic terrain, Yellowstone National Park, J. Volcanol. Geotherm. Res., 115, 207–231.

Fleischmann, DJ, 2006, Geothermal development needs in Idaho, Geothermal Energy Association publication for the Department of Energy, 51 pp.

Ge, S., 1998, Estimation of groundwater velocity in localized fracture zones from well temperature profiles, Journal of Volcanology and Geothermal Research, v. 84, , p. 93-101.

Geist, D, Teasdale, R, Sims, E, and Hughes, S, 2002a, Subsurface volcanology at TAN and controls on groundwater flow, GSA Special Paper 353, 45-59.

Genter, A., Traineau, H., 1996, Analysis of macroscopic fractures in granite in the HDR geothermal well EPS-1, Soultz-sous-Forêts, France, Journal of volcanology and geothermal research, vol. 72, no1-2, pp. 121-141.

Glen JMG and Ponce DA, 2002, Large-scale fractures related to inception of the Yellowstone hotspot: Geology, v. 30, p. 647–650.

Glen JMG, Payette S, Bouligand M, Helm-Clark C, Champion D, 2006, Regional geophysical setting of the Yellowstone Hotspot track along the Snake River Plain, Idaho, USA. EOS Trans. AGU, 87(52), V54-1698.

Goodwillie A. and Ryan B., 2009, User Guide for GeoMapApp version 2, Lamont-Doherty Earth Observatory, Columbia University, http://www.geomapapp.org

Graham D, Reid M, Jordan R, Grunder A, Leeman W, Lupton J, 2006, A Helium Isotope Perspective on Mantle Sources for Basaltic Volcanism in the Northwestern US, EOS Trans. AGU, 87(52), V43D-02.

Grauch, V.J.S., and Cordell, L., 1987, Limitations of determining density or magnetic boundaries from the horizontal gradient of gravity or pseudogravity data, Geophysics, 52, 118-121.

Hackett, W.R., R.P. Smith, and Soli Khericha, 2002, Volcanic hazards of the Idaho National Engineering and Environmental Laboratory, southeast Idaho, in Bill Bonnichsen, C.M. White, and Michael McCurry, eds., Tectonic and Magmatic Evolution of the Snake River Plain Volcanic Province: Idaho Geological Survey Bulletin 30, p. 461-482.

Hanan, BB Shervais, JW, and Vetter, SK, 2008, Yellowstone plume-continental lithosphere interaction beneath the Snake River Plain, Geology, v. 36, 51-54. DOI: 10.1130/G23935A.1

Hannsen, P., Ziolkowski, A., and Li, X. (2003), A quantitative study on the use of converted waves for sub-basalt imaging, Geophysical Prospecting, 183-193.

Hildenbrand, T.G., 1983, FFTFI - A filtering program based on two-dimensional Fourier analysis: U.S. Geological Survey Open-File Report 83-237, 29 p.

Hobson, V.R., 2009, Remote sensing of basaltic volcanics, Central Snake River Plain, Idaho, M.Sc. Report, Utah State University, 2009.

Hulen, J.B. and Nielson, D.L., 1995, Hydrothermal factors in porosity evolution and caprock formation at The Geysers steam field, California - insight from The Geysers coring project: Proceedings 20th Workshop on Geothermal Reservoir Engineering, Stanford University, p. 91-93

Innovative Technical Solutions, Inc., 2003, Geothermal Energy Resource Assessment on Military Lands: Report prepared for the Naval Air Weapons Station China Lake under Contract No. N68936-02-R-0236, 506 p.

Jablonski, H.M., 1974, World relative gravity reference network North America, Parts 1 and 2: U.S. Defense Mapping Agency Aerospace Center Reference Publication no. 25, originally published 1970, revised 1974, with supplement of IGSN 71 gravity datum values, 1261 p.

James, D, Roth, J, Fouch, M, and Carlson, R, 2009, Upper mantle velocity structure of the Pacific Northwest: Implications for geodynamical processes during the late Cenozoic, Abstract, Earthscope National Meeting, Boise Idaho, 12-15 May 2009; http://www.iris.edu/hq/esreg/page/abstracts.

James, ER Manga, M, Rose, TP, Hudson, GB, 2000, The use of temperature and the isotopes of O, H, C, and noble gases to determine the pattern and spatial extent of groundwater flow, Journal of Hydrology 237, 100–112.

Janik, A., Lyle, M., and Liberty, L.M., 2004, Seismic expression of Pleistocene paleoceanographic changes in the California Borderland from digitally acquired 3.5 kHz subbottom profiles and Ocean Drilling Program Leg 167 drilling: Journal of Geophysical Research, v. 109.

Jenks, M.D., Bonnichsen, B., Godchaux, M.M., 1998, Geologic map of the Grandview-Bruneau area, Owyhee County, Idaho, Idaho Geological Survey Technical Report 93-2, 21 p., 19 maps, scale 1:24,000.

Johnson, TM, RC Roback, TL McLing, TD Bullen, DJ DePaolo, C. Doughty, RJ Hunt, RW Smith, L. DeWayne Cecil, and MT Murrell. 2000. Groundwater 'fast paths' in the Snake River Plain aquifer: Radiogenic isotope ratios as natural groundwater tracers. Geology 28, (10) (Oct): 871-874.

Kauffman, JD, Othberg, KL, Gillerman, VS, Garwood, DL, 2005a, Geologic Map of the Twin Falls 30x60 minute Quadrangle, Idaho: Idaho Geological Survey, Moscow Idaho; DWM-43, Scale: 1:100,000.

Kauffman, JD, Othberg, KL, Shervais, JW, Cooke, MF, 2005b, Geologic Map of the Shoshone Quadrangle, Lincoln County, Idaho: Idaho Geological Survey, Moscow Idaho; DWM-44, Scale: 1:24000.

Kucks, R.P., 1999, Bouguer gravity anomaly data grid for the conterminous US: in, U.S. Geological Survey, National geophysical data grids; gamma-ray, gravity, magnetic and topographic data for the conterminous United States: U.S. Geological Survey Digital Data Series DDS-9.

Kuntz, M. A., 1992, A model-based perspective of basaltic volcanism, eastern Snake River plain, Idaho, in Link, Kuntz, and Platt, eds., Regional geology of eastern Idaho and western Wyoming, Memoir 179: Boulder, Co, Geological Society of America, p. 289-304.

Kuntz, M.A., Skipp, Betty, Champion, D.E., Gans, P.B., Van Sistine, D.P., and Snyders, S.R., 2007, Geologic map of the Craters of the Moon 30' x 60' quadrangle, Idaho: U.S. Geological Survey Scientific Investigations Map 2969, 64-p. pamphlet, 1 plate, scale 1:100,000.

Kuntz, MA, Champion, DE, Spiker, EC, Lefebvre, RH, and McBroome, LA, 1982, The great rift and the evolution of the Craters of the Moon lava field, Idaho: Idaho Bureau of Mines and Geology, Bulletin v. 26, p. 423-437.

Lewis RE, and HW Young, 1989, The Hydrothermal System in Central Twin Falls County, Idaho, USGS Water-Resources Investigations Report 88-4152, 44 pages.

Lewis, RE, and Stone, MAJ, 1988, Geohydrologic data from a 4,403-foot geothermal test hole, Mountain Home Air Force Base, Elmore County, Idaho: U.S. Geological Survey Open-File Report 88-166, 30 p.

Liberty, L.M., 1998, Seismic reflection imaging of geothermal aquifer in urban setting, Geophysics, 1285-1294.

Liberty, L.M., W.P. Clement, and M.D. Knoll, 1999, Surface and borehole seismic characterization of the Boise Hydrogeophysical Research Site, Proc. Environmental and Engineering Geophysical Society, 723-732.

Liberty, LM, Wood, SH, and Barrash, W, 2001, Seismic reflection imaging of hydrostratigraphic facies in Boise: A tale of three scales, SEG expanded abstracts, DOI:10.1190/1.1816360.

Lindholm, G.F., 1996, Summary of the Snake River regional aquifer-system analysis in Idaho and eastern Oregon: U.S. Geological Survey Professional Paper 1408-A, 59 p.

Lindholm, G.F., 1996, Summary of the Snake River regional aquifer-system analysis in Idaho and eastern Oregon: U.S. Geological Survey Professional Paper 1408-A, 59 p.

Link, PK and L. L. Mink, LL (editors), 2002, Geology, hydrogeology, and environmental remediation: Idaho National Engineering and Environmental Laboratory, Eastern Snake River Plain, Idaho: Geological Society of America Special Paper 353, Boulder, 316 pp.

Matthews, S., 2000, Geology of the Owinza Butte, Shoshone SE, and Star Lake Quadrangles: Snake River Plain, Southern Idaho, M.Sc. Thesis, University of South Carolina, 2000.

Matthews, SH, Shervais, JW, Kauffman, JD, & Othberg, KL, 2006a, Geologic Map of the Star Lake Quadrangle, Jerome and Lincoln Counties, Idaho: Idaho Geological Survey, Moscow Idaho, DWM-67 scale 1:24,000.

Matthews, SH, Shervais, JW, Kauffman, JD, & Othberg, KL, 2006b, Geologic Map of the Shoshone SE Quadrangle, Jerome and Lincoln Counties, Idaho: Idaho Geological Survey, Moscow Idaho, DWM-62 scale 1:24,000.

McCafferty, A. E., Kucks, R. P., Hill, P. L., and Racey, S. D., 1999, Aeromagnetic map for the state of Idaho; a web site for distribution of data, USGS Open-File Report: 99-371. http://pubs.usgs.gov/of/1999/ofr-99-0371/

McCurry, M, Hayden, K, Morse, L, and Mertzman, S, 2008, Genesis of post-hotspot, A-type rhyolite of the Eastern Snake River Plain volcanic field by extreme fractional crystallization of olivine tholeiite: Bulletin of Volcanology, v. 70, no. 3, p. 361-383.

McCurry, M., Watkins, AM, Parker, JL, Wright, K, and Hughes, SS, 1996, Preliminary volcanological constraints for sources of high-grade rheomorphic ignimbrites of the Cassia Mountains, Idaho: Implications for the Evolution of the Twins Falls Volcanic Center. Northwest Geology, vol. 26, 81-91.

McLing, Travis L., Robert W. Smith, and Thomas M. Johnson. 2002. Chemical characteristics of thermal water beneath the eastern Snake River Plain; Geology, Hydrogeology, and Environmental Remediation; Idaho National Engineering And Environmental Laboratory, Eastern Snake River Plain, Idaho. Special Paper - Geological Society of America 353: 205-211.

Melosh, G, Cumming, W, Casteel, J, Niggemann, K, and Fairbank, B, 2010, Seismic Reflection Data and Conceptual Models for Geothermal Development in Nevada, Proceedings World Geothermal Congress 2010, Bali, Indonesia, 25-29 April 2010, 6 pp.

Mitchell, NC, MW Lyle, MB Knappenberger and LM Liberty, 2003, Lower Miocene to present stratigraphy of the equatorial Pacific sediment bulge and carbonate dissolution anomalies, Paleoceanography, v18, 1-14.

Morgan LA, 1990, Lithologic description of the “Site E Corehole” Idaho National Engineering Laboratory, Butte County, Idaho; US Geological Survey Open File Report OF-90-487, 7 pp.

Morgan LA, Doherty DJ and Leeman WP, 1984, Ignimbrites of the eastern Snake River Plain: Evidence for major caldera-forming eruptions: Journal of Geophysical Research, v. 89, no. B10, 8665-8678.

Morse, L.H., and McCurry, M., 2002, Genesis of alteration of Quaternary basalts within a portion of the eastern Snake River Plain aquifer: Geological Society of America Special Paper 353, pp. 213-224.

Nathenson, M, TC Urban, WH Diment, and NL Nehring, 1980, Temperatures, heat flow, and water chemistry from drill holes in the Raft River geothermal system, Cassia County, Idaho, U.S. Geol. Surv. Open-File Report. 80-2001, 29 pp., 1980.

Neely, KW and Galinato, G, 2007, Geothermal power generation in Idaho: an overview of current developments and future potential, Open File Report, Idaho Office of Energy Resources, 18 pp.

Neely, KW, 1996, Production history for the four geothermal district heating systems in Boise, Idaho, Geothermal Resources Council Transactions, vol. 20, pp. 137-144.

Nielson, D. L., 2001, Deep wireline coring in geothermal reservoirs: Geothermal Resources Council Transactions, v. 25, p. 115-118

Nielson, D. L., Barton, C. A. and Keighley, K. E., 1998, Comparative study of fractures in core and borehole televiewer in well VC-2B, Valles caldera, New Mexico: Proceedings, twenty-third workshop on geothermal reservoir engineering, Stanford University, p. 283-290

Nielson, D.L., Clemente, W.C., Moore, J.N., and Powell, T.S., 1996, Fracture permeability in the Matalibong-25 corehole, Tiwi geothermal field, Philippines: Proceedings, Twenty-first workshop on geothermal reservoir engineering, Stanford University, SGP-TR-151, p. 209-216

Paillet, F.L., 1999, Geophysical reconnaissance in bedrock boreholes--finding and characterizing the hydraulically active fractures, in Morganwalp, D.W. and Buxton, H.T., eds., U.S. Geological Survey Toxic Substances Hydrology Program--Proceedings of the Technical Meeting, Charleston, South Carolina, March 8-12, 1999: U.S. Geological Survey Water-Resources Investigations Report 99-4018C, v. 3, p. 725-733.

Paillet, F.L., 2000, Using borehole wireline methods to delineate fracture flow paths in bedrock formations (Chapter 7), in Inyang, H.I., and Bruell, C.J., eds., Remediation in rock masses: Reston Vir., American Society of Civil Engineers.

Pan-American Center for Earth and Environmental Studies (PACES), 2009, Online gravity data set for the lower 48 states, USA: El Paso, University of Texas at El Paso (UTEP). [http://gis.utep.edu/index.php?option=com_content&view=article&id=197%3Agdrp-home&catid=51%3Amain-site&Itemid=59, last accessed August 11, 2009].

Peng, X and ED Humphreys, 1998, Crustal velocity structure across the eastern Snake River plain and the Yellowstone Swell. Journal of Geophysical Research, B, Solid Earth and Planets 103(4): 7171-7186.

Peterson, S., Widner, L. and Nelson, JR, 2004, Estimated Impacts Of Proposed Idaho Geothermal Energy Projects Department of Agricultural Economics and Rural Sociology, A.E. Extension Series No. 04-01.

Phillips, J.D., 2001, Designing matched bandpass and azimuthal filters for the separation of potential-field anomalies by source region and source type, Australian Society of Exploration Geophysicists, 15th Geophysical Conference and Exhibition, August 2001, Brisbane.

Pierce, K.L., and Morgan, L.A., 1992, The track of the Yellowstone hot spot--volcanism, faulting and uplift, in Link, P.K., Kuntz, M.A., and Platt, L.W., eds., Regional geology of eastern Idaho and western Wyoming: Geological Society of America Memoir 179 (in honor of Steve Oriel), p. 1-53, 24 figs., 1 color map.

Pierce, KL and Morgan, LA, 1992, The track of the Yellowstone hotspot: Volcanism, faulting, and uplift, in Regional geology of eastern Idaho and western Wyoming: Geological Society of America Memoir 179, p. 1-53.

Pierce, KL, Morgan, L.A, and Saltus, RW, 2002, Yellowstone Plume Head: Postulated Tectonic Relations to the Vancouver Slab, Continental Boundaries, and Climate, in: Bonnichsen B., White C., and McCurry M., eds., Tectonic and magmatic evolution of the Snake River Plain volcanic province, Idaho Geological Survey Bulletin 30. Moscow, ID, United States, p. 5-33.

Pujol, J. and Smithson, S.B. (1991), Seismic wave attenuation in volcanic rocks from VSP experiments, Geophysics, 56, 9, 1441-1455.

Pujol, J., Fuller, B., and Smithson, S. (1989), Interpretation of a vertical seismic profile conducted in the Columbia Plateau basalts, Geophysics, 54, 10, 1258-1266.

Regone, C. J. (1997). Measurement and identification of 3-d coherent noise generated from irregular surface carbonates. Carbonate seismology: Soc. Expl. Geophys, 281-305.

Rohe, Michael J., Richard P. Smith, and Travis McLing. 2002. Variation in aquifer hydraulic gradient related to near-decadal climate changes; geological society of america, 2002 annual meeting. Abstracts with Programs - Geological Society of America 34, (6) (Oct): 241.

Ronne, JA, Witter, JB and Thompson, GR, 2010, Exploration of Four Geothermal Properties in Nevada, Proceedings World Geothermal Congress 2010, Bali, Indonesia, 25-29 April 2010, 8 pp.

Sanyal, SK and SJ Butler, 2005. An Analysis of Power Generation Prospects From Enhanced Geothermal Systems. Geothermal Resources Council Transactions, 29.

Sass, J.H., Lachenbruch, A.H., Munroe, R.J., Green, G.W., and Moses, T.H., Jr., 1971, Heat flow in the western United States, J. Geophys. Res., 76, 6356-6431.

Schmitt, D.R., Currie, C.A., and Zhang, L., 2012, Crustal stress determination from boreholes and rock cores: Fundament principles, Tectonophysics, v. 580, pp. 1-26.

Sherman, FB, 1982, Characterization of the geothermal resources of southeastern Idaho, pp. 76-87, in Geothermal Direct Heat Program Roundup Technical Conference Proceedings, ed. C. A. Ruscetta, Earth Sci. Lab., Univ. of Utah, DOE/ID/12079-71.

Shervais, J.W., and Hanan, B.B., 2008, Lithospheric topography, tilted plumes, and the track of the Snake River-Yellowstone Hotspot, Tectonics, 27, TC5004, doi:10.1029/2007TC002181.

Shervais, J.W., Branney, M.J., Geist, D.J., Hanan, B.B., Hughes, S.S., Prokopenko, A.A., Williams, D.F., 2006a, HOTSPOT: The Snake River Scientific Drilling Project – Tracking the Yellowstone Hotspot Through Space and Time. Scientific Drilling, no 3, 56-57. Doi:10.2204/iodp.sd.3.14.2006.

Shervais, J.W., Evans, J.P., Christiansen, E.J., Schmitt, D.R., Liberty, L.M., Kessler, J.E., Potter, K.E., Jean, M.M., Sant, C.J., and Freeman, T.G., 2011, Hotspot: The Snake River Geothermal Drilling Project -- An Overview, Geothermal Resource Council Transactions 2011, 14 p.

Shervais, J.W., Gaurav Shroff, S.K. Vetter, Scott Matthews, B.B. Hanan, and J.J. McGee, 2002, Origin and evolution of the western Snake River Plain: Implications from stratigraphy, faulting, and the geochemistry of basalts near Mountain Home, Idaho, in Bill Bonnichsen, C.M. White, and Michael McCurry, eds., Tectonic and Magmatic Evolution of the Snake River Plain Volcanic Province: Idaho Geological Survey Bulletin 30, p. 343-361.

Shervais, J.W., Kauffman, J.D., Gillerman, V.S., Othberg, K.L., Vetter, S.K., Hobson, V.R., Meghan Zarnetske, M., Cooke, M.F., Matthews, S.H., and Hanan, B.B., 2005, Basaltic Volcanism of the Central and Western Snake River Plain: A Guide to Field Relations Between Twin Falls and Mountain Home, Idaho; in J. Pederson and C.M. Dehler, Guide to Field trips in the western United States, Field Guide volume 6, Geological Society of America, Boulder Colorado, 26 pages.

Shervais, J.W., Vetter, S.K. and Hanan, B.B., 2006b, A Layered Mafic Sill Complex beneath the Eastern Snake River Plain: Evidence from Cyclic Geochemical Variations in Basalt, Geology, v. 34, 365-368.

Shervais, J.W., Vetter, S.K., and Hackett, W.R., 1994, Chemical Stratigraphy of Basalts in Coreholes NPR-E and WO-2, Idaho National Engineering Laboratory, Idaho: Implications for Plume Dynamics in the Snake River Plain, in Proceedings of the VIIth International Symposium on the Observation of Continental Crust Through Drilling, Santa Fe, New Mexico, 1994, 93-96.

Shervais, JW and Vetter, SK, 2009, High-K Alkali Basalts of the Western Snake River Plain: Abrupt Transition from Tholeiitic to Mildly Alkaline Plume-Derived Basalts, Western Snake River Plain, Idaho, Journal of Volcanology and Geothermal Research, doi:10.1016/j.jvolgeores.2009.01.023.

Shervais, JW, Cooke, MF, Kauffman, JD, and Othberg, KL, 2006c, Geologic Map of the Owinza Quadrangle, Lincoln County, Idaho, Idaho Geological Survey, Moscow Idaho: Idaho Geological Survey, Moscow Idaho, DWM-64 scale 1:24,000.

Shervais, JW, Cooke, MF, Kauffman, JD, and Othberg, KL, 2006d, Geologic Map of the Owinza Butte Quadrangle, Jerome and Lincoln Counties, Idaho: Idaho Geological Survey, Moscow Idaho, DWM-65 scale 1:24,000.

Smith, R.P., D.D. Blackwell, and T.L. McLing. 2002. Ground water flow, aquifer geometry, and geothermal interactions inferred from temperature distribution; Snake River Plain Aquifer, South-Eastern Idaho; Geological Society Of America, 2002 annual meeting. Abstracts w Programs 34, (6).

Smith, R.P., Josten, N.E., and Hackett, W.R., 1994, Upper crustal seismic and geologic structure of the eastern Snake River Plain: Evidence from drill holes and regional geophysics at the Idaho National Engineering Laboratory (INEL); EOS, v.75, no.44, p.685.

Smith, RP, 2004, Geologic Setting of the Snake River Plain Aquifer and Vadose Zone, Vadose Zone Journal, Vol. 3, 47–58.

Smith, RP, DD Blackwell, TL McLing, and MJ Rohe, submitted, Temperature distribution, aquifer geometry, and groundwater flow in the Snake River Plain aquifer, Eastern Snake River Plain, Idaho.

Stewart, R. R., Gaiser, J. E., Brown, R. J., & Lawton, D. C. (2003). Converted-wave seismic exploration: Applications. Geophysics, 68(1), 40-57.

Street, L. V., and DeTar, R. E., 1987. Geothermal resource analysis in Twin Falls County, Idaho. IDWR Water Information Bulletin 30, Part 15, 46 p.

Street, LV and RE DeTar, 1987, Geothermal Resource Analysis in Twin Falls County, Idaho, in Geothermal Investigations in Idaho, IDWR Water Information Bulletin No. 30, Part 15, 46 pages.

Syberg, F.J.R., 1972, A fourier method for the regional-residual problem of potential fields, Geophysical Prospecting, v. 20, p. 47-75.

Twining, B.V., and Bartholomay, R. C., 2011. Geophysical logs and water-quality data collected for boreholes Kimama-1A and -1B, and a Kimama water supply well near Kimama, southern Idaho. U.S. Geological Survey Data Series 622 (DOE/ID 22215), 18 p., plus appendix.

U. S. Geological Survey, 2000, An Aeromagnetic Survey in Yellowstone National Park: A Web Site for Distribution of Data (on-line edition), USGS Open-File-Report 00-163, http://pubs.usgs.gov/of/2000/ofr-00-0163/

Waite GP, Smith RB and Allen RM, 2006, V_P and V_S structure of the Yellowstone hot spot from teleseismic tomography: Evidence for an upper mantle plume. Jour Geophysical Research, 111, B04303.

Whitehead, RL, Lindholm, GF, 1985, Results of geohydrologic test drilling in the eastern Snake River Plain, Gooding County, Idaho: U.S. Geological Survey Water Resources Investigations Report 84-4294, 30 p., 1 plate.

Wisian, KW, DD Blackwell, S. Bellani, JA Henfling, RA Norman, PC Lysne, A Forster, and J. Schrotter, 1998, Field comparison of conventional and new technology temperature logging systems; Geothermics, v27, n2, 131-141.

Wood, S.H., 1994, Seismic expression and geological significance of a lacustrine delta in Neogene deposits of the western Snake River Plain, Idaho, AAPG Bulletin, 78, 1, 102–121.

Wood, SH and DM Clemens, 2002, Geologic and tectonic history of the western Snake River Plain, Idaho and Oregon, in Idaho Geological Survey Bulletin 30, p. 69-103.

Xue, M. and Allen, RM, 2010, Mantle structure beneath the western United States and its implications for convection processes, Journal Of Geophysical Research, Vol. 115, B07303, doi: 10.1029/2008JB006079, 2010

Yilmaz, Ö., 2001, Seismic data analysis: processing, inversion, and interpretation of seismic data (No. 10). SEG Books.

Yuan H and Dueker K, 2005, Teleseismic P-wave Tomogram of the Yellowstone Plume, Geophysical Research Letters, vol. 32, L07304, doi:10.1029/2004GL022056.

Ziolkowski, A., Hanssen, P., Gatliff, R., Jakubowicz, H., Dobson, A., Hampson, G., Li, X.-Y. and Liu, E. (2003), Use of low frequencies for sub-basalt imaging. Geophysical Prospecting, 51: 169–182. doi: 10.1046/j.1365-2478.2003.00363.

Zoback, M.D., Barton, C.A., Castillo, D.A., Finkbeiner, T., Grollimund, B.R., Moos, D.B., Ward, C.D., Wiprut, D.J., 2003, Determination of Stress Orientation and Magnitude in Deep Wells, International Journal of Rock Mechanics & Mining Sciences, v. 40, pp. 1049 – 1076.

Appendix A

Core Handling Procedures

John Shervais and Katherine Potter

INTRODUCTION

The core collected during Project Hotspot provides a wealth of scientific knowledge about the deep hydrogeology of the SRP subsurface. Some examples of the more impressive core recovered are presented in Figures A.1-1 to A.1-4. To ensure that the core was collected and preserved properly to satisfy a host of scientific objectives the Hotspot core sampling team followed strict protocols in the field. The core handling procedures are described in the following sections.

A prerequisite for the success of Hotspot: the Snake River Scientific Drilling Project was the acquisition and documentation of continuous cores in stratigraphic sequence. We describe here the procedures followed for core handling and preparation, the splitting of the core into working and archive halves, and primary core descriptions.

Core Preparation

Core drilling was conducted 24 hours a day using wire-line techniques. Handling and curation procedures began when the inner core barrel was removed from the hole. After consultation with the core driller and a brief training program for the drilling crew regarding the importance of maintaining core orientation, sequencing and continuity, removal of the core from the inner core barrel was done by the drilling hands under the supervision of the core driller.

Removal of the Core from the Core Barrel

The core was removed from the core barrel by the drilling crew and placed in sequentially numbered PVC trays (Figure A-1). The PVC trays were securely mounted on 8” wide planks which provided stability and allowed drainage of water and drilling mud through ~5 mm diameter holes spaced evenly along the bottoms of the PVC trays. Red paint was used to mark the tops of the trays, and drillers were careful to place the top of the core at the top of the tray. Once the trays were filled with core they were fitted with end blocks and the core trays were stacked in sequence adjacent to the drilling rig until they were moved to the processing area by the core logging team (Figure A-2).

For each core run, the drilling crew prepared a wooden block with the core run number, the top and bottom driller’s depths, and the amount of core recovered. The wooden block was placed at the top of the appropriate PVC core tray and remained with the core run until the core was completely washed, marked, and boxed; the wooden blocks were place inside the core boxes with the core to mark the end of each run.

Figure A-1. Core is removed from inner core barrel by the drilling crew. Process is monitored by Science Crew to ensure that core integrity and orientation are maintained.

Figure A-2. Core runs in PVC troughs stored in Core Logging Tent before being logged. This sediment core was obtained in plastic core barrel liners, so it is simply capped and boxed for transport to the LacCore Facility in Minnesota.

Figure A-3. Initial core logging of a core run in the PVC trough. Each core run logged for rock types, structures, and other characteristics before being boxed.

Figure A-4. Diamond table saw for cutting core. Core is cut into 2-foot lengths and boxed before being photographed and packed for shipping to the USU Core Facility.

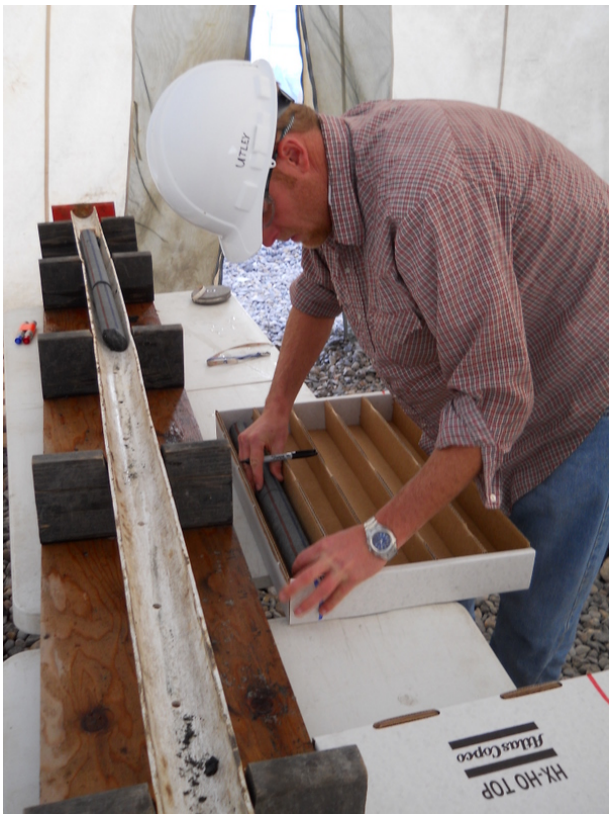

Figure A-5. Left: core is cut and boxed; above: copy stand or 5 MP resolution photos of core boxes.

After each core was moved into the core processing tent, it was washed carefully and thoroughly using water hoses and brushes to remove drilling mud and rock cuttings. Special care was taken during the washing of soil or non-coherent core to prevent disruption or loss of core. The core was then dried with heat lamps or heat guns; once dry, each individual segment of core was marked with Red and Blue lines to indicate orientation (Red on Right where core is held vertically with top of core up).

Run Information and Core Boxing

Individual core runs were placed on working tables for preliminary logging (Figure A-3). A Run Information Form (RIF) was filled out for each core run. The run number, driller's depths, date, and any unusual conditions related to the recovery of the core were noted on the RIF. The core was aligned, and individual pieces were fitted together where possible. The top of the core run being processed was compared to the bottom of the previous core run, and it was noted on the RIF whether these two pieces of core could be fitted together. The length of recovered core was measured in feet (to the nearest tenth) and this was recorded on the RIF. This length included the best estimates for lengths of rubble zones.

The core was then marked for "up" orientation with blue and red, permanent, waterproof felt-tipped pens (see Figure A.1-5.) If necessary, the surface of the core was first dried with a heat gun to prevent smudging of the pen marks. Orientation lines were marked twice on the core, on opposite sides, so that when the core was split into working and archive portions, each piece retained a set of lines. Delicate core (e.g., ash or soil) was sealed in shrink-wrap to preserve its integrity.

Preliminary identification of units was made and the location of contacts and unusual features (e.g., delicate glass-bearing sections, secondary mineralization, ash layers or baked contacts) were noted on the RIF. The core was put into core boxes that were segmented into five 2-ft long rows. The boxes were marked with top (blue) and bottom (red) labels and oriented with the top of the box at the upper left corner. Core was placed in the box beginning with the top in the upper left corner, and continuing down and to the right. The drillers' depth was marked on the box at both the top and bottom.

If necessary, the core was cut with a saw so that each 2-ft segment fit in the core box exactly (Figure A-4). The wooden core run block was placed at the end of each run, labeled with the core run number and the ending driller's depth for that run and the core run number.

After each core box was filled, it was labeled with a black waterproof felt-tipped pen. The project name (HSDP), the box number, the core run number (or run numbers if the box contains material from more than one core run) and the driller's depth range of the core segment in the box were all noted on the box and its lid. Each box was then transferred to a copy stand for a medium resolution digital photograph (5 MP) of the full box plus centimeter scale, grey scale, and color bars, before the box was closed and stacked on a pallet for storage until transport to the USU Core Processing Lab (Figure A-5).

Figure A-6. Medium resolution (5 MP) photograph of boxed core, with run identification, length scale, color bars, and greyscale bars. These photos are made in Core Logging Tent onsite as core is collected, logged, and boxed.

CORE LOGGING PROCEDURES

General Statement

Logging, i.e., the hand-specimen scale description of the core, is critical to the success of the Snake River Scientific Drilling Project since it provides the framework for all subsequent sampling and scientific study of the core.

The first step in core logging was to produce a box label for each box with all pertinent information about box number, depths, etc. Each box was then photographed with a high-resolution digital camera (15 MP Leica V2) using a copy stand with metric scales, grey scale, and Kodak standard color bars, as well as the core box information sheet (Figure A-7). Additionally, a high-resolution digital scan of each whole round core piece was made using the ICDP DMT Core Scanner. Individual scans generally corresponded to the 2-ft rows of the core box, however sections containing rubble were not scanned. Scanned images were entered into the "Drilling Information System" (DIS) database along with information on depth interval of the scan, run number, and box number in which the core piece was stored. A 360º image of the core was made by rotating the core on a set of rollers while the scanner moved down the length of the core. The result is a flat image of the outside surface of the core.

Standardized logging forms for lava flows, tephra, and sedimentary units were based on protocols from the Hawaii Scientific Drilling Project, updated for use with SRP rhyolites and sediments, and the modifications were made to the DIS database so that descriptive protocols could be accessed through drop-down menus.

Detailed Logging Procedures

Loggers were provided with a hand lens, ruler (metric and inches in tenths), references on rock and mineral classification, dilute hydrochloric acid. The log for each box of core consists of a written description of the core prepared using the standardized logging forms, which were filled out in hard copy before being upload into the ICDP DIS database (Figure A-8).

Identifying Contacts and Lithologies

Contacts between units basalt-sediment, basalt-rhyolite, rhyolite-sediment, as well as flow contacts within basalts (basalt-basalt), rhyolites (rhyolite-rhyolite), and sediments (e.g., sand-gravel). All contacts were noted on the logging forms with drillers depth and distance from the nearest upper section boundary (as defined by the DIS database). For flow contacts between basalt flows or rhyolite units, the nature and basis for the contact identification are described. Top and bottom depths of the box and the top depth for each unit in the box were recorded relative to the top depth of each run. All absolute depths are automatically calculated in the database from the relative depth information entered by the logger.

When internal boundaries were present within units (e.g., lobes of a pahoehoe flow; rubble in an aa flow; changes in sorting or grain size in hyaloclastites; glassy pillow margins; or the presence of interpillow breccia), their depths were recorded and their locations were marked with thin dashed lines on the digital image of the core box.

Figure A-7. Example of high resolution (15 MP RAW image) of boxed core taken at USU Core Facility. All high resolution images and core scans uploaded to the Drilling Information System database for archiving. These images are available to anyone wishing to study the core.

For lavas, the groundmass texture was determined (glassy, cryptocrystalline, microcrystalline, fine-grained (<1 mm), medium-grained (1-2 mm), coarse-grained (>2 mm)). Comments on the groundmass (e.g., mineralogy and texture) were added when relevant. Vesicle abundance was visually estimated in volume % (sparse (<5%), moderate (5-15%), abundant (15-30%), very abundant (>30%), and variable). Average vesicle size (small <1 mm, medium 1-5 mm, and large >5 mm), shape (round, sub-rounded, sub-angular, angular), and aspect ratio (equant, horizontally elongated, vertically elongated, inclined - if inclined, the dip relative to the axis of the core was included) were recorded. Comments were also made on the vesicle distribution within the unit.

The extent of alteration was estimated in volume % of the core as a whole (excluding alteration along fractures): fresh (<2% alteration), slightly altered (2-10% alteration), moderately altered (10-40% alteration), highly altered (>40% alteration). Secondary minerals were described and identified where possible (e.g., clays, zeolites, etc.). The extent of fracturing was estimated based on the number of fractures/foot (none, weakly fractured, (<4 fractures/ ft), moderately fractured (4-10 fractures/ft), highly fractured (>10 fractures/ft), or rubble. Loggers noted drilling induced fractures based on their lack of alteration and orientation.

When appropriate, sedimentary features were described (e.g., grain size, sorting, color, and dip of bedding). Lacustrine sediments from the Mountain Home site were recovered in plastic liners and handled differently than the other core, as described below.

Figure A-8. Detailed core logging at the USU Core Facility in Logan, Utah.

Lake Sediment Core

Sediment core from the Mountain Home site was handled differently from the other core. Because it is thought to consist entirely of Pliocene-Pleistocene lake sediments below 200 m depth, this core will be drilled with plastic core liners and sent directly to the LaCore facility at the University of Minnesota for processing. This stratigraphic boundary records the onset of glacial conditions in continental North America. As a part of the initial core description was (1) multi-sensor continuous whole-core logging; (2) core opening and splitting longwise for initial core description and high-resolution imaging; (3) smear slide observations of lithology; (4) preliminary diatom biostratigraphy on 200 samples, i.e., ca. 1 sample per 3 m involving scanning electron microscope imaging of diatoms. This latter part is listed as a part of initial core description, because it is essential to gain understanding of the preliminary age model and hence sedimentation rates and to gain better understanding of the depositional setting at the drill site. Intact clearly labeled lake sediment cores in capped and taped standard GLAD butyrate liner were shipped to the LacCore facility at the University of Minnesota.

APPENDIX B:

PUBLICATIONS AND PRESENTATIONS

Publications Resulting From This Work

Shervais, John W.; Evans, James P.; Christiansen, Eric J.; Schmitt, Douglas R.; Kessler, James A.; Potter, Katherine E.; Jean, Marlon M.; Sant, Christopher J.; Freeman, Thomas G., 2011, Project Hotspot – The Snake River Scientific Drilling Project. Geothermal Resources Council *Transactions*, vol. 35, *995-1003*.

Kessler, James A.; Evans, James P., 2011, Fracture Distribution in Slimholes Drilled for Project Hotspot: The Snake River Geothermal Drilling Project and the Implications for Fluid Flow. Geothermal Resources Council *Transactions*, vol. 35, *839-842*.

Potter, Katherine E.; Shervais, John W.; Sant, Christopher J., 2011, Project Hotspot: Insight into the Subsurface Stratigraphy and Geothermal Potential of the Snake River Plain. Geothermal Resources Council *Transactions*, vol. 35, *967-971*.

Sant, Christopher J. and John W. Shervais, 2011, Project Hotspot: Preliminary Analysis of Secondary Mineralization in Basaltic Core, Central Snake River Plain. Geothermal Resources Council *Transactions*, vol. 35, 987-989.

Twining B.V. and Bartholomay, R.C., 2011, Geophysical Logs and Water-Quality Data Collected for Boreholes Kimama-1A and -1B, and a Kimama Water Supply Well near Kimama, Southern Idaho. United States Geological Survey, Data Series 622, DOE/ID 22215, 17 pp.

Shervais, J.W., 2011, Hotspot. *DOSECC Newsletter, November 2011, vol 7, no.2, 1-4.*

Schmitt, DR, Liberty, LM, Kessler, JE, Kück, J., Kofman, R., Bishop, R., Shervais, JW, Evans, JP, Champion, DE. 2012, The ICDP Snake River Geothermal Drilling Project: Preliminary overview of borehole geophysics. *Geothermal Resources Council Transactions*, v36., 1017-1022.

Nielson, DL., Delahunty, C., and Shervais, JW, 2012, Geothermal Systems in the Snake River Plain, Idaho, Characterized by the Hotspot Project. *Geothermal Resources Council Transactions*, v36, 727-730.

Breckenridge, RP, Shervais, JW, Nielson, DE, Wood, TR, 2012, Exploration and Recourse Assessment at Mountain Home Air Force Base, Idaho Using an Integrated Team Approach. *Geothermal Resources Council Trans*, v36, 615-619.

Lachmar, TL, Freeman, T., Shervais, JW, Nielson, DE, 2012, Preliminary Results: Chemistry and Thermometry of Geothermal Water from MH-2B Test Well. *Geothermal Resources Council Transactions*, vol. 36, 689-692.

Delahunty, C., Nielson, DL, and Shervais, JW, 2012, Coring of three deep geothermal holes, Snake River Plain, Idaho. *Geothermal Resources Council Trans*., v36, 641-647.

Shervais, JW, Nielson , DL, Evans, JP, Lachmar, T, Christiansen, EH, Morgan, L., Shanks, WCP, Delahunty, C, Schmitt, DR, Liberty, LM, Blackwell, DD, Glen, JM, Kessler, JE, Potter, KE, Jean, MM, Sant, CJ, Freeman, TG. 2012, Hotspot: The Snake River Geothermal Drilling Project -- Initial Report. *Geothermal Resources Council Transactions*, v36., 767-772.

Shervais, JW, Schmitt, DR, Nielson, DL, Evans, JP, Christiansen, EH, Morgan, L., Shanks, WCP, Lachmar, T, Liberty, LM, Blackwell, DD, Glen, JM, Champion, D, Potter, KE and Kessler, JA, 2013, First results from HOTSPOT: The Snake River Plain Scientific Drilling Project, Idaho, USA: *Scientific Drilling*, no. 15, doi:10.2204/iodp.sd.15.06.2013.

Jean, M.M., Shervais, J.W., Champion, D.E., and S.K. Vetter, 2013, Geochemical and paleomagnetic variations in basalts from the Wendell Regional Aquifer Systems Analysis (RASA) drill core: evidence for magma recharge and assimilation–fractionation crystallization from the central Snake River Plain, Idaho: *Geosphere*, doi:10.1130/GES00914.1

Published Abstracts Resulting From This Work.

Shervais, John W.; Evans, James P.; Lachmar, Thomas E.; Christiansen, Eric J.; Schmitt, Douglas R.; Kessler, James A.; Potter, Katherine E.; Jean, Marlon M.; Sant, Christopher J.; Freeman, Thomas G., 2011, Project Hotspot – The Snake River Scientific Drilling Project: A Progress Report. *Geological Society of America, Program with Abstracts, Vol. 43, no. 4.*

Potter, Katherine E.; Shervais, John W.; Sant, Christopher J.; Christiansen, Eric H., 2011, Project Hotspot: Insight Into The Subsurface Stratigraphy And Petrologic Evolution Of The Snake River Plain. *Geological Society of America, Program with Abstracts, Vol. 43, no. 4.*

Kessler, James A.; Evans, James P.; Schmitt, Douglas R., 2011, Rock Property Descriptions Interpreted From Borehole Geophysical Data Collected In Slimholes Drilled For Project Hotspot: The Snake River Geothermal Drilling Project. *Geological Society of America, Program with Abstracts, Vol. 43, no. 4.*

Shervais, JW, 2011, Project Hotspot – The Snake River Scientific Drilling Project. *Geological Society of America Annual Meeting, Minneapolis, Minnesota, Abstracts with Programs, Vol 43, no. 7.*

Liberty, L.M.; D.R., Schmitt; and J.W. Shervais, 2011, Seismic imaging through volcanic rocks of the Snake River Plain, Idaho for the ICDP Project Hotspot. *EOS, Transactions of the American Geophysical Union,* S51C-2245.

Potter K.E.; J.W. Shervais; E.H. Christiansen; and R.W. Bradshaw, 2011, Project Hotspot: Subsurface stratigraphy and petrologic evolution of Snake River Plain basalts from KImama core. *EOS, Transactions of the American Geophysical Union,* V43A-2556.

Bradshaw R.W.; E.H. Christiansen; M.J. Dorais; K.E. Potter; J.W. Shervais, 2011, Project Hotspot: Mineral chemistry of high-MgO basalts from the Kimama core, Snake River Scientific Drilling Project, Idaho. *EOS, Transactions of the American Geophysical Union,* V43A-2555.

Jean M.M.; B.B. Hanan; J.W. Shervais: Plume-Lithosphere Interaction beneath the Snake River Plain, Idaho: Constraints from Pb, Sr, Nd, and Hf Isotopes. *EOS, Transactions of the American Geophysical Union,* T51H-2474.

John W. Shervais; Barry B. Hanan; Scott Vetter, 2012, Basaltic Volcanism of the Snake River Volcanic Province. *EOS, Transactions of the American Geophysical Union,* V11E-01.

Barry B. Hanan; Marlon M. Jean; John W. Shervais; David W. Graham; Scott Vetter, 2012, Interaction of Sublithospheric Mantle with a Complex Continental Lithosphere: Radiogenic Isotope Constraint. *EOS, Transactions of the American Geophysical Union,* V11E-02.

David D. Blackwell; Shari Kelley; Kamil Erkan, 2012, Thermomechanical Characteristics of the YNP/SRP Region. *EOS, Transactions of the American Geophysical Union,* V13B-2837.

Katherine E. Potter; John W. Shervais; Duane Champion; Robert A. Duncan; Eric H. Christiansen, 2012, Project Hotspot: Temporal Compositional Variation in Basalts of the Kimama Core and Implications for Magma Source Evolution, Snake River Scientific Drilling Project, Idaho. *EOS, Transactions of the American Geophysical Union,* V13B-2839.

Richard W. Bradshaw; Eric H. Christiansen; Michael J. Dorais; John W. Shervais; Katherine E. Potter, 2012, Source and Crystallization Characteristics of Basalts in the Kimama core: Project Hotspot Snake River Scientific Drilling Project, Idaho. *EOS, Transactions of the American Geophysical Union,* V13B-2840.

Duane Champion; Robert A. Duncan, 2012, Paleomagnetic and 40Ar/39Ar studies on tholeiite basalt samples from "HOTSPOT" corehole taken at Kimama, Idaho, central Snake River Plain. *EOS, Transactions of the American Geophysical Union,* V13B-2842.

Nielson, D. L. Delahunty, C and Shervais, J. W., 2012, Geothermal systems in the Snake River Plain Idaho characterized by the Hotspot Project: *EOS, Transactions of the American Geophysical Union,* V23F-06.

Presentations Resulting From This Work

Geological Society of America, Joint Rocky Mountain-Cordilleran Section Meeting, Logan, Utah, May 2011.

"Project Hotspot – The Snake River Scientific Drilling Project: A Progress Report"

Shervais, John W.; Evans, James P.; Lachmar, Thomas E.; Christiansen, Eric J.; Schmitt, Douglas R.; Kessler, James A.; Potter, Katherine E.; Jean, Marlon M.; Sant, Christopher J.; Freeman, Thomas G.

"Project Hotspot: Insight Into The Subsurface Stratigraphy And Petrologic Evolution Of The Snake River Plain."

Potter, Katherine E.; Shervais, John W.; Sant, Christopher J.; Christiansen, Eric H.

"Rock Property Descriptions Interpreted From Borehole Geophysical Data Collected In Slimholes Drilled For Project Hotspot: The Snake River Geothermal Drilling Project."

Kessler, James A.; Evans, James P.; Schmitt, Douglas R.

Geological Society of America, National Meeting, Minneapolis, Minnesota, October 2011.

"Project Hotspot – The Snake River Scientific Drilling Project: A Progress Report" Shervais, John W.; Evans, James P.; Lachmar, Thomas E.; Christiansen, Eric J.; Schmitt, Douglas R.; Kessler, James E.; Potter, Katherine E.; Jean, Marlon M.; Sant, Christopher J.; Freeman, Thomas

Earthscope Workshop for Interpretive Specialists, Teton Science Center, Jackson Wyoming, September 12, 2010.

"Plume Tales... Chasing the Yellowstone Plume through Space and Time," John W. Shervais.

National Association of Geoscience Teachers-NW Chapter, College of Southern Idaho, Twin Falls, Idaho, June 22, 2010

"Plume Tales... Chasing the Yellowstone Plume through Space and Time" John W. Shervais.

ICDP-DOSECC Town Hall at AGU Annual Meeting, San Francisco, 13 December 2010.

"The Snake River Geothermal Drilling Project: Innovative Approaches to Geothermal Exploration" John W. Shervais

Nevada Geological Society, Elko, Nevada, January 20, 2011.

"Geothermal Exploration in the Snake River Plain Volcanic Province" John W. Shervais

University of Idaho Research Center and USDA Research Center, Kimberly, Idaho, 15 April 2011.

"The Snake River Geothermal Drilling Project: Innovative Approaches to Geothermal Exploration," John W. Shervais

Geothermal Resources Council, San Diego, California, October 2011

"Project Hotspot – The Snake River Scientific Drilling Project" Shervais, John W.; Evans, James P.; Christiansen, Eric J.; Schmitt, Douglas R.; Kessler, James E.; Potter, Katherine E.; Jean, Marlon M.; Sant, Christopher J.; Freeman, Thomas G.

"Fracture Distribution in Slimholes Drilled for Project Hotspot: The Snake River Geothermal Drilling Project and the Implications for Fluid Flow" Kessler, James A.; Evans, James P.

"Project Hotspot: Insight into the Subsurface Stratigraphy and Geothermal Potential of the Snake River Plain" Potter, Katherine E.; Shervais, John W.; Sant, Christopher J.

Geothermal Resources Council, Reno, Nevada, October 2012

"The ICDP Snake River Geothermal Drilling Project: Preliminary overview of borehole geophysics." Schmitt, DR, Liberty, LM, Kessler, JE, Kück, J., Kofman, R., Bishop, R., Shervais, JW, Evans, JP, Champion, DE

"Geothermal Systems in the Snake River Plain, Idaho, Characterized by the Hotspot Project" Nielson, DL., Delahunty, C., and Shervais, JW

"Exploration and Recourse Assessment at Mountain Home Air Force Base, Idaho Using an Integrated Team Approach." Breckenridge, RP, Shervais, JW, Nielson, DE, Wood, TR

"Preliminary Results: Chemistry and Thermometry of Geothermal Water from MH-2B Test Well" Lachmar, TL, Freeman, T., Shervais, JW, Nielson, DE

"Coring of three deep geothermal holes, Snake River Plain, Idaho." Delahunty, C., Nielson, DL, and Shervais, JW

"Hotspot: The Snake River Geothermal Drilling Project -- Initial Report." Shervais, JW, Nielson , DL, Evans, JP, Lachmar, T, Christiansen, EH, Morgan, L., Shanks, WCP, Delahunty, C, Schmitt, DR, Liberty, LM, Blackwell, DD, Glen, JM, Kessler, JE, Potter, KE, Jean, MM, Sant, CJ, Freeman, TG.

American Geophysical Union, Fall Meeting, San Francisco, California, December 2011

"Seismic imaging through volcanic rocks of the Snake River Plain, Idaho for the ICDP Project Hotspot" L.M. Liberty; D.R., Schmitt; J.W. Shervais: S51C-2245.

"Project Hotspot: Subsurface stratigraphy and petrologic evolution of Snake River Plain basalts from KImama core" K.E. Potter; J.W. Shervais; E.H. Christiansen; R.W. Bradshaw: V43A-2556.

"Project Hotspot: Mineral chemistry of high-MgO basalts from the Kimama core, Snake River Scientific Drilling Project, Idaho" R.W. Bradshaw; E.H. Christiansen; M.J. Dorais; K.E. Potter; J.W. Shervais: V43A-2555.

"Plume-Lithosphere Interaction beneath the Snake River Plain, Idaho: Constraints from Pb, Sr, Nd, and Hf Isotopes" M.M. Jean; B.B. Hanan; J.W. Shervais: T51H-2474.

"Seismic imaging through volcanic rocks of the Snake River Plain, Idaho for the ICDP Project Hotspot" Liberty, L.M., Schmitt, D.R., Shervais, J.W.: S51C-2245

American Geophysical Union, Fall Meeting, San Francisco, California, December 2012

"Basaltic Volcanism of the Snake River Volcanic Province"
John W. Shervais; Barry B. Hanan; Scott Vetter; V11E-01.

"Interaction of Sublithospheric Mantle with a Complex Continental Lithosphere: Radiogenic Isotope Constraints" (Invited)
Barry B. Hanan; Marlon M. Jean; John W. Shervais; David W. Graham; Scott Vetter; V11E-02.

"Thermomechanical Characteristics of the YNP/SRP Region"
David D. Blackwell; Shari Kelley; Kamil Erkan; V13B-2837.

"Geothermal systems in the Snake River Plain Idaho characterized by the Hotspot Project"
Nielson, D. L. Delahunty, C and Shervais, J. W., V23F-06.

"Project Hotspot: Temporal Compositional Variation in Basalts of the Kimama Core and Implications for Magma Source Evolution, Snake River Scientific Drilling Project, Idaho." Katherine E. Potter; John W. Shervais; Duane Champion; Robert A. Duncan; Eric H. Christiansen; V13B-2839.

"Source and Crystallization Characteristics of Basalts in the Kimama core: Project Hotspot Snake River Scientific Drilling Project, Idaho"
Richard W. Bradshaw; Eric H. Christiansen; Michael J. Dorais; John W. Shervais; Katherine E. Potter; V13B-2840.

"Paleomagnetic and 40Ar/39Ar studies on tholeiite basalt samples from "HOTSPOT" corehole taken at Kimama, Idaho, central Snake River Plain" Duane Champion; Robert A. Duncan; V13B-2842.